



**Politechnika  
Śląska**

**Załączniki-oryginalne artykuły naukowe  
wraz z oświadczeniami**

**Rozprawa doktorska**

***Badania nad poprawą właściwości  
wytrzymałościowych tworzyw na podstawie  
biopolimerów***

**WERONIKA JANIK**

**GLIWICE 2023**



R-6079- [redacted]

13.10.2024



## Wykaz publikacji

- I. **Janik, W.**, Wojtala, A., Pietruszka, A., Dudek, G., & Sabura, E. (2021). Environmentally Friendly Melt-Processed Chitosan/Starch Composites Modified with PVA and Lignin. *Polymers*, 13(16). <https://doi.org/10.3390/polym13162685>  
IF: 4.329  
Punktacja MNiSW: 100
- II. **Janik, W.**, Nowotarski, M., Shyntum, D. Y., Banaś, A., Krukiewicz, K., Kudła, S., & Dudek, G. (2022). Antibacterial and Biodegradable Polysaccharide-Based Films for Food Packaging Applications: Comparative Study. *Materials*, 15(9). <https://doi.org/10.3390/ma15093236>  
IF: 3.623  
Punktacja MNiSW: 140
- III. **Janik, W.**, Ledniowska, K., Nowotarski, M., Kudła, S., Knapczyk-Korczak, J., Stachewicz, U., Nowakowska-Bogdan, E., Sabura, E., Nosal-Kovalenko, H., Turczyn, R., & Dudek, G. (2022). Chitosan-based films with alternative eco-friendly plasticizers: Preparation, physicochemical properties and stability. *Carbohydrate Polymers*, 120277. <https://doi.org/10.1016/j.carbpol.2022.120277>  
IF: 11.2  
Punktacja MNiSW: 140
- IV. **Janik, W.**, Nowotarski, M., Ledniowska, K., Shyntum, D. Y., Krukiewicz, K., Turczyn, R., Sabura, E., Furgoł, S., Kudła, S., & Dudek, G. (2023). Modulation of physicochemical properties and antimicrobial activity of sodium alginate films through the use of chestnut extract and plasticizers. *Scientific Reports*, 13(1). <https://doi.org/10.1038/s41598-023-38794-3>  
IF: 4.996  
Punktacja MNiSW: 140
- V. **Janik, W.**, Nowotarski, M., Ledniowska, K., Biernat, N., Abdullah, Shyntum, D. Y., Krukiewicz, K., Turczyn, R., Gołombek, K., & Dudek, G. (2023). Effect of Time on the Properties of Bio-Nanocomposite Films Based on Chitosan with Bio-Based Plasticizer Reinforced with Nanofiber Cellulose. *International Journal of Molecular Sciences*, 24(17), <https://doi.org/10.3390/ijms241713205>  
IF: 6.208  
Punktacja MNiSW: 140

## Article

# Environmentally Friendly Melt-Processed Chitosan/Starch Composites Modified with PVA and Lignin

Weronika Janik <sup>1,2,\*</sup> , Anna Wojtala <sup>1</sup>, Anna Pietruszka <sup>1</sup> , Gabriela Dudek <sup>3</sup> and Ewa Sabura <sup>1</sup>

<sup>1</sup> Łukasiewicz Research Network-The Institute of Heavy Organic Synthesis “Blachownia”, Energetyków 9, 47-225 Kędzierzyn-Koźle, Poland; anna.wojtala@icso.lukasiewicz.gov.pl (A.W.); anna.pietruszka@icso.lukasiewicz.gov.pl (A.P.); ewa.sabura@icso.lukasiewicz.gov.pl (E.S.)

<sup>2</sup> Department of Physical Chemistry and Technology of Polymers, PhD School, Silesian University of Technology, 2a Akademicka Str., 44-100 Gliwice, Poland

<sup>3</sup> Department of Physical Chemistry and Technology of Polymers, Faculty of Chemistry, Silesian University of Technology, Strzody 9, 44-100 Gliwice, Poland; gabriela.maria.dudek@polsl.pl

\* Correspondence: weronika.janik@icso.lukasiewicz.gov.pl; Tel.: +48-77-487-31-87

**Abstract:** Chitosan/starch-based composites were prepared by thermomechanical processing as an alternative to the traditional solution method, with the aim of fabricating environmentally friendly materials on a larger scale. Different contents and types of lignin and poly(vinyl alcohol), PVA were incorporated into chitosan/starch compositions to improve their mechanical properties. It was demonstrated that the presence of both lignin and PVA increases the values of tensile strength and elongation at break of the composites. Moreover, it was observed that by the selection of a type of lignin and PVA, it was possible to tailor the internal microstructure of the samples. As observed in scanning electron microscope (SEM) micrographs, the introduction of lignin and PVA resulted in the formation of a smooth surface and homogeneous samples.

**Keywords:** chitosan; starch; thermomechanical processing; lignin; PVA



**Citation:** Janik, W.; Wojtala, A.; Pietruszka, A.; Dudek, G.; Sabura, E. Environmentally Friendly Melt-Processed Chitosan/Starch Composites Modified with PVA and Lignin. *Polymers* **2021**, *13*, 2685. <https://doi.org/10.3390/polym13162685>

Academic Editors: Uroš Novak, Sanja I. Šešljija and Filipa A. Vicente

Received: 25 June 2021

Accepted: 4 August 2021

Published: 11 August 2021

**Publisher's Note:** MDPI stays neutral with regard to jurisdictional claims in published maps and institutional affiliations.



**Copyright:** © 2021 by the authors. Licensee MDPI, Basel, Switzerland. This article is an open access article distributed under the terms and conditions of the Creative Commons Attribution (CC BY) license (<https://creativecommons.org/licenses/by/4.0/>).

## 1. Introduction

Due to the increased demand for petroleum materials and the impact of their accumulation in the environment, there is a growing interest in the design of biodegradable and compostable polymers. Among a wide range of biopolymers, chitosan is the second most popular natural polymer. Chitosan is a natural bioactive polysaccharide possessing intrinsic antimicrobial activity, exhibiting exceptional physicochemical properties imparted by the presence of a polysaccharide backbone, including biodegradability, biocompatibility, and low toxicity. Due to its properties, chitosan has been extensively investigated in many fields, mainly as an environmentally friendly material for packaging applications [1–3]. Moreover, the good film-forming properties of chitosan allows the production of different films and coating materials [2–5]. Chitosan is obtained by a partial deacetylation of chitin, and the degree of deacetylation is proportional to the transformational degree of chitosan from chitin [1]. Most chitosans are insoluble in water and in commonly used organic solvents, but they can be dissolved in acidic aqueous solutions of pH below 6.3 [5]. Still, the use of chitosan at large scale is limited. The reason for this is its high costs and worse properties when compared to traditional petroleum-based plastics, such as lower barrier against water vapor, and thermal and mechanical strength. Fortunately, these properties can be improved by blending chitosan with other biopolymers [4,5].

Chitosan-based films and coatings have been recently intensively studied [2–23]. Most of the research has been focused on evaluating different preparation conditions (including the processing method) and incorporation of additives to improve the properties of composites. Currently, there are two main methods to produce films from chitosan: a wet method based on solvent casting, and a dry method [6], with the preference for wet



method due to its unquestionable simplicity [2–15]. The obtained materials, however, are fragile at small thickness. Additionally, solvent casting is hard to scale up from laboratory to industrial level, because it is a long-lasting process [6]. Only a few literature reports describe the method of chitosan plasticization by one-step extrusion process, but in these composites the amount of chitosan is less than 10 wt.%.

Recently, blends of chitosan/PVA, chitosan/starch, or chitosan/lignin have been greatly studied as promising materials for industrial applications [7–18]. Polymer blends of chitosan and PVA exhibited good thermal stability, unique morphology and reduced solubility in acid solution. FTIR study showed that PVA and chitosan were considered miscible and compatible owing to hydrogen-bonding interaction [7,8]. Moreover, the use of sorbitol as a plasticizer caused an increase in the elongation at break [9]. Composites of chitosan and starch showed good mechanical properties, especially after the addition of more starch content [10]. Furthermore, the addition of keratin fibers increased the glass temperature and the storage modulus of the obtained films [11]. The other type of biocomposite film that has recently been a subject of investigations is chitosan/lignin [12–15]. The FTIR data confirmed the formation of hydrogen bonding between the hydroxyl and carbonyl groups in chitosan with carbonyl, hydroxyl, and ether groups in lignin [12,15]. Additionally, a salt was formed between the protonated amino group of chitosan and the carboxylic group of lignin. The bond formation between the components led to the formation of a crosslinked elastic framework carrying the main mechanical load. Introduction of lignin resulted in an insignificant decrease in tensile strength and modulus of the obtained composite films, while it greatly decreased the cost of formed films.

Polymer blending by mixing two natural biopolymers (chitosan and starch) with PVA was investigated in the following studies [16–18]. The infrared spectra confirmed the good compatibility of PVA with chitosan/starch composite [16]. Additionally, several beneficial effects of PVA addition to the composite were observed: an increase of film flexibility and elongation at break [16], pore disappearance and smoothing of the surface [17], and improved mechanical and functional properties without the loss of biodegradability [18].

Another method for preparing polymer films and coatings is thermomechanical processing. As opposed to the casting method, this method can be used in industrial conditions, which allows the preparation of biodegradable materials on a larger scale. However, the plasticization of chitosan is necessary before applying this method. Glycerol, sorbitol, and xylitol are frequently used as plasticizers, and their presence provides thermoplastic material with good mechanical properties [19–22]. Furthermore, thermomechanical processing allows the use of the conventional tools for polymer processing, such as extruders, kneaders, injection molding, etc., enabling the production of a wide variety of forms and shapes in contrast to a wet method, in which only casted films are produced.

More recently, chitosan has been plasticized during a one-step extrusion process [23–26]. The plasticizing system (glycerol with acetic acid) was mixed with polyethylene [21] or keratin fiber [25]. Extrusion compounding was shown to be a promising method for the industrial processing of chitosan/starch composites due to the possibility of further molding of the materials and its high productivity. It could be used to fabricate a material with a high dispersion and distribution degree of the chitosan phase in starch.

Taking into account the versatility of thermomechanical processing, we used this method to fabricate chitosan/starch composites with lignin and PVA. To the best of our knowledge, similar composites have been only obtained by conventional casting methods [16–18]. Moreover, every previous work describing thermomechanical-processed chitosan [19,20] was associated with its low content in the composite. In our case, chitosan was one of the main components of the composite, with a content of about 30 wt.%. We measured the hydrophilic, mechanical, and thermal properties of investigated samples and analyzed their variation with sample composition.

## 2. Materials and Methods

### 2.1. Materials

Chitosan 30–100 cps ( $M_w = 250,000$ ,  $DD \geq 90\%$ ) and chitosan 100–300 cps ( $M_w = 890,000$ ,  $DD \geq 90\%$ ) were purchased from Glentham Life Sciences Ltd. (Corsham, UK). Each composite contained native potato starch purchased from Przedsiębiorstwo Przemysłu Ziemiaczanego “Trzemeszno” Sp. z o. o. (Trzemeszno, Poland), glycerol from Eurochem BGD Sp. z o.o. (Tarnów, Poland) and acetic acid 20% solution. Three types of lignin were used (dealkaline L0045 from Tokyo Chemical Industry (Tokyo, Japan), and Kraft (sulfate) ones: Lineo Classic and Lineo Classic W from Stora Enso (Stockholm, Sweden)). Three different PVA were used: Elvanol 71–30 (viscosity 27.0–33.0 mPa.s,  $M_w \sim 100,000$ , fully hydrolyzed) was provided by Kuraray Europe GmbH (Hattersheim am Main, Germany), Mowiol 20–98 (viscosity 18.5–21.5 mPa.s,  $M_w \sim 125,000$ , 98.0–98.8 mol% hydrolysis) purchased from Merck (Darmstadt, Germany) and Mowiol 8–88 (viscosity 7–9 mPa.s,  $M_w \sim 67,000$ , 86.7–88.7 mol% hydrolysis) were also purchased from Merck (Darmstadt, Germany).

### 2.2. Sample Preparation

The formulation of chitosan/starch-based samples is shown in Table 1. The appropriate amount of glycerol was incorporated in the chitosan powder and manually mixed. Then, an adequate amount of acetic acid aqueous solution (20 wt.%) was added to the chitosan/glycerol mixture to obtain a paste with final chitosan concentration of 30 wt.%. Then, starch, lignin, and PVA were introduced. The mixtures were then mechanically blended in a HaakePoly-Lab QC Reomix 600 internal batch mixer at 80 °C for 4 min, with a rotor speed of 40 rpm. Finally, the resulting materials were first hot-pressed at 110 °C, 250 bar pressure for 7 min and immediately cooled at room temperature, in the press, for 2 min.

**Table 1.** Composition of chitosan/starch-based blends.

Sample	Composition, wt.%					
	Chitosan	Starch	PVA	Lignin	Glycerol	AAAS
CH1E	30.30 <sup>CH1</sup>	15.76	21.52 <sup>E</sup>	-	10.90	21.52
CH2E	30.30 <sup>CH2</sup>	15.76	21.52 <sup>E</sup>	-	10.90	21.52
CH1EL	28.74 <sup>CH1</sup>	14.94	20.40 <sup>E</sup>	5.17 <sup>L</sup>	10.35	20.40
CH2EL	28.74 <sup>CH2</sup>	14.94	20.40 <sup>E</sup>	5.17 <sup>L</sup>	10.35	20.40
CH1ELC	28.74 <sup>CH1</sup>	14.94	20.40 <sup>E</sup>	5.17 <sup>LC</sup>	10.35	20.40
CH2ELC	28.74 <sup>CH2</sup>	14.94	20.40 <sup>E</sup>	5.17 <sup>LC</sup>	10.35	20.40
CH1ELCW	28.74 <sup>CH1</sup>	14.94	20.40 <sup>E</sup>	5.17 <sup>LCW</sup>	10.35	20.40
CH2ELCW	28.74 <sup>CH2</sup>	14.94	20.40 <sup>E</sup>	5.17 <sup>LCW</sup>	10.35	20.40
CH2L	36.10 <sup>CH2</sup>	18.77	-	6.50 <sup>L</sup>	13.00	25.63
CH2M1L	28.74 <sup>CH2</sup>	14.94	20.40 <sup>M1</sup>	5.17 <sup>L</sup>	10.35	20.40
CH2M2L	28.74 <sup>CH2</sup>	14.94	20.40 <sup>M2</sup>	5.17 <sup>L</sup>	10.35	20.40

CH1—Chitosan 100–300 cpi; CH2—Chitosan 30–100 cpi; E—PVA Elvanol 71–30; L—Lignin TCI; LC—Lignin StornaEnso Classic; LCW—Lignin StornaEnso Classic W; M1—PVA Mowiol 20–98; M2—PVA Mowiol 8–88; AAAS—Acetic Acid Aqueous Solution.

### 2.3. Moisture Content (MC), Swelling Degree (SD), and Total Soluble Matter (TSM)

Moisture content (MC) was determined by a gravimetric method. Weighed samples of a mass ~1 g were dried in an air-circulating oven at 105 °C for 24 h. After this time, the samples were once again weighed. Moisture content was calculated as the percentage of weight loss based on the original weight. Triplicate measurements of MC were conducted for each sample, and the average MC was calculated. A swelling degree (SD) study was



performed by putting dried samples into 100 mL distilled water at room temperature for 24 h. All samples were weighed before and after swelling. Total soluble matter (TSM) was determined by immersing samples in 100 mL of distilled water at 25 °C for 24 h. After this time, the samples were dried in an air-circulating oven at 105 °C for 24 h. TSM was calculated in relation to the dry mass, and it was expressed as the percentage of sample dry matter solubilized.

#### 2.4. Mechanical Properties

Tensile tests were performed by means of an Instron 4466 machine. The tests were carried out at ambient temperature with the indications of PN-EN ISO 527: 2012, sheets 1 and 2. A constant stretching rate of 100 mm/min was applied. Mechanical properties were determined from the average of five measurements.

#### 2.5. Scanning Electron Microscopy (SEM)

Surface morphology of the composite samples was studied using a HITACHI TM3000 scanning electron microscope at a 10 kV accelerating voltage and a chamber pressure of about  $9 \times 10^{-3}$  Pa. Cross-sectional SEM samples were made by freeze fracturing with liquid nitrogen.

#### 2.6. Thermogravimetric Analysis (TGA)

Thermogravimetric analysis was carried out using a Mettler Toledo TGA 2 Thermobalance. The samples (5 mg) were heated up in an open platinum crucible (Pt 70  $\mu$ L), in the temperature range 30–1100 °C, with the heating rate  $\beta = 20$  °C/min, in the dynamic (100 mL/min) nitrogen or air atmosphere. The thermographs were analyzed with the use of the STARe Thermal Analysis Software.

#### 2.7. Differential Scanning Calorimetry (DSC)

DSC measurements were performed using a Mettler Toledo DSC 822e Differential Scanning Calorimeter. Measurements were carried out in two or three stages for  $m_s \sim 5$  mg in an aluminum crucible (Al 40  $\mu$ L) closed with perforated lid, under a nitrogen flow of 50 mL/min according to the temperature program below:

The investigated samples were first heated from 0 °C to 220 °C with the heating rate  $\beta = 10$  °C/min, then cooled to 0 °C at 10 °C/min, and finally, the second heating was performed to 220 °C at 10 °C/min. The investigated samples were first heated from  $-60$  °C to 220 °C at 10 °C/min, then from  $-60$  °C to 300 °C with the same heating rate.

### 3. Results

#### 3.1. Moisture Content, Swelling Degree, and Total Soluble Matter

Figure 1, Figure 2, Figure 3 show the moisture content (MC), swelling degree (SD), and total soluble matter (TSM) of the chitosan/starch-based samples. As can be seen in Figure 1, MC values are similar (around 10%) for all investigated samples. Regarding the composites prepared with different chitosan (CH1 and CH2), it is noticed that the type of chitosan has a slight influence on the moisture content, of about 1 wt.%. In the case of a swelling degree (Figure 2), it can be noticed that the highest value of this parameter (about 200%) is obtained for compositions CH1E and CH2E, with the absence of lignin. This behavior can be explained by the physical crosslinking of hydrophilic polymers with lignin via H-bonds. Lignin partially “blocks” hydrophilic sites of glycerol and chitosan by hydrogen bonds with OH groups, leaving less OH groups to interact with water molecules, resulting in lower SD values [27]. Significant values are also observed for CH2M1L and CH2M2L samples, both containing PVA, which is not fully hydrolyzed. PVA is widely recognized as a crystalline water-soluble polymer. The degree of crystallinity depends on the degree of hydrolysis, and higher degree of hydrolysis causes higher crystallinity. According to [28] the swelling behavior closely correlates with the crystallinity. Therefore, the increase in the swelling ratio is expected to arise from the degradation of crystalline

phase leading to the increase in the presence of amorphous one. The lowest SD value is observed in the case of CH2ELC and CH2ELCW samples where kraft lignin is used. Among the various types of lignin, kraft lignin is much less soluble in water at neutral or acidic pH because of the lack of hydrophilic groups [29]. Considering the total soluble matter for chitosan/starch-based samples, it can be noticed that this parameter is similar for all investigated samples. The exception is the CH2M2L sample, where TSM reaches a value 30% higher than for other samples. Compared to other samples, only this sample contains PVA with the lowest percentage of hydrolysis (86.7–88.7 mol%). The partially hydrolyzed PVA possesses residual acetate groups, which are essentially hydrophobic, and can generate a steric hindrance that disturbs the arrangement of the intermolecular chains in PVA and inhibits the formation of hydrogen bonds between the molecular chains. The presence of an adequate number of these acetate groups enhances composite solubility in water.

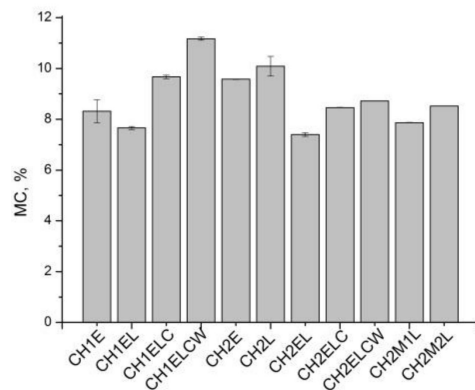


Figure 1. Moisture content (MC) for chitosan/starch-based samples.

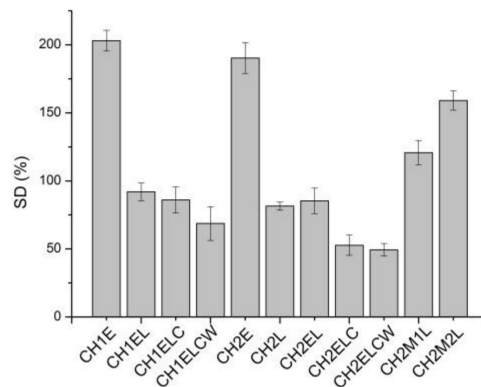


Figure 2. Swelling degree (SD) for chitosan/starch-based samples.

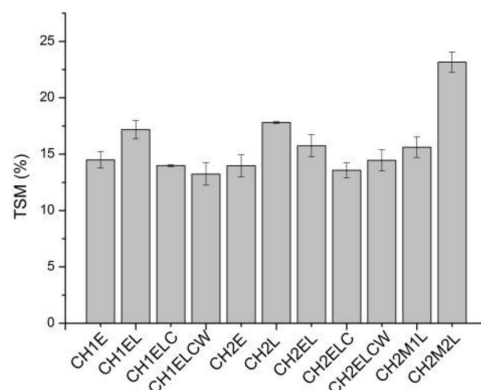
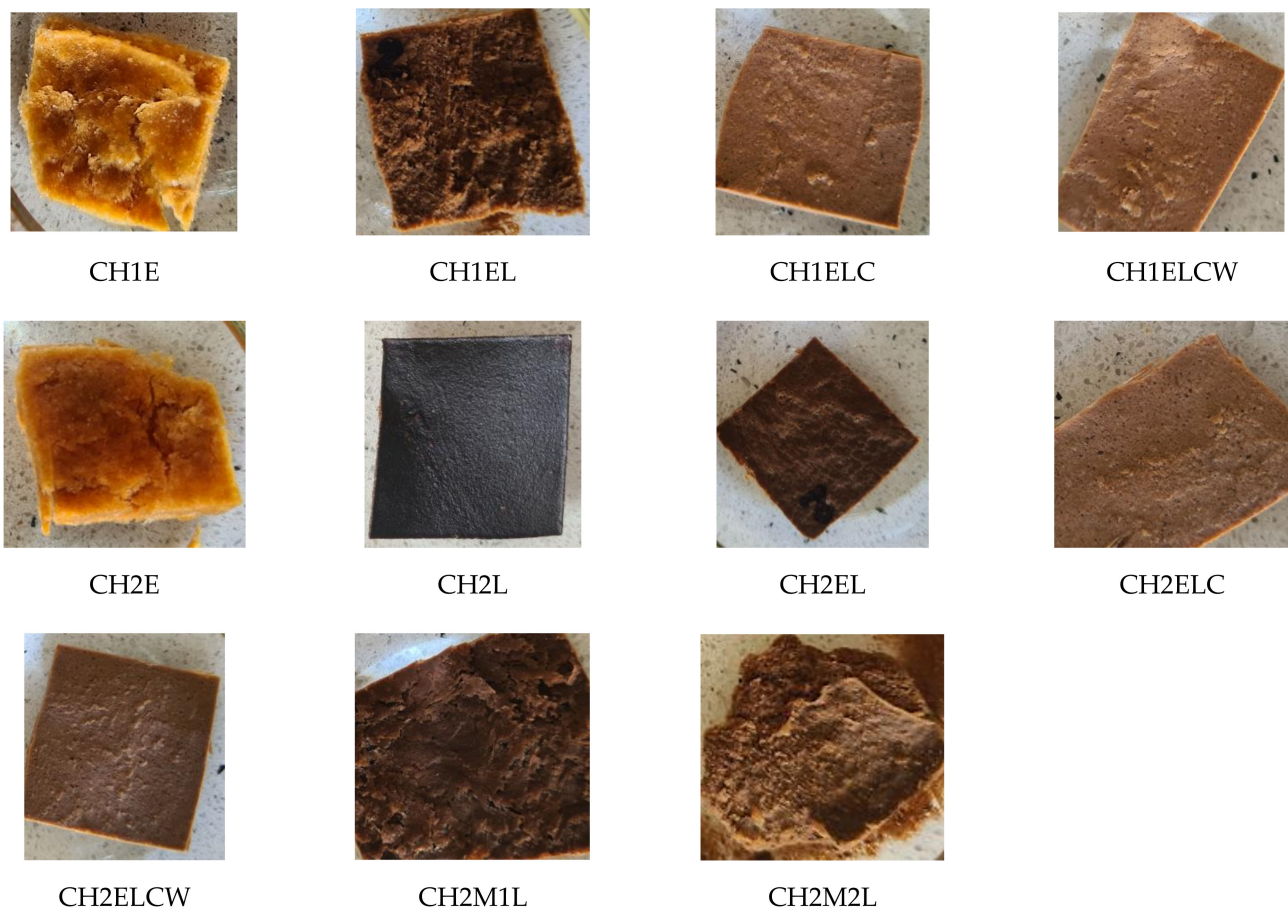


Figure 3. Total soluble matter (TSM) for chitosan/starch-based samples.



Figure 4 shows optical images of samples after immersion in water for 24 h. As can be seen, chitosan/starch-based samples swell after immersion in water. The smoothest surface after swelling is observed for the sample CH2L suggesting its most homogeneous structure. Nevertheless, it can be seen that most of the samples retained their structure and shape. The most visible degradation of a sample can be observed for CH2M2L, which suggests its lowest resistance to water, as confirmed by the results of SD and TSM measurements. However, it can be seen that swelling is lower for samples with lignin and regarding to the obtained results, the lowest value is observed for the composite modified with LCW. This indicates that the type of lignin influences on the structure of the investigated composites, probably due to the presence of chemical interactions between amino groups in chitosan and methoxy together with hydroxy groups in lignin [30]. A tighter structure leads to a decrease in swelling.



**Figure 4.** Chitosan/starch-based samples after immersion in water for 24 h.

### 3.2. Mechanical Properties

The effect of lignin and PVA content on the mechanical properties is shown in Figure 5, Figure 6, Figure 7. Regarding the composites prepared with different chitosan (CH1 and CH2), it is noticed that the type of chitosan has a slight influence on the mechanical properties of composites. In the case of tensile strength, a difference of about 2 wt.% is observed whereas elongation at break and nominal elongation at break vary by about 4% for both types of chitosan. However, tensile strength and elongation at break increases for samples modified with lignin, which is expected to arise from the interactions between chitosan/starch and lignin. This result is different from described by Rosova et al. [15], where the addition of lignin resulted in a decrease in tensile strength and elongation at break in chitosan samples. Even though mechanical properties of the samples can be

mainly linked to the physicochemical characteristic of the polymers and plasticizers, it should be also taken into account that interactions between polymers and plasticizer could vary with the inclusion of additional ingredients, such as lignin or PVA. Different results were observed by Chen et al. [12], where tensile strength increased with the increase in lignin content up to 20 wt.% and decreased after reaching this value. Meanwhile, the value of elongation at break also increased, so it was concluded that lignin can be used as a compatibilizer in chitosan-based samples. Regarding the composites prepared with different lignin (L, LC and LCW), it is noticed that the type of lignin has an influence on the mechanical properties of composites. In the case of tensile strength, the highest value is observed for CH1EL and CH2EL, where lignin L is used. Considering elongation at break and nominal elongation at break, a slight difference is noted, about 3 wt.%. It is noticed that PVA also influences the mechanical properties of composites. Samples modified with PVA exhibit an increase in tensile strength and decrease in elongation at break. The differences in the results between the types of PVA are associated with distribution and density of intermolecular and intramolecular interactions in the network created in chitosan/starch samples modified with PVA [31]. Regarding the composites prepared with different PVA (E, M1 and M2), the highest value is observed in the case of the CH2M2L sample, which contains PVA with the lowest percentage of hydrolysis.

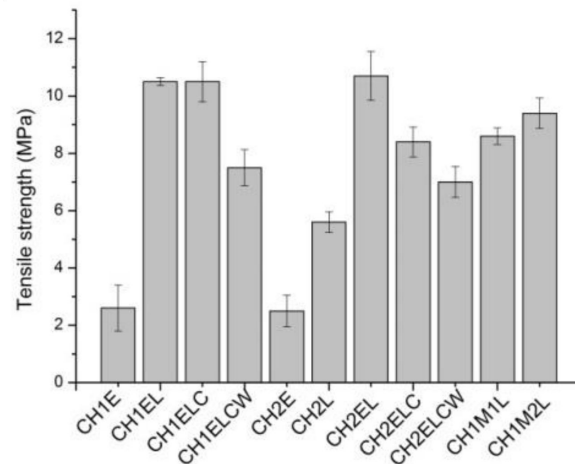


Figure 5. Tensile strength for chitosan/starch-based samples.

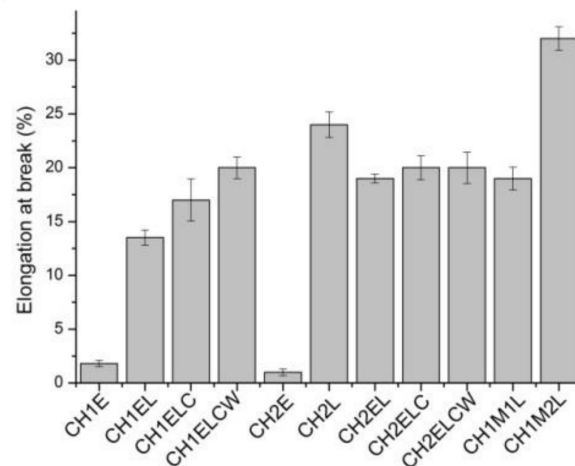


Figure 6. Elongation at break for chitosan/starch-based samples.



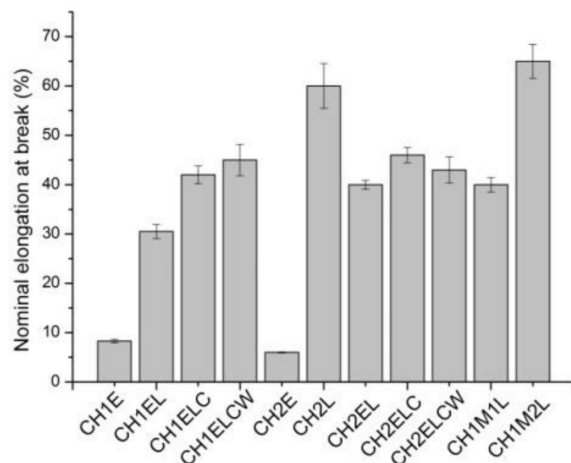


Figure 7. Nominal elongation at break for chitosan/starch-based samples.

### 3.3. Morphology

Figure 8 shows scanning electron microscopy (SEM) images of chitosan/starch-based samples. For all samples, a homogeneous structure is observed demonstrating that the chitosan/starch-based samples modified with lignin and/or PVA had a smooth, flat surface. Lignin is present here in the form of irregularly shaped particles, and PVA seems to be entirely dissolved. SEM images show that regardless of the type of lignin, it is evenly distributed in the polymer matrix, and no voids are noticed in the polymer matrix. The surface of CH2E sample without lignin appears to be relatively smoother than that of CH2L composite (6.5 wt.% L). Despite this, it must be emphasized that proper interfacial interaction is an important factor when lignin or other fillers are to be used to improve mechanical properties [32]. According to the mechanical properties results, it is noticed that lignin significantly increases the mechanical properties of the chitosan/starch-based samples. This indicates good interaction between the components, and it is proven by these SEM images, where the samples showed smooth surfaces. Karua and Saho also prepared starch/chitosan samples with the addition of PVA [17]. In this case, an increasing PVA content ranging from 0 to 10 wt.% resulted in the increase in the tensile strength of blends. Moreover, the corresponding SEM images showed that upon the addition of PVA, the surface of the blend became smooth, and the pores disappeared. In our case, SEM images confirm that the samples with PVA appears to be relatively smoother than those without it. In summary, SEM images confirm the homogeneity of dispersion of lignin and PVA in the chitosan/starch matrix, providing a confirmation that the conditions of processing were appropriate.

### 3.4. Thermal Analysis

Figure 9, Figure 10, Figure 11 show the TG/DTG curves for the chitosan/starch-based samples as well as pure starch, pure chitosan, pure PVA, and pure lignin. For chitosan/starch-based samples, it can be observed that some specific degradations for chitosan and its crosslinked products occurred. At higher temperatures a degradation of PVA byproducts is also observed [33]. Two main weight losses occurred at the temperature ranges of 200–400 °C and 480–600 °C. The first weight loss is assigned to a rapid decomposition of polymer segments of PVA, chitosan, and starch due to the thermal scission of the polymer backbone. The second weight loss is caused by the degradation of the byproducts generated from PVA during its thermal degradation [34] and lignin. For all chitosan/starch-based samples, the two main weight losses were observed each with one  $T_{\text{onset}}$ , which indicates significant interactions between the components [35]. It should be also taken into account that the  $T_{\text{onset}}$  is different for the obtained samples, which should be associated with intramolecular interactions in the samples. The strong hydrogen-bonding interaction between the groups should also increase thermal stability as the formation of a

confined structure in the chitosan/starch-based samples [5]. This is observed in the case of samples modified with lignin, where the  $T_{\text{onset}}$  values in the second stage were higher than for samples without lignin. An additional weight loss in the region of 200 °C can be observed in the DTG curves for samples modified with lignin. This was not observed either on the curve for pure lignin or for the non-modified samples (Figure 11). It should be also noted that for all samples, there is a single event representing the pyrolysis of glycerol observed in the range 130–260 °C [36].

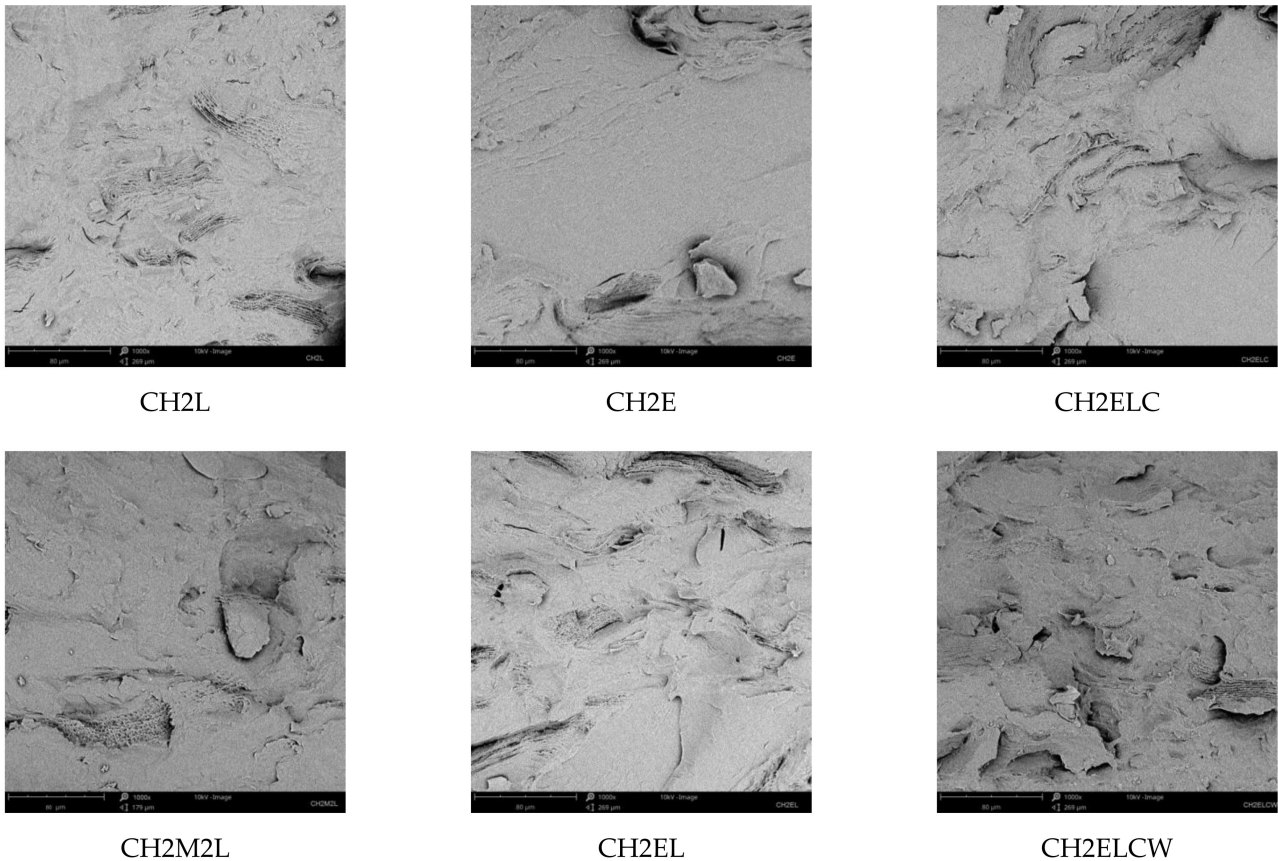


Figure 8. SEM images of chitosan/starch-based samples modified with PVA and lignin, 1000×.

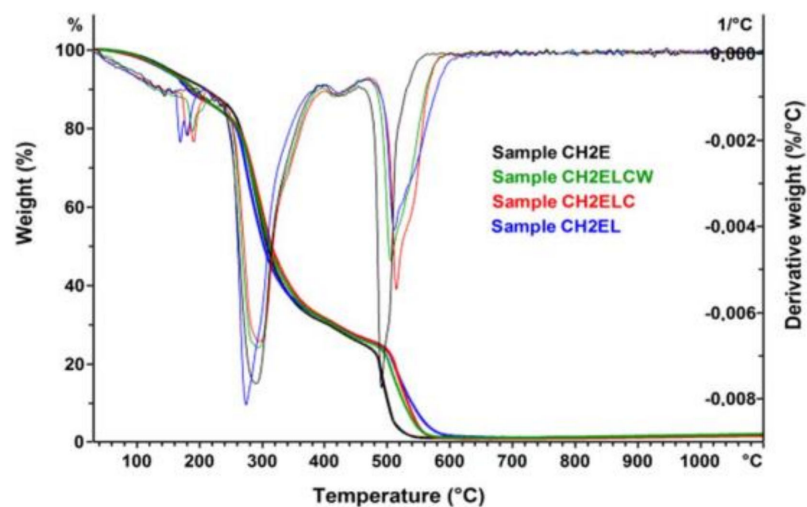


Figure 9. TG and DTG curves of chitosan/starch-based samples.



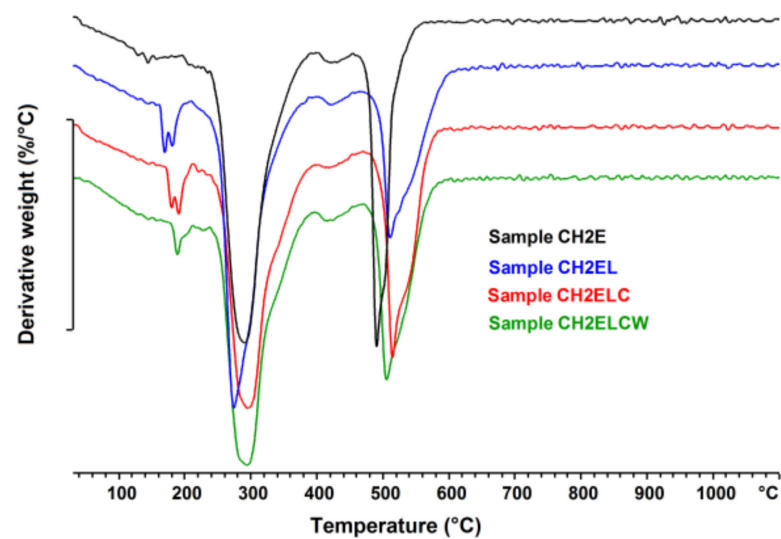


Figure 10. DTG curves of chitosan/starch-based samples.

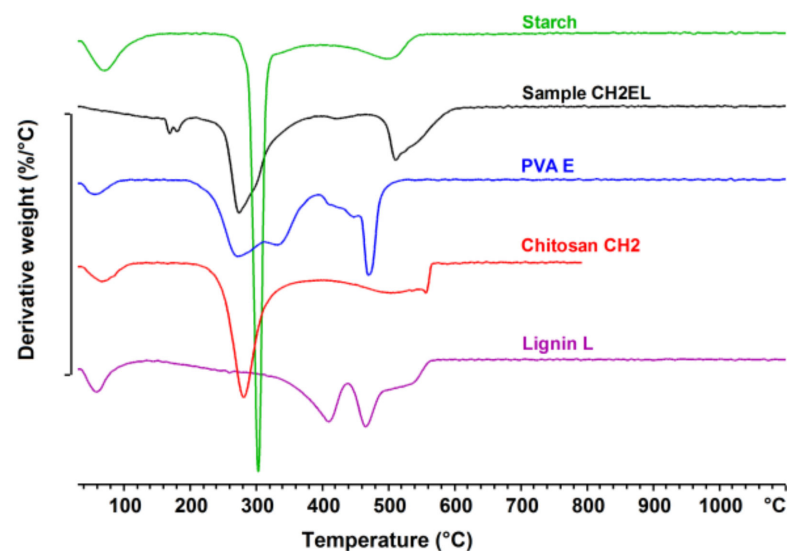


Figure 11. DTG curves of sample CH2EL, pure starch, PVA E, chitosan CH2 and lignin L.

Figures 12 and 13 show the transitions detected in the thermograms of pure lignin used in the chitosan/starch-based samples. The DSC thermogram showed a wide endothermic peak between 20–150 °C assigned to the loss of water. The highest water content is noticed for lignin LCW. Moreover, at temperature of about 0 °C, an additional endothermic peak of the DSC curve is observed, and is associated with the content of freezable water in this type of lignin. Taking into account the enthalpy of fusion and water evaporation of pure LCW, it can be concluded that it contains both freezable water and non-freezable bound water. For both lignin and chitosan, a thermal event was registered. The glass transition temperature was determined using the enthalpy calculation procedure given by Richardson [37], and the values were presented in Table 2. The glass transition temperature is clearly higher for lignin than for chitosan. Moreover, the highest glass transition temperature is observed for lignin L. Figure 14 shows the differential scanning calorimetric scans of the prepared chitosan/starch-based samples. In the first heating curve, a wide endothermic peak between 30–180 °C is observed, which is related to the evaporation of water present in the sample. This transition is no longer observed at the second heating scans. The DSC thermogram shows an endothermic peak between 180–220 °C which is

attributed to the melting of PVA, while an exothermic peak starting above 250 °C indicates a thermal decomposition of prepared samples.

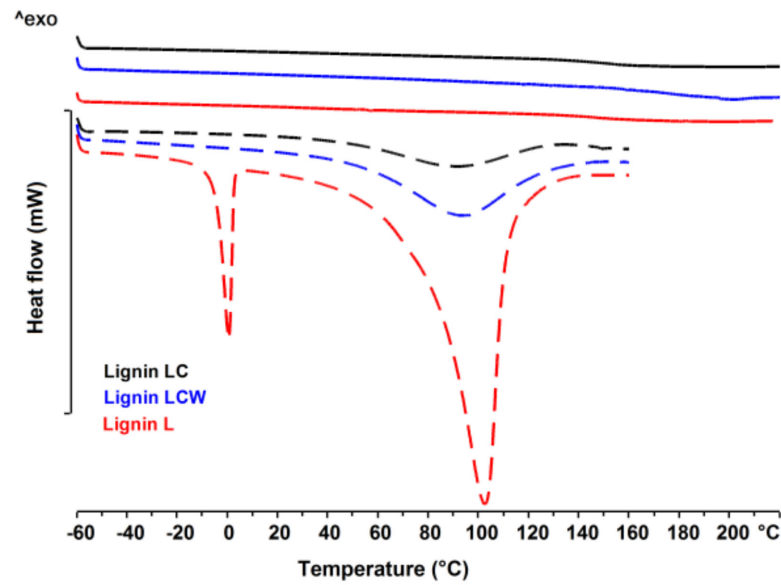


Figure 12. DSC curves of various lignin; 1st heating (dotted line) and 2nd heating (solid line).

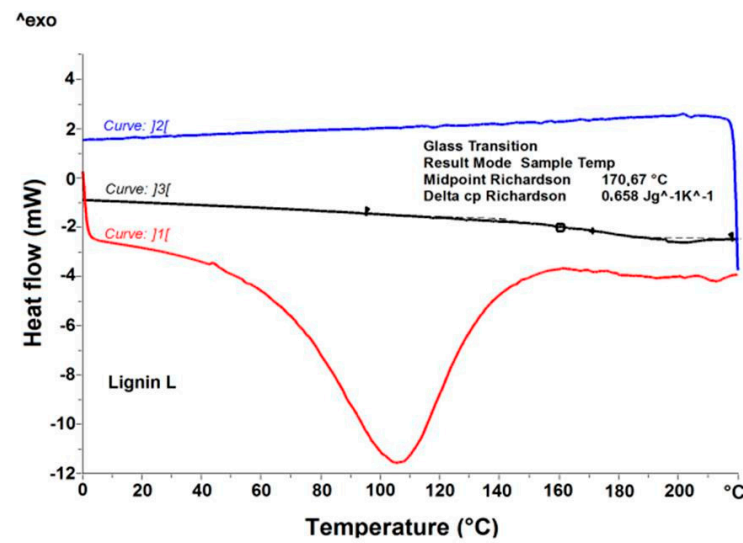
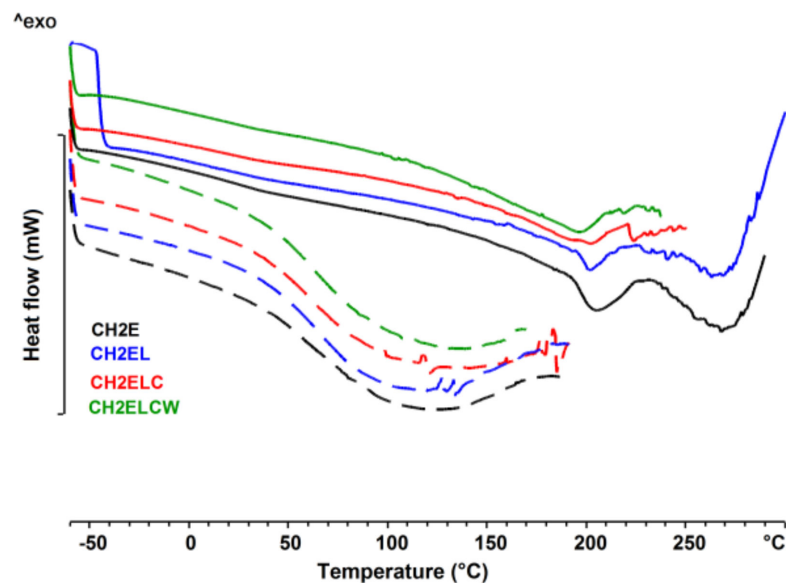


Figure 13. DSC determination of glass transition temperature (T<sub>g</sub>) and change in heat capacity (C<sub>p</sub>) for Lignin L.

Table 2. Glass transition temperatures and their associated change in heat capacity.

Sample	T <sub>g</sub> (°C)	ΔC <sub>p</sub> (J·g <sup>-1</sup> ·K <sup>-1</sup> )
Lignin LC	148.4	0.374
Lignin LCW	154.2	0.325
Lignin L	170.7	0.658
Chitosan CH2	89.8	0.457



**Figure 14.** DSC curves of chitosan/starch-based samples; 1st heating (dotted line) and 2nd heating (solid line).

#### 4. Conclusions

Herein, we describe the fabrication and characterization of environmentally friendly chitosan/starch-based composite materials modified with lignin and PVA. This is the first study reporting samples containing significant amount of chitosan, with a content of about 30 wt.%, prepared via thermomechanical processing. The physicochemical characterization of composites involved the determination of moisture content, swelling degree, total soluble matter, tensile strength, and elongation at break. The results showed that the type of lignin and PVA had a significant influence on the structure of the samples, with the superior mechanical characteristics exhibited by the materials modified with lignin. Furthermore, the addition of PVA was found to increase the tensile strength and decreased the elongation at break. Due to the higher value of tensile strength and similar value of elongation at break, investigated composite materials exhibit better mechanical properties than chitosan/starch compositions produced by extrusion process and containing less than 10 wt.% of chitosan. Moreover, strong hydrogen-bonding interaction between the groups in the chitosan/starch-based samples increased the thermal stability of investigated composites. SEM images showed a good dispersion of lignin and PVA within the composite material, showing smooth surfaces and a high level of homogeneity. The best results were obtained for samples containing both investigated components, i.e., ~20 wt.% PVA and ~5 wt.% lignin, for which tensile strength and nominal elongation at break were equal to ~9 MPa and ~40%, respectively. The performed study proved that the use of lignin and PVA in chitosan/starch composites is a suitable method for obtaining a thermomechanical-processed material. Due to the fact that thermomechanical processing is the most popular method used in the production of packaging, and biopolymers are popular materials on the packaging market, the presented studies can contribute to broaden the applicability of biopolymers at a large scale. Still, the presented results are preliminary, and further research is necessary to improve material properties for industrial application.

#### 5. Patents

The patent was registered under the number P.438269.

**Author Contributions:** Conceptualization, W.J.; data curation, W.J., A.W., A.P., E.S., G.D.; formal analysis, W.J., A.W., E.S., G.D.; funding acquisition, W.J.; investigation, W.J., A.W., E.S., G.D.; methodology, W.J., A.W., E.S.; project administration, W.J., A.W.; resources, W.J.; supervision, G.D.; validation,



W.J., A.W., A.P.; visualization, W.J.; writing—Original draft preparation, W.J., A.P.; writing—Review and editing, W.J., G.D. All authors have read and agreed to the published version of the manuscript.

**Funding:** Article Processing Charge was financed by the Ministry of Education and Science of Poland under grant No BZ/21/23. This research was co-financed by the Ministry of Education and Science of Poland under grant No DWD/4/21/2020.

**Data Availability Statement:** Not applicable.

**Acknowledgments:** Authors would like to thank the Silesian University of Technology for the partial financial support under the projects no 04/040/SDU/10-22-02 and 04/040/BKM21/0168.

**Conflicts of Interest:** The authors report no conflicts of interest.




## References

1. Kumari, S.; Kumar Annamareddy, S.H.; Abanti, S.; Kumar Rath, P. Physicochemical Properties and Characterization of Chitosan Synthesized from Fish Scales, Crab and Shrimp Shells. *Int. J. Biol. Macromol.* **2017**, *104*, 1697–1705. [[CrossRef](#)]
2. Leceta, I.; Guerrero, P.; de la Caba, K. Functional Properties of Chitosan-Based Films. *Carbohydr. Polym.* **2013**, *93*, 339–346. [[CrossRef](#)]
3. Ke, C.-L.; Deng, F.-S.; Chuang, C.-Y.; Lin, C.-H. Antimicrobial Actions and Applications of Chitosan. *Polymers* **2021**, *13*, 904. [[CrossRef](#)] [[PubMed](#)]
4. Souza, V.G.L.; Pires, J.R.A.; Rodrigues, C.; Coelho, I.M.; Fernando, A.L. Chitosan Composites in Packaging Industry—Current Trends and Future Challenges. *Polymers* **2020**, *12*, 417. [[CrossRef](#)] [[PubMed](#)]
5. van den Broek, L.A.M.; Knoop, R.J.I.; Kappen, F.H.J.; Boeriu, C.G. Chitosan Films and Blends for Packaging Material. *Carbohydr. Polym.* **2015**, *116*, 237–242. [[CrossRef](#)]
6. Zhang, Y.; Liu, B.-L.; Wang, L.-J.; Deng, Y.-H.; Zhou, S.-Y.; Feng, J.-W. Preparation, Structure and Properties of Acid Aqueous Solution Plasticized Thermoplastic Chitosan. *Polymers* **2019**, *11*, 818. [[CrossRef](#)] [[PubMed](#)]
7. Casey, L.; Wilson, L. Investigation of Chitosan-PVA Composite Films and Their Adsorption Properties. *J. Geosci. Environ. Prot.* **2015**, *3*, 78–84. [[CrossRef](#)]
8. Choo, K.; Ching, Y.C.; Chuah, C.H.; Julai, S.; Liou, N.-S. Preparation and Characterization of Polyvinyl Alcohol-Chitosan Composite Films Reinforced with Cellulose Nanofiber. *Materials* **2016**, *9*, 644. [[CrossRef](#)]
9. Ali, M.; Gherissi, A. Synthesis and Characterization of the Composite Material PVA/Chitosan/5% Sorbitol with Different Ratio of Chitosan. *Int. J. Mech. Mechatron. Eng.* **2017**, *17*, 15–28.
10. Sakkara, S.; Nataraj, D.; Venkatesh, K.; Reddy, N. Influence of Alkali Treatment on the Physicochemical and Mechanical Properties of Starch Chitosan Films. *Starch—Stärke* **2019**, *71*, 1800084. [[CrossRef](#)]
11. Flores-Hernández, C.G.; Colin-Cruz, A.; Velasco-Santos, C.; Castaño, V.M.; Almendarez-Camarillo, A.; Olivás-Armendariz, I.; Martínez-Hernández, A.L. Chitosan–Starch–Keratin Composites: Improving Thermo-Mechanical and Degradation Properties Through Chemical Modification. *J. Polym. Environ.* **2018**, *26*, 2182–2191. [[CrossRef](#)]
12. Chen, L.; Tang, C.; Ning, N.; Wang, C.; Fu, Q.; Zhang, Q. Preparation and Properties of Chitosan/Lignin Composite Films. *Chin. J. Polym. Sci.* **2009**, *27*, 739–746. [[CrossRef](#)]
13. Pandharipande, S.L.; Pujari, N.; Deshmukh, K. Synthesis and Characterisation of Biocomposite Films of Chitosan and Lignin. *Int. J. Eng. Res. Technol.* **2016**, *5*, 626–636. [[CrossRef](#)]
14. Kopania, E.; Wiśniewska-Wrona, M. Biopolymer Composites Based on Lignin and Microcrystalline Chitosan. *Prog. Chem. Appl. Chitin Its Deriv.* **2016**, *21*, 122–134. [[CrossRef](#)]
15. Rosova, E.; Smirnova, N.; Dresvyanina, E.; Smirnova, V.; Vlasova, E.; Ivan'kova, E.; Sokolova, M.; Maslennikova, T.; Malafeev, K.; Kolbe, K.; et al. Biocomposite Materials Based on Chitosan and Lignin: Preparation and Characterization. *Cosmetics* **2021**, *8*, 24. [[CrossRef](#)]
16. Gomes, A.M.M.; da Silva, P.L.; e Moura, C.D.L.; da Silva, C.E.M.; Ricardo, N.M.P.S. Study of the Mechanical and Biodegradable Properties of Cassava Starch/Chitosan/PVA Blends. *Macromol. Symp.* **2011**, *299*, 220–226. [[CrossRef](#)]
17. Karua, C.S.; Sahoo, A. Synthesis and Characterization of Starch/Chitosan Composites. *Mater. Today Proc.* **2020**, *33*, 5179–5183. [[CrossRef](#)]
18. Kochkina, N.E.; Lukin, N.D. Structure and Properties of Biodegradable Maize Starch/Chitosan Composite Films as Affected by PVA Additions. *Int. J. Biol. Macromol.* **2020**, *157*, 377–384. [[CrossRef](#)]
19. Epure, V.; Griffon, M.; Pollet, E.; Avérous, L. Structure and Properties of Glycerol-Plasticized Chitosan Obtained by Mechanical Kneading. *Carbohydr. Polym.* **2011**, *83*, 947–952. [[CrossRef](#)]
20. Matet, M.; Heuzey, M.-C.; Pollet, E.; Aji, A.; Avérous, L. Innovative Thermoplastic Chitosan Obtained by Thermo-Mechanical Mixing with Polyol Plasticizers. *Carbohydr. Polym.* **2013**, *95*, 241–251. [[CrossRef](#)] [[PubMed](#)]
21. Meng, Q.; Heuzey, M.-C.; Carreau, P.J. Hierarchical Structure and Physicochemical Properties of Plasticized Chitosan. *Biomacromolecules* **2014**, *15*, 1216–1224. [[CrossRef](#)]
22. Chen, P.; Xie, F.; Tang, F.; McNally, T. Unexpected Plasticization Effects on the Structure and Properties of Polyelectrolyte Complexed Chitosan/Alginate Materials. *ACS Appl. Polym. Mater.* **2020**, *2*, 2957–2966. [[CrossRef](#)]

23. Mendes, J.F.; Paschoalin, R.T.; Carmona, V.B.; Sena Neto, A.R.; Marques, A.C.P.; Marconcini, J.M.; Mattoso, L.H.C.; Medeiros, E.S.; Oliveira, J.E. Biodegradable Polymer Blends Based on Corn Starch and Thermoplastic Chitosan Processed by Extrusion. *Carbohydr. Polym.* **2016**, *137*, 452–458. [[CrossRef](#)] [[PubMed](#)]
24. Matet, M.; Heuzey, M.-C.; Ajji, A.; Sarazin, P. Plasticized Chitosan/Polyolefin Films Produced by Extrusion. *Carbohydr. Polym.* **2015**, *117*, 177–184. [[CrossRef](#)] [[PubMed](#)]
25. Flores-Hernandez, C.G.; Martinez-Hernandez, A.L.; Colin-Cruz, A.; Martinez-Bustos, F.; Castaño, V.M.; Olivas-Armendariz, I.; Almendarez-Camarillo, A.; Velasco-Santos, C. Starch Modified With Chitosan and Reinforced With Feather Keratin Materials Produced by Extrusion Process: An Alternative to Starch Polymers. *Starch—Stärke* **2018**, *70*, 1700295. [[CrossRef](#)]
26. Pelissari, F.M.; Yamashita, F.; Grossmann, M.V.E. Extrusion Parameters Related to Starch/Chitosan Active Films Properties. *Int. J. Food Sci. Technol.* **2011**, *46*, 702–710. [[CrossRef](#)]
27. Liu, R.; Dai, L.; Xu, C.; Wang, K.; Zheng, C.; Si, C. Lignin-Based Micro- and Nanomaterials and Their Composites in Biomedical Applications. *ChemSusChem* **2020**, *13*, 4266–4283. [[CrossRef](#)] [[PubMed](#)]
28. Puspitasari, T.; Raja, K.M.L.; Pangerteni, D.S.; Patriati, A.; Putra, E.G.R. Structural Organization of Poly(vinyl alcohol) Hydrogels Obtained by Freezing/Thawing and J-Irradiation Processes: A Small-Angle Neutron Scattering (SANS) Study. *Procedia Chem.* **2012**, *4*, 186–193. [[CrossRef](#)]
29. Konduri, M.; Kong, F.; Fatehi, P. Production of carboxymethylated lignin and its application as a dispersant. *Eur. Polym. J.* **2015**, *70*, 371–383. [[CrossRef](#)]
30. Yu, O.; Kim, K.H. Lignin to Materials: A Focused Review on Recent Novel Lignin Applications. *Appl. Sci.* **2020**, *10*, 4626. [[CrossRef](#)]
31. Nasalapure, A.V.; Chalannavar, R.K.; Malabadi, R.B. Preparation of Poly(Vinyl Alcohol)/Chitosan/Starch Blends and Studies on Thermal and Surface Properties. *AIP Conf. Proc.* **2018**, *1953*, 100060. [[CrossRef](#)]
32. Wang, K.; Loo, L.S.; Goh, K.L. A Facile Method for Processing Lignin Reinforced Chitosan Biopolymer Microfibres: Optimising the Fibre Mechanical Properties through Lignin Type and Concentration. *Mater. Res. Express* **2016**, *3*, 035301. [[CrossRef](#)]
33. Arora, S.; Lal, S.; Sharma, C.; Aneja, K. Synthesis, Thermal and Antimicrobial Studies of Chitosan/Starch/Poly(Vinyl Alcohol) Ternary Blend Films. *Chem. Sin.* **2011**, *2*, 75–86.
34. Grande, G.; Pessan, L.A.; Carvahlo, A. Thermoplastic blends of chitosan: A method for the preparation of high thermally blends with polyesters. *Carboh. Polym.* **2018**, *191*, 44–52. [[CrossRef](#)] [[PubMed](#)]
35. Wu, H.; Wan, Y.; Cao, X.; Wu, Q. Interlocked chitosan/poly(DL-lactide) blends. *Mater. Lett.* **2008**, *62*, 330–334. [[CrossRef](#)]
36. Almazrouei, M.; Samad, T.E.; Janajreh, I. Thermogravimetric Kinetics and High Fidelity Analysis of Crude Glycerol. *Energy Procedia* **2017**, *142*, 1699–1705. [[CrossRef](#)]
37. Manley, T.R. *Calorimetry and Thermal Analysis of Polymers*, Edited by V. B. F. Mathot. Hanser, Munich, 1994. pp. 377. ISBN 3-446-17511-3. *Polym. Int.* **1995**, *37*, 83. [[CrossRef](#)]

## Article

# Antibacterial and Biodegradable Polysaccharide-Based Films for Food Packaging Applications: Comparative Study

Weronika Janik <sup>1,2,\*</sup> , Michał Nowotarski <sup>3</sup>, Divine Yutefar Shyntum <sup>4</sup>, Angelika Banaś <sup>3</sup>, Katarzyna Krukiewicz <sup>3</sup> , Stanisław Kudła <sup>1</sup> and Gabriela Dudek <sup>3</sup> 

- <sup>1</sup> Łukasiewicz Research Network—The Institute of Heavy Organic Synthesis “Blachownia”, Energetyków 9, 47-225 Kędzierzyn-Koźle, Poland; stanislaw.kudla@icso.lukasiewicz.gov.pl
- <sup>2</sup> Department of Physical Chemistry and Technology of Polymers, PhD School, Silesian University of Technology, 2a Akademicka Str., 44-100 Gliwice, Poland
- <sup>3</sup> Department of Physical Chemistry and Technology of Polymers, Faculty of Chemistry, Silesian University of Technology, Strzody 9, 44-100 Gliwice, Poland; michnow566@student.polsl.pl (M.N.); angeban429@student.polsl.pl (A.B.); katarzyna.krukiewicz@polsl.pl (K.K.); gabriela.maria.dudek@polsl.pl (G.D.)
- <sup>4</sup> Biotechnology Centre, Silesian University of Technology, B. Krzywoustego 8, 44-100 Gliwice, Poland; divine.yutefar.shyntum@polsl.pl
- \* Correspondence: weronika.janik@icso.lukasiewicz.gov.pl; Tel.: +48-77-487-31-87

**Abstract:** One of the major objectives of food industry is to develop low-cost biodegradable food packaging films with optimal physicochemical properties, allowing for their large-scale production and providing a variety of applications. To meet the expectations of food industry, we have fabricated a series of solution-cast films based on common biodegradable polysaccharides (starch, chitosan and alginate) to be used in food packaging applications. Selected biopolymers were modified by the addition of glycerol and oxidized sucrose (starch), glycerol (chitosan), and glycerol and calcium chloride (alginate), as well as being used to form blends (starch/chitosan and starch/alginate, respectively). A chestnut extract was used to provide antibacterial properties to the preformed materials. The results of our studies showed that each modification reduced the hydrophilic nature of the polymers, making them more suitable for food packaging applications. In addition, all films exhibited much higher barrier properties to oxygen and carbon dioxide than commercially available films, such as polylactic acid, as well as exhibiting antimicrobial properties against model Gram-negative and Gram-positive bacteria (*Escherichia coli* and *Staphylococcus epidermidis*, respectively), as well as yeast (*Candida albicans*).

**Keywords:** starch; chitosan; alginate; biopolymers; polysaccharide; modification; barrier properties



**Citation:** Janik, W.; Nowotarski, M.; Shyntum, D.Y.; Banaś, A.; Krukiewicz, K.; Kudła, S.; Dudek, G. Antibacterial and Biodegradable Polysaccharide-Based Films for Food Packaging Applications: Comparative Study. *Materials* **2022**, *15*, 3236. <https://doi.org/10.3390/ma15093236>

Academic Editors: Pavel Kopel and Ewelina Jamróz

Received: 4 April 2022

Accepted: 27 April 2022

Published: 29 April 2022

**Publisher's Note:** MDPI stays neutral with regard to jurisdictional claims in published maps and institutional affiliations.



**Copyright:** © 2022 by the authors. Licensee MDPI, Basel, Switzerland. This article is an open access article distributed under the terms and conditions of the Creative Commons Attribution (CC BY) license (<https://creativecommons.org/licenses/by/4.0/>).

## 1. Introduction

As the environment becomes increasingly polluted with plastics, there is an urgent need for the development of biodegradable polymers applicable in industry. Currently, these are polysaccharides, such as starch, chitosan and alginates, that serve as the most popular biodegradable polymers. However, the raw polysaccharide-based materials do not exhibit the appropriate physicochemical properties necessary for food packaging applications [1–4]. Therefore, numerous recent studies [3,5–9] focus on the modification of such biopolymers. Unfortunately, the modification of biodegradable polymers is not as obvious as in the case of conventional synthetic polymers, since each polysaccharide, due to its chemical structure, requires a different modification method. Additionally, it is known that the introduction of some modifications can have an adverse effect on the process of biodegradation. Since biodegradable polymers are primarily used in the packaging market, modifiers must be non-hazardous and considered as safe for food contact.

The most common modification route for starch is plasticization, and the most commonly used plasticizer is glycerol [5–7]. This modification is used to improve the elongation,



distribution, flexibility, elasticity, and rigidity of the film [8–11]. Moreover, the addition of plasticizers can change the continuity and thus improve the properties of starch-based films [5]. Another popular way to modify starch is by using crosslinking, e.g., with natural organic acids (lactic acid, malic acid and citric acid). The presence of acidic crosslinking agents leads to the decrease in swelling, water uptake and water vapor permeability of materials, and these effects are proportional to the amount of a crosslinker [12–14]. Furthermore, the presence of organic acids was found to improve the tensile strength of starch films [15,16], as well as to reduce water vapor permeability, and to increase thermal properties without affecting biodegradability of investigated films [17,18]. Xu et al. [19] used oxidized sucrose as a starch crosslinking agent, and the obtained films were found to be strong and ductile.

Chitosan can be modified through the addition of plasticizers or crosslinking agents (citric acid) [20–24]. Similarly to the case of starch, plasticizers improve the elongation, distribution, flexibility, elasticity, and rigidity of chitosan-based films [25–27]. Chitosan, due to its chemical nature, does not always require additional modifications beyond plasticization. It dissolves only in acidic conditions, so it is not as highly soluble in water as other polysaccharides. Nevertheless, crosslinking with citric acid can provide some additional benefits, for instance the improvement in mechanical, thermal and moisture barrier properties when compared to the unmodified chitosan film [21,22]. Another approach for chitosan modification is the use of glycidol [28–31]. The resulting chitosan derivatives form micelles, hydrogels or membranes, and are commonly used for drug/gene delivery.

For sodium alginates, the most common modification is the use of calcium chloride as a crosslinking agent [32–34]. Recent results indicate that the swelling properties of alginate films decrease after the addition of  $\text{CaCl}_2$ , which is due to the crosslinking reaction between the carboxyl group of alginate and calcium ions [33,35,36]. Modified alginate films exhibited higher tensile stress and tensile strain compared to the unmodified films [33,34]. Giz et al. [34] revealed a synergistic effect when alginate films were crosslinked with  $\text{CaCl}_2$  and plasticized with glycerol, as they observed an increase in tensile strength and a decrease in elongation at break as the result of this “double” modification route.

Another approach to achieve suitable physical and mechanical properties of biodegradable films is to fabricate blends by mixing two or three polymers. The results of infrared spectroscopy, scanning electron microscopy and X-ray diffraction have confirmed the compatibility between starch, chitosan and alginate, due to the presence of strong interactions such as hydrogen bonds, as well as ionic interactions [37–39]. Moreover, such films are generally homogeneous, thin, smooth, with good coherence and no visual defects [40,41].

Numerous comparisons of the same non-modified and modified biodegradable polymers can be found in the literature [32,42–46]. Unfortunately, there is still limited data showing how polymers of different chemical structures belonging to the same group differ in their properties. Therefore, we have decided to perform a comparative study using three non-modified and modified polysaccharides, namely starch, chitosan and alginate. In the present study, starch was modified by the addition of oxidized sucrose (crosslinking agent) and glycerol (plasticizer), chitosan was modified by the addition of glycerol (plasticizer), and alginate was modified by the addition of  $\text{CaCl}_2$  (crosslinking agent) and glycerol (plasticizer). Additionally, we have fabricated polymer blends by mixing two polysaccharides to form starch/chitosan and starch/alginate, respectively. All materials were modified with a chestnut extract, which is known from its antimicrobial activity [47]. Preformed films were characterized to assess their applicability as food packaging materials, and the following properties were determined: hydrophilic properties (moisture content, swelling degree, total soluble matter, water contact angle), barrier properties (oxygen and carbon dioxide permeability), and mechanical properties (tensile strength, elongation at break). Furthermore, antimicrobial properties of developed films, which are of great interest for storing food, were also investigated. The performance of polysaccharide-based films was compared with the performance of a commercially available poly(lactic acid) (PLA) film.

## 2. Materials and Methods

### 2.1. Materials

Starch was purchased from Heuschen & Schrouff OFT B.V. Chitosan 30–100 cps (MW = 250,000, DD  $\geq$  90%) was purchased from Sigma-Aldrich (St. Louis, MI, USA). Sodium alginate (Brookfield viscosity 350–550 mPas, c = 1 wt.% at 20 °C) was supplied by Acros Organics (Branchburg, NJ, USA). Acetic acid was purchased from POCH S. A. (Gliwice, Poland) (99.5–99.9%) and chestnut extract Farmatan ( $\geq$ 76% tannins) was provided by Tanin Sevnica (Sevnica, Slovenia). Calcium chloride (purity  $\geq$  96%) was purchased from Avantor Performance Materials (Radnor, PA, USA). Glycerol was produced by Nortchem (Los Angeles, CA, USA). Oxidized sucrose was prepared using sucrose from Pfeifer & Langen Polska (Poznań, Poland), sodium periodate (>98%) from Acros Organics and barium chloride purchased from STANLAB Sp. J. Lublin (Lublin, Poland).

### 2.2. Film Preparation

#### 2.2.1. Modified Starch-Based Films

##### Preparation of Oxidized Sucrose

Oxidized sucrose was prepared according to a slightly modified protocol described in Wang et al. [48]. In short, 6.50 g sucrose and 12.90 g sodium periodate were dissolved in 200 mL distilled water and stirred at room temperature (24 °C) on a magnetic stirrer (IKA, Staufen, Germany) at 1000 rpm for 24 h. Approximately 7 g of barium chloride was then added to the solution and stirred at 5 °C for 1 h to allow complete precipitation. The solution was filtered, and the filtrate was stored in a fridge (5 °C) for further use.

##### Preparation of Modified Starch-Based Films

Starch solution (5%, *w/w*) was prepared by dispersing starch with chestnut extract (0.75% *w/v*) and glycerol (40%, *w/w* based on the mass of starch) in water. Oxidized sucrose (15 % *w/w* based on the mass of starch) was added, and the mixture was stirred at 90 °C for 30 min. The solution was poured onto Teflon-coated plates. The cast films were dried overnight at room temperature (24 °C) and later peeled from the plates. The starch films were then incubated/dried in an air oven at 160 °C for 4 min.

#### 2.2.2. Modified Chitosan-Based Films

Chitosan solution (2%, *w/w*) was prepared by dispersing chitosan in acetic acid solution (1%, *v/v*) with chestnut extract (0.75% *w/v*) and glycerol (30%, *w/w* based on the mass of chitosan). The mixture was agitated overnight on a magnetic stirrer (IKA, Staufen, Germany) at 1000 rpm and room temperature (24 °C). Afterwards, the mixture was homogenized at 6000 rpm for 5 min with an homogenizator (Ultra-Turrax T50, IKA, Staufen, Germany) and left overnight. The mixture was cast on Petri dishes and left overnight at room temperature (24 °C) to dry.

#### 2.2.3. Modified Alginate-Based Films

Alginate solution (1%, *w/w*) was prepared by dispersing sodium alginate with chestnut extract (0.75% *w/v*) and glycerol (30%, *w/w* based on the mass of alginate) in water and stirring overnight on a magnetic stirrer (IKA, Staufen, Germany) at 1000 rpm and room temperature (24 °C). Afterwards, the mixture was homogenized at 6000 rpm for 5 min with an homogenizator (Ultra-Turrax T50, IKA, Staufen, Germany) and left overnight. The mixture was cast on Petri dishes and left overnight at room temperature (24 °C) to dry. The cast films were peeled from the plates and soaked in 40 mL 2.5% CaCl<sub>2</sub> solution for 2 h. Thereafter, the films were washed with distilled water and dried at room temperature.

#### 2.2.4. Modified Starch and Chitosan-Based Films

Starch and chitosan solution was prepared by dispersing starch (2%, *w/w*) and chitosan (2%, *w/w*) with chestnut extract (0.75% *w/v*) and glycerol (30%, *w/w* based on the mass of starch and chitosan) in acetic acid solution (1%, *v/v*), and stirring overnight on a magnetic

stirrer (IKA, Staufen, Germany) at 1000 rpm and at 100 °C. Afterwards, the mixture was homogenized for 5 min at 6000 rpm with an homogenizer (Ultra-Turrax T50, IKA, Staufen, Germany) and left overnight. Thereafter, oxidized sucrose (15% *w/w* based on the mass of starch) was added and stirred at 90 °C for 30 min. The solution was poured onto Petri dishes and the cast films were dried overnight at room temperature (24 °C) and later peeled from the plates. The films were then treated in an air oven at 160 °C for 4 min.

### 2.2.5. Modified Starch and Alginate-Based Films

Starch and alginate solution was prepared by dispersing starch (5%, *w/w*) and alginate (1%, *w/w*) with chestnut extract (0.75% *w/v*) and glycerol (30%, *w/w* based on the mass of starch and alginate) in distilled water and stirring overnight on a magnetic stirrer at 1000 rpm and at 100 °C. Afterwards, the mixture was homogenized at 6000 rpm for 5 min with an homogenizer (Ultra-Turrax T50, IKA, Staufen, Germany) and left overnight. Then, oxidized sucrose (10% *w/w* based on the mass of starch) was added and stirred at 90 °C for 30 min. The solution was poured onto Petri dishes and the cast films were dried overnight at room temperature (24 °C) and later peeled from the plates. The films were then treated in an air oven at 160 °C for 4 min. The abbreviations of all obtained films are shown in Table 1.

**Table 1.** Abbreviations of samples investigated in this study.

Abbreviations	ST	CH	ALG	STCH	STALG
Sample	Modified starch-based film	Modified chitosan-based film	Modified alginate-based film	Modified starch and chitosan-based film	Modified starch and alginate-based film

### 2.3. Measurement of Film Thickness

The film thickness was measured with a digimatic micrometer (Mitutoyo Absolute, Tester Sangyo Co., Ltd., Tokyo, Japan). Twenty values were randomly taken at different locations for each film, and the average value was determined as the final result.

### 2.4. Measurement of Moisture Content, Swelling Degree and Total Soluble Matter

Moisture content (*MC*), swelling degree (*SD*) and total soluble matter (*TSM*) were determined using a gravimetric three-step method. Square samples with an area of 1 cm<sup>2</sup> were cut from the films and weighed on an analytical balance (*M*<sub>1</sub>). Then, the samples were dried at 100 °C for 24 h and weighed again (*M*<sub>2</sub>). Thereafter, the analyzed film pieces were placed in 30 mL of distilled water, left at room temperature (24 °C) for 24 h and weighed again (*M*<sub>3</sub>). In the last step, the samples were dried at 100 °C for 24 h and weighed (*M*<sub>4</sub>). The measurements were repeated five times and the average value was determined. *MC*, *SD* and *TSM* were calculated as follows:

$$MC(\%) = \frac{(M_1 - M_2)}{M_1} \times 100 \quad (1)$$

$$SD(\%) = \frac{(M_3 - M_2)}{M_2} \times 100 \quad (2)$$

$$TSM(\%) = \frac{(M_2 - M_4)}{M_2} \times 100 \quad (3)$$

### 2.5. Measurement of Contact Angle

The contact angle between water and the films was measured using an optical contact angle meter and a contour analysis systems (OCA15 from DataPhysic, Filderstadt, Germany) at room temperature (24 °C). Deionized water (1 µL) was carefully dropped onto the films and contact angles were determined from the average of ten measurements.



### 2.6. Measurement of Oxygen and Carbon Dioxide Permeability

Oxygen and carbon dioxide permeability was determined using an isobaric apparatus (Supplementary Information, Figure S1). The samples in a form of a disk with an area of about 6 cm<sup>2</sup> were sealed in a diffusion chamber. In the chamber, compressed oxygen (class 5.0) or carbon dioxide (technical gas) were supplied at a controlled flow rate to keep the pressure constant in that compartment. The flow of the chambers was connected to a manometer to ensure the equality of pressures (from 0.05 to 1.0 MPa).

Before the measurement, the samples were degassed for 24 h and then placed in the apparatus to condition for 2 h with the appropriate gas. The permeation coefficient was determined as follows:

$$P = \frac{V \times l}{S \times \Delta p} \quad (4)$$

where  $V$  is the volumetric flow (mol·s<sup>-1</sup>),  $l$  is the sample thickness (m),  $S$  is the sample activate area (m<sup>2</sup>) and  $\Delta p$  is the pressure difference on both sides of the film (Pa).

### 2.7. Measurement of Mechanical Properties

Mechanical properties, including tensile strength and elongation at break, were performed by means of an Instron 4466 machine at a speed of 5 mm/min at room temperature. Films were cut into strips (80 mm × 20 mm) for measurement. Final values of tensile strength and elongation at break were determined from the average of ten measurements.

### 2.8. Measurement of Antimicrobial Properties

Before using the chestnut extract for the fabrication of polysaccharide-based foils, its antimicrobial properties were assessed against model Gram-positive bacteria (*Staphylococcus epidermidis* ATCC12228), Gram-negative bacteria (*Escherichia coli* ATCC25922) and yeasts (*Candida albicans* ATCC18804) using an inhibition zone assay [49] (Supplementary Information, Figure S2). This experiment confirmed superior antimicrobial properties of chestnut extract, particularly when compared with other investigated plant extracts, including those derived from nettle, grape, and graviola.

Antimicrobial activity of polysaccharide films was determined against standard bacterial isolates, i.e., Gram-negative bacteria *Escherichia coli* ATCC25922 (*E. coli*) and Gram-positive bacteria *Staphylococcus epidermidis* ATCC12228 (*S. epidermidis*), as well as yeast (*Candida albicans* ATCC18804), by a serial dilution following co-culture with each film. Briefly, a single bacterial colony was cultured in 10 mL of Mueller-Hinton broth (MHB) at 37 °C overnight. Thereafter, bacteria from a 1 mL of cultures were collected by centrifugation (7000 × *g*, 3 min, 4 °C), and resuspended in a sterile saline solution. The optical density was normalized to 0.5 McFarland standard (approximately 1.5 × 10<sup>8</sup> CFU/mL) using a densitometer. Finally, 100 µL of the normalized cultures were inoculated into sterile bottles containing 4 mL M9 minimal supplemented glucose and the given film to be analyzed. The resulting mixture was then incubated overnight at 37 °C in a shaking incubator, followed by a serial dilution plating on MHB for CFU/mL determination. Experiments were repeated four times and the results presented as the log<sub>10</sub> of the average CFU/mL.

### 2.9. Scanning Electron Microscopy

Surface morphology of the films was studied using a Phenom ProX scanning electron microscope at a 10 kV accelerating voltage.

### 2.10. Fourier-Transform Infrared Spectroscopy

The infrared (FTIR) spectra of the films were recorded in the 4000–650 cm<sup>-1</sup> range with a resolution of 2 cm<sup>-1</sup> using a Spectrum Two spectrometer (Perkin Elmer). For measurements, films were cut into small discs and placed tightly between the sensor and support to ensure good contact. For each spectrum, 25 scans were taken. These analyses were performed in duplicate at room temperature.

### 3. Results and Discussion

The images of ST, CH, ALG, STCH, STALG films are shown in Figure 1. As it can be noticed, all obtained films are homogeneous and they have a slightly brownish color due to the addition of a chestnut extract. The thickness of prepared films ranges between 40  $\mu\text{m}$  for alginate films to 110  $\mu\text{m}$  for films based on alginate and starch. The commercially available PLA-based film had a thickness of 7  $\mu\text{m}$ .

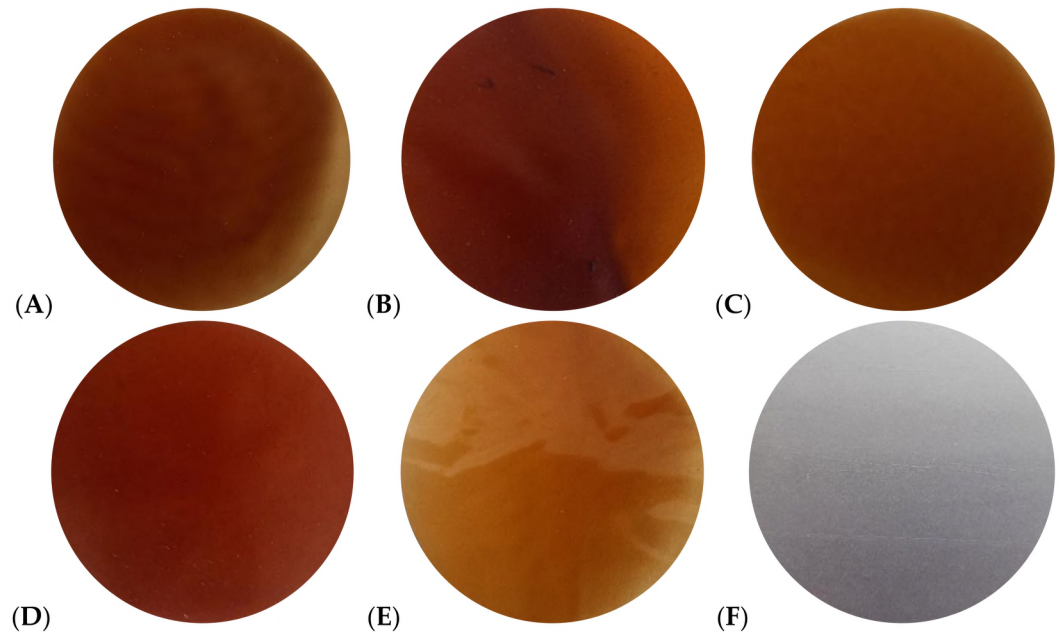


**Figure 1.** Physical appearance of the modified: (A) starch-based (ST) film; (B) chitosan-based (CH) film; (C) alginate-based (ALG) film; (D) starch and chitosan-based (STCH) film; (E) starch and alginate-based (STALG) film; (F) commercially available PLA-based film.

#### 3.1. Moisture Content, Swelling Degree and Total Soluble Matter

The MC, SD and TSM values of the obtained films are shown in Figure 2. These material properties are related to the film's sensitivity to water and moisture, which is one of the major areas of interest in the design of food packaging materials. MC indicates the total volume of empty space occupied by water molecules in the network microstructure of the film [50]. As shown in Figure 2A, the MC values are the lowest for the commercially available PLA-based sample (about 5%) and the highest for the starch-based sample (about 22%). The chitosan and alginate-based samples also showed higher moisture content than PLA (about 17% and 16%, respectively). It is worth noting that the samples based on two polysaccharides, i.e., STCH and STALG, showed much lower MC values than these polymers separately (about 10% for both samples). Similar MC values were observed for other films based on starch [51], chitosan [52,53], alginate [54,55] and their blends [56,57]. In the case of SD (Figure 2B), which is an undesirable property of a film, especially if it is intended for packaging applications [58], it can be noticed that the highest value of this parameter is obtained for STALG and STCH (about 1400% and 700%, respectively). Additionally, in this case, the different behavior of the two-component samples compared to the single-polymer based samples can be observed. Samples based on a single polysaccharide had a much lower SD value than their combinations. The lowest SD value was observed for PLA (i.e., about 5%), and the nearest values were observed for ST and CH (about 60% and 40%, respectively).

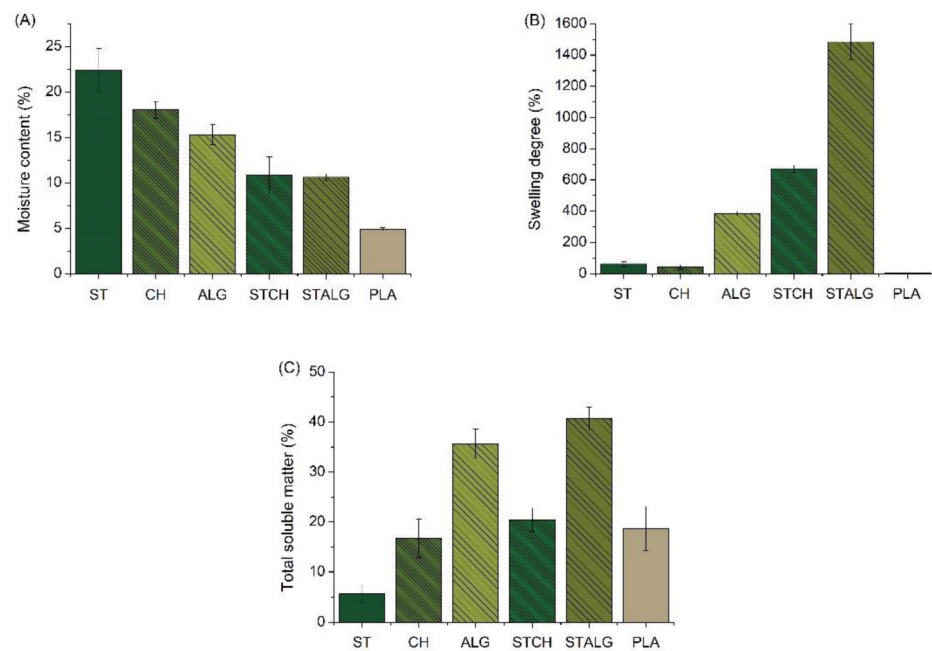


**Figure 2.** Moisture content (A), swelling degree (B) and total soluble matter (C) of the starch-based (ST), chitosan-based (CH), alginate-based (ALG), starch and chitosan-based (STCH) and starch and alginate-based (STALG) films and the commercially available PLA-based film ( $p < 0.05$ ).

Balakrishnan et al. [59] also prepared films using starch as a matrix and oxidized sucrose as a crosslinking agent. After crosslinking, a reduction in film swelling was observed, indicating that the acetal bond had a strong influence on the swelling behavior of the films, acting as a barrier that prevents water molecules from passing through, causing the films to swell [19,48,59]. In this case, swelling was reduced by up to half for films prepared with oxidized sucrose. On the other hand, Rodríguez et al. [60] studied the SD of chitosan films modified with different content of glycerol and observed that the amount of glycerol significantly affected the swelling behavior of the film. Li et al. [61] studied the influence of the crosslinking agent content (calcium chloride) on the swelling behavior of alginate-based films. They noticed that the SD values of the films decreased significantly when the concentration of  $\text{CaCl}_2$  was increased to 6% *w/v*. The results indicated that the total degree of cross-linking of the films increased with  $\text{CaCl}_2$  concentration.

TSM is another important factor in selecting films for specific applications. Solubility is a desirable property in many cases, such as for food encapsulation. However, for foods with high moisture content, water resistance and integrity are required, and high solubility of the film is disadvantageous. In our case, low solubility in water is desirable, and considering the TSM values (Figure 2C), it can be noticed that this parameter is similar for CH, STCH and PLA samples (about 18%). However, the lowest value was observed for ST film (about 5%) and the highest value for ALG and STALG (about 35 and 40%, respectively). These values show that each modification had the desired effect, as previous studies indicate that the films based on the pure polysaccharides used in this study are almost completely soluble [62]. ST and CH samples show the lowest SD and TSM values among all obtained samples, indicating their best properties for use as food films. Compared to the commercially available PLA sample, the TSM properties of the ST film are even better (Figure 2C), indicating that the films obtained in the present study fully meet the hydrophobicity requirements of commercially available films.

### 3.2. Contact Angle

The water contact angle values of the obtained films are shown in Figure 3 to understand the effect of the modifiers on the wettability of the films. This parameter is a good indicator of the hydrophilicity, because as the wettability of the surface increases,



the contact angle decreases [53]. It is well known that the water contact angle ( $\theta$ ) value of  $\theta < 90^\circ$  indicates the hydrophilic nature of the test sample, while  $\theta > 90^\circ$  represents its hydrophobic nature [63,64]. The values for all investigated films were less than  $90^\circ$ , indicating hydrophilicity of the surfaces. The most hydrophilic film was found to be STCH and ST, with a contact angle of about  $40^\circ$  and  $55^\circ$ , respectively. Bastos et al. [65] observed that the unmodified starch film had a contact angle of  $55^\circ$ , which decreased rapidly with time if the droplet remained on the surface due to water absorption. The addition of glycerol increased the hydrophilic behavior of the film [66,67], but in our case the additional modification with oxidized sucrose caused the contact angle value to remain the same as the unmodified film. On the other hand, Balakrishnan et al. [59], who examined the contact angle of films based on pure starch and modified with oxidized sucrose, showed that the reduction in hydroxyl groups in the crosslinked sample due to the reaction between starch and oxidized sucrose resulted in a reduction in hydrophilic properties. The pure starch film without modifier showed the lowest contact angle (about  $33^\circ$ ), which was due to the presence of a large number of hydroxyl groups in starch. For films prepared with oxidized sucrose, the contact angle increased to about  $92^\circ$ . The authors hypothesized that [59] that during film drying the aldehyde groups in the oxidized sucrose sample reacted with the hydroxyl groups of starch and formed water stable acetal bonds. Other samples, including PLA, shows a contact angle of approximately  $70^\circ$ . Although this value still indicates the hydrophilic nature of the film, the use of PLA films in the packaging market indicates that this level of hydrophilicity is sufficient for food packaging. Therefore, it can be concluded that the CH, ALG and STALG films obtained in this study should be the best alternative to commercially available films, including those based on PLA. Previous studies [53,68,69] demonstrated that the contact angle for pure chitosan film was approximately  $105^\circ$ . As estimated in our research, the contact angle values for chitosan equals to  $71^\circ$  due to the modification with hydrophilic glycerol. Taverna et al. [70] determined the contact angle for films based on pure alginate, which was about  $25^\circ$ . Its value increased after treatment of the film with  $\text{CaCl}_2$ , which is related to the lower water absorption capacity of the crosslinked films. Such a relationship can also be observed in our study, in which the contact angle for ALG and STALG was about  $70^\circ$ .

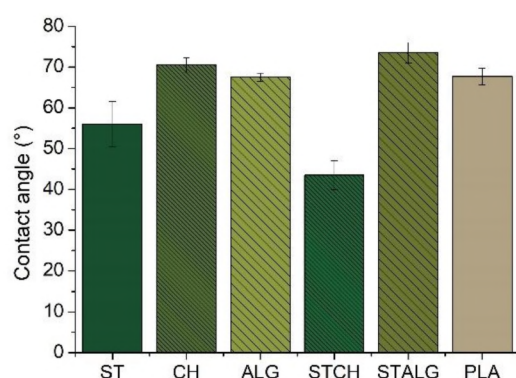


**Figure 3.** Contact angle of the starch-based (ST), chitosan-based (CH), alginate-based (ALG), starch and chitosan-based (STCH) and starch and alginate-based (STALG) films and the commercially available PLA-based film ( $p < 0.05$ ).

### 3.3. Oxygen and Carbon Dioxide Permeability

Oxygen and carbon dioxide permeability values are shown in Figure 4. Oxygen and carbon dioxide are the most common gases studied in food packaging applications. The permeation of oxygen from the air into the package should be avoided due to deterioration of product properties caused by oxidation during long-term storage. On the other hand, carbon dioxide can potentially reduce the food degradation, leading to a significant increase in shelf life [71,72]. Maintaining a certain level of carbon dioxide concentration along with the desired oxygen concentration that have been introduced during food packaging is

helpful in preserving different types of food. Therefore, high barrier properties of the film are very important for food packaging films [73]. The highest oxygen and carbon dioxide permeabilities were observed for PLA, indicating its low barrier properties compared to the films obtained in the present study. All other films provided good barrier properties to O<sub>2</sub> and CO<sub>2</sub>. ST films showed almost no detectable O<sub>2</sub> permeability, while CH and ALG films showed permeability values of about 2 and 3 × 10<sup>−10</sup> cm<sup>3</sup> /m·s·Pa, respectively. The CO<sub>2</sub> permeability was much lower than that of O<sub>2</sub>, i.e., about 1 × 10<sup>−11</sup> cm<sup>3</sup> /m·s·Pa and 2.5 × 10<sup>−12</sup> cm<sup>3</sup> /m·s·Pa, respectively. This effect was also observed for other similar polymers previously [72,74].

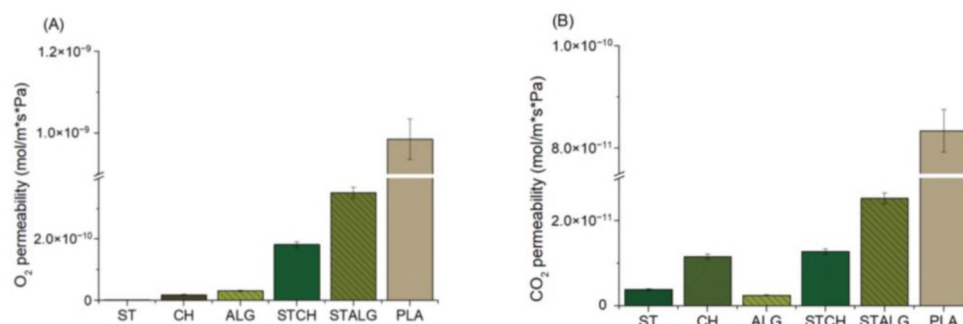


**Figure 4.** Oxygen (A) and carbon dioxide (B) permeability of the starch-based (ST), chitosan-based (CH), alginate-based (ALG), starch and chitosan-based (STCH) and starch and alginate-based (STALG) films and the commercially available PLA-based film ( $p < 0.05$ ).

O<sub>2</sub> permeation is generally lower when compared to CO<sub>2</sub> permeation, due to the decrease in diffusivity and increase in solubility with decreasing permeant size (O<sub>2</sub> molecular diameter is 3.1 Å and CO<sub>2</sub> molecular diameter is 3.4 Å, respectively) [75]. García et al. [76] used plasticizers (glycerol and sorbitol) to improve the barrier properties of starch-based films. They observed that O<sub>2</sub> permeability was significantly lower (10<sup>−10</sup> cm<sup>3</sup> /m·s·Pa) than for CO<sub>2</sub> (10<sup>−9</sup> cm<sup>3</sup> /m·s·Pa), indicating a selective effect of these films on gas permeability, which the authors attributed to the higher solubility of CO<sub>2</sub> in the starch films. It was also observed that the CO<sub>2</sub> and O<sub>2</sub> permeabilities for the unplasticized films were significantly higher than those for the plasticized films, which was attributed to the presence of pores and cracks on the surface of the unplasticized films. On the other hand, Butnaru et al. [77] investigated the effect of plasticizer for O<sub>2</sub> and CO<sub>2</sub> permeability of chitosan films. The O<sub>2</sub> permeability values for the reference chitosan film were 67 mL/m<sup>2</sup>, and after the addition of plasticizer, the O<sub>2</sub> permeability was higher at 212 and 134 mL/m<sup>2</sup>, respectively. The increased O<sub>2</sub> values can be attributed to the plasticization effect of the biopolymer by the plasticizer molecules [78]. The plasticization effect results in increased mobility of oxygen molecules due to disruption of hydrogen bonds, creating additional sites for oxygen solvation [79]. In turn, the presence of the plasticizer led to improved barrier properties for CO<sub>2</sub>, achieving half the CO<sub>2</sub> values compared to pure chitosan [77]. It is worth noting that the films based on two polymers showed a different characteristics than the films based on a single polymer. In the case of oxygen permeability for films based on two polysaccharides (Figure 4A), the barrier properties of STCH and STALG films decreased significantly, by as much as about 70% and 90%, respectively, compared to ST, CH and ALG films. On the other hand, the lowest permeability values for carbon dioxide (Figure 4B) were recorded for ST and ALG, but the combination of these two polymers (STALG) resulted in a significant increase in permeability. In contrast, the high barrier properties of starch in the ST sample did not contribute to the reduced permeability of carbon dioxide when combined with chitosan. STCH sample showed barrier properties at the same level as CH. These results could mean a lower degree of interaction between starch and chitosan than in the case of starch and alginate, causing easier migration of oxygen and carbon dioxide molecules through the film. Nevertheless, the results obtained for all the investigated films in the



present study outperformed the commercial food packaging films used today, such as PLA films or even low-density polyethylene (LDPE) [53,80].

### 3.4. Mechanical Properties

Mechanical properties of investigated films are summarized in Figure 5. They are important in evaluating the quality of food packaging films, since they are used to assess the ability of packaging materials to maintain integrity under various stresses that occur during processing and storage of packaged foods [77]. It can be seen that the tensile strength values (Figure 5A) are the highest for the commercially available PLA-based film (about 30 MPa). This value is about 70% higher when compared with CH and STCH and as much as 95% higher when compared with ST, ALG and STALG. The lowest tensile strength values were noted for ST and ALG (about 2 MPa) and the highest for CH (about 8 MPa). The combination of the weakest samples, i.e., ST and ALG, did not improve their properties, since the tensile strength of STALG remained around 5 MPa. On the other hand, the combination of ST and CH slightly improved the tensile strength to 12 MPa (as noted for STCH). This shows that in some cases the addition of a polymer with a weaker tensile strength can increase the mechanical properties of the final material. The same relationship was observed by Tan et al. [81], who investigated the effects of starch concentration, chitosan and glycerol content on mechanical properties of their composites. An optimum tensile strength of 5.19 MPa was obtained with the combination of these two polysaccharides, in which the concentrations were: starch 5 wt.%; chitosan 20 wt.%; glycerol 40 wt.%. Elongation at break results (Figure 5B) also show that the highest values were noted for the commercial PLA sample (about 460%). In this case, the value is also significantly higher than for the samples obtained in this study (by about 80% when compared to ST, CH, STALG and by as much as about 95% for ALG and STCH). Djalila et al. [37] studied the physicomechanical properties of films based on starch, alginate and their mixture, and noted a clear increase in the elongation at break from about 5% to 19% of the films when the alginate content increased from 0% to 50%. On the other hand, Xu et al. [82] investigated and compared the mechanical properties of chitosan and starch-based films at different ratios and at a concentration gradient of 0.5. The results showed that the tensile strength and elongation at break of the films first increased and then decreased with increasing starch content. The maximum elongation at break of the film with a starch to chitosan weight ratio of 1.5:1 reached 60%. Balakrishnan et al. [59] studied the effect of crosslinking starch with oxidized sucrose on the mechanical properties of investigated films and found a significant improvement after adding the modifier to pure starch. A maximum threefold increase in tensile strength was obtained with a slight deterioration in elongation at break.

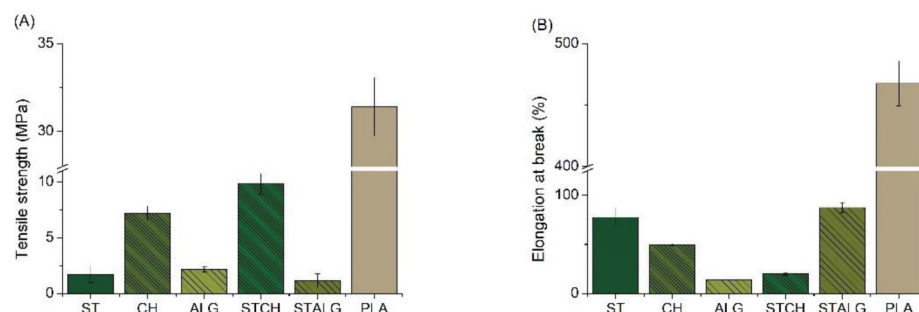


**Figure 5.** Tensile strength (A) and elongation at break (B) of the starch-based (ST), chitosan-based (CH), alginate-based (ALG), starch and chitosan-based (STCH) and starch and alginate-based (STALG) films and the commercially available PLA-based film ( $p < 0.05$ ).

The increase in strength properties is mainly due to the good compatibility of starch with oxidized sucrose, which results from chemical and physical interactions between starch and the crosslinking agent. On the other hand, crosslinked films have a slightly



lower elongation percentage due to the limited mobility of the starch macromolecular chain. Rhim [83] studied alginate films prepared with and without  $\text{CaCl}_2$  treatment and demonstrated an increase in the tensile strength of and a concurrent decrease in elongation at break when  $\text{CaCl}_2$  was applied to the alginate films. The same observation was also found in our study, in which the elongation at break also decreases with an increase in tensile strength. Another property was observed by Ibrahim et al. [33], who also studied alginate films modified with  $\text{CaCl}_2$ . In this case, the alginate films showed an increase in tensile strength with an increase in elongation at break after modification. The mechanical properties of the alginate films increased up to 4 times after immersion in  $\text{CaCl}_2$ . The improvement in the mechanical properties of the films may be due to the crosslinking reaction between  $\text{Ca}^{2+}$  ions and the carboxyl group of alginate. The crosslinking can be formed by simple ionic bridging of two carboxyl groups on adjacent polymer chains with calcium ions [84]. Even though polysaccharide-based films have not been found to outperform commercial PLA films from the point of view of their mechanical properties, acquired results did not stand out of other literature proceedings describing this class of materials. The best tensile strength results were obtained for CH and STCH (i.e., about 8 MPa and 10 MPa, respectively), and the best elongation at break properties were obtained for ST and STALG (i.e., about 78% and 88%, respectively). Obviously, further research is needed to improve their properties, but the results obtained so far can be considered as satisfying.

### 3.5. Antimicrobial Properties

The results of antimicrobial assays demonstrated that different films obtained in this study caused a significant reduction in the growth of both model Gram-positive and Gram-negative bacteria, such as *S. epidermidis* (Figure 6A), and *E. coli* (Figure 6B). In particular, a 4–5 log reduction in the growth of *S. epidermidis* was observed while for *E. coli* there was a 5 log reduction for CH and over a 7–8 log reduction when co-cultured with starch-based, alginate-based, and both polymer blend films. Moreover, the study showed that starch-based films were more resistant to *E. coli* bacterial pathogens than chitosan-based films.

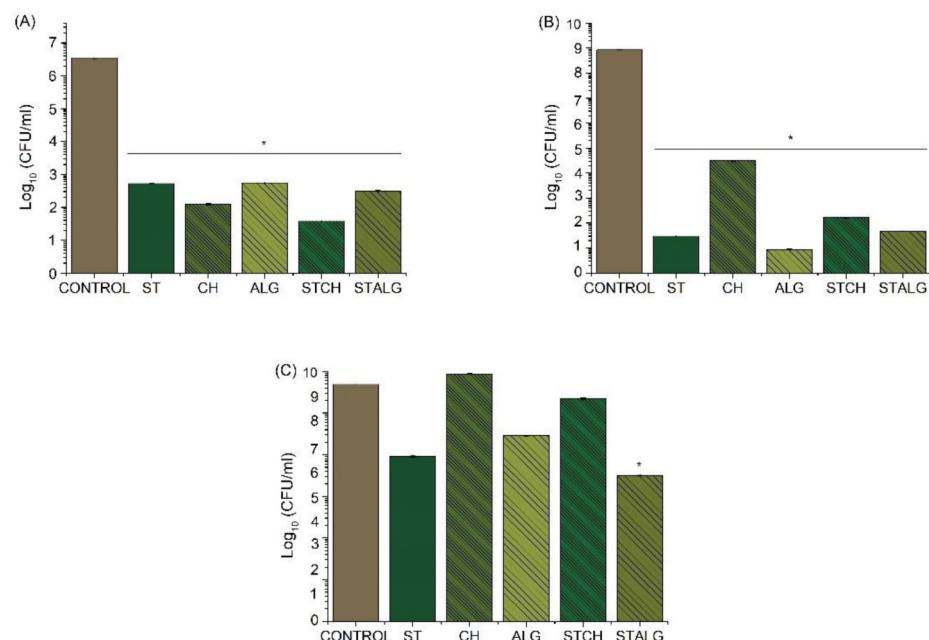


**Figure 6.** The effect of modified polysaccharide films on the viability of *S. epidermidis* cells (A), *E. coli* cells (B) and *C. albicans* (C); unpaired *t*-Test: \*  $p < 0.05$ .

It is important to indicate that the primary source of antibacterial activity of investigated films was the presence of a chestnut extract, which is a rich source of polyphenolic compounds, phenolic acids, and tannins [85,86]. Since the amount of chestnut extract was

the same in all investigated films, the difference in antibacterial effects should be associated with a biopolymer matrix and the presence of modifiers. For instance, Priya et al. [87] studied the antimicrobial activity of PVA starch cross-linked samples and found that both the crosslinking agent and plasticizer induced antimicrobial properties. In our study, starch was crosslinked with oxidized sucrose, which led to acetal formation able to release cationic ions interacting with the anionic charges of microbial cell membranes through electrostatic bonding. This specific interaction led to increased cell peripherality and leakage of intercellular components, which ultimately induced cell death [88]. It is also expected that the low film permeability could reduce the attraction of bacterial species [89].

On the other hand, the antibacterial properties of chitosan could be easily justified by its ability to bind to the negatively charged bacterial cell wall and cause disruption of the cell, followed by its interactions with DNA leading to cell death [90]. It is also known that the presence of chitosan can affect an efflux of particular ions ( $K^+$ ,  $Ca^{2+}$ ,  $H^+$ ,  $Cl^-$ ) and increase transmembrane potential difference in the cells, altering the ionic balance required for microorganisms to maintain their vitality [91]. Still, the antibacterial properties of chitosan are dependent on its molecular weight, degree of deacetylation, concentration, pH, chitosan source, temperature, as well as a type of microorganisms and a cell growth phase [92]. Superior antibacterial properties of ALG foils when compared with other investigated materials could be associated with the presence of  $CaCl_2$ . Recent studies [93,94] show that  $CaCl_2$  exhibits an inhibitory effect on microbial growth, as demonstrated in the example of *Ralstonia pseudosolanacearum*. The antibacterial activity mechanism of  $CaCl_2$  is based on its ability to arrest the swarming motility of bacteria, disrupt their physiological functions and, finally, inhibit the formation of a mature biofilm.

Although a chestnut extract was found to exhibit antifungal properties, not all investigated polysaccharide-based foils were observed to follow this behavior (Figure 6C). An antifungal effect was noted for STALG, ST and ALG, but no effect of antifungal activity was observed in any of chitosan-based foils, even though chitosan itself is known to exhibit antifungal properties [91]. We expect this behavior to be associated with a limited solubility of chitosan at neutral pH, which restricts its intrinsic antifungal activity and limits the release of a chestnut extract.

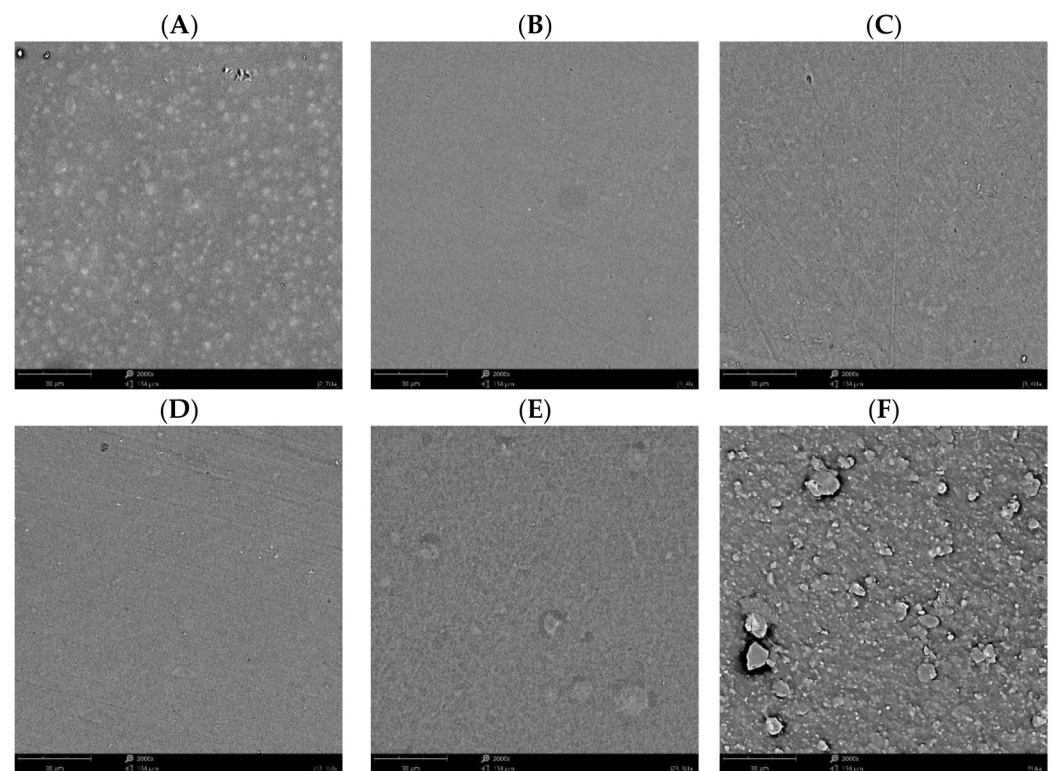
The results of microbiological investigations confirmed that fabricated polysaccharide-based films can be regarded as having antibacterial activity towards *E. coli* and *S. epidermidis*. It should be highlighted that commercially used packaging materials, for instance, PLA, alone and unmodified did not show antimicrobial activity [95]. Therefore, modified polysaccharide-based films, as confirmed by previous studies (Table 2), perfectly match current trends in packaging industry to apply bioactive and biodegradable materials for the development of antibacterial and antioxidative packaging systems functionalized with natural bioactive agents.

### 3.6. Scanning Electron Microscopy

Figure 7 shows scanning electron microscopy (SEM) images of the obtained polysaccharide-based and commercially available PLA films. For all the obtained samples, a homogeneous structure is observed, indicating that the modified films have a smooth, flat surface in the case of the ST film, the presence of undissolved particles of chestnut extract in the polymer matrix is noted. Nevertheless, the blends of starch with other polymers, i.e., chitosan or alginate (sample STCH and STALG, respectively) show that the extract appears to be completely dissolved. For the commercially available PLA film, unspecified particles are noted which may indicate the use of fillers in the present film to modify the physicochemical properties of the material. As noted, when analyzing mechanical properties of samples, PLA film was found to have the highest mechanical properties, which is most likely due to the presence of a filler. Many studies [101–103] noted that fillers significantly improve the mechanical properties of samples, including materials based on polysaccharides. Nevertheless, the SEM images confirm the homogeneity of the chestnut extract dispersion in the polymer matrix and the compatibility of the polymers.

**Table 2.** Polysaccharide-based films containing different plant extracts exhibiting antimicrobial activity towards particular microorganisms.

Biopolymer	Antimicrobial Agent	Microorganisms	Ref.
Chitosan	Chestnut extract	<i>E. coli</i> , <i>B. subtilis</i>	[96]
Chitosan	Chestnut extract	<i>P. fluorescens</i> , <i>E. coli</i> , <i>P. commune</i>	[97]
Chitosan	Chestnut extract	<i>E. coli</i> , <i>S. epidermidis</i>	This study
Chestnut starch-chitosan	<i>Cornus officinalis</i> fruit extract, glycerol monolaurate, nisin, pine needle essential oil	<i>E. coli</i> , <i>S. aureus</i> , <i>L. monocytogenes</i>	[98]
Starch	Chestnut extract	<i>E. coli</i> , <i>S. epidermidis</i>	This study
Alginate	Nisin, $\epsilon$ -polylysine, olive extract, nettle extract, green tea extract	<i>E. coli</i> , <i>S. aureus</i>	[99]
Alginate	Algae extract, aminoglycosides	<i>E. coli</i>	[100]
Alginate	Chestnut extract, CaCl <sub>2</sub>	<i>E. coli</i> , <i>S. epidermidis</i> , <i>C. albicans</i>	This study

**Figure 7.** SEM images of: (A) starch-based (ST) film; (B) chitosan-based (CH) film; (C) alginate-based (ALG) film; (D) starch and chitosan-based (STCH) film; (E) starch and alginate-based (STALG) film; (F) commercially available PLA-based film.

### 3.7. Fourier-Transform Infrared Spectroscopy

FTIR spectra are useful for observing and understanding the molecular interactions that polymers engage in with various modifications. Figure 8 illustrates the FTIR spectra of unmodified and modified polysaccharide films and their blends, as well as a comparison of all obtained samples. The FTIR spectra of unmodified and modified starch films (Figure 8A) showed clear changes in the spectral regions primarily due to the use of oxidized sucrose



and glycerol, as a peak at  $3450\text{ cm}^{-1}$  is noted, which is attributed to the stretching vibration of the -OH groups, and at  $2960\text{ cm}^{-1}$ , which can be attributed to the stretching vibration of the -CH bond [18,104]. The absorption band between  $1000$  and  $1200\text{ cm}^{-1}$  was characteristic of -CO stretching of the polysaccharide skeleton [105].

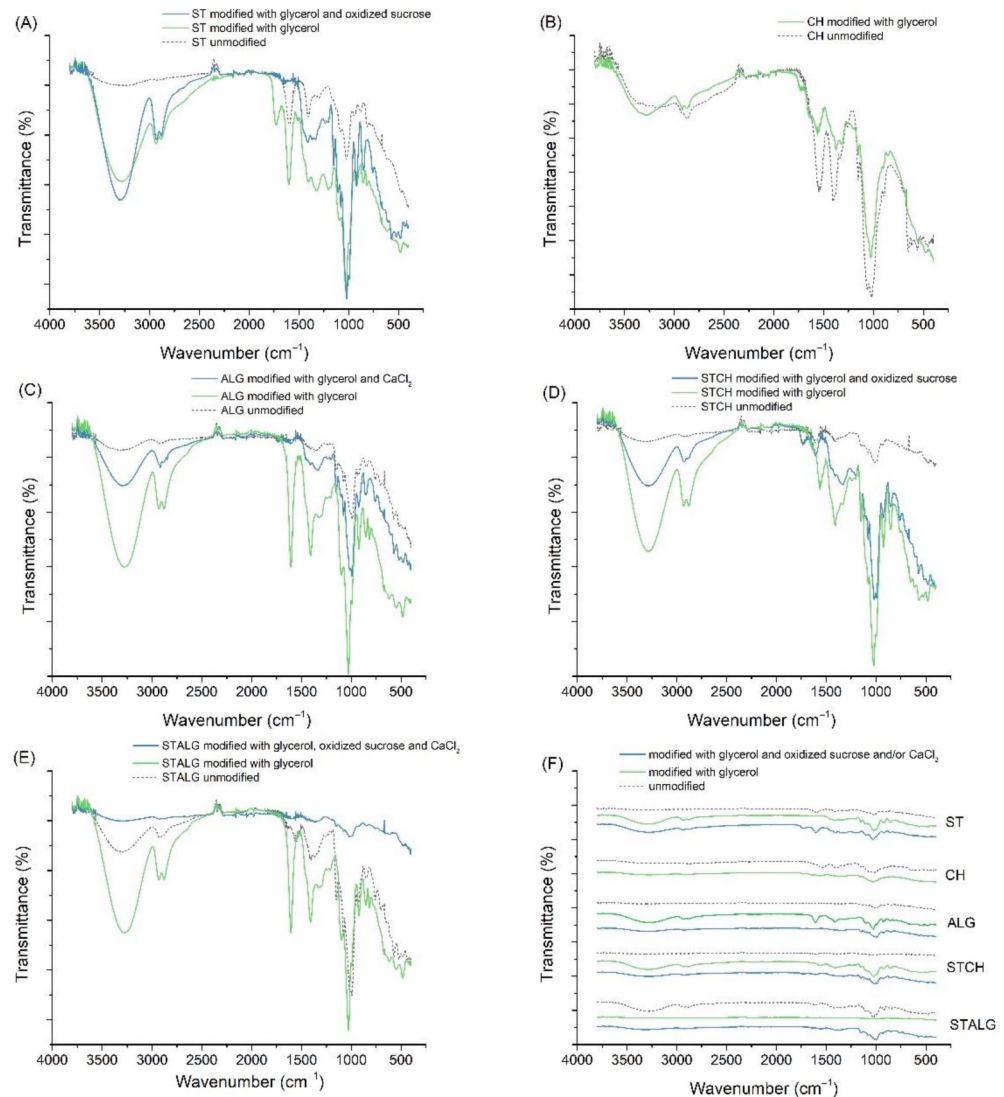


**Figure 8.** FTIR spectra of ST films (A), CH films (B), ALG films (C), STCH films (D), STALG films (E) and a summary of all spectra (F).

FTIR spectra of unmodified and modified chitosan films (Figure 8B) are almost comparable, indicating that glycerol did not change the structure of chitosan but only interacted with it. Chitosan exhibited two strong vibrational bands at  $1645$  and  $1584\text{ cm}^{-1}$ ; these bands are attributed to the vibrations of amide I and amide II, respectively [106]. It has been reported that the deformation vibrations of amines usually produce strong or very strong bands in the region of  $1638$ – $1575\text{ cm}^{-1}$  [107]. A broad band in the range of about  $3600$ – $3100\text{ cm}^{-1}$  is attributed to N-H and OH-O stretching vibrations. This band is also related to some extent to the intermolecular hydrogen bonds of the chitosan molecules [108].

The spectra of alginate films are shown in Figure 8C. As alginate is modified with glycerol, the O-H stretching peak ( $\sim 3380\text{ cm}^{-1}$ ) has a much higher intensity due to the O-H groups derived from glycerol. On the other hand, when additionally modified with calcium chloride, the O-H stretching peak becomes narrower and of greater intensity compared to the unmodified sample, but lower than when modified with glycerol by itself. This is characteristic of an increase in intramolecular bonding [109]. The O-H shoulder (at



3250  $\text{cm}^{-1}$ ), corresponding to the intermolecular binding, also becomes narrower and has higher intensity. The  $-\text{COO}^-$  peaks at  $\sim 1650$  and  $1420 \text{ cm}^{-1}$  (asymmetric and symmetric stretching, respectively) become broader and more intense after glycerol and their intensity strongly decreases after additional modification with calcium chloride. This is because this peak is characteristic of the ionic bonding. When calcium ions replace sodium ions in the alginate structure, the charge density, radius and atomic mass of the cation change, creating a new environment around the carbonyl group [109]. In the region  $1150\text{--}1000 \text{ cm}^{-1}$ , a set of intense peaks can be observed that can be attributed to C-C and C-O stretching vibrations [110].

The FTIR spectra obtained for STCH are shown in Figure 8D. It can be observed that the unmodified STCH film as well as the modified film show a broad absorption band centered at  $3380 \text{ cm}^{-1}$ , which can be attributed to N-H and O-H stretching vibrations [111]. The peak is definitely more intense when modified with glycerol alone. After modification with oxidized sucrose, the intensity decreases suggesting higher interactions with O-H groups for the STCH sample than for the ST sample (Figure 8A). The peak at  $2918 \text{ cm}^{-1}$  can be attributed to the asymmetric C-H stretching vibrations of methylene groups, and the peak at about  $2876 \text{ cm}^{-1}$  to the  $-\text{CH}_3$  group of acetylamino groups in chitosan [18,104]. Their amount decreased in the modified film with glycerol and oxidized sucrose compared to the modified only with glycerol sample, which may be due to the reaction of chitosan with sodium periodate, which leads to the elimination of acetamido groups by strong oxidant and strong acid [112]. The band at  $1645 \text{ cm}^{-1}$  can be attributed to the C-O stretching vibration of the residual amide bond [113]. On the other hand, the band at  $1597 \text{ cm}^{-1}$  can be attributed to N-H bending vibrations of chitosan, which disappeared in the modified sample with oxidized sucrose by reaction with aldehydes from oxidized sucrose products [112]. The band at  $1412 \text{ cm}^{-1}$  is a C-N stretching vibration in chitosan and the peak at  $1080 \text{ cm}^{-1}$  is attributed to C-O stretching vibration [113]. The bands in the  $1000$  and  $1100 \text{ cm}^{-1}$  region are attributed to the C-O bond of the C-O-H group in starch [114]. The intensity of these bands is significantly reduced for the unmodified sample, suggesting high interactions between the starch itself with chitosan.

The spectra of modified and unmodified starch- and alginate-based films are shown in Figure 8E. A strong absorption due to -OH stretching vibration ( $3400 \text{ cm}^{-1}$ ) was noted in the FTIR spectra. It is typical of polymeric association of hydroxyl groups [115]. As can be seen, the highest intensity was recorded for the sample modified with glycerol only, and the additional modification with calcium chloride caused the intensity to drop below that recorded for the unmodified sample. This explains the hydrophilicity results of these films, which were found to be lower than for the STCH sample. The peaks at values from about  $1600 \text{ cm}^{-1}$  to  $1400 \text{ cm}^{-1}$  can be attributed to asymmetric and symmetric stretching vibrations of  $-\text{COO}^-$  [116]. The spectra of the modified blend with glycerol, oxidized sucrose and calcium chloride exhibit lower intensities, which indicates intermolecular interaction through hydrogen bond formation between  $-\text{COO}^-$  groups in alginate and -OH groups in starch [115].

#### 4. Conclusions

In this study, modified films based on starch, chitosan, alginate and their compositions with a chestnut extract were prepared by a solution casting method. An extensive characterization of as-formed films revealed that polysaccharides are promising materials for food packaging industry. Particular materials were shown to match the requirements of commercially available films, for example low swelling degree (starch and chitosan), low total soluble material (starch), optimal hydrophilicity (chitosan alginate, and starch/alginate), and high barrier properties with respect to  $\text{O}_2$  and  $\text{CO}_2$  (all investigated films). An important benefit of polysaccharide-based films containing chestnut extract was their antibacterial nature verified against *E. coli*, *S. epidermidis*, and *C. albicans*. Even though the mechanical properties of investigated materials were satisfactory, they were still worse than the ones of a commercially available PLA film. However, SEM studies showed that the commercially

available PLA film contains particles indicating the use of a filler, which can significantly improve the mechanical properties. Therefore, further studies with the use of fillers are planned for starch, chitosan, alginate films and their blends.

Due to the fact that polysaccharides are becoming an increasingly popular alternative to traditional plastics in packaging production, the research presented herein may contribute to expanding the applicability of biopolymers through an easier selection of the polymer matrix. This is a comparative study and further research, especially in direction of improving mechanical properties, is needed for further application of polysaccharides in industry.

**Supplementary Materials:** The following supporting information can be downloaded at: <https://www.mdpi.com/article/10.3390/ma15093236/s1>, Figure S1: Schematic diagram of experimental apparatus for gas permeability testing; Figure S2: Antimicrobial activity of four commercially available extracts: chestnut (K), graviola (G), grape (W), nettle (P) tested against model Gram-positive bacteria (*S. epidermidis*), Gram-negative bacteria (*E. coli*) and yeasts (*C. albicans*); control well was filled with deionized water (ddH<sub>2</sub>O).

**Author Contributions:** Conceptualization, W.J. and G.D.; methodology, W.J., G.D., K.K., S.K. and D.Y.S.; software, W.J. and M.N.; validation, W.J., G.D., M.N., A.B. and D.Y.S.; formal analysis, G.D.; investigation, W.J.; resources, G.D.; data curation, M.N. and A.B.; writing—original draft preparation, W.J.; writing—review and editing, G.D. and K.K.; visualization, W.J.; supervision, G.D. and S.K.; project administration, G.D.; funding acquisition, G.D. All authors have read and agreed to the published version of the manuscript.

**Funding:** Publication supported by the Excellence Initiative—Research University program implemented at the Silesian University of Technology, year 2022 under the project no 04/040/SDU/10-21-04. W.J. would like to thank the Ministry of Education and Science of Poland for providing support under the project no DWD/4/21/2020.

**Institutional Review Board Statement:** Not applicable.

**Informed Consent Statement:** Not applicable.

**Data Availability Statement:** Not applicable.

**Conflicts of Interest:** The authors declare no conflict of interest.

## References

1. Thakur, R.; Pristijono, P.; Scarlett, C.J.; Bowyer, M.; Singh, S.P.; Vuong, Q.V. Starch-Based Films: Major Factors Affecting Their Properties. *Int. J. Biol. Macromol.* **2019**, *132*, 1079–1089. [[CrossRef](#)] [[PubMed](#)]
2. Azeredo, H.M.C.; Waldron, K.W. Crosslinking in Polysaccharide and Protein Films and Coatings for Food Contact—A Review. *Trends Food Sci. Technol.* **2016**, *52*, 109–122. [[CrossRef](#)]
3. Bhattacharya, A.; Ray, P. Basic Features and Techniques. In *Polymer Grafting and Crosslinking*; John Wiley & Sons: Hoboken, NJ, USA, 2008; pp. 7–64. ISBN 978-0-470-41481-1.
4. Yong, S.K.; Shrivastava, M.; Srivastava, P.; Kunhikrishnan, A.; Bolan, N. Environmental Applications of Chitosan and Its Derivatives. In *Reviews of Environmental Contamination and Toxicology*; Springer: Cham, Switzerland, 2015; Volume 233, pp. 1–43. [[CrossRef](#)]
5. Wang, B.; Yu, B.; Yuan, C.; Guo, L.; Liu, P.; Gao, W.; Li, D.; Cui, B.; Abd El-Aty, A.M. An Overview on Plasticized Biodegradable Corn Starch-Based Films: The Physicochemical Properties and Gelatinization Process. *Crit. Rev. Food Sci. Nutr.* **2021**, *62*, 1–11. [[CrossRef](#)]
6. Domene-López, D.; García-Quesada, J.C.; Martín-Gullón, I.; Montalbán, M.G. Influence of Starch Composition and Molecular Weight on Physicochemical Properties of Biodegradable Films. *Polymers* **2019**, *11*, 1084. [[CrossRef](#)] [[PubMed](#)]
7. Özeren, H.D.; Olsson, R.T.; Nilsson, F.; Hedenqvist, M.S. Prediction of Plasticization in a Real Biopolymer System (Starch) Using Molecular Dynamics Simulations. *Mater. Des.* **2020**, *187*, 108387. [[CrossRef](#)]
8. Esmaeili, M.; Pircheraghi, G.; Bagheri, R. Optimizing the Mechanical and Physical Properties of Thermoplastic Starch via Tuning the Molecular Microstructure through Co-Plasticization by Sorbitol and Glycerol. *Polym. Int.* **2017**, *66*, 809–819. [[CrossRef](#)]
9. Khan, B.; Bilal Khan Niazi, M.; Samin, G.; Jahan, Z. Thermoplastic Starch: A Possible Biodegradable Food Packaging Material—A Review. *J. Food Process Eng.* **2017**, *40*, e12447. [[CrossRef](#)]
10. Ibrahim, M.I.J.; Sapuan, S.M.; Zainudin, E.S.; Zuhri, M.Y.M. Physical, Thermal, Morphological, and Tensile Properties of Cornstarch-Based Films as Affected by Different Plasticizers. *Int. J. Food Prop.* **2019**, *22*, 925–941. [[CrossRef](#)]

11. Basiak, E.; Lenart, A.; Debeaufort, F. How Glycerol and Water Contents Affect the Structural and Functional Properties of Starch-Based Edible Films. *Polymers* **2018**, *10*, 412. [[CrossRef](#)]
12. Prachayawarakorn, J.; Tamseekhram, J. Chemical Modification of Biodegradable Cassava Starch Films by Natural Mono-, Di- and Tri-Carboxylic Acids. *Songklanakarin J. Sci. Technol.* **2019**, *41*, 8.
13. Utomo, P.; Nizardo, N.M.; Saepudin, E. *Crosslink Modification of Tapioca Starch with Citric Acid as a Functional Food*; AIP Publishing: Depok, Indonesia, 2020; p. 040055.
14. Olsson, E. Effects of Citric Acid on Starch-Based Barrier Coatings. Ph.D. Thesis, Karlstads Universitet, Karlstads, Sweden, 2013.
15. Reddy, N.; Yang, Y. Citric Acid Cross-Linking of Starch Films. *Food Chem.* **2010**, *118*, 702–711. [[CrossRef](#)]
16. Shen, L.; Xu, H.; Kong, L.; Yang, Y. Non-Toxic Crosslinking of Starch Using Polycarboxylic Acids: Kinetic Study and Quantitative Correlation of Mechanical Properties and Crosslinking Degrees. *J. Polym. Environ.* **2015**, *23*, 588–594. [[CrossRef](#)]
17. Tanetrungroj, Y.; Prachayawarakorn, J. Effect of Dual Modification on Properties of Biodegradable Crosslinked-Oxidized Starch and Oxidized-Crosslinked Starch Films. *Int. J. Biol. Macromol.* **2018**, *120*, 1240–1246. [[CrossRef](#)]
18. Canisag, H. *Bio-Crosslinking of Starch Films with Oxidized Sucrose*; University of Nebraska-Lincoln: Lincoln, NE, USA, 2015.
19. Xu, H.; Canisag, H.; Mu, B.; Yang, Y. Robust and Flexible Films from 100% Starch Cross-Linked by Biobased Disaccharide Derivative. *ACS Sustain. Chem. Eng.* **2015**, *3*, 2631–2639. [[CrossRef](#)]
20. Guerrero, P.; Muxika, A.; Zarandona, I.; de la Caba, K. Crosslinking of Chitosan Films Processed by Compression Molding. *Carbohydr. Polym.* **2019**, *206*, 820–826. [[CrossRef](#)] [[PubMed](#)]
21. Ponnusamy, P.G.; Sundaram, J.; Mani, S. Preparation and Characterization of Citric Acid Crosslinked Chitosan-Cellulose Nanofibrils Composite Films for Packaging Applications. *J. Appl. Polym. Sci.* **2021**, *139*, 52017. [[CrossRef](#)]
22. Khouri, J.; Penlidis, A.; Moresoli, C. Viscoelastic Properties of Crosslinked Chitosan Films. *Processes* **2019**, *7*, 157. [[CrossRef](#)]
23. Epure, V.; Griffon, M.; Pollet, E.; Avérous, L. Structure and Properties of Glycerol-Plasticized Chitosan Obtained by Mechanical Kneading. *Carbohydr. Polym.* **2011**, *83*, 947–952. [[CrossRef](#)]
24. Ma, X.; Qiao, C.; Wang, X.; Yao, J.; Xu, J. Structural Characterization and Properties of Polyols Plasticized Chitosan Films. *Int. J. Biol. Macromol.* **2019**, *135*, 240–245. [[CrossRef](#)]
25. Sun, Y.; Liu, Z.; Zhang, L.; Wang, X.; Li, L. Effects of Plasticizer Type and Concentration on Rheological, Physico-Mechanical and Structural Properties of Chitosan/Zein Film. *Int. J. Biol. Macromol.* **2020**, *143*, 334–340. [[CrossRef](#)]
26. Sinaga, M.Z.E.; Gea, S.; Zuhra, C.F.; Sihombing, Y.A.; Zaidar, E.; Sebayang, F.; Ningsih, T.U. The Effect of Plasticizers and Chitosan Concentration on the Structure and Properties of *Gracilaria* sp.-Based Thin Films for Food Packaging Purpose. *Polimery* **2021**, *66*, 119–126. [[CrossRef](#)]
27. Sun, L.; Sun, J.; Chen, L.; Niu, P.; Yang, X.; Guo, Y. Preparation and Characterization of Chitosan Film Incorporated with Thinned Young Apple Polyphenols as an Active Packaging Material. *Carbohydr. Polym.* **2017**, *163*, 81–91. [[CrossRef](#)] [[PubMed](#)]
28. Dudek, G.; Turczyn, R. New Type of Alginate/Chitosan Microparticle Membranes for Highly Efficient Pervaporative Dehydration of Ethanol. *RSC Adv.* **2018**, *8*, 39567–39578. [[CrossRef](#)]
29. Araújo Carneiro, E.; Pessoa Bastos, A.; Oliveira, U.; Matos, L.; Sabino Adriano, W.; Monteiro, R.; dos Santos, J.; Gonçalves, L. Improving the catalytic features of the lipase from *rhizomucor miehei* immobilized on chitosan-based hybrid matrices by altering the chemical activation conditions. *Quím. Nova* **2020**, *43*, 1234–1239. [[CrossRef](#)]
30. Aranaz, I.; Harris, R.; Heras, A. Chitosan Amphiphilic Derivatives. Chemistry and Applications. *Curr. Org. Chem.* **2010**, *14*, 308–330. [[CrossRef](#)]
31. Madera-Santana, T.J.; Mendez, C.; Rodríguez, J. An Overview of the Chemical Modifications of Chitosan and Its Advantages. *Green Mater.* **2018**, *6*, 131–142. [[CrossRef](#)]
32. Castro-Yobal, M.A.; Contreras-Oliva, A.; Saucedo-Rivalcoba, V.; Rivera-Armenta, J.L.; Hernández-Ramírez, G.; Salinas-Ruiz, J.; Herrera-Corredor, A. Evaluation of Physicochemical Properties of Film-Based Alginate for Food Packing Applications. *E-Polym.* **2021**, *21*, 82–95. [[CrossRef](#)]
33. Ibrahim, S.F.; Mohd Azam, N.A.N.; Mat Amin, K.A. Sodium Alginate Film: The Effect of Crosslinker on Physical and Mechanical Properties. *IOP Conf. Ser. Mater. Sci. Eng.* **2019**, *509*, 12063. [[CrossRef](#)]
34. Giz, A.S.; Berberoglu, M.; Bener, S.; Aydelik-Ayazoglu, S.; Bayraktar, H.; Alaca, B.E.; Catalgil-Giz, H. A Detailed Investigation of the Effect of Calcium Crosslinking and Glycerol Plasticizing on the Physical Properties of Alginate Films. *Int. J. Biol. Macromol.* **2020**, *148*, 49–55. [[CrossRef](#)]
35. Szekalska, M.; Sosnowska, K.; Czajkowska-Kośnik, A.; Winnicka, K. Calcium Chloride Modified Alginate Microparticles Formulated by the Spray Drying Process: A Strategy to Prolong the Release of Freely Soluble Drugs. *Materials* **2018**, *11*, 1522. [[CrossRef](#)]
36. Russo, R.; Malinconico, M.; Santagata, G. Effect of Cross-Linking with Calcium Ions on the Physical Properties of Alginate Films. *Biomacromolecules* **2007**, *8*, 3193–3197. [[CrossRef](#)] [[PubMed](#)]
37. Djalila, A.; Aicha, S. Development and Characterization of Biodegradables Packaging Obtained from Biopolymers Mixture. *J. Macromol. Sci. Part A* **2018**, *55*, 11–16. [[CrossRef](#)]
38. Li, H.; Gao, X.; Wang, Y.; Zhang, X.; Tong, Z. Comparison of Chitosan/Starch Composite Film Properties before and after Cross-Linking. *Int. J. Biol. Macromol.* **2013**, *52*, 275–279. [[CrossRef](#)] [[PubMed](#)]
39. Wu, J.; Zhong, F.; Li, Y.; Shoemaker, C.F.; Xia, W. Preparation and Characterization of Pullulan–Chitosan and Pullulan–Carboxymethyl Chitosan Blended Films. *Food Hydrocoll.* **2013**, *30*, 82–91. [[CrossRef](#)]

40. Wu, H.; Lei, Y.; Lu, J.; Zhu, R.; Xiao, D.; Jiao, C.; Xia, R.; Zhang, Z.; Shen, G.; Liu, Y.; et al. Effect of Citric Acid Induced Crosslinking on the Structure and Properties of Potato Starch/Chitosan Composite Films. *Food Hydrocoll.* **2019**, *97*, 105208. [[CrossRef](#)]
41. da Silva Raposo, A.K.; Paixão, L.C.; Rocha, A.A.; Lopes, I.A.; Santos, G.A.S.; Ribeiro, G.A.C.; de Menezes, A.S.; Barros Filho, A.K.D.; Santana, A.A. Characterization of Biodegradable Films Produced from Mixtures of Alginate, Starch and Babassu Fibers. *J. Polym. Environ.* **2021**, *29*, 1212–1226. [[CrossRef](#)]
42. Sivaselvi, K.; Ghosh, P. Characterization of Modified Chitosan Thin Film. *Mater. Today Proc.* **2017**, *4*, 442–451. [[CrossRef](#)]
43. Ismail, H.; Zaaba, N. Effect of Unmodified and Modified Sago Starch on Properties of (Sago Starch)/Silica/PVA Plastic Films. *J. Vinyl Addit. Technol.* **2014**, *20*, 185–192. [[CrossRef](#)]
44. Shrestha, B.; Dhungana, P.K.; Dhital, S.; Adhikari, B. Evaluation of Modified Sorghum Starches and Biodegradable Films. *J. Food Sci. Technol. Nepal* **2018**, *10*, 11–17. [[CrossRef](#)]
45. Kaczmarek, B. Improving Sodium Alginate Films Properties by Phenolic Acid Addition. *Materials* **2020**, *13*, 2895. [[CrossRef](#)]
46. Elzamy, R.A.; Mohamed, H.M.; Mohamed, M.I.; Zaky, H.T.; Harding, D.R.K.; Kandile, N.G. New Sustainable Chemically Modified Chitosan Derivatives for Different Applications: Synthesis and Characterization. *Arab. J. Chem.* **2021**, *14*, 103255. [[CrossRef](#)]
47. Razvy, M.A.; Faruk, M.O.; Hoque, M.A. Environment Friendly Antibacterial Activity of Water Chestnut Fruits. *J. Biodivers. Environ. Sci.* **2011**, *1*, 26–34.
48. Wang, P.; Sheng, F.; Tang, S.; Din, Z.; Chen, L.; Nawaz, A.; Hu, C.; Xiong, H. Synthesis and Characterization of Corn Starch Crosslinked with Oxidized Sucrose. *Starch-Starke* **2018**, *71*, 1800152. [[CrossRef](#)]
49. Martí, M.; Frígols, B.; Serrano-Aroca, A. Antimicrobial Characterization of Advanced Materials for Bioengineering Applications. *JoVE J. Vis. Exp.* **2018**, *138*, e57710. [[CrossRef](#)] [[PubMed](#)]
50. Wang, J.; Shang, J.; Ren, F.; Leng, X. Study of the Physical Properties of Whey Protein: Sericin Protein-Blended Edible Films. *Eur. Food Res. Technol.* **2010**, *231*, 109–116. [[CrossRef](#)]
51. Cervera, M.F.; Karjalainen, M.; Airaksinen, S.; Rantanen, J.; Krogars, K.; Heinämäki, J.; Colarte, A.I.; Yliruusi, J. Physical Stability and Moisture Sorption of Aqueous Chitosan–Amylose Starch Films Plasticized with Polyols. *Eur. J. Pharm. Biopharm.* **2004**, *58*, 69–76. [[CrossRef](#)]
52. Mujtaba, M.; Morsi, R.E.; Kerch, G.; Elsabee, M.Z.; Kaya, M.; Labidi, J.; Khawar, K.M. Current Advancements in Chitosan-Based Film Production for Food Technology; A Review. *Int. J. Biol. Macromol.* **2019**, *121*, 889–904. [[CrossRef](#)]
53. Leceta, I.; Guerrero, P.; de la Caba, K. Functional Properties of Chitosan-Based Films. *Carbohydr. Polym.* **2013**, *93*, 339–346. [[CrossRef](#)]
54. Olivás, G.I.; Barbosa-Cánovas, G.V. Alginate–Calcium Films: Water Vapor Permeability and Mechanical Properties as Affected by Plasticizer and Relative Humidity. *LWT–Food Sci. Technol.* **2008**, *41*, 359–366. [[CrossRef](#)]
55. Coupland, J.N.; Shaw, N.B.; Monahan, F.J.; Dolores O’Riordan, E.; O’Sullivan, M. Modeling the Effect of Glycerol on the Moisture Sorption Behavior of Whey Protein Edible Films. *J. Food Eng.* **2000**, *43*, 25–30. [[CrossRef](#)]
56. Hiremani, V.D.; Gasti, T.; Masti, S.P.; Malabadi, R.B.; Chougale, R.B. Polysaccharide-Based Blend Films as a Promising Material for Food Packaging Applications: Physicochemical Properties. *Iran. Polym. J.* **2022**, *31*, 503–518. [[CrossRef](#)]
57. Thawien, B. Plasticizer Effect on the Properties of Biodegradable Blend from Rice Starch-Chitosan. *Songklanakarin J. Sci. Technol.* **2008**, *30*, 149–165.
58. Suput, D.; Lazic, V.; Popović, S.; Hromis, N.; Bulut, S. Biopolymer Films Synthesis and Characterisation. *J. Process. Energy Agric.* **2017**, *21*, 9–12. [[CrossRef](#)]
59. Balakrishnan, P.; Sreekala, M.S.; Geethamma, V.G.; Kalarikkal, N.; Kokol, V.; Volova, T.; Thomas, S. Physicochemical, Mechanical, Barrier and Antibacterial Properties of Starch Nanocomposites Crosslinked with Pre-Oxidised Sucrose. *Ind. Crops Prod.* **2019**, *130*, 398–408. [[CrossRef](#)]
60. Rodríguez, J.; Madera-Santana, T.J.; Sánchez-Machado, D.; Lopez-Cervantes, J.; Valdez, H. Chitosan/Hydrophilic Plasticizer-Based Films: Preparation, Physicochemical and Antimicrobial Properties. *J. Polym. Environ.* **2014**, *22*, 41–51. [[CrossRef](#)]
61. Li, J.; Wu, Y.; He, J.; Huang, Y. A New Insight to the Effect of Calcium Concentration on Gelation Process and Physical Properties of Alginate Films. *J. Mater. Sci.* **2016**, *51*, 5791–5801. [[CrossRef](#)]
62. Guo, M.Q.; Hu, X.; Wang, C.; Ai, L. *Polysaccharides: Structure and Solubility*; IntechOpen: London, UK, 2017; ISBN 978-953-51-3650-7.
63. Gontard, N.; Guilbert, S.; Cuq, J.-L. Edible Wheat Gluten Films: Influence of the Main Process Variables on Film Properties Using Response Surface Methodology. *J. Food Sci.* **1992**, *57*, 190–195. [[CrossRef](#)]
64. Vogler, E.A. Structure and Reactivity of Water at Biomaterial Surfaces. *Adv. Colloid Interface Sci.* **1998**, *74*, 69–117. [[CrossRef](#)]
65. Bastos, D.C.; Santos, A.E.F.; da Fonseca, M.D.; Simão, R.A. Inducing Surface Hydrophobization on Cornstarch Film by SF6 and HMDSO Plasma Treatment. *Carbohydr. Polym.* **2013**, *91*, 675–681. [[CrossRef](#)]
66. Pongjanyakul, T.; Puttipipatkachorn, S. Alginate-Magnesium Aluminum Silicate Films: Effect of Plasticizers on Film Properties, Drug Permeation and Drug Release from Coated Tablets. *Int. J. Pharm.* **2007**, *333*, 34–44. [[CrossRef](#)]
67. Jouki, M.; Khazaei, N.; Ghasemlou, M.; HadiNezhad, M. Effect of Glycerol Concentration on Edible Film Production from Cress Seed Carbohydrate Gum. *Carbohydr. Polym.* **2013**, *96*, 39–46. [[CrossRef](#)] [[PubMed](#)]
68. Britto, D.; Assis, O. A Novel Method for Obtaining a Quaternary Salt of Chitosan. *Carbohydr. Polym.* **2007**, *69*, 305–310. [[CrossRef](#)]
69. Hsieh, C.-Y.; Tsai, S.-P.; Wang, D.-M.; Chang, Y.-N.; Hsieh, H.-J. Preparation of -PGA/Chitosan Composite Tissue Engineering Matrices. *Biomaterials* **2005**, *26*, 5617–5623. [[CrossRef](#)] [[PubMed](#)]



70. Taverna, M.E.; Busatto, C.A.; Saires, P.J.; Bertero, M.P.; Sedran, U.A.; Estenoz, D.A. Bio-Composite Films Based on Alginate and Rice Husk Tar Microparticles Loaded with Eugenol for Active Packaging. *Waste Biomass Valorization* **2022**, *13*, 1–10. [[CrossRef](#)]
71. Siracusa, V. Food Packaging Permeability Behaviour: A Report. *Int. J. Polym. Sci.* **2012**, *2012*, e302029. [[CrossRef](#)]
72. Siracusa, V.; Rocculi, P.; Romani, S.; Rosa, M.D. Biodegradable Polymers for Food Packaging: A Review. *Trends Food Sci. Technol.* **2008**, *12*, 634–643. [[CrossRef](#)]
73. Lee, D.S.; Wang, H.J.; Jaisan, C.; An, D.S. Active Food Packaging to Control Carbon Dioxide. *Packag. Technol. Sci.* **2022**, *35*, 213–227. [[CrossRef](#)]
74. Siracusa, V.; Romani, S.; Gigli, M.; Mannozzi, C.; Cecchini, J.P.; Tylewicz, U.; Lotti, N. Characterization of Active Edible Films Based on Citral Essential Oil, Alginate and Pectin. *Materials* **2018**, *11*, 1980. [[CrossRef](#)]
75. Robertson, G.L. Optical, Mechanical and Barrier Properties of Thermoplastic Polymers. In *Food Packaging*; CRC Press: Boca Raton, FL, USA, 2012; ISBN 978-0-429-10540-1.
76. Garcia, M.; Martino, M.; Zaritzky, N. Lipid Addition to Improve Barrier Properties of Edible Starch-Based Films and Coatings. *J. Food Sci.* **2000**, *65*, 941–944. [[CrossRef](#)]
77. Butnaru, E.; Stoleru, E.; Brebu, M.A.; Darie-Nita, R.N.; Bargan, A.; Vasile, C. Chitosan-Based Bionanocomposite Films Prepared by Emulsion Technique for Food Preservation. *Materials* **2019**, *12*, 373. [[CrossRef](#)]
78. Caner, C.; Vergano, P.J.; Wiles, J.L. Chitosan Film Mechanical and Permeation Properties as Affected by Acid, Plasticizer, and Storage. *J. Food Sci.* **2006**, *63*, 1049–1053. [[CrossRef](#)]
79. Aguirre-Loredo, R.Y.; Rodríguez-Hernández, A.I.; Chavarría-Hernández, N. Physical Properties of Emulsified Films Based on Chitosan and Oleic Acid. *CyTA–J. Food* **2014**, *12*, 305–312. [[CrossRef](#)]
80. Miller, K.S.; Krochta, J.M. Oxygen and Aroma Barrier Properties of Edible Films: A Review. *Trends Food Sci. Technol.* **1997**, *8*, 228–237. [[CrossRef](#)]
81. Tan, S.X.; Ong, H.C.; Andriyana, A.; Lim, S.; Pang, Y.L.; Kusumo, F.; Ngoh, G.C. Characterization and Parametric Study on Mechanical Properties Enhancement in Biodegradable Chitosan-Reinforced Starch-Based Bioplastic Film. *Polymers* **2022**, *14*, 278. [[CrossRef](#)] [[PubMed](#)]
82. Xu, Y.X.; Kim, K.M.; Hanna, M.A.; Nag, D. Chitosan–Starch Composite Film: Preparation and Characterization. *Ind. Crops Prod.* **2005**, *21*, 185–192. [[CrossRef](#)]
83. Rhim, J.-W. Physical and Mechanical Properties of Water Resistant Sodium Alginate Films. *LWT–Food Sci. Technol.* **2004**, *37*, 323–330. [[CrossRef](#)]
84. Pavlath, A.E.; Gossett, C.; Camirand, W.; Robertson, G.H. Ionomeric Films of Alginic Acid. *J. Food Sci.* **1999**, *64*, 61–63. [[CrossRef](#)]
85. Pinto, G.; De Pascale, S.; Aponte, M.; Scaloni, A.; Addeo, F.; Caira, S. Polyphenol Profiling of Chestnut Pericarp, Integument and Curing Water Extracts to Qualify These Food By-Products as a Source of Antioxidants. *Molecules* **2021**, *26*, 2335. [[CrossRef](#)]
86. Silva, V.; Falco, V.; Dias, M.I.; Barros, L.; Silva, A.; Capita, R.; Alonso-Calleja, C.; Amaral, J.S.; Igrejas, G.; Ferreira, I.C.F.R.; et al. Evaluation of the Phenolic Profile of *Castanea sativa* Mill. By-Products and Their Antioxidant and Antimicrobial Activity against Multiresistant Bacteria. *Antioxid. Basel Switz.* **2020**, *9*, 87. [[CrossRef](#)]
87. Priya, B.; Gupta, V.K.; Pathania, D.; Singha, A.S. Synthesis, Characterization and Antibacterial Activity of Biodegradable Starch/PVA Composite Films Reinforced with Cellulosic Fibre. *Carbohydr. Polym.* **2014**, *109*, 171–179. [[CrossRef](#)]
88. Nicosia, A.; Gieparda, W.; Foksowicz-Flaczyk, J.; Walentowska, J.; Wesolek, D.; Vazquez, B.; Prodi, F.; Belosi, F. Air Filtration and Antimicrobial Capabilities of Electrospun PLA/PHB Containing Ionic Liquid. *Sep. Purif. Technol.* **2015**, *154*, 154–160. [[CrossRef](#)]
89. Zhang, S.D.; Zhang, Y.R.; Wang, Y.Z.; Wang, X.L. Effect of Crosslink on Properties of Thermoplastics Dialdehyde Sweet Potato Starch. *Adv. Mater. Res.* **2013**, *629*, 391–395. [[CrossRef](#)]
90. Atay, H.Y. Antibacterial Activity of Chitosan-Based Systems. In *Functional Chitosan*; Springer: Singapore, 2019; pp. 457–489. [[CrossRef](#)]
91. Peña, A.; Sánchez, N.S.; Calahorra, M. Effects of Chitosan on *Candida Albicans*: Conditions for Its Antifungal Activity. *BioMed Res. Int.* **2013**, *2013*, 527549. [[CrossRef](#)] [[PubMed](#)]
92. Li, J.; Zhuang, S. Antibacterial Activity of Chitosan and Its Derivatives and Their Interaction Mechanism with Bacteria: Current State and Perspectives. *Eur. Polym. J.* **2020**, *138*, 109984. [[CrossRef](#)]
93. Alahakoon, A.U.; Jayasena, D.D.; Jung, S.; Kim, H.J.; Kim, S.H.; Jo, C. Antimicrobial Effect of Calcium Chloride Alone and Combined with Lactic Acid Injected into Chicken Breast Meat. *Korean J. Food Sci. Anim. Resour.* **2014**, *34*, 221–229. [[CrossRef](#)]
94. Rajamma, S.B.; Raj, A.; Kalampalath, V.; Eapen, S.J. Elucidation of Antibacterial Effect of Calcium Chloride against *Ralstonia Pseudosolanacearum* Race 4 Biovar 3 Infecting Ginger (*Zingiber Officinale* Rosc.). *Arch. Microbiol.* **2021**, *203*, 663–671. [[CrossRef](#)] [[PubMed](#)]
95. Turalija, M.; Bischof, S.; Budimir, A.; Gaan, S. Antimicrobial PLA Films from Environment Friendly Additives. *Compos. Part B Eng.* **2016**, *102*, 94–99. [[CrossRef](#)]
96. Körge, K.; Bajić, M.; Likožar, B.; Novak, U. Active Chitosan–Chestnut Extract Films Used for Packaging and Storage of Fresh Pasta. *Int. J. Food Sci. Technol.* **2020**, *55*, 3043–3052. [[CrossRef](#)]
97. Körge, K.; Šeme, H.; Bajić, M.; Likožar, B.; Novak, U. Reduction in Spoilage Microbiota and Cyclopiazonic Acid Mycotoxin with Chestnut Extract Enriched Chitosan Packaging: Stability of Inoculated Gouda Cheese. *Foods* **2020**, *9*, 1645. [[CrossRef](#)]
98. Mei, J.; Yuan, Y.; Guo, Q.; Wu, Y.; Li, Y.; Yu, H. Characterization and Antimicrobial Properties of Water Chestnut Starch-Chitosan Edible Films. *Int. J. Biol. Macromol.* **2013**, *61*, 169–174. [[CrossRef](#)]

99. Alirezalu, K.; Yaghoubi, M.; Poorsharif, L.; Aminnia, S.; Kahve, H.I.; Pateiro, M.; Lorenzo, J.M.; Muneke, P.E.S. Antimicrobial Polyamide-Alginate Casing Incorporated with Nisin and  $\epsilon$ -Polylysine Nanoparticles Combined with Plant Extract for Inactivation of Selected Bacteria in Nitrite-Free Frankfurter-Type Sausage. *Foods* **2021**, *10*, 1003. [[CrossRef](#)] [[PubMed](#)]
100. Kumar, L.; Brice, J.; Toberer, L.; Klein-Seetharaman, J.; Knauss, D.; Sarkar, S.K. Antimicrobial Biopolymer Formation from Sodium Alginate and Algae Extract Using Aminoglycosides. *PLoS ONE* **2019**, *14*, e0214411. [[CrossRef](#)] [[PubMed](#)]
101. Azeredo, H.M.C.; Mattoso, L.H.C.; Avena-Bustillos, R.J.; Filho, G.C.; Munford, M.L.; Wood, D.; McHugh, T.H. Nanocellulose Reinforced Chitosan Composite Films as Affected by Nanofiller Loading and Plasticizer Content. *J. Food Sci.* **2010**, *75*, N1–N7. [[CrossRef](#)]
102. Chen, Q.; Liu, Y.; Chen, G. A Comparative Study on the Starch-Based Biocomposite Films Reinforced by Nanocellulose Prepared from Different Non-Wood Fibers. *Cellulose* **2019**, *26*, 2425–2435. [[CrossRef](#)]
103. Zhao, Y.; Troedsson, C.; Bouquet, J.-M.; Thompson, E.M.; Zheng, B.; Wang, M. Mechanically Reinforced, Flexible, Hydrophobic and UV Impermeable Starch-Cellulose Nanofibers (CNF)-Lignin Composites with Good Barrier and Thermal Properties. *Polymers* **2021**, *13*, 4346. [[CrossRef](#)]
104. Colussi, R.; Pinto, V.Z.; El Halal, S.L.M.; Vanier, N.L.; Villanova, F.A.; Marques e Silva, R.; da Rosa Zavareze, E.; Dias, A.R.G. Structural, Morphological, and Physicochemical Properties of Acetylated High-, Medium-, and Low-Amylose Rice Starches. *Carbohydr. Polym.* **2014**, *103*, 405–413. [[CrossRef](#)] [[PubMed](#)]
105. Zhang, Y.; Han, J.H. Plasticization of Pea Starch Films with Monosaccharides and Polyols. *J. Food Sci.* **2006**, *71*, E253–E261. [[CrossRef](#)]
106. Gao, C.; Stading, M.; Wellner, N.; Parker, M.; Noel, T.; Mills, E.; Belton, P. Plasticization of a Protein-Based Film by Glycerol: A Spectroscopic, Mechanical, and Thermal Study. *J. Agric. Food Chem.* **2006**, *54*, 4611–4616. [[CrossRef](#)]
107. Fundo, J.F.; Galvis-Sanchez, A.C.; Delgadillo, I.; Silva, C.L.M.; Quintas, M.A.C. The Effect of Polymer/Plasticiser Ratio in Film Forming Solutions on the Properties of Chitosan Films. *Food Biophys.* **2015**, *10*, 324–333. [[CrossRef](#)]
108. Liu, H.; Adhikari, R.; Guo, Q.; Adhikari, B. Preparation and Characterization of Glycerol Plasticized (High-Amylose) Starch-Chitosan Films. *J. Food Eng.* **2013**, *116*, 588–597. [[CrossRef](#)]
109. Sartori, C.; Finch, D.S.; Ralph, B.; Gilding, K. Determination of the Cation Content of Alginate Thin Films by FTIR Spectroscopy. *Polymer* **1997**, *38*, 43–51. [[CrossRef](#)]
110. Salmieri, S.; Lacroix, M. Physicochemical Properties of Alginate/Polycaprolactone-Based Films Containing Essential Oils. *J. Agric. Food Chem.* **2006**, *54*, 10205–10214. [[CrossRef](#)] [[PubMed](#)]
111. Atangana, E.; Chiweshe, T.T.; Roberts, H. Modification of Novel Chitosan-Starch Cross-Linked Derivatives Polymers: Synthesis and Characterization. *J. Polym. Environ.* **2019**, *27*, 979–995. [[CrossRef](#)]
112. Xi, X.; Pizzi, A.; Lei, H.; Zhang, B.; Chen, X.; Du, G. Environmentally Friendly Chitosan Adhesives for Plywood Bonding. *Int. J. Adhes. Adhes.* **2022**, *112*, 103027. [[CrossRef](#)]
113. Queiroz, M.; Melo, K.; Sabry, D.; Sasaki, G.; Rocha, H. Does the Use of Chitosan Contribute to Oxalate Kidney Stone Formation? *Mar. Drugs* **2014**, *13*, 141. [[CrossRef](#)]
114. Nobrega, M.; Olivato, J.; Müller, C.; Yamashita, F. Biodegradable Starch-Based Films Containing Saturated Fatty Acids: Thermal, Infrared and Raman Spectroscopic Characterization. *Polim.-Cienc. E Tecnol.* **2012**, *22*, 475–480. [[CrossRef](#)]
115. Siddaramaiah; Swamy, T.M.M.; Ramaraj, B.; Lee, J.H. Sodium Alginate and Its Blends with Starch: Thermal and Morphological Properties. *J. Appl. Polym. Sci.* **2008**, *109*, 4075–4081. [[CrossRef](#)]
116. Sáenz-Santos, C.; Oyedara, O.; García Tejada, Y.; Romero Bastida, C.; García-Oropesa, E.; Villalobo, E.; Rodríguez-Perez, M. Active Biopolymeric Films Inoculated with *Bdellovibrio bacteriovorus*, a Predatory Bacterium. *Coatings* **2021**, *11*, 605. [[CrossRef](#)]



# Antibacterial and Biodegradable Polysaccharide-Based Films for Food Packaging Applications: Comparative Study

Weronika Janik, Michał Nowotarski, Divine Yutefar Shyntum, Angelika Banaś, Katarzyna Krukiewicz, Stanisław Kudła, Gabriela Dudek

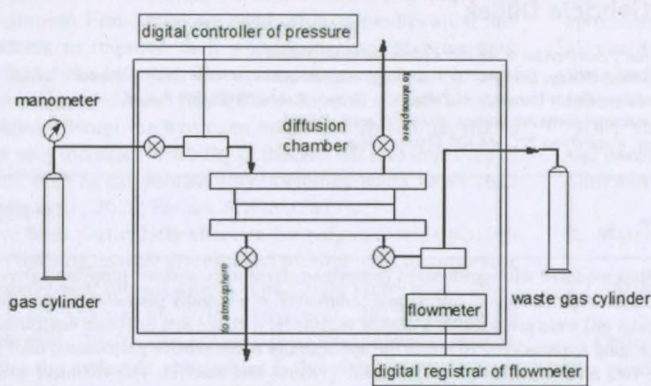


Figure S1. Schematic diagram of experimental apparatus for gas permeability testing.

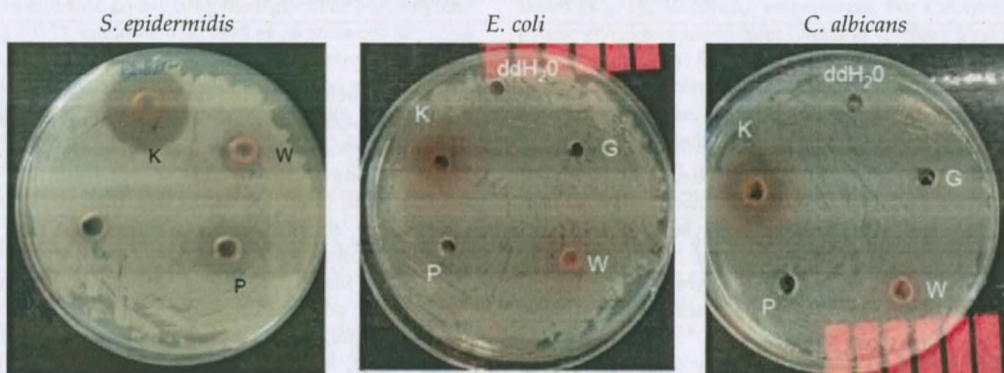
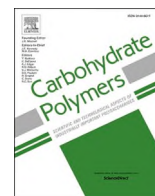


Figure S2. Antimicrobial activity of four commercially available extracts: chestnut (K), graviola (G), grape (W), nettle (P) tested against model Gram-positive bacteria (*S. epidermidis*), Gram-negative bacteria (*E. coli*) and yeasts (*C. albicans*); control well was filled with deionized water (ddH<sub>2</sub>O).



# Chitosan-based films with alternative eco-friendly plasticizers: Preparation, physicochemical properties and stability

Weronika Janik<sup>a,b,\*</sup>, Kerstin Ledniowska<sup>a,b</sup>, Michał Nowotarski<sup>c</sup>, Stanisław Kudła<sup>a</sup>, Joanna Knapczyk-Korczak<sup>d</sup>, Urszula Stachewicz<sup>d</sup>, Ewa Nowakowska-Bogdan<sup>a</sup>, Ewa Sabura<sup>a</sup>, Hanna Nosal-Kovalenko<sup>a</sup>, Roman Turczyn<sup>c,e</sup>, Gabriela Dudek<sup>c</sup>

<sup>a</sup> Lukaszewicz Research Network - Institute of Heavy Organic Synthesis "Blachownia", Energetyków 9, 47-225 Kędzierzyn-Koźle, Poland

<sup>b</sup> Department of Physical Chemistry and Technology of Polymers, Joint Doctoral School, Silesian University of Technology, Akademicka 2a, 44-100 Gliwice, Poland

<sup>c</sup> Department of Physical Chemistry and Technology of Polymers, Faculty of Chemistry, Silesian University of Technology, Strzody 9, 44-100 Gliwice, Poland

<sup>d</sup> AGH University of Science and Technology, Faculty of Metals Engineering and Industrial Computer Science, 30-023 Cracow, Poland

<sup>e</sup> Centre for Organic and Nanohybrid Electronics, Silesian University of Technology, Konarskiego 22B, 44-100 Gliwice, Poland

## ARTICLE INFO

### Keywords:

Chitosan  
Plasticizer  
Films  
Polysaccharide  
Physico-chemical characterization  
Mechanical properties

## ABSTRACT

Chitosan-based films modified with synthesized (propylene glycol monoacetate, propylene glycol esters of fatty acids, and epoxidized propylene glycol esters) and commercial eco-friendly plasticizers (epoxidized soybean oil and epoxidized palm oil) were prepared by a casting technique, with the aim to obtain environmentally friendly materials for packaging applications. To assess the applicability of alternative plasticizers, their properties were compared to the two most common plasticizers, i.e. glycerol and sorbitol. The chemical structure of newly synthesized plasticizers was verified by gas chromatography with mass detector, infrared spectroscopy and <sup>1</sup>H NMR; and their acid, epoxy, iodine, and saponification values were determined. Plasticized chitosan-based films were characterized in terms of hydrophilic, barrier, thermal, mechanical properties, zeta potential and morphology, confirming their flexibility and homogeneity. The research confirmed that the alternative plasticizers introduced by us are more effective than commercially available ones, exhibiting lower hydrophilicity and superior mechanical properties compared to samples plasticized with traditional plasticizers. Moreover, these properties were found to be even better after ageing for 10 months.

## 1. Introduction

Food packaging plays an important role in protecting food from external environment, ensuring food quality and extending its shelf life. Unfortunately, most of the packaging used on the market today is made of petroleum-based polymers, such as polypropylene or polyesters, which cause environmental pollution due to their non-biodegradable nature (Ncube et al., 2020). In consequence, there is an urgent demand for developing biomaterials that can replace petroleum-based plastics.

A number of studies have been conducted so far on the use of polysaccharides in food packaging (Mohamed et al., 2020). Current research is mainly concerned with obtaining films from such polysaccharides as

cellulose, starch, chitosan, or sodium alginate (Mohamed et al., 2020; Swain & Mohanty, 2018). Cellulose films are mostly fabricated from cellulose derivatives such as methylcellulose or carboxymethyl cellulose, which are further modified with polyethylene glycol, silver nanoparticles or nanocellulose to improve their physicochemical properties (Cazón et al., 2017). Starch (mainly from corn, rice, wheat, cassava and potatoes) is primarily plasticized with glycerol, xylitol, or sorbitol (Zhao et al., 2021). Starch films currently available on the market are primarily blended with polyesters, mainly polylactic acid (Muller et al., 2017). On the other hand, sodium alginate films are primarily cross-linked with calcium ions, leading to improved water barrier properties and mechanical resistance (Cazón et al., 2017). Another polysaccharide, chitosan, shows good gelation and film formation properties, as well as

\* Corresponding author at: Lukaszewicz Research Network - Institute of Heavy Organic Synthesis "Blachownia", Energetyków 9, 47-225 Kędzierzyn-Koźle, Poland.

E-mail addresses: [weronika.janik@icso.lukasiewicz.gov.pl](mailto:weronika.janik@icso.lukasiewicz.gov.pl) (W. Janik), [kerstin.ledniowska@icso.lukasiewicz.gov.pl](mailto:kerstin.ledniowska@icso.lukasiewicz.gov.pl) (K. Ledniowska), [michnow566@student.polsl.pl](mailto:michnow566@student.polsl.pl) (M. Nowotarski), [stanislaw.kudla@icso.lukasiewicz.gov.pl](mailto:stanislaw.kudla@icso.lukasiewicz.gov.pl) (S. Kudła), [jknapczyk@agh.edu.pl](mailto:jknapczyk@agh.edu.pl) (J. Knapczyk-Korczak), [ustachew@agh.edu.pl](mailto:ustachew@agh.edu.pl) (U. Stachewicz), [ewa.nowakowska@icso.lukasiewicz.gov.pl](mailto:ewa.nowakowska@icso.lukasiewicz.gov.pl) (E. Nowakowska-Bogdan), [ewa.sabura@icso.lukasiewicz.gov.pl](mailto:ewa.sabura@icso.lukasiewicz.gov.pl) (E. Sabura), [hanna.nosal@icso.lukasiewicz.gov.pl](mailto:hanna.nosal@icso.lukasiewicz.gov.pl) (H. Nosal-Kovalenko), [roman.turczyn@polsl.pl](mailto:roman.turczyn@polsl.pl) (R. Turczyn), [gabriela.maria.dudek@polsl.pl](mailto:gabriela.maria.dudek@polsl.pl) (G. Dudek).

<https://doi.org/10.1016/j.carbpol.2022.120277>

Received 27 July 2022; Received in revised form 17 October 2022; Accepted 26 October 2022

Available online 29 October 2022

0144-8617/© 2022 Elsevier Ltd. All rights reserved.



good antioxidant activity and excellent antimicrobial activity, with effective inhibition of most fungi, gram-negative and gram-positive bacteria (Zhao et al., 2021). When combined with additives such as antibacterial extracts, it is possible to obtain chitosan-based antibacterial food films, which are of great interest for packaging applications. In particular, these properties distinguish chitosan from other polysaccharides (Zhao et al., 2021).

Chitosan is a polymer derived through the deacetylation of chitin, which is one of the most common polysaccharides in nature (Bakshi et al., 2020; Priyadarshi et al., 2018). Solubility of chitosan depends on many factors, such as degree of deacetylation, molecular weight, distribution of acetyl groups along the main chain and type of acid used for its protonation (Cazón & Vázquez, 2019; Pardo-Castaño & Bolaños, 2019). Nevertheless, it is important that chitosan is soluble in dilute acid solutions at pH below 6.5 due to the presence of amino groups (Bakshi et al., 2020; Sami El-banna et al., 2019). For this reason acids, such as acetic or lactic acid, are frequently used to dissolve chitosan (Melro et al., 2020; Tambunan & Chamidah, 2021). Despite many promising properties of chitosan films, they are rigid without modification and require plasticizers to improve their physico-mechanical properties. Addition of plasticizers into the film formulation reduces frictional forces between polymer chains. Plasticizer molecules placed between the polymer chains disrupt the hydrogen bonds and spread the chains apart, what not only increases flexibility of the film but also improves its other properties, such as gas permeability, including water vapor (Ballesteros-Mártinez et al., 2020; Farhan & Hani, 2017).

Polyols have been particularly effective for polysaccharide plasticization. For that purpose, mainly glycerol and sorbitol were incorporated into most chitosan-based films (Castelló et al., 2018; Epure et al., 2011; Liu et al., 2014; Ma, Qiao, et al., 2019; Matet et al., 2013; Priyadarshi et al., 2018; Sun et al., 2020). This is due to their low molecular weight, since the smaller the molecule, the greater is the plasticizing effect on the polymer matrix (Murrieta et al., 2019). However, it is known that the hydrophilicity of plasticized films increases due to the presence of hydroxyl groups in glycerol and sorbitol (Vieira et al., 2011). Furthermore, small molecules diffuse to the film surface, especially during long term storage, resulting in secondary film brittleness. For this reason, searching for other plasticizers is still an issue. The literature suggests that other polyols, such as ethylene glycol, propylene glycol or polyethylene glycol (Vieira et al., 2011), could be also used as plasticizers. Suyatma et al. (2005) studied the effects of ethylene glycol, propylene glycol, polyethylene glycol and glycerol on the mechanical and surface properties of chitosan films that were stored for 3 and 20 weeks. Glycerol and polyethylene glycol were found to be more suitable as plasticizers of chitosan than ethylene and propylene glycol. In addition, chitosan films containing 20 wt% glycerol or polyethylene glycol showed good stability for 5 months. Meanwhile, Caicedo et al. (2022) used glycerol, sorbitol and polyethylene glycol as plasticizers for starch/PVOH/chitosan films. The sample plasticized with sorbitol at 30 wt% was found to have the lowest water vapor permeability, the highest elongation at break and better thermal resistance than samples prepared with other plasticizers. Alternative plasticizers are still being sought, including oils such as palm oil (Hasan et al., 2020), rosehip seed oil (Darie-Niță et al., 2021), epoxidized chia seed oil (Dominguez-Candela et al., 2021), epoxidized soybean oil (Alhanish & Abu Ghalia, 2021) olive oil or corn oil (Giannakas et al., 2017) and fatty acids (Srinivasa et al., 2007). On the other hand, Vlacha et al. (2016) proposed oleic acid as a plasticizer for chitosan films. Samples prepared with this plasticizer were shown to be a better barrier to water vapor. Unfortunately, other properties (including mechanical and hydrophilic) were worse than they were for glycerol. Similar conclusions can be drawn from other works (Matet et al., 2013; Rodríguez-Núñez et al., 2014; Thawien, 2008), which also indicated that glycerol and sorbitol are the most effective plasticizers for chitosan at this time. Unfortunately, samples obtained with these plasticizers, do not solve the problem of brittleness or hydrophilic character of chitosan-based materials.

In this paper, we propose alternative plasticizers (APs) as modifiers for chitosan-based films to tackle the aforementioned drawbacks. We propose three different mixtures of plasticizers based on renewable raw materials such as propylene glycol, acetic acid, oleic acid and succinic acid. Propylene glycol has been already proven to have good plasticizing properties (Ibrahim et al., 2020) and acids such as acetic acid, oleic acid and succinic acid can also act as plasticizers (Chen et al., 2008; Qiao et al., 2021; Vlacha et al., 2016). In addition, all substrates used by us are environmentally friendly, the synthesis process does not require purification steps and a previous study (Ledniowska et al., 2022) has shown that such plasticizer mixtures have a low migration rate. To the best of our knowledge, such plasticizer mixtures have not been studied in the context of biodegradable films. Thus, this work focuses on the evaluation of suitability of chitosan films containing alternative plasticizers and chestnut extract as packaging films, mainly in the food industry. For this purpose, mechanical, hydrophilic, structural, thermal, zeta potential and ageing properties of chitosan films were determined. In addition, two commercially available alternative plasticizers (CAPs), namely epoxidized soybean oil (EPOS) and epoxidized palm oil (EPOP), were also used in this study. To assess the applicability of APs as plasticizers, their performance was compared with the performance of the two most common used plasticizers for chitosan, i.e. glycerol (GLY) and sorbitol (SOR). The influence of plasticizer type on the mechanical, hydrophilic, and barrier properties of the films was investigated for freshly prepared films and after 10 months of storage.

## 2. Material and methods

### 2.1. Materials

Chitosan (viscosity: 0.03–0.1 Pa·s, MW = 250 kg/mol, DD ≥ 90 %) was purchased from Sigma-Aldrich (Steinheim, Germany). Acetic acid was purchased from Avantor (Gliwice, Poland) (99.5–99.9 %) and chestnut extract Farmatan (≥76 % tannins) was provided by Tanin Sevnica (Sevnica, Slovenia). Glycerol was supplied by Merck (Darmstadt, Germany), while sorbitol by Sigma-Aldrich (Steinheim, Germany). Epoxidized soybean oil and epoxidized palm oil were from Inbra Indústrias Químicas LTDA (Sao Paulo, Brasil) and Malaysian Palm Oil Board (Kajang, Malaysia), respectively. For the synthesis of APs, propylene glycol purchased from Chempur (Piekary Śląskie, Poland), acetic acid (99.5–99.9 %) from Avantor (Gliwice, Poland), oleic acid (90.0 %) from Alfa Aesar (Ward Hill, MA, USA), and succinic acid (≥99.5 %) from POL-AURA (Zabrze, Poland) were used. Methanesulfonic acid (>99.0 %) from TCI (Zwijndrecht, Belgium) was used as a catalyst. Cyclohexene and toluene (both pure p.a.) from Chempur (Piekary Śląskie, Poland) were used as solvents. Formic acid (85.0 %), hydrogen peroxide (30.0 %) and di-sodium hydrogen phosphate dihydrate (pure p.a.) from Chempur (Piekary Śląskie, Poland) were used for epoxidation reaction and purification of epoxidized esters. Sodium hydrogen carbonate (pure p.a.) from Chempur (Piekary Śląskie, Poland) was used for purification of acetic acid esters.

### 2.2. Plasticizer preparation

Esterification and epoxidation reactions were carried out in a glass reactor with a capacity of 500 or 1000 cm<sup>3</sup>, equipped with a mechanical stirrer, a temperature controller with a Pt-100 temperature sensor, Dean-Stark trap (for esterification reactions), reflux condenser and dropping funnel (for selected reactions). The reactor was heated using a heating mantle with automatic temperature control.

#### 2.2.1. Synthesis of mixed esters based on propylene glycol and acetic acid (OC)

Propylene glycol (167.4 g) was esterified with acetic acid (120.7 g), where 25 wt% of the amount of acetic acid was placed in the reactor, while the remaining amount was added dropwise over 6 h. The process

was carried out for 24 h using methanesulfonic acid (0.58 g) as a catalyst at a temp. of 80 °C, with intensive stirring (400 rpm) and nitrogen bubbling. Cyclohexane (57.5 g) was used to remove water released as a by-product from the reaction mixture and collected in the Dean-Stark trap. The main product was poured into a separating funnel and purified consequently with saturated NaHCO<sub>3</sub> solution, distilled water (6 wt %) and cyclohexane (15 wt%) and then separated into two phases. The bottom layer was removed, while the rest was distilled off in a rotary evaporator under reduced pressure. The schematic route of OC plasticizer synthesis is shown in Fig. 1.

### 2.2.2. Synthesis of mixed esters based on succinic acid, propylene glycol and oleic acid (KBOL)

Mixed esters based on succinic acid, propylene glycol and oleic acid were synthesized in two steps. In the first step, propylene glycol (226.4 g) was esterified with oleic acid (600.0 g). The process was carried out for 8 h using methanesulfonic acid (1.70 g) as a catalyst at a temp. of 120 °C, with stirring at 400 rpm and nitrogen bubbling. Toluene (82.8 g) was used to remove water released as a by-product from the reaction mixture and collected in the Dean-Stark trap. At the end of the reaction, the remaining toluene was distilled from the reaction mixture in a rotary evaporator under reduced pressure. In the second step, succinic acid (35.4 g) and the catalyst (0.47 g) were added to the mixture obtained in the first step of the synthesis (200.0 g). Toluene (25.0 g) was used to remove water released as a by-product from the reaction mixture and collected in the Dean-Stark trap. The synthesis was carried out for 8 h at 120 °C, in the same way as it was in the first step. The schematic route of KBOL plasticizer synthesis is shown in Fig. 2.

### 2.2.3. Synthesis of epoxidized mixed esters based on succinic acid, propylene glycol and oleic acid (EPKBOL)

Epoxidized mixed esters based on succinic acid, propylene glycol and oleic acid were synthesized in three step process. The first and second steps were carried out according to the method described in 2.2.2. In the second stage, 41.4 g of succinic acid and 0.50 g of the catalyst were added to 200 g of the reaction mixture. The epoxidation reaction was the third step, in which formic acid (16.3 g) was added to the reaction mixture (148.3 g) of the second step. Thereafter, hydrogen peroxide (152.5 g) was added dropwise for about 1 h. The whole process was carried out for 4 h at 60 °C with intensive stirring. After this time, the

obtained product was placed in a separating funnel and allowed to separate into two phases for about 1 h. The bottom layer, containing mainly water, formic acid and hydrogen peroxide, was removed, and the upper layer, containing the epoxidized mixed ester, was purified using aqueous solution of Na<sub>2</sub>HPO<sub>4</sub> (0.1 M) and distilled water, until pH value was close to 7. The purified product was dried using a vacuum evaporator. The schematic route of EPKBOL plasticizer synthesis is shown in Fig. 3.

### 2.3. Film preparation

Chitosan solutions were prepared according to Guo et al. (2019). Chitosan (2 %, w/v) was dissolved into 1.0 % (v/v) acetic acid aqueous solution with 30 % (w/w) plasticizer (GLY, SOR, EPOS, EPOP, OC, KBOL or EPKBOL) based on the mass of chitosan, by stirring with a magnetic stirrer at 800 rpm and room temp. for 24 h. Chestnut extract (0.75 % (w/v)) was added into the polymer solutions to obtain an active film according to the previous studies (Janik et al., 2022). The solutions were then homogenized for 5 min at 6000 rpm and were left overnight to let air bubbles disappear. Finally, the chitosan solutions were cast over Petri dishes (46 g per 12 × 12 cm dish) and dried at room temperature. Obtained films were named according to the plasticizers used, i.e. GLY film, SOR film, EPOS film, EPOP film, OC film, KBOL film and EPKBOL film, respectively.

### 2.4. Plasticizers characteristic

#### 2.4.1. Gas chromatography

PerkinElmer Autosystem XL gas chromatograph with an on-column injector, a ZB-5HT capillary chromatography column (length 15 m, i. d. 0.32 mm, 0.10 μm film) and a flame ionization detector (FID) was used for quantitative analysis of the compounds. Temperature for the injector was 50 °C and for the detector was 380 °C. Helium was used as the carrier gas at a pressure of 70 kPa in a temperature mode programmed from 50 to 370 °C.

Agilent Technologies 7890A gas chromatograph with a Mass Hunter software, a DB-5HT capillary column (length 30 m, i.d. 0.25 mm) and a mass detector (MSD type 7000 GC/MS Triple Quad) with a temperature mode programmed from 80 to 340 °C was used for qualitative identification of the reaction mixture components.

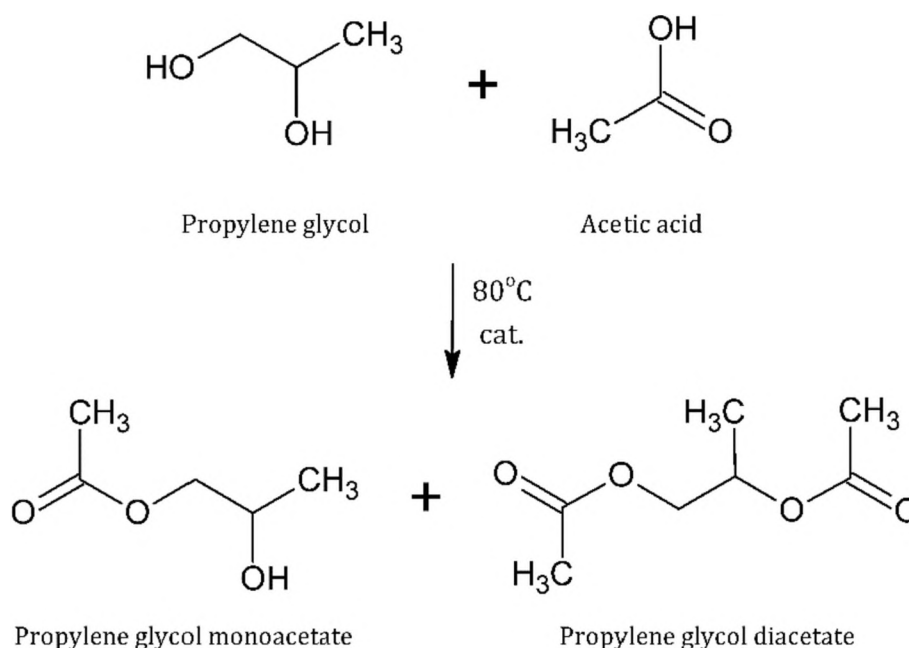


Fig. 1. Schematic route of OC plasticizer synthesis.

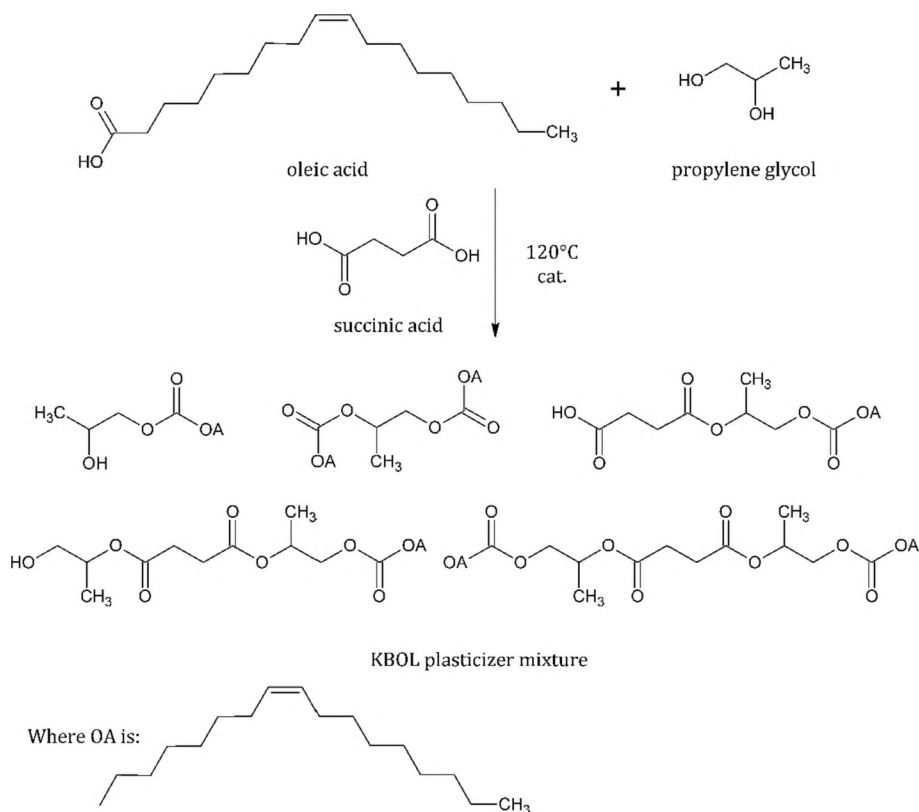


Fig. 2. Schematic route of KBOL plasticizer synthesis.

#### 2.4.2. Acid value, epoxy value, iodine value, saponification value, ester value and water content

The acid, epoxy, iodine and saponification values were determined according to PN-EN 14104:2004, PN-C-89085-13:1987, PN 87/C-04281:1987 and PN-EN ISO 3657:2004 standards, respectively. By subtracting the acid value from the saponification value, the ester value was calculated. The water content was determined using a 870 KF Titrimo Plus titration assembly (Metrohm), according to PN-ISO 760:2001 standard.

#### 2.4.3. Fourier-Transform Infrared Spectroscopy (FTIR)

FTIR Nicolet Model 6700 spectrophotometer fitted with the Omnic software (THERMO Scientific) was used for recording the infrared spectra based on PN-ISO 6286:1994 standard. FTIR tests were carried out using ZnSe 60 crystals and the SMART ATR reflection device.

#### 2.4.4. $^1\text{H}$ Nuclear Magnetic Resonance ( $^1\text{H}$ NMR)

$^1\text{H}$  NMR spectra of post reaction mixtures of all synthesized plasticizers were collected using a Varian UNITY INOVA 300 MHz spectrometer in  $\text{CDCl}_3$  as a solvent and TMS as internal standard.

### 2.5. Film characteristic

#### 2.5.1. Thickness

The film thickness was measured using a digital micrometer (Mitutoyo Absolute Tester, Tokyo Sangyo Co. Ltd., Japan) with a resolution of 0.001 mm. The values presented were calculated as an average value of twenty measurements taken at different points for each sample.

#### 2.5.2. Moisture content, swelling degree and total soluble matter

Moisture content (MC), swelling degree (SD), and total soluble matter (TSM) were determined gravimetrically according to the method described by Deng et al. (2020). The films were cut into  $2\text{ cm} \times 2\text{ cm}$  squares, then weighed and dried in an air-circulating oven at  $105\text{ }^\circ\text{C}$  for

24 h. After that the samples were weighed again and MC was calculated as the percentage of weight loss based on the original weight. The dried samples were then immersed into 100 mL of distilled water at  $25\text{ }^\circ\text{C}$  for 24 h. After removing the free surface water, the swollen films were weighed and SD was calculated as the percentage of weight loss based on the dry sample and after immersion it into water. The samples were dried once more at  $105\text{ }^\circ\text{C}$  for 24 h to get the final dry mass. TSM was calculated in relation to the dry mass, and it was expressed as the percentage of sample dry matter solubilized. The entire procedure was repeated for all samples after storage for 10 months.

#### 2.5.3. Contact angle

The wettability of the films was measured using an optical contact angle tester and the contour analysis systems (OCA15, DataPhysic). A  $1\text{ }\mu\text{L}$  droplet of distilled water was carefully deposited onto the film surface. After water droplet was stabilized, the contact angle of the sample was examined. The wettability was determined from the average of ten measurements. The entire procedure was repeated for all samples after storage for 10 months.

#### 2.5.4. Gas permeability

Oxygen and carbon dioxide permeability (OP and CDP, respectively) were determined using an isobaric apparatus as described in (Janik et al., 2022) according to the PN-EN ISO 2556:2002 standard. Pressurized oxygen (class 5.0) and carbon dioxide (technical gas) were used. The films in the form of disks with surface area of ca.  $6\text{ cm}^2$  were placed in a diffusion chamber. Before measurements, the samples were degassed for 24 h and then conditioned in the apparatus for 2 h with the appropriate gas. The measurements were performed at room temperature and at a controlled pressure in the range of 0.05 to 1.0 MPa. The gas flow rate was measured during the experiment using the El-Flow select flow meter (with a range of  $0\text{--}0.7\text{ cm}^3/\text{min}$ ). The permeation coefficient was determined according to eq. (1), where  $V$  is the volumetric flow ( $\text{mol}\cdot\text{s}^{-1}$ ),  $l$  is the sample thickness (m),  $S$  is the sample area ( $\text{m}^2$ ) and  $\Delta p$

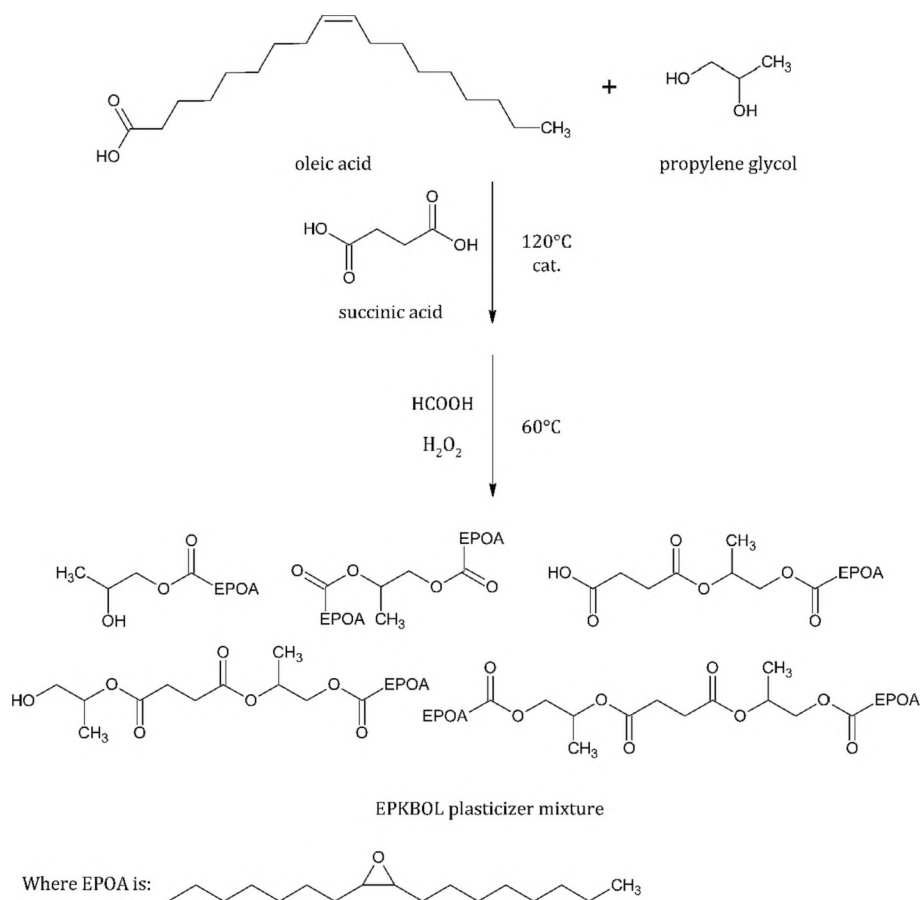


Fig. 3. Schematic route of EPKBOL plasticizer synthesis.

is the pressure difference on both sides of the film (Pa).

$$P = \frac{V \times l}{S \times \Delta p} \quad (1)$$

Water vapor permeability (WVP) was determined according to the ASTM E96-02 standard. The film samples in the form of discs (24.64 mm diameter) were mounted on a glass cell containing silica gel. The test glass cell was placed in a desiccator with NaBr, which generated a water-vapor differential pressure of 2854.23 Pa. The cell was weighed every 60 min for 8 h. Water vapor permeability was determined from the average of three measurements.

#### 2.5.5. Zeta potential analysis

The surface charge of the chitosan-based films was assessed by the zeta potential at the film-water interface. Streaming zeta potential was measured using the electrokinetic analyzer (SurPASS 3, Anton Paar, Austria). All samples based on chitosan were placed in the Adjustable Gap Cell for Planar Samples with dimensions of 20 × 10 mm. Samples were mounted in the holder using a double-sided adhesive tape. The adjustable gap ranged from 110 to 140 μm to avoid any material swelling effect on the measurement. Prior the zeta potential tests, all samples were rinse at least 6 times in 0.01 M KCl solution with pH of 5.9 to establish the cell constant. pH value of KCl solution was controlled by progressive addition of 0.05 M KOH. The zeta potential measurement was performed 3 times for each sample at a fixed pH = 5.85.

#### 2.5.6. Mechanical properties

Tensile tests of a film strip (8 cm × 2 cm) were performed by Instron 4466 testing machine. The tests were carried out at room temperature according to ASTM D882. A constant stretching rate of 5 mm/min was applied. Mechanical properties were determined from the average of

five measurements. The entire procedure was repeated for all samples after storage them for 10 months.

#### 2.5.7. Biodegradability

Biodegradation (soil degradability) of chitosan films with APs was carried out according to the method reported by De Carli et al. (2022). Small pieces of dry film samples (2 × 3 cm) were buried 5 cm below the surface of the soil in plastic containers. About 10 mL of water was added to the samples daily to keep the soil moisture at 40 %. After 15 days of incubation at 25 ± 1.0 °C, final weights of the samples were measured. Soil degradability was calculated as the percentage of weight loss based on the original weight. All tests were performed in triplicate.

#### 2.5.8. Morphological properties

The surface and cross-section morphologies of the film samples were studied using Phenom ProX equipped with the 3D Roughness Reconstruction software working at 10 kV acceleration voltage. Cross-sectional SEM samples were made by freeze fracturing in liquid nitrogen. Additionally, surface roughness of all investigated films was measured by the 3D RR software module of SEM and using the Filmetrics Profilm3D® optical profilometer in WLI normal mode, with 10× objective and 4× digital zoom option.

#### 2.5.9. Fourier-Transform Infrared Spectroscopy

FTIR spectra of the films were recorded in the range of 4000–650 cm<sup>-1</sup> with a resolution of 2 cm<sup>-1</sup> using a Spectrum Two spectrometer (Perkin Elmer). Films were cut into small discs and placed tightly between the sensor and support to ensure good contact. For each spectrum 25 scans were taken. These analyses were performed in duplicate at room temperature.



### 2.5.10. Thermal analysis

Thermogravimetric analysis (TGA) was carried out using a Mettler Toledo TGA 2 Thermo-balance. The samples (10 mg) were heated up in an open platinum crucible (Pt 70  $\mu$ L), in the temperature range 30–800 °C, with the heating rate  $\beta = 20$  °C/min, in the dynamic (100 mL/min) nitrogen (inert atmosphere, thermal stability) or air (oxidative atmosphere; thermoxidative stability) atmosphere. The thermographs were analyzed with the use of the STARE Thermal Analysis Software.

Differential Scanning Calorimetry (DSC) measurements were performed using the Mettler Toledo DSC 822e Differential Scanning Calorimeter. DSC curves of each film were obtained from the second heating run at a rate of 10 °C/min, after the first run of heating up to 190 °C and cooling to 0 °C at the same rate, under nitrogen atmosphere. The weight of each sample film was about 10 mg.

### 2.6. Statistical analysis

Experimental data were analyzed for statistical significance by analysis of variance (ANOVA) and Tukey's multiple range test with a  $p < 0.05$  significance level. Data were evaluated by OriginPro 8.5.0 software (OriginLab, Northampton, MA, USA).

## 3. Results and discussion

### 3.1. Plasticizer characterization

Each synthesized plasticizer was prepared by esterification reaction. EPKBOL plasticizer was additionally subjected to epoxidation reaction. The plasticizers were analyzed by GC/FID and GC/MS and their chemical compositions are shown in Table 1.

OC plasticizer was synthesized from propylene glycol and acetic acid (Fig. 1). The aim of this synthesis was to obtain as many monoesters of acetic acid and propylene glycol as possible, because they contain free hydroxyl groups which can interact with the hydroxyl groups of chitosan via hydrogen bonding (Chen et al., 2018). Since the esterification reaction is not selective, esters mixture containing 67.0 wt% of propylene glycol monoacetate and 9.4 wt% of propylene glycol diacetate was obtained. Due to the use of an excess of propylene glycol, 21.1 wt% of the compound remained in the final mixture. Analysis of mass spectra collected for each main components present on the chromatogram confirmed the presence of four compounds in OC plasticizer, i.e. propylene glycol acetate (two isomers), propylene glycol diacetate, and unreacted substrates: acetic acid and propylene glycol. The mass spectra and fragmentation analysis are presented in Supplementary Data (Figs. S1–S2), as well as  $^1\text{H}$  NMR spectrum of OC plasticizer (Fig. S7). Analysis of  $^1\text{H}$  NMR spectrum confirms the presence of all aforementioned species (Table S1). Moreover, the content of each component

**Table 1**  
Composition of OC, KBOL and EPKBOL plasticizers determined by gas chromatography.

Compound	OC (wt %)	KBOL (wt %)	EPKBOL (wt %)
Acetic acid	2.3	–	–
Propylene glycol	21.1	0.4	0.1
Succinic acid	–	0.0	0.0
Propylene glycol monoacetate	67.0	–	–
Propylene glycol diacetate	9.4	–	–
Propylene glycol succinate	–	1.1	0.6
Oleic acid	–	2.3	–
Epoxidized oleic acid	–	–	2.4
Propylene glycol monooleate	–	11.5	7.3
Propylene glycol dioleate	–	33.2	34.9
Succinic acid, propylene glycol and oleic acid mixed esters	–	15.2	16.2
Non-volatile components	–	33.5	35.6
Others	0.3	2.9	2.9

obtained from  $^1\text{H}$  NMR spectrum is consistent with the GC data (see Fig. S7 and Table S2 in Supplementary Data).

KBOL and EPKBOL plasticizers were both obtained by similar methods - the difference is that more succinic acid was used during the second step of EPKBOL synthesis; the compound was also subjected to epoxidation reaction. In this reaction, the unsaturated bonds of oleic acid moieties were oxidized with performic acid to introduce oxirane rings into the EPKBOL structure. The purpose of this approach was to obtain two different plasticizers that can interact with chitosan in different ways. KBOL is a mixture of structures containing hydroxyl groups but also carboxyl groups that can bond amino groups of chitosan (Brasselet et al., 2019). In contrast, EPKBOL, due to the presence of oxirane rings, can bond both amino and hydroxyl groups of chitosan, depending on the pH (Jain et al., 2013; Kumar et al., 2004). Table 1 shows the compositions of KBOL and EPKBOL before the epoxidation, as it was assumed the reaction did not affect ester bonds and ester composition.

In the first synthesis step for both plasticizers, mono- and diesters of oleic acid and propylene glycol were obtained. In the second step, succinic acid was added. During reaction with propylene glycol, its succinate was produced (1.1 wt% and 0.6 wt% for KBOL and EPKBOL, respectively). Subsequently, in the reaction of succinic acid with propylene glycol monooleate, mixed esters of succinic acid, propylene glycol and oleic acid were obtained (15.2 wt% and 16.2 wt% for KBOL and EPKBOL, respectively). After the second step, 11.5 wt% and 7.3 wt% of propylene glycol monooleate and 33.2 wt% and 34.9 wt% of propylene glycol dioleate remained in KBOL and EPKBOL, respectively. Succinic acid reacting with propylene glycol most probably formed not only esters but also oligoesters by oligomerization reactions of these two compounds. This is indicated by the high content of non-volatile components in the products. The oligomerization products, marked as non-volatile components in Table 1, are responsible for 33.5 wt% and 35.6 wt% of mass for KBOL and EPKBOL, respectively. A slight difference in the amount of succinic acid added does not significantly affect the final plasticizer composition. Mass spectra confirmed the presence of five compounds, i.e. propylene glycol monooleate (two isomers), propylene glycol dioleate, oleic acid, propylene glycol, succinic acid mixed esters (two isomers) in KBOL, and also five components of EPKBOL, i.e. epoxidized propylene glycol monooleate (two isomers), epoxidized propylene glycol dioleate, epoxidized oleic acid propylene glycol, succinic acid mixed esters (two isomers) and epoxidized oleic acid. However, epoxidized mixed esters of oleic acid propylene glycol and succinic acid were not seen on the EPKBOL chromatogram. The epoxidation reaction takes place under relatively mild conditions and should not affect the content of the different types of esters (this is confirmed by the analogous KBOL and EPKBOL ester values - Table 2). Therefore, it can be assumed that epoxidized mixed esters of oleic acid propylene glycol and succinic acid are also present in the analyzed EPKBOL sample. However, due to the lower volatility of these esters, their presence could not be confirmed by GC/MS. The corresponding mass spectra of identified compounds and the fragmentation patterns are shown in Figs. S3–S6 (Supplementary Data). The structures of all components of both oleic acid based plasticizer, found from GS/MS, are also confirmed by the  $^1\text{H}$  NMR analysis (Supplementary Data, Figs. S8–S9). Their interpretation is summarized in Tables S3 and S5 (Supplementary Data).

**Table 2**  
Chemical properties of the synthesized plasticizers.

Properties	OC	KBOL	EPKBOL
Acid value (mg KOH/g)	21.0	22.1	12.0
Epoxy value (mol/100 g)	–	–	0.19
Iodine value (g I <sub>2</sub> /100 g)	0.0	53.0	5.7
Saponification value (mg KOH/g)	417	305	296
Ester value (mg KOH/g)	392	283	284
Water content (wt%)	0.55	0.33	0.19

The structures of the synthesized plasticizers were also analyzed by FTIR. The spectra of OC, KBOL, and EPKBOL are shown in Fig. S10 (Supplementary Data) and their main IR peaks with corresponding functional groups are shown in Table S5 (Supplementary Data). The FTIR spectra for each plasticizer (OC, KBOL and EPKBOL) show a strong stretching vibration band at  $1736\text{ cm}^{-1}$ , which can be attributed to the carbonyl bond (C=O), characteristic for ester groups. Additionally, the occurrence of esterification reaction is confirmed by the presence of ester C—O—C bond stretching vibration bands at  $1043\text{ cm}^{-1}$  and  $1232\text{ cm}^{-1}$  for OC; at  $1082\text{ cm}^{-1}$  and  $1156\text{ cm}^{-1}$  for KBOL; at  $1082\text{ cm}^{-1}$  and  $1154\text{ cm}^{-1}$  for EPKBOL. The spectra show a strong and broad O—H stretching vibration band for OC at  $3427\text{ cm}^{-1}$  and a weak band at  $3464\text{ cm}^{-1}$  for KBOL and EPKBOL. These bands correspond to the hydroxyl groups in the unreacted propylene glycol, and also to their monoesters (containing one free hydroxyl group). GC analysis confirms the presence of these compounds in each sample, but for OC the amount of unreacted glycol and monoesters is ca. 7 times higher than for KBOL and EPKBOL, what is also seen in the bands intensity. At  $2924/2925\text{ cm}^{-1}$  and  $2854/2855\text{ cm}^{-1}$  for KBOL and EPKBOL, respectively, bands are present, corresponding to the C—H stretching vibrations of fatty acid hydrocarbon chains moiety. In the FTIR spectra of OC, there are three weak bands at  $2882\text{ cm}^{-1}$ ,  $2936\text{ cm}^{-1}$  and  $2974\text{ cm}^{-1}$ , corresponding to the C—H stretching vibrations of acetic acid hydrocarbon chain moiety. The FTIR spectra for KBOL, unlike for other synthesized esters, exhibit an absorption band at  $3009\text{ cm}^{-1}$ , which corresponds to the C—H stretching

and deformation vibrations in unsaturated —HC=CH— bonds. It indicates the presence of unsaturated C=C bonds in the structure of KBOL. Its absence in EPKBOL indicates a reaction involving unsaturated bonds.

The chemical properties, such as acid value, iodine value, saponification value, ester value and water content were determined for the plasticizers and are shown in Table 2. This values provide an additional confirmation for the occurrence of esterification and epoxidation reactions, respectively. The epoxy value was determined only for EPKBOL and it was  $0.19\text{ mol}/100\text{ g}$ , what confirms formation of oxirane rings, further acknowledged by the iodine number. In the case of OC plasticizer, the iodine number was equal to zero since therein are no unsaturated bonds. For KBOL, the iodine number was  $53.0\text{ g I}_2/100\text{ g}$ , while for EPKBOL after epoxidation, it decreased to  $5.7\text{ g I}_2/100\text{ g}$ . It indicated a low content of unsaturated bonds, and confirmed the efficiency of the epoxidation reaction. Acid values were equal to  $21.0\text{ mg KOH/g}$ ,  $22.1\text{ mg KOH/g}$  and  $12.0\text{ mg KOH/g}$  for OC, KBOL and EPKBOL, respectively. The saponification value was determined for each plasticizer to calculate the ester value. OC had the highest ester value of  $392\text{ mg KOH/g}$  - for KBOL and EPKBOL the ester values were almost identical:  $283\text{ mg KOH/g}$  and  $284\text{ mg KOH/g}$ , respectively. This difference is due to the size of the individual molecules. The ratio of acetic acid and propylene glycol esters molecules (short chain structures) to OC will be higher than the amount of succinic acid, propylene glycol and oleic acid esters molecules (long chain structures). All plasticizers were characterized by low water content, below  $0.6\%$ .

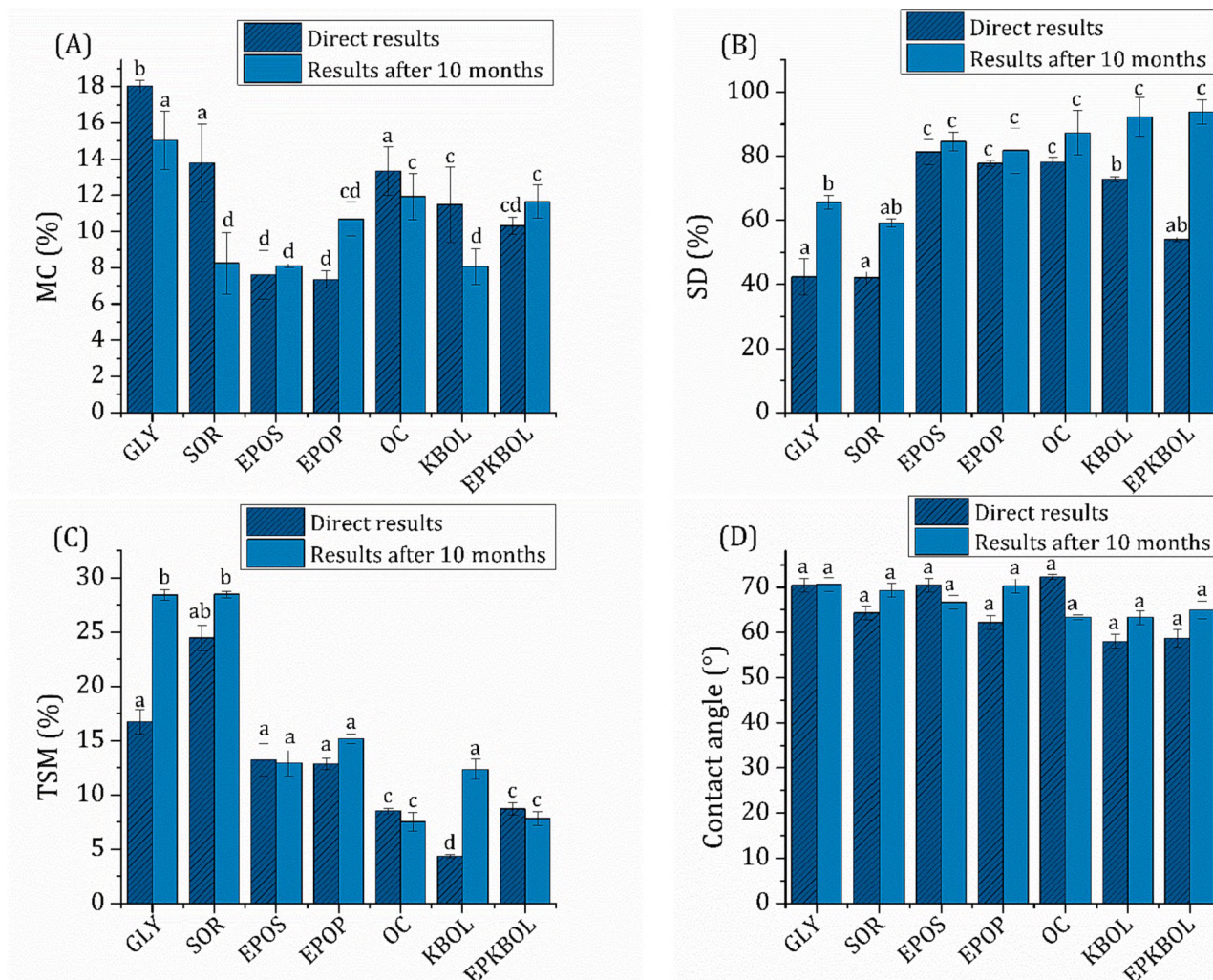


Fig. 4. Moisture content (A), swelling degree (B), total soluble matter (C) and contact angle (D) for chitosan-based films; different lowercase letters indicate significantly different value at  $p < 0.05$  using Tukey's Multiple Range Test.



### 3.2. Film characterization

At a macroscopic scale, all films were homogeneous with a brownish color due to the presence of a chestnut extract (see Supplementary Data, Fig. S11). All films had a similar thickness of ca. 90  $\mu\text{m}$ .

#### 3.2.1. Hydrophobicity

Hydrophobicity was determined by moisture content, swelling degree, total soluble matter and contact angle measurements. MC, SD and TSM were determined immediately after film preparation (direct results:  $\text{MC}^{\text{DR}}$ ,  $\text{SD}^{\text{DR}}$ ,  $\text{TSM}^{\text{DR}}$ ) and after 10 months of storage (results after 10 months:  $\text{MC}^{10}$ ,  $\text{SD}^{10}$ ,  $\text{TSM}^{10}$ ). The results, summarized in Fig. 4, indicate the ability of the films to interact with water molecules. As shown in Fig. 4A, all  $\text{MC}^{\text{DR}}$  values for the films with APs decreased, compared to the control films (GLY and SOR). In contrast, the  $\text{MC}^{10}$  for sorbitol was much lower and decreased by almost a half, compared to the fresh sample.  $\text{MC}^{\text{DR}}$  values are similar (around 8 %) for the samples prepared with CAPs, what is >50 % less than for the GLY and SOR control samples. In the case of CAPs, the  $\text{MC}^{10}$  results remained the same for EPOS before and after ageing and increased slightly, to about 11 % for EPOP. Regarding the films prepared with the three synthesized plasticizers, it was noticed that the type of plasticizer had a slight (ca. 1.5 %) influence on the  $\text{MC}^{\text{DR}}$ . A similar relationship was observed for the values of  $\text{MC}^{10}$ . In the case of SD (Fig. 4B), it can be noticed that the  $\text{SD}^{\text{DR}}$  value was almost 50 % higher for all the films with APs, compared to GLY and SOR films (with an exception for  $\text{SD}^{\text{DR}}$  of EPKBOL, for which the value increased by about 30 %, compared to GLY). Similar relationship was observed after 10 months. All the  $\text{SD}^{10}$  values for APs are higher than for glycerol and sorbitol, but the difference is slightly smaller, by about 25 %, than for the direct results. On the other hand,  $\text{TSM}^{\text{DR}}$  and  $\text{TSM}^{10}$  values (Fig. 4C) are lower for all films with APs, compared to the GLY film, and especially to the SOR film measured directly, which has the highest  $\text{TSM}^{\text{DR}}$  value of about 25 %. The results obtained after 10 months of ageing also suggest that the films with glycerol and sorbitol show the highest  $\text{TSM}^{10}$  values - ca. 28 % for both films, while the values for APs were at least half as high. Therefore, these results indicate that the APs films are more resistant to destruction by contact with water than the GLY and SOR films. MC, SD and TSM values for chitosan-based films with plasticizers were described in several studies (Leceta et al., 2013; Ma et al., 2017; Debandi et al., 2016). For instance, Ma et al. who used glycerol as a plasticizer indicated that the SD values increased with an increase in the glycerol concentration in the films. On the other hand, Debandi et al. reported that the SD value increased until the glycerol content of 30 % and decreased at a plasticizer content of 50 %. Leceta et al. observed that the TSM value increased with the increase in the amount of glycerol in the sample. The observation suggests specific interactions between plasticizer and water.

To investigate the effect of APs on film hydrophobicity, contact angle values for chitosan films were determined (Fig. 4D). According to our results, the contact angle for the chitosan film without plasticizer (but containing chestnut extract) is about 45°. It can be observed that the addition of APs increased contact angle value to about 60° (EPOP, KBOL, EPKBOL) and to about 70° (EPOS, OC). The reference plasticizers (GLY and SOR) also caused the contact angle values to increase to about 70° and 65°, respectively. Analyzing the results for samples aged for 10 months, no significant changes are observed in the values of contact angle. The results for GLY and SOR after 10 months are similar to APs. The contact angle values for all films is <90°, indicating the hydrophilic nature of the surfaces. Nevertheless, plasticizers used in this study caused reduction of hydrophilic character of chitosan. According to Chen et al. (2021) the lower surface hydrophilicity of films containing plasticizers is due to the compaction of biopolymer chains that reduces free volume and assists binding between plasticizer and chitosan polar groups, reducing thus the amount of free polar groups.

#### 3.2.2. Gas permeability and zeta potential

In order to use films in packaging applications, high barrier properties are required, reflecting the ability of oxygen, carbon dioxide and water vapor molecules to pass through the film. In addition, the surface charge of the packaging material is also an important aspect, which is the primary parameter for increasing or suppressing interactions of compounds dissolved in aqueous solution with the surface of the packaging (Zemljic et al., 2020). The literature indicates that changes in the physical properties of the films are closely related to the nature of the polyelectrolytes of the biopolymer components and their ability to affect microstructural network through ion groups (Sabbah & Esposito, 2016). For this reason, the zeta potential for the obtained films was also determined. As it can be seen in Fig. 5A, the zeta potential of chitosan film without plasticizer (containing only chestnut extract) was equal to  $-4.28 \pm 0.39$  mV. Numerous studies have shown that the zeta potential for neat chitosan is positive and at pH value at which our measurements were made (5.85) the zeta potential values for neat chitosan were reported between +11 and +17 mV (Mehdizadeh et al., 2022; Ni et al., 2021), while modification of chitosan by different additives causes changes of the potential- both directions of the change are possible (Maciel et al., 2017). Pavlátková et al. showed that the value of the zeta potential depends on the type of used extract (Pavlátková et al., 2022). In our case, the chestnut extract lowered the zeta potential to negative values. Neri et al. (2010) investigated the composition of chestnut extract and showed that its main components are starch, sucrose, proteins and lipids. Polysaccharides, like starch impact on the decrease of zeta potential because they contain hydroxyl groups which can create electrostatic interactions with positively charged amino groups of chitosan (Ahmad et al., 2020; Nobeyama et al., 2018; Voci et al., 2022). No significant deviation in zeta potential for films containing plasticizers was observed. This means that the type of plasticizer has not the dominant effect on the zeta potential of the chitosan film, and the negative value of zeta potential is only related to the presence of chestnut extract.

When it comes to the permeability of  $\text{O}_2$ ,  $\text{CO}_2$  and  $\text{H}_2\text{O}$ , there are several factors that may be responsible for the observed differences. Among them are the physical state of the plasticizer, their molecular weight, and the structure of the film as a result of the chemical interaction of the plasticizer (Srinivasa et al., 2007). Oxygen, carbon dioxide and water vapor permeability values of the films under investigation are shown in Fig. 5B. The highest OP, CDP and WVP values were observed for EPOP film, indicating its low barrier properties, compared to the films with other plasticizers. This is probably due to the greater surface roughness of this film compared to films containing other plasticizers (see Supplementary Data, Table S6). The relation between roughness of a film and water vapor permeability was studied by Ma, Yang, et al. (2019) and Ramon and Hoek (2013). They showed that an increase in roughness leads to increased water permeability. All the films with APs exhibited higher barrier properties, compared to GLY, SOR and CAPs films. EPKBOL film showed almost no detectable  $\text{O}_2$  and  $\text{CO}_2$  permeability, while OC and KBOL films showed permeability ( $\text{cm}^3 \text{m}^{-1} \text{s}^{-1} \text{Pa}^{-1}$ ) ca. 5 and  $8 \times 10^{-12}$  for  $\text{O}_2$  and ca.  $4 \times 10^{-13}$  and  $3 \times 10^{-12}$  for  $\text{CO}_2$ , respectively. Caicedo et al. (2022) investigated the effect of the amount and type of plasticizer (glycerol and sorbitol) on WVP values. The barrier results were similar to those obtained in this study (at levels ranging from  $10^{-12} \text{g} \cdot \text{m}^{-1} \text{s}^{-1} \text{Pa}^{-1}$  to  $10^{-12} \text{g} \cdot \text{m}^{-1} \text{s}^{-1} \text{Pa}^{-1}$ ) and it was also proven that the films obtained with both plasticizers did not show different barrier results, but the WVP values increased as the amount of plasticizer increased. An increase in gas permeability can be expected when the material is plasticized, which increases the mobility of polymer chains and thus decreases the resistance of the film to gas permeation. This effect, in turn, can be significantly offset by good barrier properties of the plasticizer itself and its ability to effectively fill small voids in the polymer matrix (Srinivasa et al., 2007). In addition, Jiménez-Regalado et al. (2021) showed that the film that absorbed the most moisture was the one that provided the best barrier to water vapor

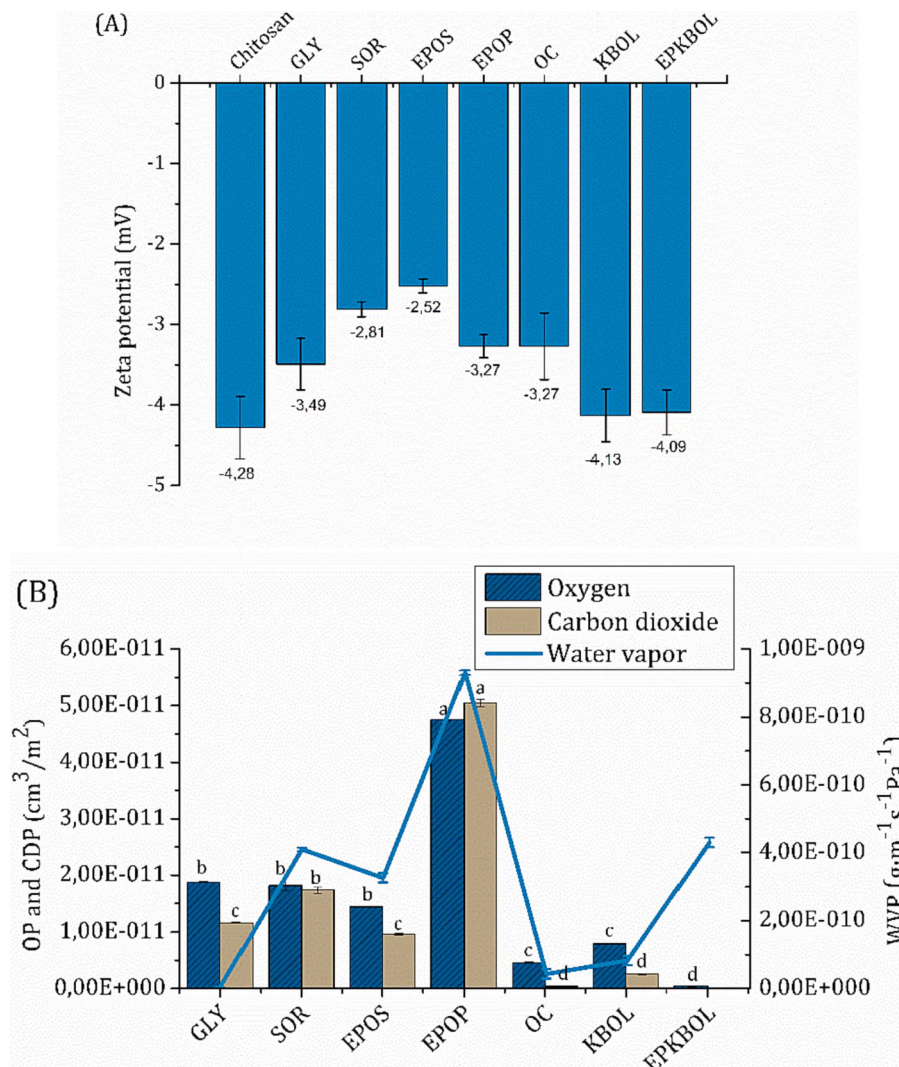


Fig. 5. Zeta potential (A), carbon dioxide and water vapor permeability (B) for chitosan-based films, different lowercase letters indicate significantly different value at  $p < 0.05$  using Tukey's Multiple Range Test.

what is also observed in this study, e.g., GLY film with the highest MC value has the best barrier to water vapor, and EPOP film with the lowest MC value has the lowest WVP value. The presence of water molecules and their interaction with the polar groups of chitosan through inter-chain hydrogen bonds gradually reduce the cohesion energy of the polymer, leading to plasticization of the matrix and an increase in the diffusion coefficient (Jiménez-Regalado et al., 2021). On the other hand, Sabbah et al. (2019) conducted barrier studies of chitosan films plasticized with spermidine and/or glycerol and compared them with commercially available films used as food casings. Their results showed that the films with the addition of these plasticizers showed similar barrier properties compared to commercial film against oxygen and carbon dioxide, but increased permeability against water vapor. In our case, it can be seen that APs have the greatest ability to fill small voids in the polymer matrix. This is due to the different interactions of various esters and their epoxidized derivatives having different molecular weights.

### 3.2.3. Mechanical properties

Mechanical properties of polymer materials are largely related to the distribution and density of intermolecular and intramolecular interactions in the network formed within e.g. chitosan films (Leceta et al., 2013). Tensile strength (TS) and elongation at break (EB) for chitosan films were measured immediately after the film preparation (direct

results:  $TS^{DR}$ ,  $EB^{DR}$ ) and after 10 months of its storage ( $TS^{10}$ ,  $EB^{10}$ ) to determine the effect of APs on the mechanical properties. The characteristic stress-strain curves of the films are illustrated in Fig. 6. It can be seen that the presence of APs, particularly EPOS, EPOP and OC, has a positive effect on the mechanical properties of the films compared to GLY and SOR. For films with APs, the investigated samples displayed  $TS^{DR}$  values spanning from ~1 to 10 MPa and  $TS^{10}$  values in the range of approx. 2–3 MPa. Although the highest  $TS^{DR}$  results were recorded for KBOL and GLY, their  $EB^{DR}$  was lower than for most APs (only EPKBOL showed  $EB^{DR}$  at a comparable level). Moreover, the glycerol- and sorbitol-based films after 10 months of ageing were to brittle, even for handling them. Nevertheless, direct tests for the films prepared with GLY and SOR showed that these types of plasticizer had strong influence on the mechanical properties of the film. In the case of SOR, the measured properties of the film were about 1 MPa ( $TS^{DR}$ ) and 10 % ( $EB^{DR}$ ), which were the lowest values for all of the performed tests. Such weak mechanical properties of chitosan films plasticized with sorbitol were also reported by Rodríguez-Núñez et al. (2014), where elongation at break was about 2 % and tensile strength was about 40 MPa. Comparing the APs used in this study, it can be stated that most of them improve the  $EB^{DR}$  by about 30–46 % (EPOS, EPOP and OC), with the exception of KBOL, which caused a slight decrease of 7 %. Nevertheless, this decrease is balanced by an increase in  $TS^{DR}$  of about 30 %, compared to GLY and up to about 80 %, compared to SOR. Other chitosan samples with APs



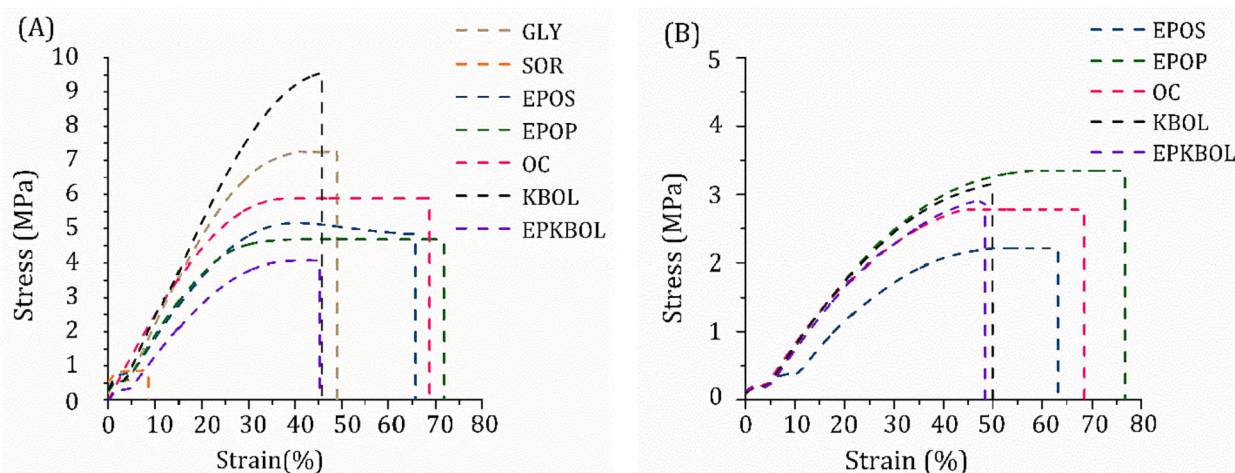


Fig. 6. Stress vs. strain curves of chitosan-based films: A) direct results; B) results after 10 months, different lowercase letters indicate significantly different value at  $p < 0.05$  using Tukey's Multiple Range Test.

(EPOS, EPOP, OC) showed an increase in  $TS^{DR}$  over sorbitol and a decrease in  $TS^{DR}$  from 20 to 40 %, compared to glycerol. Additionally, the significant advantage of the APs, compared to sorbitol and glycerol, is that all EB values for the APs showed no deterioration over 10 months. The samples were not as brittle as those with glycerol and sorbitol, indicating a much lower loss of these plasticizers from chitosan over time. Such changes in mechanical properties under the influence of various plasticizers and time are the result of weakening of different intermolecular forces between adjacent chitosan chains, resulting in an increase in free volume and a decrease in mechanical properties (Debandi et al., 2016). The inclusion of APs either increased or resulted in equally good mechanical properties of the films compared to GLY, which was due to the fact that added plasticizers could establish intermolecular hydrogen bonding interactions with the matrix, making the films more resistant (Tan et al., 2020; Zhang et al., 2020). Of the plasticizers we synthesized, the best film mechanical properties were provided by OC plasticizer, containing primarily propylene glycol monoacetate, but also propylene glycol diacetate, acetic acid and propylene glycol in its mixture. Therefore, it can be concluded that these compounds show better plasticizing activity than larger molecule like propylene glycol succinate, oleic acid, propylene glycol monooleate, propylene glycol dioleate or succinic acid, propylene glycol and oleic acid mixed esters.

### 3.2.4. Biodegradability

The soil degradation study of the obtained films showed that after 15 days, the films were completely degraded. The application of APs to the films did not change the degradation properties in the soil. Chitosan films using the alternative plasticizers proposed in this research can be considered as fully biodegradable materials.

### 3.2.5. Morphological analysis

The external and internal structure of chitosan films containing investigated plasticizers was presented by imaging their surface and cross-section, as illustrated in Fig. S12 (Supplementary Data). Investigated films were smooth, compact and without any crack or pores. The cross-section of SEM images indicated a uniform smooth interface. These observations confirmed good interaction and compatibility of the chitosan-based films obtained with glycerol, sorbitol and APs. Also no changes were noticed between the films obtained with two commercial APs plasticizers and our proposed APs.

### 3.2.6. Fourier-Transform Infrared Spectroscopy

FTIR spectroscopy was used to evaluate interactions between plasticizers and chitosan. The shifts and changes in intensity of the

characteristic peaks in the spectra reflect the physical bonds and chemical interactions between the substances and characterize their compatibility. Fig. 7 shows FTIR spectra of unplasticized and plasticized chitosan-based materials. The spectra of unplasticized, GLY and SOR films (Fig. 7A) are almost the same, indicating that glycerol and sorbitol did not change the structure of chitosan but only interacted with it. The spectra of GLY and SOR films exhibited only slightly lower intensities, which indicates intermolecular interaction through hydrogen bond formation. The most significant differences in spectral intensity are observed for CAPs and APs (Figs. 7B–C and 7D–F, respectively). The absorption bands between 1200 and 870  $\text{cm}^{-1}$  are characteristic for -CO stretching vibrations and could be considered as a specific region of the polysaccharide skeleton (Long et al., 2021). Their lowest intensity was observed for films with alternative plasticizers, most notably EPOP, OC and KBOL. Chitosan exhibited two strong vibrational bands at 1550 and 1400  $\text{cm}^{-1}$ , which were attributed to the vibrations of amide I and amide II, respectively (Leceta et al., 2013). For EPOP, OC and KBOL, these bands were almost imperceptible, suggesting strong interactions (mainly intermolecular hydrogen bonding interactions) between these plasticizers and the polymer matrix. The peaks in the range of 2900 and 2800  $\text{cm}^{-1}$  are characteristic to the methyl group. In the case of OC and EPKBOL, these bands were almost imperceptible, which also suggested their strong interaction with chitosan. A broad band in the range of about 3600–3000  $\text{cm}^{-1}$  is attributed to the N–H and OH–O stretching vibrations (Xu et al., 2019). This band is also related to some extent to the intermolecular hydrogen bonds of the chitosan molecules (Jančić et al., 2021). For both CAPs and APs, the intensity of this band was significantly lower compared to unplasticized chitosan or GLY and SOR films.

### 3.2.7. Thermal analysis

Thermal and thermoxidative stability of neat chitosan and the chitosan-based films was evaluated by a thermogravimetric analysis and differential scanning calorimetry. In TGA, two parameters were measured: the temperature of the onset of degradation ( $T_{\text{onset}}$ ) and the temperature at which thermal degradation results in 50 % weight loss ( $T_d^{50}$ ). In turn, DSC allowed determining the glass transition temperature of the obtained materials. The results are summarized in Table S7 (Supplementary Data) and the obtained TG curves for the two different atmospheres are shown in Fig. 8. The results indicate that all plasticized films exhibit similar thermal degradation behavior to chitosan. They undergo an initial slight weight loss at around 100 °C and then sharp weight loss from 200 to 350 °C. The first stage is related to the evaporation of water and residual acetic acid present in the polymer matrix (Souza et al., 2019). Whereas the second thermal event is attributed to

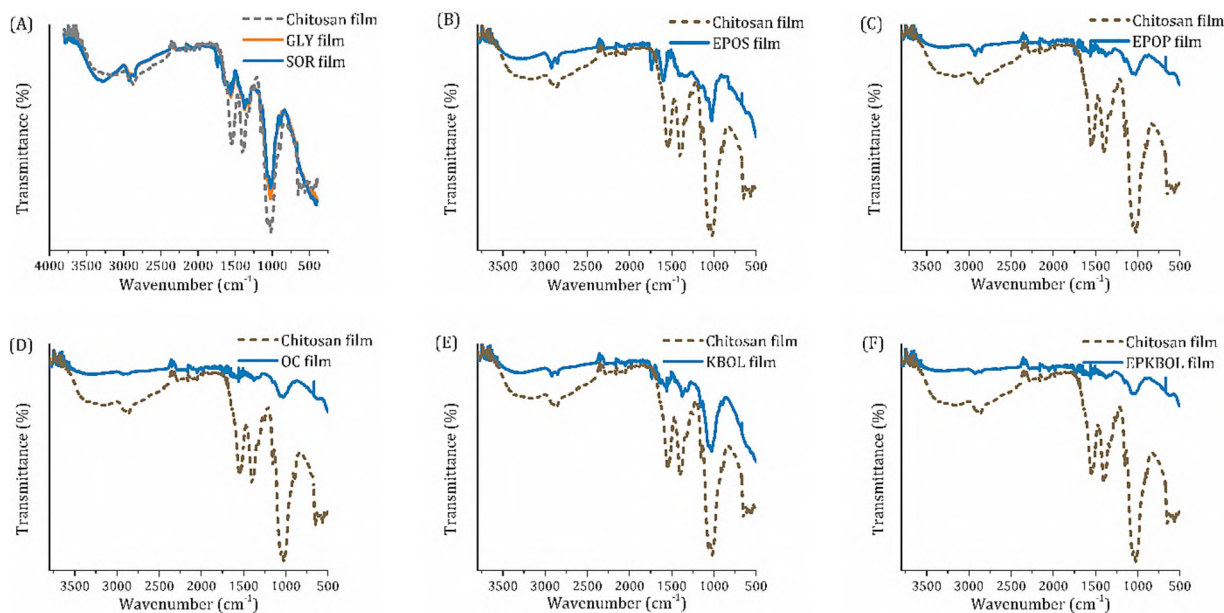


Fig. 7. FTIR spectra of pure chitosan and: A) GLY, SOR; B) EPOS; C) EPOP; D) OC; E) KBOL and F) EPKBOL films.

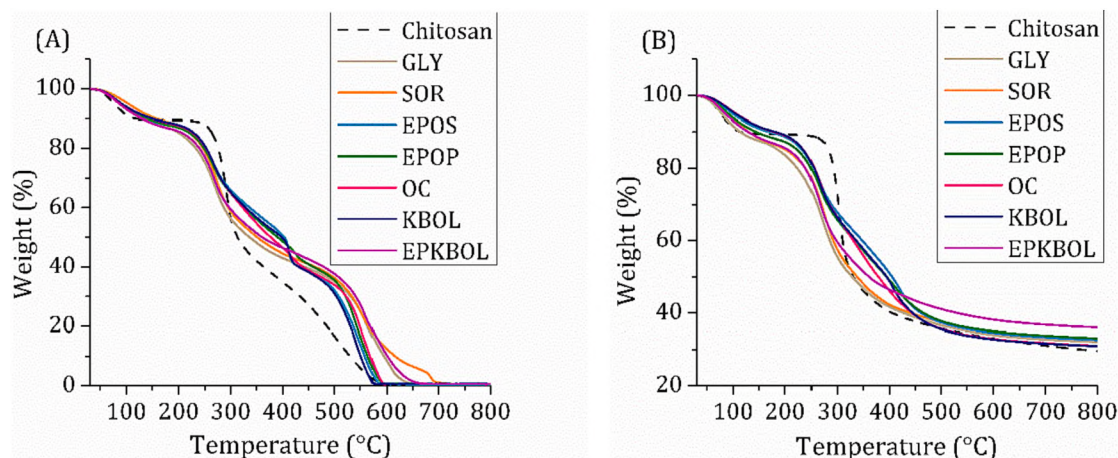


Fig. 8. TG curves of chitosan and chitosan-based films: A) in air; B) in nitrogen.

polymer decomposition (Szymańska & Winnicka, 2015). In the case of chitosan, the main thermal degradation step begins at 300 °C, which is associated with the highest weight loss ( $\approx 60\%$ ). This result may be due to degradation of the polysaccharide and deacetylation of chitosan (Corazzari et al., 2015). The third step, occurring in the temperature above 400 °C in air, can be associated with the oxidative degradation of carbonaceous residue formed during the previous step (Lim et al., 2015; Ma, Qiao, et al., 2019). The most significant difference can be observed when comparing the initial thermal degradation for neat and plasticized chitosan. As shown in Table S7 (Supplementary Data), the onset decomposition temperature in an air atmosphere was 256.9 °C for chitosan and decreased to 213.8 °C for GLY film, and to about 220 °C for all other films. A similar relationship was observed in a nitrogen atmosphere.

It is also worth noting that at temperatures above 300 °C, the neat chitosan displayed a higher rate of thermal decomposition than the plasticized films, especially CAPs and APs (an increase in  $T_d^{50}$  of about 90 °C). This can be attributed to the good interaction that occurs between the alternative plasticizers and the chitosan matrix, as evidenced by the FTIR spectra and SEM cross-section images. This result was also supported by Wang et al. (2006), Lavorgna et al. (2010) and Kusmono

and Abdurrahim (2019), who found that the thermal stability at higher temperature of the plasticized film was better compared to the control film due to the formation of cross-linking network induced by hydrogen bonds. Among our APs films, EPKBOL is found to have the lowest thermal stability, with values similar to GLY and SOR. On the other hand, DSC results show that the  $T_g$  of neat chitosan is 189 °C and the inclusion of a plasticizer results in a decrease of  $T_g$ . This is consistent with results obtained by other (Dong et al., 2004; Ma, Qiao, et al., 2019). GLY, SOR and EPKBOL films showed similar  $T_g$  of about 160 °C, while other samples showed a lower  $T_g$  of about 150 °C. According to our thermoanalytical studies, it can be concluded that the nature of plasticizer has an insignificant influence on the thermal stability of chitosan films.

#### 4. Conclusions

Chitosan-based films were prepared using commercial and alternative, environmentally friendly plasticizers that were synthesized from compounds such as propylene glycol, acetic acid and succinic acid. These plasticizers were characterized by GC/FID and GC/MS and their key chemical properties were determined. The structures of the obtained



plasticizers were confirmed by  $^1\text{H}$  NMR. Commercial plasticizers, such as epoxidized palm oil and epoxidized soybean oil, were also used to compare them with the traditional plasticizers, i.e. glycerol and sorbitol.

The results indicate that the innovative plasticizers OC, KBOL and EPKBOL improve the properties of chitosan film in comparison with films containing GLY, SOR or commercially available EPOS, EPOP plasticizers. The films with novelty plasticizers are less hydrophilic than those prepared with traditional plasticizers, suggesting a potential solution to the problems of destructive effects caused by moisture (the TSM results, among others, are lower for all APs films, compared to the GLY film and especially to the SOR film, which showed the highest TSM<sup>DR</sup> value of about 25 %). In addition, the films provide an effective barrier to oxygen, carbon dioxide and water vapor, which helps to maintain the product quality. Furthermore, the addition of APs improves the mechanical properties of the films. Taking into account the deterioration over time, chitosan films with APs exhibit undoubtedly much better properties than those containing traditional plasticizers (above all, elongation at break was maintained at about 50 % for KBOL and EPKBOL and about 80 % for EPOS, EPOP and OC). Our study shows that comparing all the results with each other, the most effective plasticizer turned out to be the OC plasticizer. It exhibits the best elongation at break and as good barrier and hydrophilic properties as the other APs.

### CRedit authorship contribution statement

**Author contributions:** Conceptualization, W.J. and G.D.; methodology, W.J., K.L., J.K-K., U.S., E.N-B., E.S., H.N-K., R.T. and G.D.; software, W.J., K.L., M.N. and R.T.; validation, W.J., K.L. J.K-K., U.S., E.N-B., E.S., H.N-K., R.T. and G.D.; formal analysis, G.D.; investigation, W. J., K.L.; resources, W.J., K.L., G.D.; data curation, W.J., K.L. and M.N.; writing—original draft preparation, W.J., K.L.; writing—review and editing, R.T. and G.D.; visualization, W.J.; supervision, G.D. and S.K.; project administration, W.J.; funding acquisition, W.J. All authors have read and agreed to the published version of the manuscript.

### Formatting of funding sources

This research was co-financed by the Ministry of Education and Science of Poland under grant No DWD/4/21/2020.

### Declaration of competing interest

The authors declare that they have no known competing financial interests or personal relationships that could have appeared to influence the work reported in this paper.

### Data availability

Data will be made available on request.

### Appendix A. Supplementary data

Supplementary data to this article can be found online at <https://doi.org/10.1016/j.carbpol.2022.120277>.

### References

- Ahmad, M., Gani, A., Masoodi, F. A., & Rizvi, S. H. (2020). Influence of ball milling on the production of starch nanoparticles and its effect on structural, thermal and functional properties. *International Journal of Biological Macromolecules*, *151*, 85–91. <https://doi.org/10.1016/j.ijbiomac.2020.02.139>
- Alhanish, A., & Abu Ghaliya, M. (2021). Developments of biobased plasticizers for compostable polymers in the green packaging applications: A review. *Biotechnology Progress*, *37*(6), Article e3210. <https://doi.org/10.1002/btpr.3210>
- Bakshi, P. S., Selvakumar, D., Kadirvelu, K., & Kumar, N. S. (2020). Chitosan as an environment friendly biomaterial – A review on recent modifications and applications. *International Journal of Biological Macromolecules*, *150*, 1072–1083. <https://doi.org/10.1016/j.ijbiomac.2019.10.113>

- Ballesteros-Martínez, L., Pérez-Cervera, C., & Andrade-Pizarro, R. (2020). Effect of glycerol and sorbitol concentrations on mechanical, optical, and barrier properties of sweet potato starch film. *NFS Journal*, *20*, 1–9. <https://doi.org/10.1016/j.nfs.2020.06.002>
- Brasselet, C., Pierre, G., Dubessay, P., Dols-Lafargue, M., Coulon, J., Maupeu, J., Vallet-Courbin, A., de Baynast, H., Doco, T., Michaud, P., & Delattre, C. (2019). Modification of chitosan for the generation of functional derivatives. *Applied Sciences*, *9*(7), 1321. <https://doi.org/10.3390/app9071321>
- Caicedo, C., Díaz-Cruz, C. A., Jiménez-Regalado, E. J., & Aguirre-Loredo, R. Y. (2022). Effect of plasticizer content on mechanical and water vapor permeability of maize starch/PVOH/chitosan composite films. *Materials (Basel, Switzerland)*, *15*(4), 1274. <https://doi.org/10.3390/ma15041274>
- Castelló, M. E., Anbinder, P. S., Amalvy, J. I., & Peruzzo, P. J. (2018). Production and characterization of chitosan and glycerol-chitosan films. *MRS Advances*, *3*(61), 3601–3610. <https://doi.org/10.1557/adv.2018.589>
- Cazón, P., & Vázquez, M. (2019). Applications of chitosan as food packaging materials. In G. Crini, & E. Lichtfouse (Eds.), *Sustainable agriculture reviews 36: Chitin and chitosan: Applications in food, agriculture, pharmacy, medicine and wastewater treatment* (pp. 81–123). Springer International Publishing. [https://doi.org/10.1007/978-3-030-16581-9\\_3](https://doi.org/10.1007/978-3-030-16581-9_3)
- Cazón, P., Velazquez, G., Ramírez, J. A., & Vázquez, M. (2017). Polysaccharide-based films and coatings for food packaging: A review. *Food Hydrocolloids*, *68*, 136–148. <https://doi.org/10.1016/j.foodhyd.2016.09.009>
- Chen, M., Runge, T., Wang, L., Li, R., Feng, J., Shu, X.-L., & Shi, Q.-S. (2018). Hydrogen bonding impact on chitosan plasticization. *Carbohydrate Polymers*, *200*, 115–121. <https://doi.org/10.1016/j.carbpol.2018.07.062>
- Chen, P., Xie, F., Tang, F., & McNally, T. (2021). Influence of plasticiser type and nanoclay on the properties of chitosan-based materials. *European Polymer Journal*, *144*, Article 110225. <https://doi.org/10.1016/j.eurpolymj.2020.110225>
- Chen, P.-H., Kuo, T.-Y., Liu, F.-H., Hwang, Y.-H., Ho, M.-H., Wang, D.-M., Lai, J.-Y., & Hsieh, H.-J. (2008). Use of dicarboxylic acids to improve and diversify the material properties of porous chitosan membranes. *Journal of Agricultural and Food Chemistry*, *56*(19), 9015–9021. <https://doi.org/10.1021/jf801081e>
- Corazzari, I., Nisticò, R., Turci, F., Faga, M. G., Franzoso, F., Tabasso, S., & Magnacca, G. (2015). Advanced physico-chemical characterization of chitosan by means of TGA coupled on-line with FTIR and GCMS: Thermal degradation and water adsorption capacity. *Polymer Degradation and Stability*, *112*, 1–9. <https://doi.org/10.1016/j.polyimdegradstab.2014.12.006>
- Darie-Niță, R. N., Răpă, M., Sivertsvik, M., Rosnes, J. T., Popa, E. E., Dumitriu, R. P., Marincaș, O., Matei, E., Predescu, C., & Vasile, C. (2021). PLA-based materials containing bio-plasticizers and chitosan modified with rosehip seed oil for ecological packaging. *Polymers*, *13*(10), 1610. <https://doi.org/10.3390/polym13101610>
- De Carli, C., Aylanc, V., Mouffok, K. M., Santamaria-Echart, A., Barreiro, F., Tomás, A., Pereira, C., Rodrigues, P., Vilas-Boas, M., & Falcao, S. I. (2022). Production of chitosan-based biodegradable active films using bio-waste enriched with polyphenol propolis extract envisaging food packaging applications. *International Journal of Biological Macromolecules*, *213*, 486–497. <https://doi.org/10.1016/j.ijbiomac.2022.05.155>
- Debandi, M. V., Bernal, C., & Francois, N. J. (2016). Development of biodegradable films based on chitosan/glycerol blends suitable for biomedical applications. *Journal of Tissue Science & Engineering*, *07*(03). <https://doi.org/10.4172/2157-7552.1000187>
- Deng, L., Li, X., Miao, K., Mao, X., Han, M., Li, D., Mu, C., & Ge, L. (2020). Development of disulfide bond crosslinked Gelatin/ε-polylysine active edible film with antibacterial and antioxidant activities. *Food and Bioprocess Technology*, *13*(4), 577–588. <https://doi.org/10.1007/s11947-020-02420-1>
- Dominguez-Candela, I., Ferri, J. M., Cardona, S. C., Lora, J., & Fombuena, V. (2021). Dual plasticizer/thermal stabilizer effect of epoxidized chia seed oil (Salvia hispanica L.) to improve ductility and thermal properties of poly(lactic acid). *Polymers*, *13*(8), 1283. <https://doi.org/10.3390/polym13081283>
- Dong, Y., Ruan, Y., Wang, H., Zhao, Y., & Bi, D. (2004). Studies on glass transition temperature of chitosan with four techniques. *Journal of Applied Polymer Science*, *93* (4), 1553–1558. <https://doi.org/10.1002/app.20630>
- Epure, V., Griffon, M., Pollet, E., & Avérous, L. (2011). Structure and properties of glycerol-plasticized chitosan obtained by mechanical kneading. *Carbohydrate Polymers*, *83*(2), 947–952. <https://doi.org/10.1016/j.carbpol.2010.09.003>
- Farhan, A., & Hani, N. M. (2017). Characterization of edible packaging films based on semi-refined kappa-carrageenan plasticized with glycerol and sorbitol. *Food Hydrocolloids*, *64*, 48–58. <https://doi.org/10.1016/j.foodhyd.2016.10.034>
- Giannakas, A., Patsaoura, A., Barkoula, N.-M., & Ladavos, A. (2017). A novel solution blending method for using olive oil and corn oil as plasticizers in chitosan based organoclay nanocomposites. *Carbohydrate Polymers*, *157*, 550–557. <https://doi.org/10.1016/j.carbpol.2016.10.020>
- Guo, Y., Chen, X., Yang, F., Wang, T., Ni, M., Chen, Y., Yang, F., Huang, D., Fu, C., & Wang, S. (2019). Preparation and characterization of chitosan-based ternary blend edible films with efficient antimicrobial activities for food packaging applications. *Journal of Food Science*, *84*(6), 1411–1419. <https://doi.org/10.1111/1750-3841.14650>
- Hasan, M., Gopakumar, D. A., Olaiya, N. G., Zarlaidda, F., Alfian, A., Aprinasari, C., Alfatah, T., Rizal, S., & Khalil, H. P. S. A. (2020). Evaluation of the thermomechanical properties and biodegradation of brown rice starch-based chitosan biodegradable composite films. *International Journal of Biological Macromolecules*, *156*, 896–905. <https://doi.org/10.1016/j.ijbiomac.2020.04.039>
- Ibrahim, Y. H.-E. Y., Regdon, G., Kristó, K., Kelemen, A., Adam, M. E., Hamedelnel, E. I., & Sovány, T. (2020). Design and characterization of chitosan/citrate films as carrier for oral macromolecule delivery. *European Journal of Pharmaceutical Sciences*, *146*, Article 105270. <https://doi.org/10.1016/j.ejps.2020.105270>



- Jain, A., Gulbake, A., Shilpi, S., Jain, A., Hurkat, P., & Jain, S. K. (2013). A new horizon in modifications of chitosan: Syntheses and applications. *Critical Reviews in Therapeutic Drug Carrier Systems*, 30(2), 91–181. <https://doi.org/10.1016/j.critrevtherdrugcarriersyst.2013005678>
- Jancić, U., Božić, M., Hribernik, S., Mohan, T., Kargl, R., Kleinschek, K. S., & Gorgieva, S. (2021). High oxygen barrier chitosan films neutralized by alkaline nanoparticles. *Cellulose*, 28(16), 10457–10475. <https://doi.org/10.1007/s10570-021-04195-w>
- Janik, W., Nowotarski, M., Shyntum, D. Y., Banaś, A., Krukiewicz, K., Kudła, S., & Dudek, G. (2022). Antibacterial and biodegradable polysaccharide-based films for food packaging applications: Comparative study. *Materials*, 15(9), 3236. <https://doi.org/10.3390/ma15093236>
- Jiménez-Regalado, E. J., Caicedo, C., Fonseca-García, A., Rivera-Vallejo, C. C., & Aguirre-Loredo, R. Y. (2021). Preparation and physicochemical properties of modified corn starch-chitosan biodegradable films. *Polymers*, 13(24), 4431. <https://doi.org/10.3390/polym13244431>
- Kumar, M. N. V. R., Muzzarelli, R. A. A., Muzzarelli, C., Sashiwa, H., & Domb, A. J. (2004). Chitosan chemistry and pharmaceutical perspectives. *Chemical Reviews*, 104(12), 6017–6084. <https://doi.org/10.1021/cr030441b>
- Kusmono, & Abdurrahim, I. (2019). Water sorption, antimicrobial activity, and thermal and mechanical properties of chitosan/clay/glycerol nanocomposite films. *Heliyon*, 5(8). <https://doi.org/10.1016/j.heliyon.2019.e02342>
- Lavorgna, M., Piscitelli, F., Mangiacapra, P., & Buonocore, G. G. (2010). Study of the combined effect of both clay and glycerol plasticizer on the properties of chitosan films. *Carbohydrate Polymers*, 82(2), 291–298. <https://doi.org/10.1016/j.carbpol.2010.04.054>
- Leceta, I., Guerrero, P., & de la Caba, K. (2013). Functional properties of chitosan-based films. *Carbohydrate Polymers*, 93(1), 339–346. <https://doi.org/10.1016/j.carbpol.2012.04.031>
- Ledniowska, K., Nosal-Kovalenko, H., Janik, W., Krasuska, A., Stańczyk, D., Sabura, E., Bartoszewicz, M., & Rybak, A. (2022). Effective, environmentally friendly PVC plasticizers based on succinic acid. *Polymers*, 14(7), 1295. <https://doi.org/10.3390/polym14071295>
- Lim, B. Y., Poh, C. S., Voon, C. H., & Salmah, H. (2015). Rheological and thermal study of chitosan filled thermoplastic elastomer composites. *Applied Mechanics and Materials*, 754–755, 34–38. <https://doi.org/10.4028/www.scientific.net/AMM.754-755.34>
- Liu, M., Zhou, Y., Zhang, Y., Yu, C., & Cao, S. (2014). Physicochemical, mechanical and thermal properties of chitosan films with and without sorbitol. *International Journal of Biological Macromolecules*, 70, 340–346. <https://doi.org/10.1016/j.ijbiomac.2014.06.039>
- Long, X., Hu, X., Liu, S., Pan, C., Chen, S., Li, L., Qi, B., & Yang, X. (2021). Insights on preparation, structure and activities of *Gracilaria lemaneiformis* polysaccharide. *Food Chemistry: X*, 12, Article 100153. <https://doi.org/10.1016/j.fochx.2021.100153>
- Ma, X., Qiao, C., Wang, X., Yao, J., & Xu, J. (2019). Structural characterization and properties of polyols plasticized chitosan films. *International Journal of Biological Macromolecules*, 135, 240–245. <https://doi.org/10.1016/j.ijbiomac.2019.05.158>
- Ma, X., Yang, Z., Yao, Z., Guo, H., Xu, Z., & Tang, C. Y. (2019). Tuning roughness features of thin film composite polyamide membranes for simultaneously enhanced permeability, selectivity and anti-fouling performance. *Journal of Colloid and Interface Science*, 540, 382–388. <https://doi.org/10.1016/j.jcis.2019.01.033>
- Ma, Y., Xin, L., Tan, H., Fan, M., Li, J., Jia, Y., Ling, Z., Chen, Y., & Hu, X. (2017). Chitosan membrane dressings toughened by glycerol to load antibacterial drugs for wound healing. *Materials Science and Engineering: C*, 81, 522–531. <https://doi.org/10.1016/j.msec.2017.08.052>
- Maciel, V. B. V., Yoshida, C. M. P., Pereira, S. M. S. S., Goycoolea, F. M., & Franco, T. T. (2017). Electrostatic self-assembled chitosan-pectin nano- and microparticles for insulin delivery. *Molecules*, 22(10), 1707. <https://doi.org/10.3390/molecules22101707>
- Matet, M., Heuzey, M.-C., Pollet, E., Ajji, A., & Avérous, L. (2013). Innovative thermoplastic chitosan obtained by thermo-mechanical mixing with polyol plasticizers. *Carbohydrate Polymers*, 95(1), 241–251. <https://doi.org/10.1016/j.carbpol.2013.02.052>
- Mehdizadeh, A., Shahidi, S.-A., Shariatfar, N., Shiran, M., & Ghorbani-HasanSarai, A. (2022). Physicochemical characteristics and antioxidant activity of the chitosan/zein films incorporated with *Pulicaria gnaphalodes* L. extract-loaded nanoliposomes. *Journal of Food Measurement and Characterization*, 16(2), 1252–1262. <https://doi.org/10.1007/s11694-021-01250-9>
- Melro, E., Antunes, F., Silva, G., Cruz, I., Ramos, P., Carvalho, F., & Alves, L. (2020). Chitosan films in food applications. Tuning film properties by changing acidic dissolution conditions. *Polymers*, 13, 1. <https://doi.org/10.3390/polym13010001>
- Mohamed, S. A. A., El-Sakhawy, M., & El-Sakhawy, M. A.-M. (2020). Polysaccharides, protein and lipid-based natural edible films in food packaging: A review. *Carbohydrate Polymers*, 238, Article 116178. <https://doi.org/10.1016/j.carbpol.2020.116178>
- Muller, J., Gonzalez-Martinez, C., & Chiralt, A. (2017). Poly(lactic) acid (PLA) and starch bilayer films, containing cinnamaldehyde, obtained by compression moulding. *European Polymer Journal*, 95. <https://doi.org/10.1016/j.eurpolymj.2017.07.019>
- Murrieta, C., Soto-Valdez, H., Pacheco-Aguilar, R., Torres, W., Rodríguez-Félix, F., Ramírez-Wong, B., Santacruz, H., Santos, I., Olibarría-Rodríguez, G., & Marquez Rios, E. (2019). Effect of different polyalcohols as plasticizers on the functional properties of squid protein film (*Dosidicus gigas*). *Coatings*, 9, 77. <https://doi.org/10.3390/coatings9020077>
- Ncube, L. K., Ude, A. U., Ogunmuyiwa, E. N., Zulkifli, R., & Beas, I. N. (2020). Environmental impact of food packaging materials: A review of contemporary development from conventional plastics to polylactic acid based materials. *Materials*, 13(21), 4994. <https://doi.org/10.3390/ma13214994>
- Neri, L., Dimitri, G., & Sacchetti, G. (2010). Chemical composition and antioxidant activity of cured chestnuts from three sweet chestnut (*Castanea sativa* Mill.) ecotypes from Italy. *Journal of Food Composition and Analysis*, 23(1), 23–29. <https://doi.org/10.1016/j.jfca.2009.03.002>
- Ni, Y., Shi, S., Li, M., Zhang, L., Yang, C., Du, T., Wang, S., Nie, H., Sun, J., Zhang, W., & Wang, J. (2021). Visible light responsive, self-activated bionanocomposite films with sustained antimicrobial activity for food packaging. *Food Chemistry*, 362, Article 130201. <https://doi.org/10.1016/j.foodchem.2021.130201>
- Nobeyama, T., Mori, M., Shigyou, K., Takata, K., Pandian, G. N., Sugiyama, H., & Murakami, T. (2018). Colloidal stability of lipid/protein-coated nanomaterials in salt and sucrose solutions. *ChemistrySelect*, 3(28), 8325–8331. <https://doi.org/10.1002/slct.201801180>
- Pardo-Castaño, C., & Bolaños, G. (2019). Solubility of chitosan in aqueous acetic acid and pressurized carbon dioxide-water: Experimental equilibrium and solubilization kinetics. *The Journal of Supercritical Fluids*, 151, 63–74. <https://doi.org/10.1016/j.supflu.2019.05.007>
- Pavlatková, L., Sedlářková, J., Pleva, P., Peer, P., Uysal-Unalan, I., & Janalíková, M. (2022). Bioactive zein/chitosan systems loaded with essential oils for food-packaging applications. *Journal of the Science of Food and Agriculture*. <https://doi.org/10.1002/jsfa.11978>
- Priyadarshi, R., Sauraj, Kumar, B., & Negi, Y. S. (2018). Chitosan film incorporated with citric acid and glycerol as an active packaging material for extension of green chilli shelf life. *Carbohydrate Polymers*, 195, 329–338. <https://doi.org/10.1016/j.carbpol.2018.04.089>
- Qiao, C., Ma, X., Wang, X., & Liu, L. (2021). Structure and properties of chitosan films: Effect of the type of solvent acid. *LWT*, 135, Article 109984. <https://doi.org/10.1016/j.lwt.2020.109984>
- Ramon, G. Z., & Hoek, E. M. V. (2013). Transport through composite membranes, part 2: Impacts of roughness on permeability and fouling. *Journal of Membrane Science*, 425–426, 141–148. <https://doi.org/10.1016/j.memsci.2012.08.004>
- Rodríguez-Núñez, J. R., Madera-Santana, T. J., Sánchez-Machado, D. I., López-Cervantes, J., & Soto Valdez, H. (2014). Chitosan/hydrophilic plasticizer-based films: Preparation, physicochemical and antimicrobial properties. *Journal of Polymers and the Environment*, 22(1), 41–51. <https://doi.org/10.1007/s10924-013-0621-z>
- Sabbah, M., Di Pierro, P., Cammarota, M., Dell'Olmo, E., Arciello, A., & Porta, R. (2019). Development and properties of new chitosan-based films plasticized with spermidine and/or glycerol. *Food Hydrocolloids*, 87, 245–252. <https://doi.org/10.1016/j.foodhyd.2018.08.008>
- Sabbah, M., & Esposito, M. (2016). Insight into zeta potential measurements in biopolymer film preparation. *Journal of Biotechnology & Biomaterials*, 6. <https://doi.org/10.4172/2155-952X.1000e126>
- Sami El-banna, F., Mahfouz, M. E., Leporatti, S., El-Kemary, M., & A. N. Hanafy, N. (2019). Chitosan as a natural copolymer with unique properties for the development of hydrogels. *Applied Sciences*, 9(11), 2193. <https://doi.org/10.3390/app9112193>
- Souza, V. G. L., Pires, J. R. A., Rodrigues, C., Rodrigues, P. F., Lopes, A., Silva, R. J., Caldeira, J., Duarte, M. P., Fernandes, F. B., Coelho, I. M., & Fernando, A. L. (2019). Physical and morphological characterization of chitosan/montmorillonite films incorporated with ginger essential oil. *Coatings*, 9(11), 700. <https://doi.org/10.3390/coatings9110700>
- Srinivasa, P. C., Ramesh, M. N., & Tharanathan, R. N. (2007). Effect of plasticizers and fatty acids on mechanical and permeability characteristics of chitosan films. *Food Hydrocolloids*, 21(7), 1113–1122. <https://doi.org/10.1016/j.foodhyd.2006.08.005>
- Sun, Y., Liu, Z., Zhang, L., Wang, X., & Li, L. (2020). Effects of plasticizer type and concentration on rheological, physico-mechanical and structural properties of chitosan/zein film. *International Journal of Biological Macromolecules*, 143, 334–340. <https://doi.org/10.1016/j.ijbiomac.2019.12.035>
- Suyatma, N. E., Tighzert, L., Copinet, A., & Coma, V. (2005). Effects of hydrophilic plasticizers on mechanical, thermal, and surface properties of chitosan films. *Journal of Agricultural and Food Chemistry*, 53(10), 3950–3957. <https://doi.org/10.1021/jf048790+>
- Swain, S. K., & Mohanty, F. (2018). Polysaccharides-based bionanocomposites for food packaging applications. In M. Jawaid, & S. K. Swain (Eds.), *Bionanocomposites for packaging applications* (pp. 191–208). Springer International Publishing. [https://doi.org/10.1007/978-3-319-67319-6\\_10](https://doi.org/10.1007/978-3-319-67319-6_10)
- Szymańska, E., & Winnicka, K. (2015). Stability of chitosan—A challenge for pharmaceutical and biomedical applications. *Marine Drugs*, 13(4), 1819–1846. <https://doi.org/10.3390/md13041819>
- Tambunan, J., & Chamidah, A. (2021). Effect of acetic and citric acid solvent combination with cinnamon oil on quality of edible packaging from chitosan. *IOP Conference Series: Earth and Environmental Science*, 919, Article 012033. <https://doi.org/10.1088/1755-1315/919/1/012033>
- Tan, W., Zhang, J., Zhao, X., Li, Q., Dong, F., & Guo, Z. (2020). Preparation and physicochemical properties of antioxidant chitosan ascorbate/methylcellulose composite films. *International Journal of Biological Macromolecules*, 146, 53–61. <https://doi.org/10.1016/j.ijbiomac.2019.12.044>
- Thawien, B. (2008). Plasticizer effect on the properties of biodegradable blend from rice starch-chitosan. *Songklanakarin Journal of Science and Technology*, 30.
- Vieira, M. G. A., da Silva, M. A., dos Santos, L. O., & Beppu, M. M. (2011). Natural-based plasticizers and biopolymer films: A review. *European Polymer Journal*, 47(3), 254–263. <https://doi.org/10.1016/j.eurpolymj.2010.12.011>
- Vlacha, M., Giannakas, A., Katapodis, P., Stamatis, H., Ladavos, A., & Barkoula, N.-M. (2016). On the efficiency of oleic acid as plasticizer of chitosan/clay nanocomposites and its role on thermo-mechanical, barrier and antimicrobial properties – Comparison with glycerol. *Food Hydrocolloids*, 57, 10–19. <https://doi.org/10.1016/j.foodhyd.2016.01.003>

- Voci, S., Gagliardi, A., Salvatici, M. C., Fresta, M., & Cosco, D. (2022). Influence of the dispersion medium and cryoprotectants on the physico-chemical features of gliadin- and zein-based nanoparticles. *Pharmaceutics*, *14*(2), 332. <https://doi.org/10.3390/pharmaceutics14020332>
- Wang, X., Du, Y., Yang, J., Wang, X., Shi, X., & Hu, Y. (2006). Preparation, characterization and antimicrobial activity of chitosan/layered silicate nanocomposites. *Polymer*, *47*(19), 6738–6744. <https://doi.org/10.1016/j.polymer.2006.07.026>
- Xu, J., Xia, R., Zheng, L., Yuan, T., & Sun, R. (2019). Plasticized hemicelluloses/chitosan-based edible films reinforced by cellulose nanofiber with enhanced mechanical properties. *Carbohydrate Polymers*, *224*, Article 115164. <https://doi.org/10.1016/j.carbpol.2019.115164>
- Zemljčić, L. F., Plohl, O., Vesel, A., Luxbacher, T., & Potrč, S. (2020). Physicochemical characterization of packaging foils coated by chitosan and polyphenols colloidal formulations. *International Journal of Molecular Sciences*, *21*(2), 495. <https://doi.org/10.3390/ijms21020495>
- Zhang, N., Bi, F., Xu, F., Yong, H., Bao, Y., Jin, C., & Liu, J. (2020). Structure and functional properties of active packaging films prepared by incorporating different flavonols into chitosan based matrix. *International Journal of Biological Macromolecules*, *165*, 625–634. <https://doi.org/10.1016/j.ijbiomac.2020.09.209>
- Zhao, Y., Li, B., Li, C., Xu, Y., Luo, Y., Liang, D., & Huang, C. (2021). Comprehensive review of polysaccharide-based materials in edible packaging: A sustainable approach. *Foods*, *10*(8), 1845. <https://doi.org/10.3390/foods10081845>

SUPPLEMENTARY DATA

# Chitosan-Based Films with Alternative Eco-friendly Plasticizers: Preparation, Physicochemical Properties and Stability

Weronika Janik, Kerstin Ledniowska, Michał Nowotarski, Stanisław Kudła, Joanna Knapczyk-Korczak, Urszula Stachewicz, Ewa Nowakowska-Bogdan, Ewa Sabura, Hanna Nosal-Kovalenko, Roman Turczyn, Gabriela Dudek

## CONTENTS

1. PLASTICIZER CHARACTERIZATION .....	2
1.1. Identification analysis of plasticizer components by GC/MS method .....	2
1.2. <sup>1</sup> H NMR and FTIR of synthesized plasticizers .....	10
2. FILM CHARACTERIZATION .....	16
2.1. Physical appearance .....	16
2.2. Roughness characteristics.....	16
2.3. Morphological analysis.....	17
2.4. Thermal analysis of chitosan-based films.....	17



# 1. PLASTICIZER CHARACTERIZATION

## 1.1. Identification analysis of plasticizer components by GC/MS method

Gas chromatography with mass spectrometry (GC/MS) was used for the qualitative analysis of components present in a post reaction mixture after each plasticizer synthesis. The proposed structure and their fragmentation pattern is shown in a simplified way, showing the key, most intense ions that appears in mass spectrum.

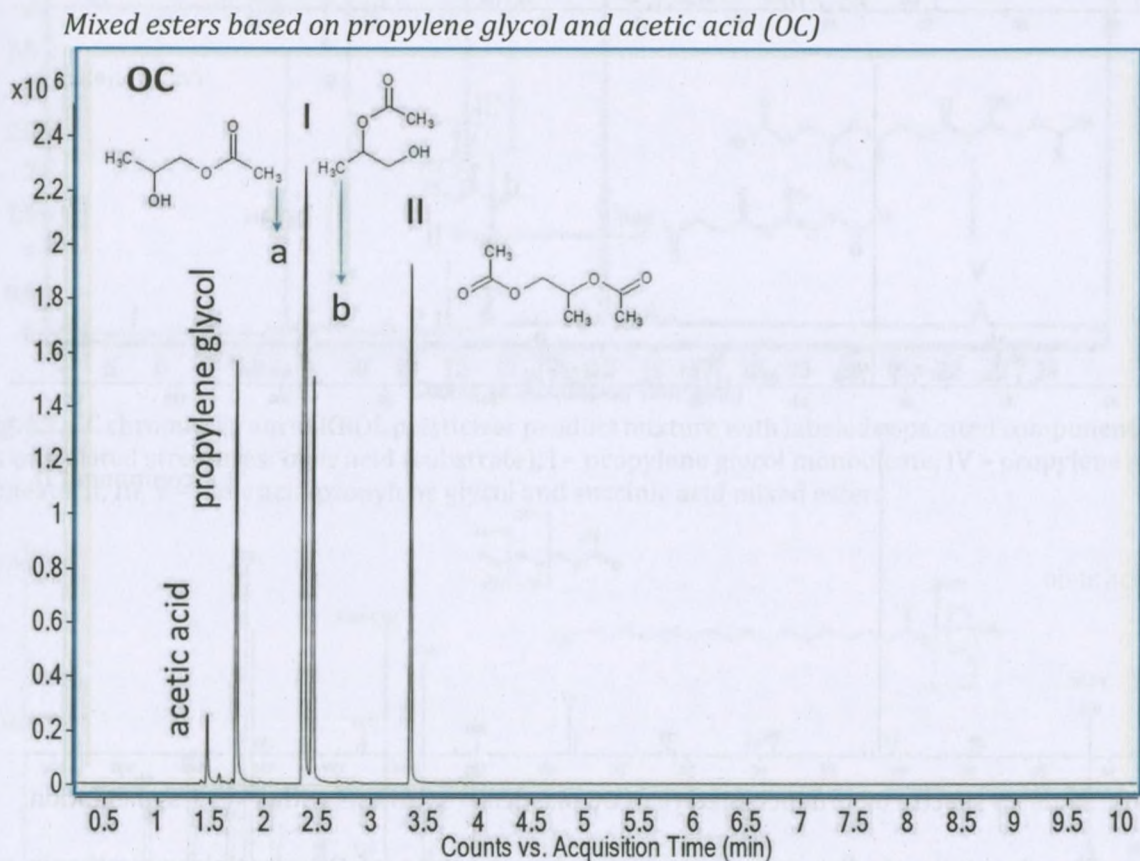


**Fig. S1.** GC chromatogram of OC plasticizer product mixture with labeled separated components and its postulated structures: acetic acid, propylene glycol, I – propylene glycol acetate (two isomers) and II – propylene glycol diacetate.



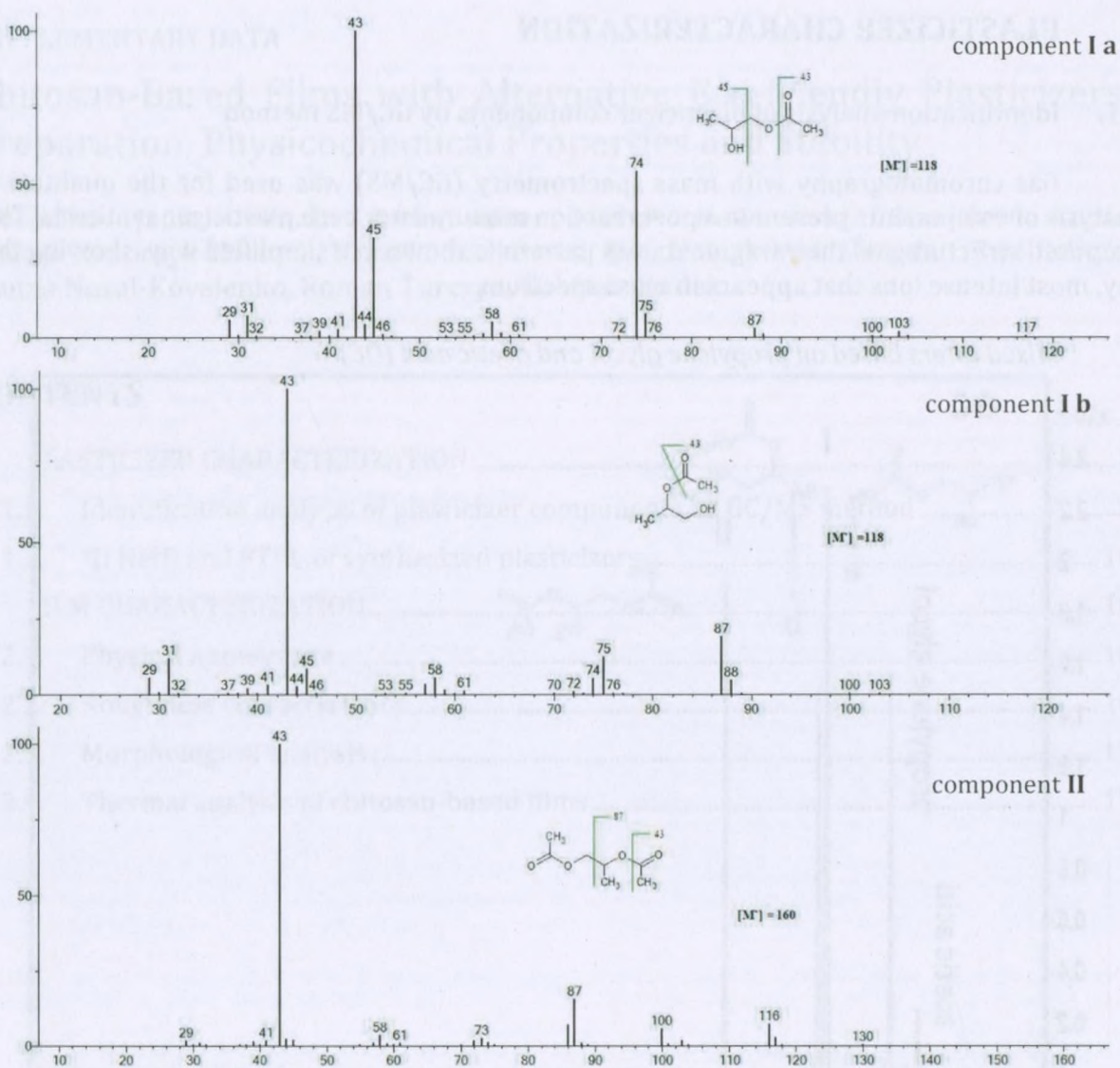
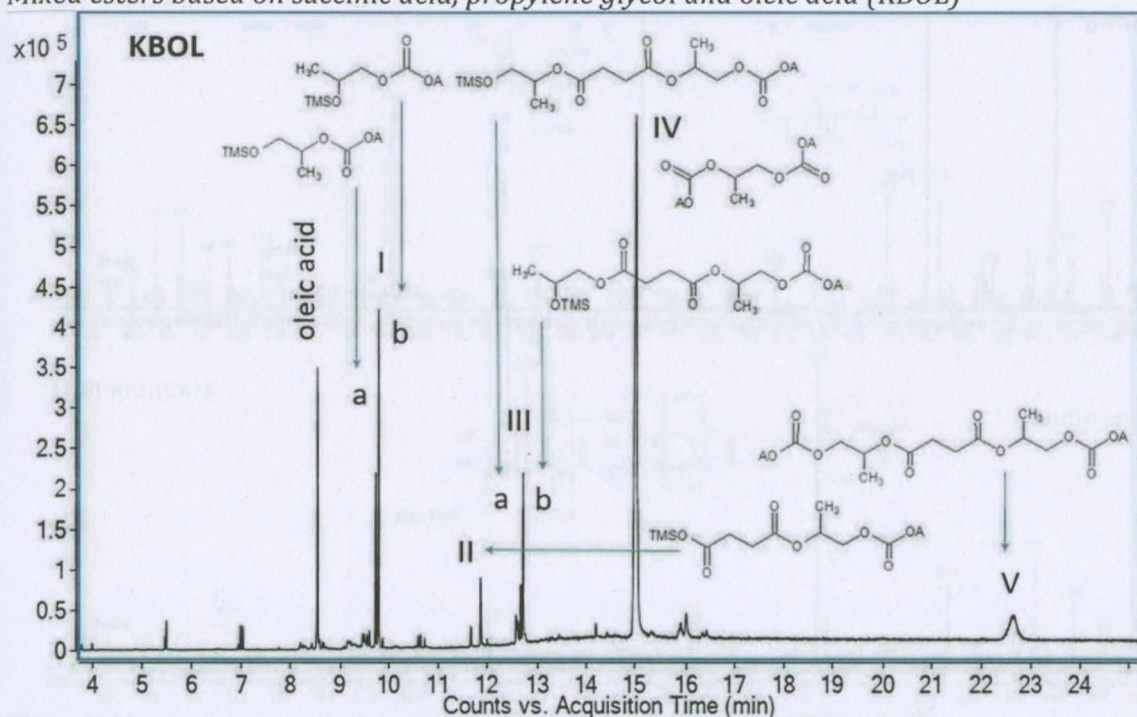


**Fig. S2.** Mass spectra of product mixture of OC plasticizer synthesis with a key fragmentation.

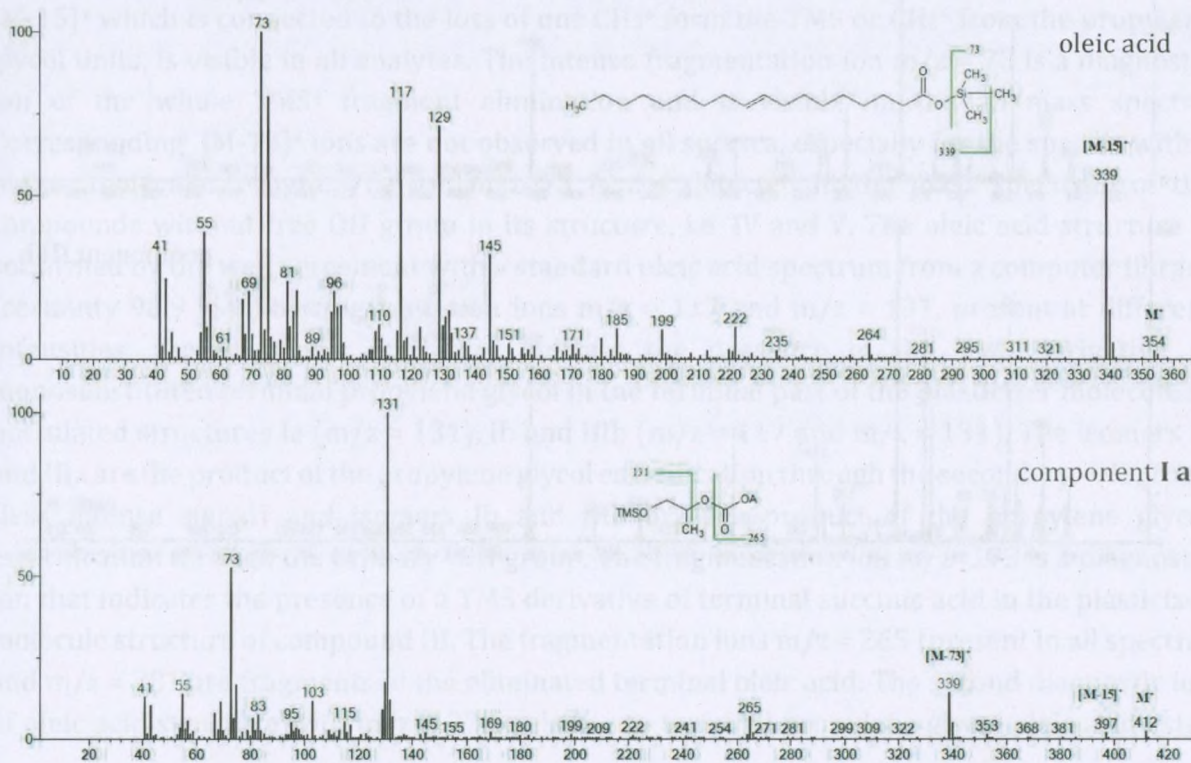
The structure of all components of product mixture of OC plasticizer synthesis are identified based on the comparison with the standard spectra from commercial digital library supplied by GC/MS producer. The agreement certainty are: for acetic acid – 97.2 %, for propylene glycol – 98.5 %, for two propylene glycol acetate compound I b (2-hydroxypropyl acetate) – 89.4 % and compound I a (1-hydroxypropan-2-yl acetate) – 90.2 %, for propylene glycol diacetate compound II – 87.6 %.



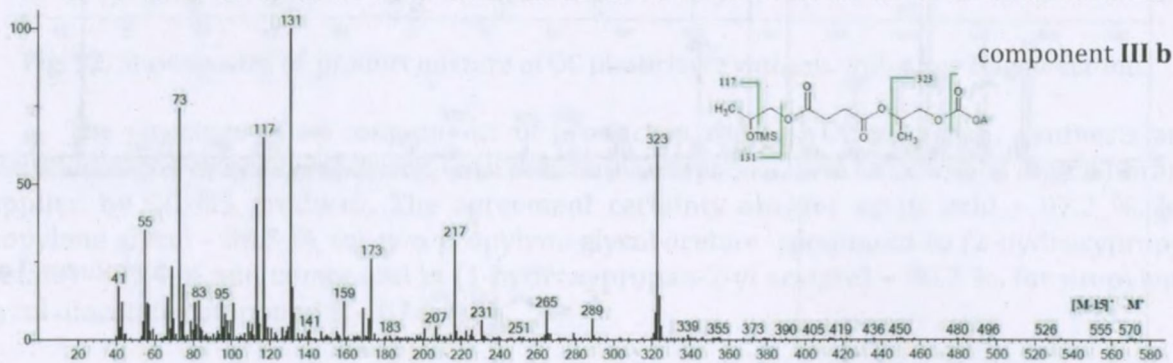
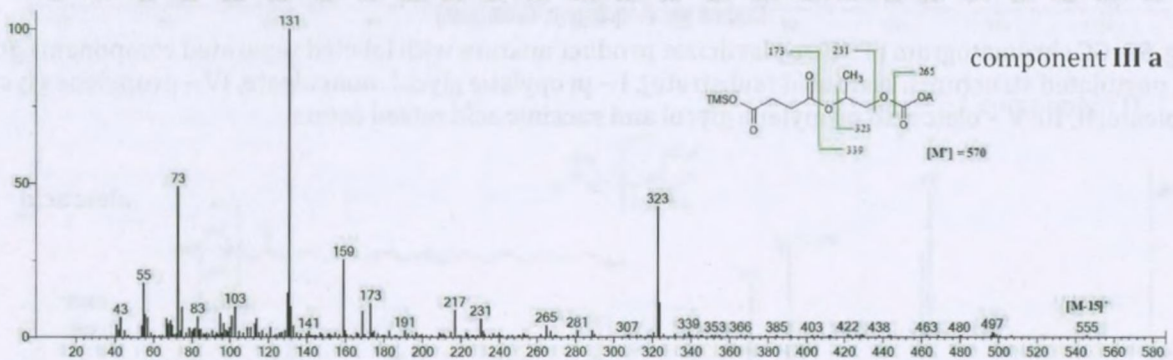
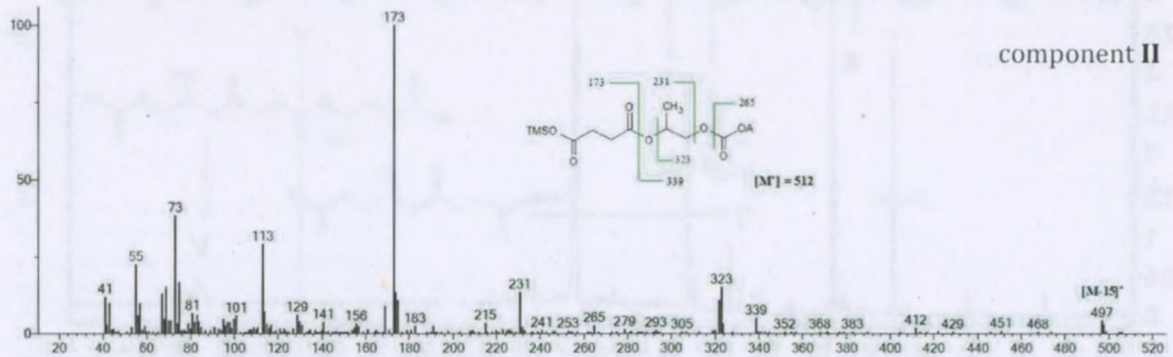
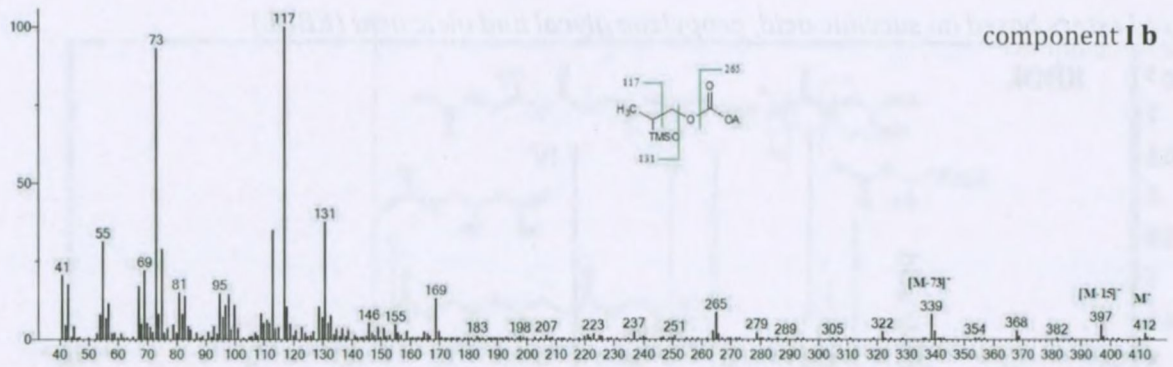
Mixed esters based on succinic acid, propylene glycol and oleic acid (KBOL)



**Fig. S3.** GC chromatogram of KBOL plasticizer product mixture with labeled separated components and its postulated structures: oleic acid (substrate), I – propylene glycol monooleate, IV – propylene glycol dioleate, II, III, V – oleic acid propylene glycol and succinic acid mixed esters







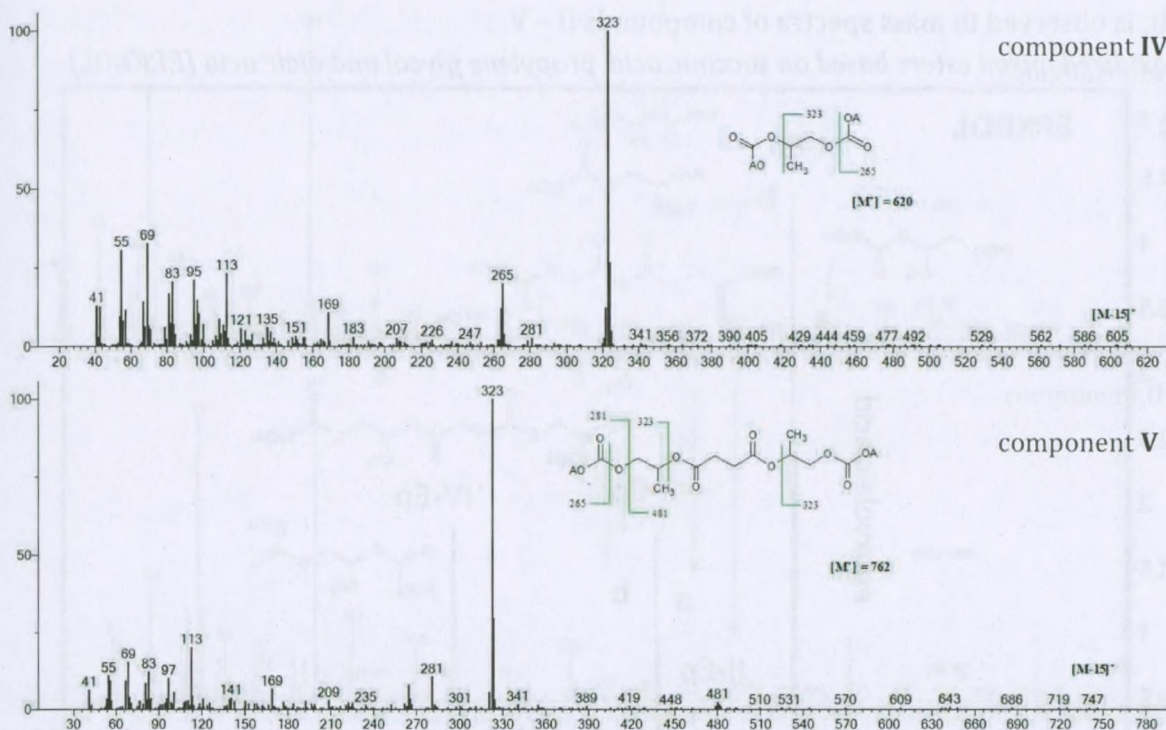


**Fig. S4.** Mass spectrum of oleic acid form product mixture of KBOL plasticizer synthesis with key fragmentation.

The molecular ion is not detectable in some proposed molecule structure, but the ion  $[M-15]^+$  which is connected to the loss of one  $CH_3^+$  from the TMS or  $CH_3^+$  from the propylene glycol units, is visible in all analytes. The intense fragmentation ion  $m/z = 73$  is a diagnostic ion of the whole TMS<sup>+</sup> fragment elimination and is visible on the all mass spectra. Corresponding  $[M-73]^+$  ions are not observed in all spectra, especially for the species with a higher molecular weight. The ion  $m/z=73$  is not detected in the mass spectrum of the compounds without free OH group in its structure, i.e. IV and V. The oleic acid structure is confirmed by the well agreement with a standard oleic acid spectrum from a computer library (certainty 98.9 %). The fragmentation ions  $m/z = 117$  and  $m/z = 131$ , present at different intensities, are diagnostic ions that indicate the presence of the TMS derivative of monosubstituted terminal propylene glycol in the terminal part of the plasticizer molecule in postulated structures Ia ( $m/z = 131$ ), Ib and IIIb ( $m/z = 117$  and  $m/z = 131$ ). The isomers Ia and IIIa are the product of the propylene glycol esterification through the secondary -OH group (less intense signal) and isomers Ib and IIIb are the product of the propylene glycol esterification through the primary -OH group. The fragmentation ion  $m/z=173$  is a diagnostic ion that indicates the presence of a TMS derivative of terminal succinic acid in the plasticizer molecule structure of compound III. The fragmentation ions  $m/z = 265$  (present in all spectra) and  $m/z = 281$  are fragments of the eliminated terminal oleic acid. The second diagnostic ion of oleic acid structure with  $m/z = 323$ , relating to terminal propylene glycol oleic acid ester



unit, is observed in mass spectra of compounds II – V.

*Epoxidized mixed esters based on succinic acid, propylene glycol and oleic acid (EPKBOL)*

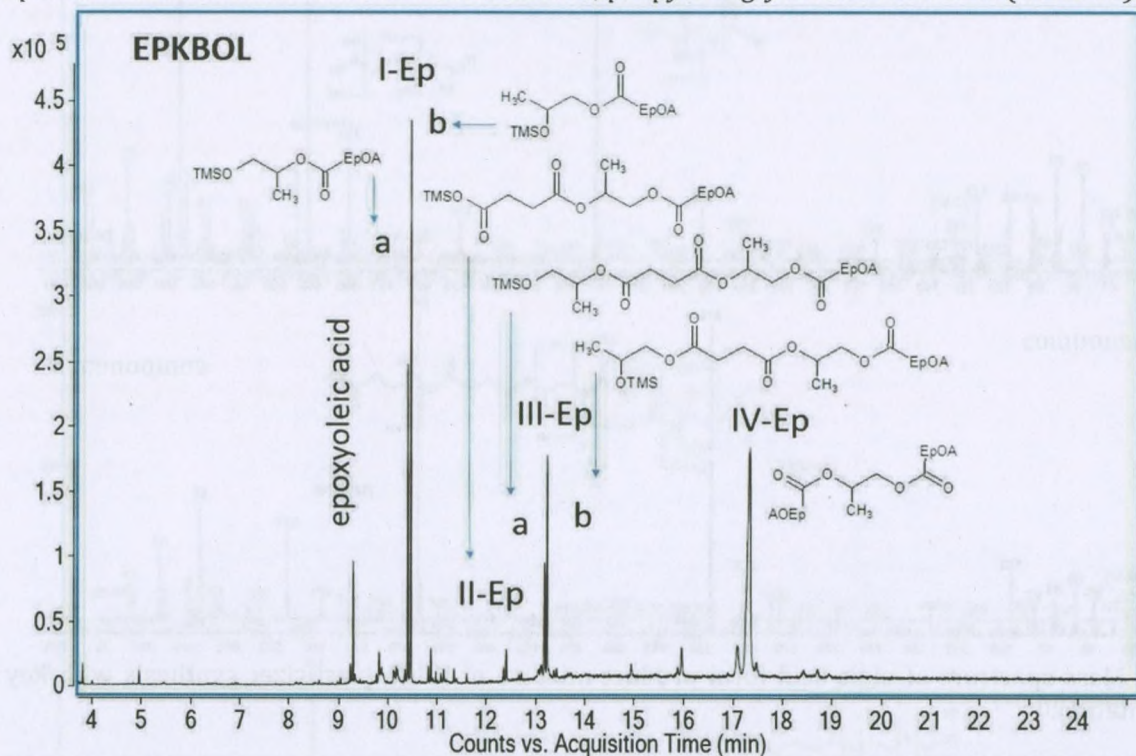
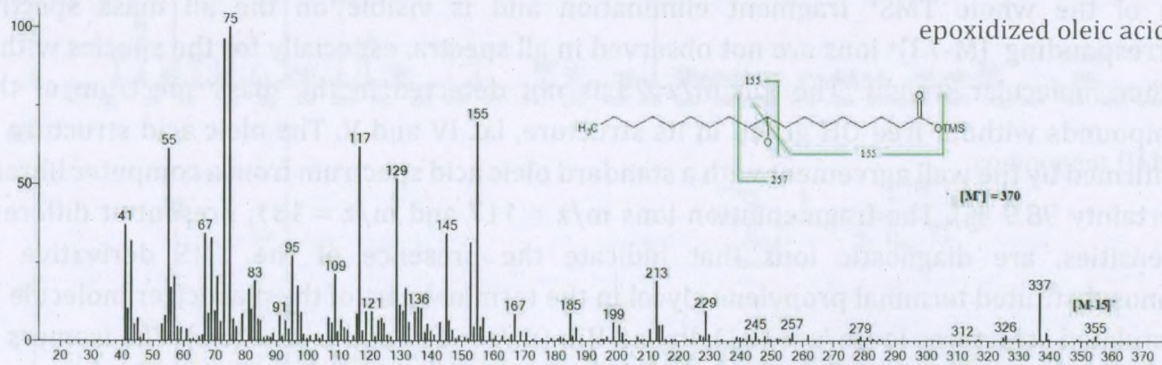
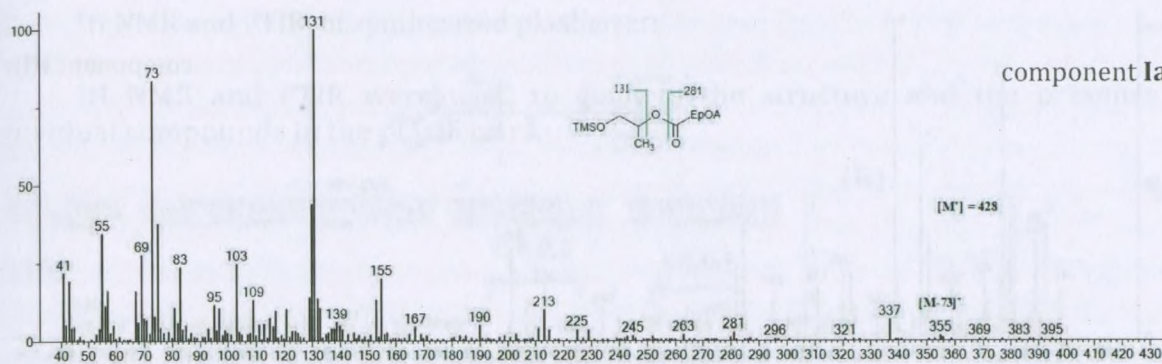


**Fig. S5.** GC chromatogram of EPKBOL plasticizer product mixture with labeled separated components and its postulated structures: epoxidized oleic acid, I – epoxidized propylene glycol monooleate, IV – epoxidized propylene glycol dioleate, II, III – epoxidized oleic acid propylene glycol and succinic acid mixed esters

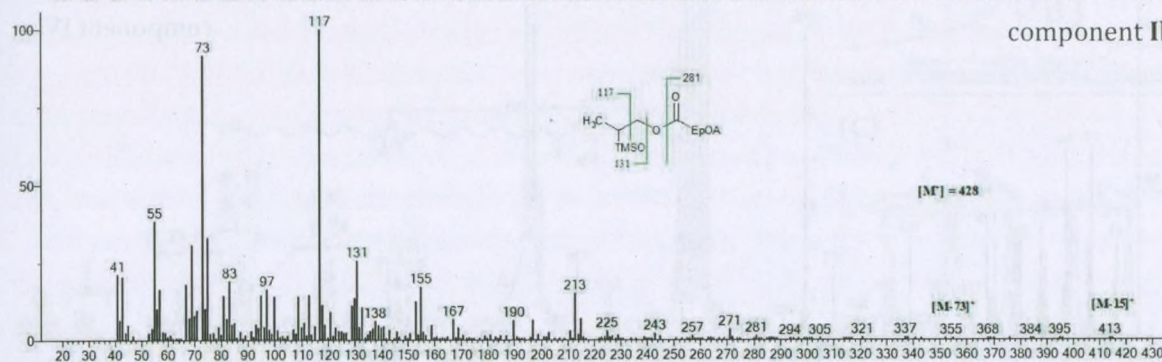




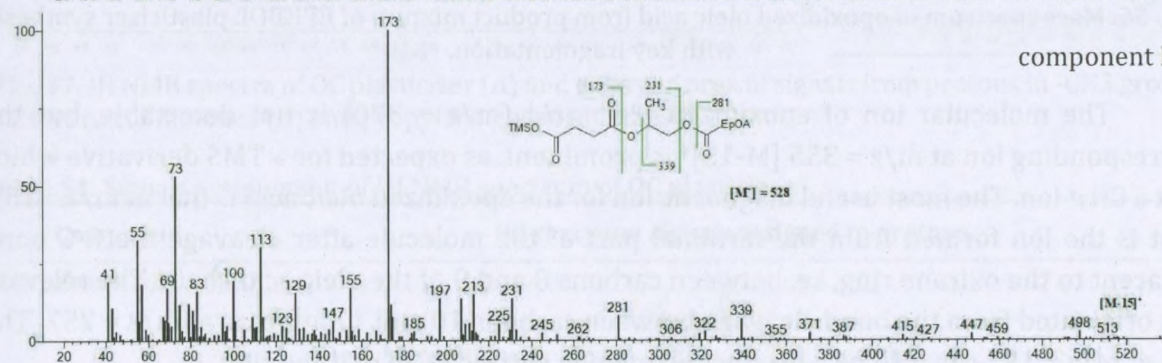
component Ia



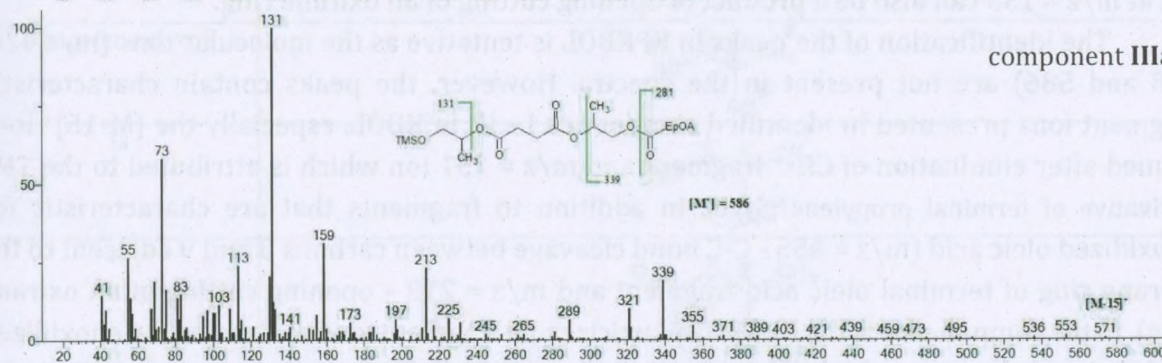
component Ib



component II



component IIIa





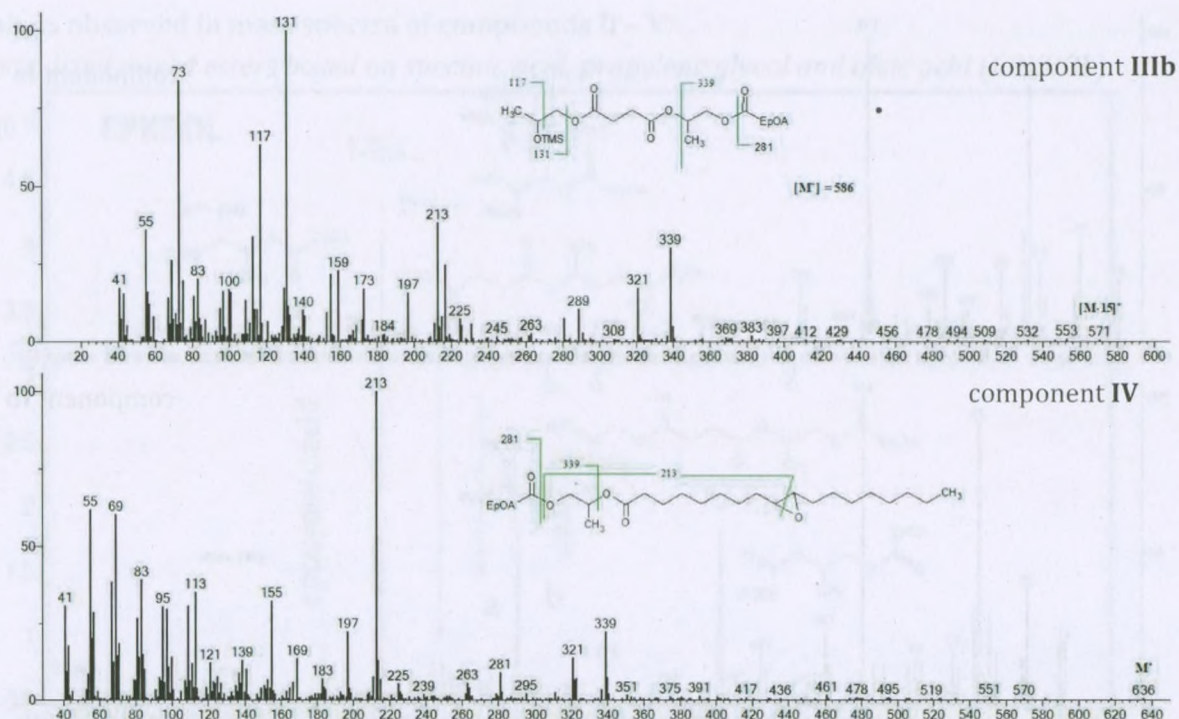


**Fig. S6.** Mass spectrum of epoxidized oleic acid from product mixture of EPKBOL plasticizer synthesis with key fragmentation.

The molecular ion of epoxidized oleic acid ( $m/z = 370$ ) is not detectable, but the corresponding ion at  $m/z = 355$   $[M-15]^+$  is prominent, as expected for a TMS derivative which lost a  $CH_3^+$  ion. The most useful diagnostic ion for the epoxidized oleic acid is that at  $m/z = 155$ , that is the ion formed from the terminal part of the molecule after cleavage the C-C bond adjacent to the oxirane ring, i.e. between carbons 8 and 9 of the oleic acid chain. The relevant ion originated from the bond cleavage between carbons 10 and 11 appears at  $m/z = 257$ . The ion at  $m/z = 155$  can also be a product of opening cutting of an oxirane ring.

The identification of the peaks in EPKBOL is tentative as the molecular ions ( $m/z$  428, 528 and 586) are not present in the spectra. However, the peaks contain characteristic fragment ions presented in identified compounds I - III in KBOL, especially the  $[M-15]^+$  ions formed after elimination of  $CH_3^+$  fragment and  $m/z = 131$  ion which is attributed to the TMS derivative of terminal propylene glycol. In addition to fragments that are characteristic for epoxidized oleic acid ( $m/z = 155$  - C-C bond cleavage between carbons 8 and 9 adjacent to the oxirane ring of terminal oleic acid fragment and  $m/z = 213$  - opening cutting of an oxirane ring). In the components of the EPKBOL plasticizer, all fragment ions containing the epoxidized acid moiety have a mass higher by 16 u than the analogues fragments in analyzed KBOL, for example  $m/z = 281$  observed in EPKBOL spectrum and  $m/z = 265$  in KBOL or  $m/z = 339$  in EPKBOL and  $m/z = 323$  in KBOL, respectively. This repeating difference in mass indicates the presence of an extra oxygen atom in EPKBOL structure confirming the successful oxidation of unsaturated bond and formation of an epoxy group in identified components of EPKBOL.



## 1.2. <sup>1</sup>H NMR and FTIR of synthesized plasticizers

<sup>1</sup>H NMR and FTIR were used to confirm the structure and the presence of individual compounds in the plasticizers.

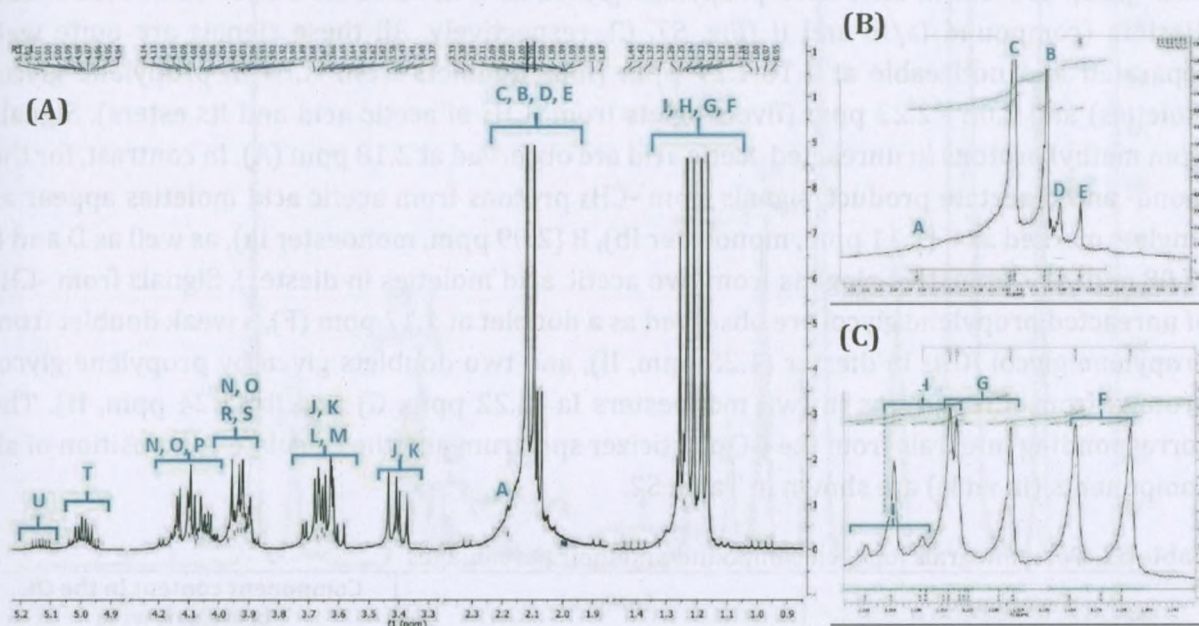


**Fig. S7.** <sup>1</sup>H NMR spectra of OC plasticizer (A) and enlarged area of signals from protons in -CH<sub>3</sub> group in acetic acid moieties (B) and propylene glycol moieties (C).

**Table S1.** Signals assignment of <sup>1</sup>H NMR spectrum of OC plasticizer

Compound	OC spectrum signals assigned to protons
Acetic acid	<chem>CC(=O)O</chem>
Propylene glycol	<chem>CC(O)CO</chem>
Ia	<chem>CC(O)CO</chem>
Ib	<chem>CC(O)OC</chem>
II	<chem>CC(=O)OCC(OC(=O)C)CO</chem>



The composition of the OC plasticizer was determined from the  $^1\text{H}$  NMR analysis based on the relative intensities (integrals) of the signals from the methyl  $-\text{CH}_3$  groups present in the structure of acetic acid and its moieties in monoesters and diesters (Fig. S7. B), and the methyl  $-\text{CH}_3$  group present in unreacted propylene glycol, as well as in the structure of mono- and diesters (compound Ia/Ib and II (Fig. S7. C), respectively). All these signals are quite well separated and noticeable at 1.16-1.27 ppm (four doublets from  $-\text{CH}_3$  in propylene glycol moieties) and 2.06 - 2.23 ppm (five singlets from  $-\text{CH}_3$  of acetic acid and its esters). Signals from methyl protons in unreacted acetic acid are observed at 2.18 ppm (A). In contrast, for the mono- and diacetate product, signals from  $-\text{CH}_3$  protons from acetic acid moieties appear as singlets marked as C (2.11 ppm, monoester Ib), B (2.09 ppm, monoester Ia), as well as D and E (2.08 and 2.07 ppm, two singlets from two acetic acid moieties in diester). Signals from  $-\text{CH}_3$  of unreacted propylene glycol are observed as a doublet at 1.17 ppm (F), a weak doublet from propylene glycol  $-\text{CH}_3$  in diester (1.25 ppm, II), and two doublets given by propylene glycol protons from  $-\text{CH}_3$  groups in two monoesters Ia (1.22 ppm, G) and Ib (1.24 ppm, H). The corresponding integrals from the OC plasticizer spectrum and the calculate composition of all components (in wt%) are shown in Table S2.

**Table S2.** Total integrals for each compound and their percentages

Compound	Integrals	Component content in the OC plasticizer, wt%
Acetic acid	0.71	1.76
Propylene glycol	6.80	21.38
Ia	4.70	40.67
Ib	8.33	22.95
II	2.00	13.24



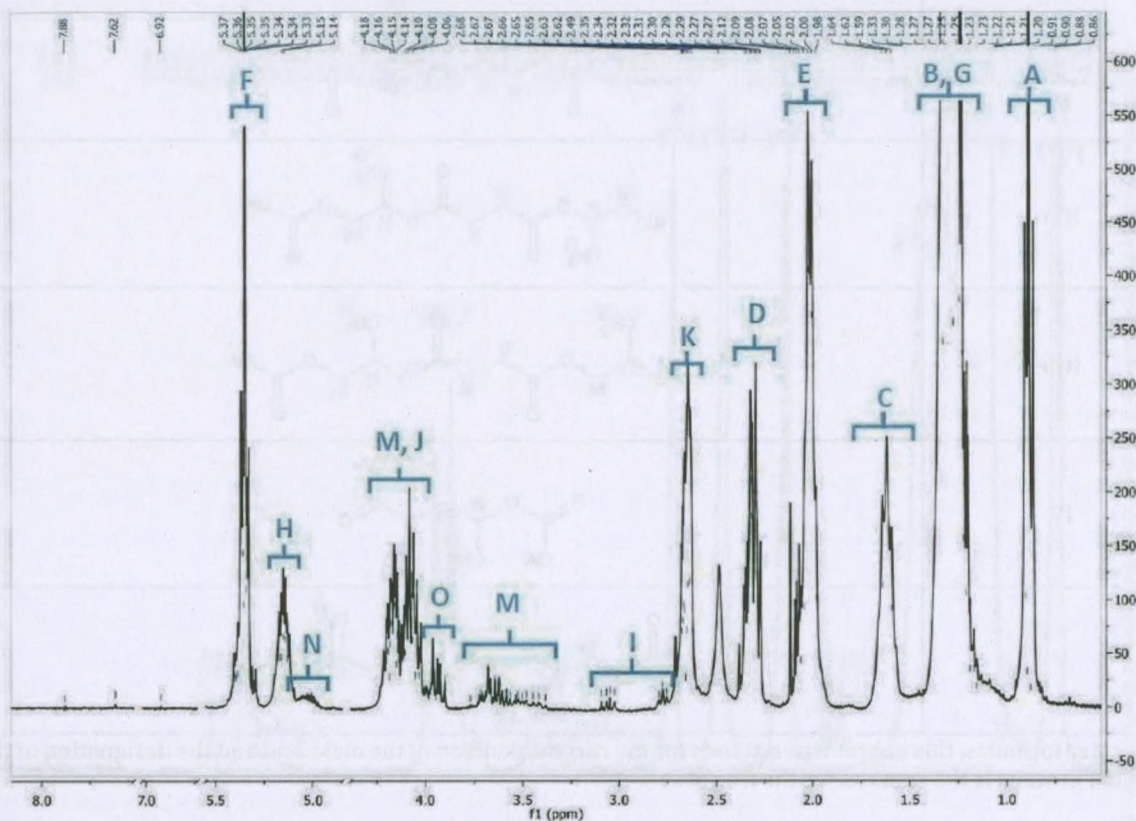


Fig. S8.  $^1\text{H}$  NMR spectra of KBOL plasticizer

Table S3.  $^1\text{H}$  NMR interpretation for KBOL plasticizer

Compound	KBOL spectrum signals assigned to protons
Oleic acid (OA*)	
Propylene glycol	
Ia	
Ib	

II	
IIIa	
IIIb	
IV	
V	

\*in the ester formulas, this abbreviation stands for the carbon skeleton of the oleic acid and the designation of the individual protons is the same as for the free acid



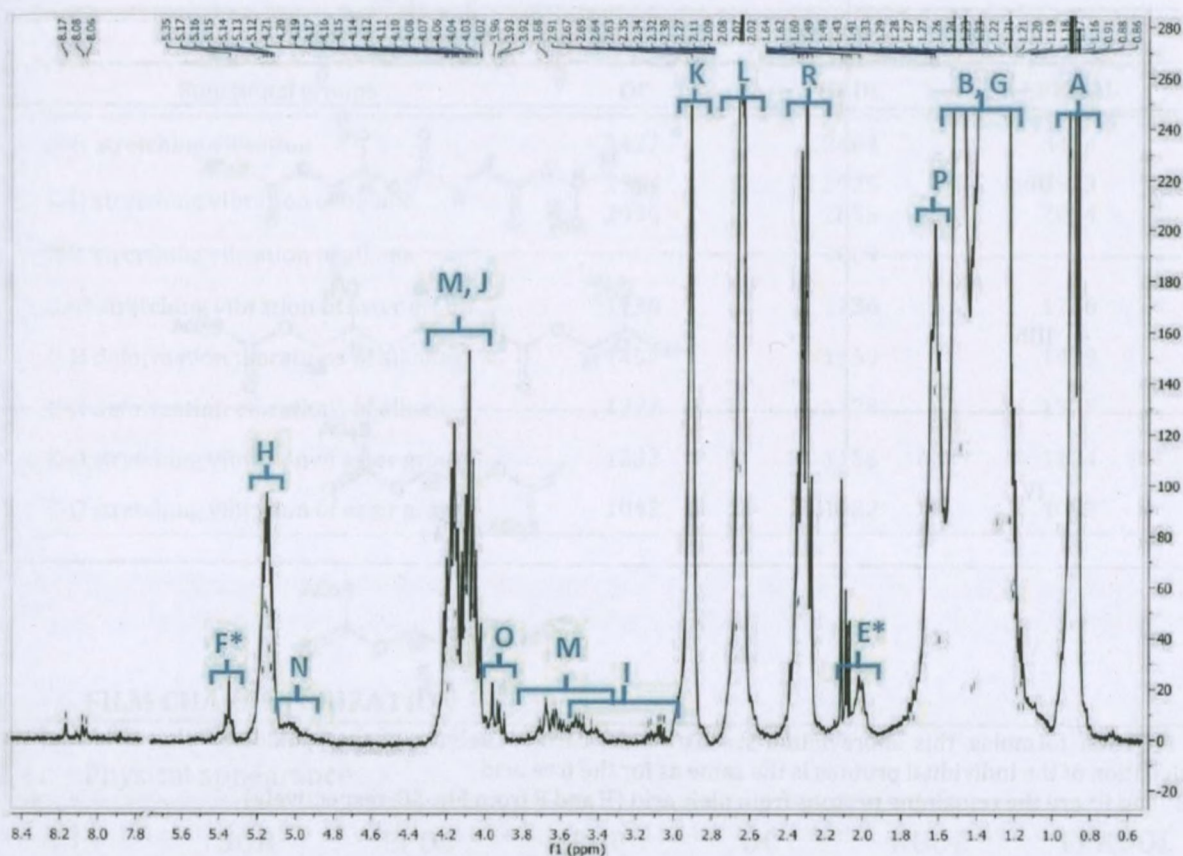
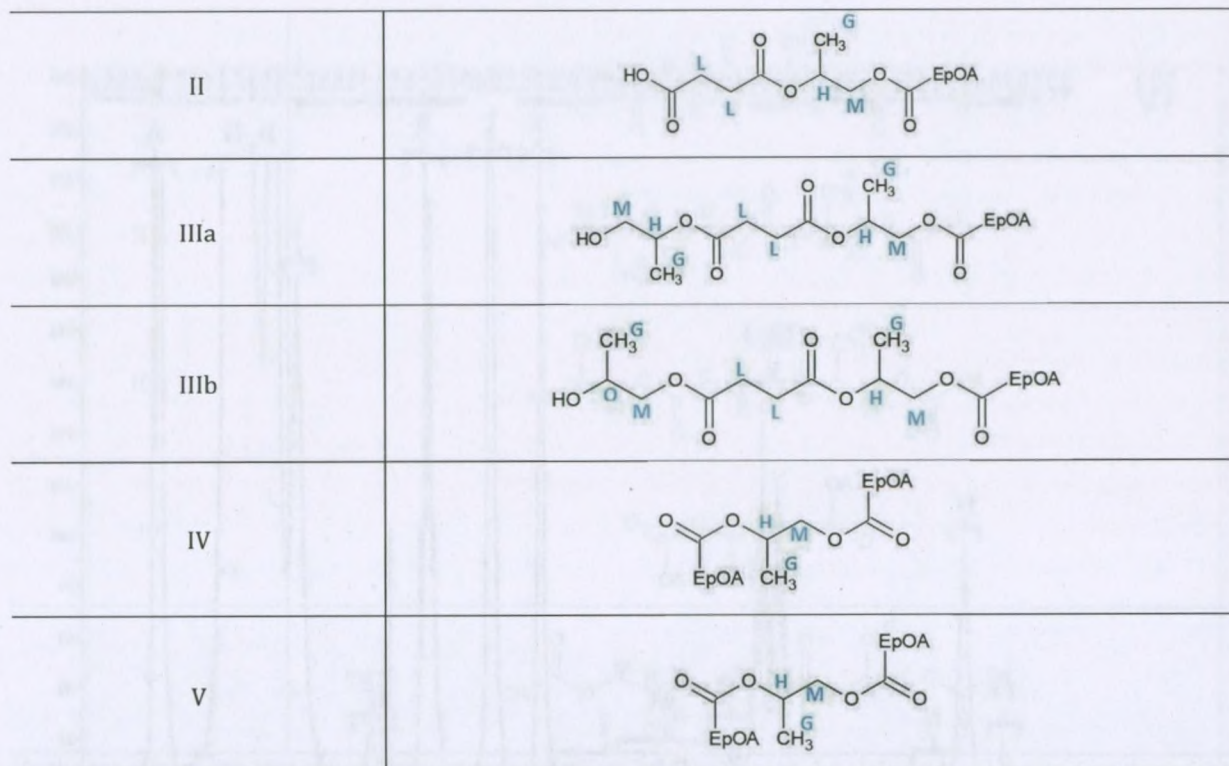


Fig. S9.  $^1\text{H}$  NMR spectra of EPKBOL plasticizer

Table S4.  $^1\text{H}$  NMR interpretation for EPKBOL plasticizer components

Compound	EPKBOL spectrum signals assigned to protons
EpOA*	
Propylene glycol	
Ia	
Ib	



\*in the ester formulas, this abbreviation stands for the carbon skeleton of the epoxidized oleic acid and the designation of the individual protons is the same as for the free acid

\*\* E\* and F\* are the remaining protons from oleic acid (E and F from Fig. S8, respectively)

The structures of the synthesized plasticizers were also confirmed by FT-IR. The obtained spectra confirmed the presence of characteristic functional groups of the plasticizers.

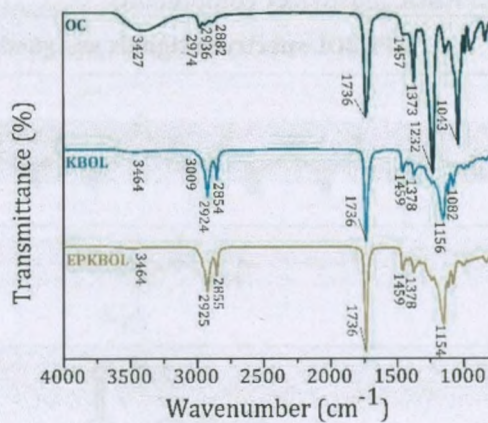


**Fig. S10.** FTIR spectra of OC, KBOL and EPKBOL plasticizer.



**Table S5..** Main IR peaks and corresponding functional groups of OC, KKBOL and EPKBOL

Functional groups	Peak (cm <sup>-1</sup> )		
	OC	KBOL	EPKBOL
O-H stretching vibration	3427	3464	3464
C-H stretching vibration of alkane	2974	2925	2923
	2936	2855	2854
C-H stretching vibration of alkene	–	3009	–
C=O stretching vibration of ester group	1736	1736	1736
C-H deformation vibrations of alkane	1457	1459	1459
C-H deformation vibrations of alkane	1373	1378	1378
C-O stretching vibration of ester group	1232	1156	1154
C-O stretching vibration of ester group	1043	1082	1082

## 2. FILM CHARACTERIZATION

### 2.1. Physical appearance

**Fig. S11.** Physical appearance of the chitosan-based films

### 2.2. Roughness characteristics

The measurements of surface roughness was carried out using two methods: optical profilometer and from SEM using dedicated 3D RR module. The obtained results are presented in Table S6 and showed that the surface of all investigated films were rather smooth. Due to the edge effects observed for the measurement conducted with SEM, the results obtained from the profilometer seem to be more reliable, especially the roughness of the bottom layer. As can be seen, the bottom layer of the films was smoother than the top layer due to the dispersion of the chestnut grains just under the surface. Considering the results from the profilometer, the roughness range of the bottom surface was between 0.16 and 0.96  $\mu\text{m}$ , while that of the top surface was between 1.00 and 1.83  $\mu\text{m}$ .



**Table S6.** Surface roughness for chitosan-based films

Sample	Surface roughness $S_a$ , $\mu\text{m}$			
	Top layer		Bottom layer	
	optical profilometer	SEM 3D RR	optical profilometer	SEM 3D RR
GLY	1.25	2.17	0.20	1.23
SOR	1.22	1.91	0.16	1.19
EPOS	1.00	1.46	0.23	1.00
EPOP	1.83	1.19	0.96	0.94
OC	1.38	2.04	0.20	0.99
KBOL	1.51	1.03	0.23	0.93
EPKBOL	1.43	1.32	0.62	1.16

### 2.3. Morphological analysis

The external and internal structure of chitosan films containing investigated plasticizers was presented by imaging their surface and cross-section, as illustrated in Fig. S12.

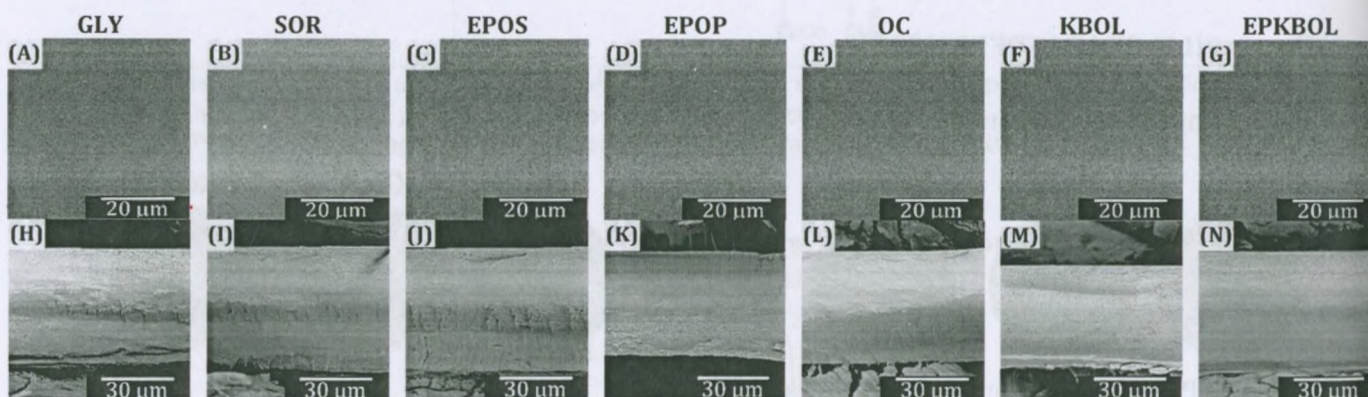


**Fig. S12.** SEM images of the surface of (A) GLY, (B) SOR, (C) EPOS, (D) EPOP, (E) OC, (F) KBOL and (G) EPKBOL film, the cross-section of (H) GLY, (I) SOR, (J) EPOS, (K) EPOP, (L) OC, (M) KBOL and (N) EPKBOL film.

### 2.4. Thermal analysis of chitosan-based films

The thermal stability of neat chitosan and the chitosan-based films were evaluated by thermogravimetric analysis and differential scanning calorimetry. In TGA, two parameters were measured: the temperature of the onset of degradation ( $T_{\text{onset}}$ ) and the temperature at which thermal degradation results in 50% weight loss ( $T_{\text{d50}}$ ). In turn, DSC allowed determining the glass transition temperature of the obtained materials. The results are summarized in Table S7.




**Table S7.** Thermal stability parameters of the tested samples according to TG and glass transition temperature determined from DSC measurements.

Sample	Thermal stability (N <sub>2</sub> )		Thermooxidative stability (air)		Glass transition temperature
	<i>T</i> <sub>onset</sub> /°C	<i>T</i> <sub>50%</sub> /°C	<i>T</i> <sub>onset</sub> /°C	<i>T</i> <sub>50%</sub> /°C	<i>T</i> <sub>g</sub> /°C
<b>Chitosan</b>	265.7	330.0	256.9	313.2	189.2
<b>GLY</b>	195.8	327.8	213.8	336.4	167.3
<b>SOR</b>	224.2	337.4	219.4	351.4	167.9
<b>EPOS</b>	223.6	405.1	227.1	403.2	158.9
<b>EPOP</b>	224.7	394.3	225.4	390.9	155.3
<b>OC</b>	228.7	378.6	227.7	377.5	152.5
<b>KBOL</b>	225.7	394.5	226.8	398.7	155.6
<b>EPKBOL</b>	223.4	360.3	223.1	360.8	164.6



OPEN

## Modulation of physicochemical properties and antimicrobial activity of sodium alginate films through the use of chestnut extract and plasticizers

Weronika Janik<sup>1,2</sup>, Michał Nowotarski<sup>3</sup>, Kerstin Ledniowska<sup>1,2</sup>, Divine Yufetar Shyntum<sup>4</sup>, Katarzyna Krukiewicz<sup>3,5</sup>, Roman Turczyn<sup>3,5</sup>, Ewa Sabura<sup>1</sup>, Simona Furgo<sup>1</sup>, Stanisław Kudła<sup>1</sup> & Gabriela Dudek<sup>3</sup>

Due to the growing demand for robust and environmentally friendly antimicrobial packaging materials, biopolymers have recently become extensively investigated. Although biodegradable biopolymers usually lack mechanical properties, which makes it inevitable to blend them with plasticizers. The purpose of this study was to investigate plasticization efficiency of bio-based plasticizers introduced into sodium alginate compositions containing chestnut extract and their effect on selected film properties, including primarily mechanical and antibacterial properties. The films were prepared by the casting method and sodium alginate was cross-linked with calcium chloride. Six different plasticizers, including three commercially available ones (glycerol, epoxidized soybean oil and palm oil) and three synthesized plasticizers that are mixtures of bio-based plasticizers, were used to compare their influence on the film properties. Interactions between the polymer matrix and the plasticizers were investigated using Fourier transform infrared spectroscopy. The morphological characteristics of the films were characterized by scanning electron microscopy. Thermal properties, tensile strength, elongation at break, hydrophilic, and barrier properties of the obtained films were also determined. To confirm the obtaining of active films through the use of chestnut extract and to study the effect of the proposed plasticizers on the antibacterial activity of the extract, the obtained films were tested against bacteria cultures. The final results showed that all of the obtained films exhibit a hydrophilic character and high barrier effect to oxygen, carbon dioxide and water vapor. In addition, sodium alginate films prepared with chestnut extract and the plasticizer proposed by us, showed better mechanical and antimicrobial properties than the films obtained with chestnut extract and the commercially available plasticizers.

Recently, there has been a growing interest in innovative and environmentally friendly antimicrobial packaging materials based on biodegradable polymers that extend the shelf life of food<sup>1</sup>. Among various packaging materials, petroleum-based plastics are dominant, especially for their low production cost and very good mechanical properties. However, their non-biodegradable nature has become a serious threat to the environment<sup>2</sup>. An alternative to non-biodegradable plastics are materials based on polysaccharides and among them, those based on starch, chitosan and sodium alginate have been the most popular<sup>3</sup>.

Sodium alginate, which is extracted from brown seaweed, is one of the most popular biodegradable polymers. The chemical structure of alginate consists of  $\beta$ -D-mannuronic acid (M) and  $\beta$ -L-guluronic acid (G)<sup>4</sup>. The monomers in the polymer chains are arranged alternately in GG and MM blocks, along with MG blocks<sup>5</sup>. Sodium

<sup>1</sup>Łukasiewicz Research Network—Institute of Heavy Organic Synthesis “Blachownia”, 47-225 Kędzierzyn-Koźle, Poland. <sup>2</sup>Department of Physical Chemistry and Technology of Polymers, PhD School, Silesian University of Technology, 44-100 Gliwice, Poland. <sup>3</sup>Department of Physical Chemistry and Technology of Polymers, Faculty of Chemistry, Silesian University of Technology, 44-100 Gliwice, Poland. <sup>4</sup>Biotechnology Centre, Silesian University of Technology, 44-100 Gliwice, Poland. <sup>5</sup>Centre for Organic and Nanohybrid Electronics, Silesian University of Technology, 44-100 Gliwice, Poland. ✉email: weronika.janik@icso.lukasiewicz.gov.pl



alginate has high compatibility with most anionic substances, film-forming ability and is fully biodegradable<sup>6</sup>. However, pure sodium alginate films exhibit high water solubility, relatively poor mechanical properties and weak antimicrobial activity, making it necessary to modify them for use in packaging<sup>7,8</sup>. An important property of alginates is their ability to react with multivalent metal cations, specifically calcium ions. The ions form connections between MM and GG blocks of the polymer, yielding a three-dimensional network<sup>5</sup>. The cross-linked sodium alginate lose their hydrophilic character, what improves its water barrier properties and reduces water solubility<sup>9,10</sup>. Mechanical properties are also significantly improved by cross-linking<sup>11</sup>, as well as by the use of proper plasticizers, which improve flexibility of the films and expand their potential applications<sup>12</sup>.

In general, unmodified sodium alginate films are very brittle and fragile, what limits their application<sup>13</sup>. The use of plasticizers results in an increase in elongation at break and a decrease in tensile strength of the films<sup>14</sup>. In the case of biodegradable films, it is also important that the plasticizer has to be eco-friendly, biodegradable and non-toxic. The most commonly used plasticizers are polyols, of which glycerol<sup>15–20</sup> and sorbitol<sup>21–24</sup> are the most often incorporated into the alginate matrix. Jost et al.<sup>21</sup> compared the efficiency of glycerol and sorbitol as plasticizers (20–50 wt%) for alginate films, finding that both positively affected mechanical properties, but led to differences in barrier properties. Incorporation of glycerol into the matrix increased permeability of oxygen and water vapor, while sorbitol had no effect on barrier properties. In another study, Jost and Stramm<sup>22</sup> investigated the effects of glycerol, sorbitol and triethanolamine (20–50 wt%) as plasticizers of alginate and cornstarch films and they found that glycerol was more effective than sorbitol in mechanical properties improvement, while triethanolamine appeared to be as effective as glycerol, but it had a different effect on barrier properties. Triethanolamine reduced the water vapor and oxygen permeability of the film, while glycerol led to their increase, and sorbitol had no effect at all. Among polyols, mannitol (12.5–50 wt%)<sup>25</sup>, diethylene glycol (20 wt%)<sup>26</sup>, isopropanol (30 wt%)<sup>27</sup> or polyethylene glycol (10–30 wt%)<sup>26–28</sup> were also used for the plastification of sodium alginate films. In addition to glycerol and sorbitol, Olivas and Barbosa-Canovas<sup>23</sup> proposed fructose and polyethylene glycol (PEG-8000) as plasticizers (40 wt%). Glycerol, sorbitol and fructose led to a significant increase in elongation at break of investigated films, when compared to PEG-8000. Water vapor permeability for films with fructose and with sorbitol showed the lowest values, while with PEG-8000—the highest. It was also found that PEG-8000 was incompatible with alginate, what was evidenced by phase separation. On the other hand, Paixao et al.<sup>29</sup> used glycerol (Gly), tributyl citrate (TC) and their mixture as plasticizers for sodium alginate (70%TC + 30%Gly, 60%TC + 40%Gly, 50%TC + 50%Gly, 30%TC + 70%Gly and 10%TC + 90%Gly). The addition of tributyl citrate made the film less hygroscopic, as it was confirmed by solubility and water vapor permeability tests. Tributyl citrate and its mixture with glycerol increased tensile strength of the films, with higher values observed at higher concentrations of glycerol. Films plasticized with tributyl citrate and its mixture with glycerol were opaque, while films with glycerol were transparent. Aadil and Jha<sup>28</sup> prepared films based on alginate and lignin using three different plasticizers: glycerol, polyethylene glycol and epichlorohydrin (10–15 wt%). The film with glycerol showed higher solubility and swelling values compared to films with the other plasticizers. In contrast, the film with polyethylene glycol had the highest tensile strength. In addition, films based on alginate and lignin in the presence of epichlorohydrin showed the highest thermal stability and better physico-mechanical and UV light barrier properties, and could be successfully used in packaging and coating applications. Unfortunately, epichlorohydrin can be used at low concentrations only, as it is toxic at higher ones.

Besides modifying mechanical properties, one of the other desirable modification of alginate is to obtain packaging materials with antimicrobial properties. Such materials can significantly reduce the number of undesirable microorganisms in food. Antibacterial activity of sodium alginate-based films can be provided by adding to the polymer matrix various bioactive nanoparticles, such as ZnO, Ag, CuO, or natural extracts<sup>30–33</sup>. A wide range of such extracts can be found in the literature, including extracts of white ginseng<sup>34</sup>, green tea<sup>35</sup>, peanut red skin<sup>36</sup> or roselle hibiscus<sup>37</sup>. In addition, antibacterial properties of alginate films can also be provided by tansy essential oil<sup>38</sup>, lemongrass essential oil<sup>30</sup>, basil leaf ethanol extract<sup>39</sup> or brown propolis extract<sup>40</sup>. Chestnut extracts used as antibacterial agents in different polysaccharide-based films have been indicated by recent studies<sup>41–45</sup> as well. Since chestnut extract is a rich source of polyphenolic compounds, phenolic acids, and tannins<sup>46–48</sup>, its presence in the packaging material is expected to provide antibacterial activity over a wide range of bacterial strains, either by a direct killing of bacteria or by attenuation of bacterial pathogenicity<sup>49</sup>. To be active, chestnut extract should migrate from the internal space of the material to its surface, to be in contact with bacterial cells. Since the addition of the plasticizer leads to higher free volume between polymer chains, it should also allow the chestnut extract particles to migrate and fully reveal the antibacterial properties. In consequence, it should be possible to modulate antibacterial properties of sodium alginate films by using deliberately selected plasticizers. In addition to the antimicrobial properties that nanomaterials bring to food packaging, concerns about the safety of nanomaterials should not be ignored. A number of researchers<sup>50–55</sup> have investigated the problem of safety of using the nanomaterials to provide so-called active, or antibacterial, films. Studies have focused on the risk of migration of nanoparticles from packaging materials into food and their impact on consumer health<sup>56</sup>. It has been found that due to the small size, nanomaterials can bioaccumulate in the body's organs and tissues<sup>53,57</sup>. Extended migration studies are therefore needed before marketing antibacterial packaging with nano-additives. Even if a substance is GRAS (generally regarded as safe), additional testing is required to assess the risks associated with its nano counterparts, since the physicochemical properties of nanostates differ significantly from those of macrostates<sup>53</sup>. The aim of the present study was to investigate plasticization efficiency of bio-based plasticizers introduced into sodium alginate compositions containing chestnut extract and their effect on selected film properties, suitable for food packaging applications. Effects of six plasticizers (three commercially available, i.e. glycerol, epoxidized soybean oil and palm oil, and three mixtures synthesized by us: (i) esters of propylene glycol with acetic acid, (ii) esters of propylene glycol with oleic acid and succinic acid, (iii) epoxidized esters based on propylene glycol, oleic acid and succinic acid, on the mechanical and physicochemical properties, including moisture content, swelling degree, total soluble matter content and gas permeability (oxygen, carbon dioxide and water vapor) were studied.

Structural changes (infrared spectroscopy) and thermal properties (thermogravimetric analysis) of the materials as well as surface topography of the films (scanning electron microscopy) were also investigated. To confirm the antimicrobial activity of the films prepared with chestnut extract and different plasticizers, microbiological tests were conducted with the use of *Escherichia coli*, *Staphylococcus epidermidis*, and *Candida albicans*.

## Materials and methods

**Materials.** Sodium alginate (Brookfield viscosity 350–550 mPa·s,  $c=1\%$ , w/w at 20 °C) was supplied by Across Organics (Geel, Belgium). Chestnut extract Farmatan ( $\geq 76\%$  tannins) was provided by Tanin Sevnica (Sevnica, Slovenia). Calcium chloride (purity  $\geq 96\%$ ) and acetic acid (99.5–99.9%) were purchased from Avantor Performance Materials (Gliwice, Poland). Glycerol was supplied by Merck (Darmstadt, Germany), while epoxidized soybean oil and epoxidized palm oil were from Inbra Indústrias Químicas LTDA (Sao Paulo, Brasil) and Malaysian Palm Oil Board (Kajang, Malaysia), respectively. Propylene glycol, cyclohexene and toluene (both pure p.a.), formic acid (85.0%), hydrogen peroxide (30.0%), disodium hydrogen phosphate dihydrate and sodium hydrogen carbonate (pure p.a.) were purchased from Chempur (Piekary Śląskie, Poland). Oleic acid (90.0%) was supplied by Alfa Aesar (Ward Hill, MA, USA), and succinic acid ( $\geq 99.5\%$ ) by POL-AURA (Zabrze, Poland). Methanesulfonic acid ( $> 99.0\%$ ) was provided by TCI (Zwijndrecht, Belgium).

**Preparation of the bio-based plasticizer mixtures.** Plasticizer mixtures were prepared as described in our previous study<sup>58,59</sup>. In short, esterification reactions (propylene glycol with acetic acid, propylene glycol with oleic acid and succinic acid) and epoxidation reactions (epoxidation of mixed esters based on propylene glycol, oleic acid and succinic acid) were carried out in a glass reactor of 500 or 1000 cm<sup>3</sup> volume, equipped with a mechanical stirrer, a temperature controller, Dean-Stark trap (for esterification reactions), reflux condenser and dropping funnel (for selected reactions). The schematic route of the synthesis is shown in Figs. S1, S2 and S3 (Supplementary).

**Preparation of the antibacterial films.** Sodium alginate films with chestnut extract and different plasticizers were prepared by casting method and then subjected to cross-linking reaction with calcium chloride (Fig. 1), according to the method described in our previous study<sup>41</sup>. In short, aqueous sodium alginate solution (1%, w/w) was prepared by dispersing sodium alginate with chestnut extract (0.75%, w/v) and a selected plasticizer (30%, w/w based on the mass of alginate)—Table 1. The films were obtained by casting the solution (46 g) onto Petri dishes (12 × 12 cm dish) thus obtaining a thickness of ca. 50 μm. After drying (24 h), the films were subjected to a cross-linking process. For this purpose, 40 ml of a 2.5% calcium chloride solution was poured onto the dried film and left on the film for 2 h under cover. After this time, the film was rinsed with distilled water and laid out on a paper towel, which was pressed to prevent the film from wrinkling during drying.

**Mechanical properties.** Mechanical properties i.e. tensile strength and elongation at break of sodium alginate films with chestnut extract and various plasticizers were examined using Instron 4466 testing machine. The analysis was performed on film samples 2 cm × 8 cm. The samples were stretched at a speed of 5 mm/min at room temperature. Final values were calculated as the average of ten measurements. During testing of the mechanical properties, the thickness of the film was measured using a digital micrometer (Mitutoyo Absolute Tester, Tokyo Sangyo Co. Ltd., Japan) with a resolution of 0.001 mm. The values presented were calculated as an average value of 10 measurements taken at different points for each sample.

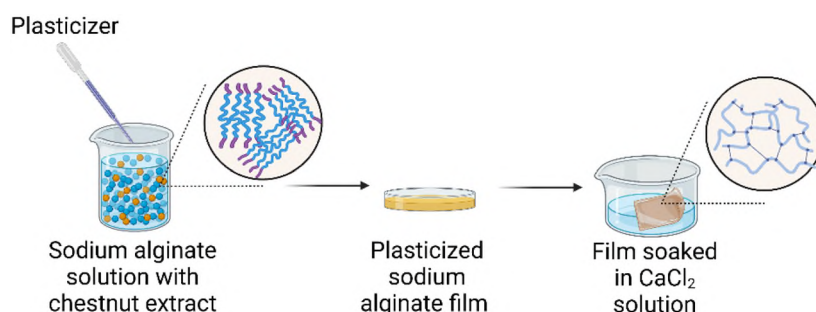


**Figure 1.** Preparation of plasticized and crosslinked sodium alginate films.

Symbol	CP1	CP2	CP3	MP1	MP2	MP3
Plasticizer	Commercial			Synthesized		
Description	Glycerol	Epoxidized soybean oil	Epoxidized palm oil	Mixed esters of propylene glycol and acetic acid	Mixed esters of propylene glycol, oleic acid and succinic acid	Epoxidized mixed esters of propylene glycol, oleic acid and succinic acid

**Table 1.** Samples under investigations.



**Hydrophilic properties.** Hydrophilicity of sodium alginate films with chestnut extract and various plasticizers was analyzed using three-step gravimetric method (moisture content—MC, swelling degree—SD, and total soluble matter—TSM) and by determination of the contact angle values. Film samples with surface area of 1 cm<sup>2</sup> were weighed ( $M_1$ ), dried at 100 °C for 24 h and weighed again ( $M_2$ ).

$$MC(\%) = \frac{(M_1 - M_2)}{M_1} \times 100 \quad (1)$$

The samples were then placed in 30 mL of distilled water, left at room temperature for 24 h and weighed again ( $M_3$ ).

$$SD(\%) = \frac{(M_3 - M_2)}{M_2} \times 100 \quad (2)$$

In the final step, the samples were dried at 100 °C for 24 h and weighed ( $M_4$ ). Measurements were repeated five times and the average value was calculated. TSM values were calculated using the following formulae:

$$TSM(\%) = \frac{(M_2 - M_4)}{M_2} \times 100 \quad (3)$$

The water contact angle of the film surface was measured using an optical contact angle meter and a contour analysis system (OCA15 from DataPhysic). Droplets of distilled water (1 μL) were examined at ten points on each sample. All measurements were performed at ambient temperature (ca. 24 °C).

**Barrier properties.** Oxygen and carbon dioxide permeability of the sodium alginate films with chestnut extract and various plasticizers were determined using an isobaric apparatus<sup>58</sup>. The samples with a circular surface area of 60 mm<sup>2</sup> were degassed for 24 h and conditioned with the appropriate gas in the apparatus prior to testing for 2 h. Then, the diffusion chamber was sealed and compressed oxygen (class 5.0) or carbon dioxide (technical gas) was supplied at a controlled flow rate to keep the pressure constant. The permeation coefficient was determined as follows:

$$P = \frac{V \times l}{S \times \Delta p} \quad (4)$$

where V is the volumetric flow (mol s<sup>-1</sup>), l is the sample thickness (m), S is the sample area (m<sup>2</sup>) and Δp is the pressure difference on both sides of the sample (Pa).

Water vapor transmission rate (WVTR) and water vapor permeability (WVP) of sodium alginate films with chestnut extract and various plasticizers were determined according to the methodology proposed by Aguirre-Loredo et al.<sup>60</sup> and Jiménez-Regalado et al.<sup>61</sup>. The samples, in the form of discs, were mounted on a glass container (internal diameter of 24.64 mm) with silica gel in its interior (~0% relative humidity, RH) and sealed with a liquid paraffin. After the paraffin solidified, the cup was weighed in order to calculate the initial weight. The covered glass container was then placed in a desiccator containing a supersaturated saline solution of BaCl<sub>2</sub> (90% RH), generating a water-vapor differential pressure of 2854.23 Pa. The glass container was weighed seven times at 60 min intervals. The determinations were made in triplicate. The WVTR and WVP values were determined as follows:

$$WVTR = \frac{m}{tA} \quad (5)$$

$$WVP = WVTR \times L\Delta p \quad (6)$$

where Δm/Δt is the moisture weight gain in time (g/s), A is the exposed surface area of the film (m<sup>2</sup>), L is the thickness of the film (mm), and Δp is the difference in partial pressure (2854.23 Pa).

**Surface morphology.** The morphology of the sodium alginate films with chestnut extract and various plasticizers was examined by a scanning electron microscopy (Phenom ProX) at 10 kV accelerating voltage, as well as an optical profilometer (Filmetrics Profilm 3D, KLA Co.). Surface roughness was obtained according to ISO 25178 via arithmetical mean height area roughness parameter ( $S_a$ ).

**Antimicrobial activity.** Antimicrobial activity of sodium alginate films with chestnut extract and various plasticizers, as well as a control sample (sodium alginate film plasticized with glycerol, without chestnut extract) was determined against *Escherichia coli* ATCC25922, *Staphylococcus epidermidis* ATCC12228, and *Candida albicans* ATCC18804. The samples in the form of discs (10 mm in diameter) were placed in 12-well plates containing 200 μl of M9 minimal medium supplemented with glucose as the sole carbon source. Thereafter, 20 μl of the targeted bacterial culture, normalized to 10<sup>4</sup> CFU/ml, was inoculated into each well and incubated overnight at 37 °C with shaking at 150 rpm. Overnight cultures were serially diluted in double distilled autoclaved water and plated on LB agar to determine CFU/ml of recovered targeted bacteria. All experiments were performed in triplicates and repeated three times.

Statistical significance analysis was performed using an unpaired, two-tailed Student's t-test (JMP software v.5; SAS Institute Inc., Cary, NC, U.S.A.). The CFU/ml of surviving bacteria, when co-cultured in the presence

of alginate films, was compared to the no treatment control (alginate film with no chestnut extract). *P* values of less than 0.05 were considered to be statistically significant.

**Thermal analysis.** Thermal and thermoxidative stability of neat sodium alginate and the sodium alginate films with chestnut extract and various plasticizers were investigated by thermogravimetric analysis (TGA) and differential scanning calorimetry (DSC). Thermogravimetric analysis was carried out using Mettler Toledo TGA 2 Thermo-balance. The sodium alginate film samples (about 5 mg) were heated up in an open platinum crucible (Pt 70  $\mu$ L), in the temperature range from 30 to 800 °C at the heating rate  $\beta = 10$  °C/min, in the dynamic (100 mL/min) nitrogen (inert atmosphere) or air (oxidative atmosphere) atmosphere. Two parameters were measured: the temperature of the onset of degradation ( $T_{onset}$ ), the temperature at maximum degradation ( $T_{peak}$ ) and weight loss on evaporation of water ( $\Delta m$ ). The thermographs (thermogravimetric (TG) curves and derivative thermogravimetric (DTG) curves) were analyzed using the STARe Thermal Analysis Software.

Differential Scanning Calorimetry (DSC) measurements were performed using Mettler Toledo DSC 822e Differential Scanning Calorimeter. The alginate film samples (about 5 mg) were heated in an aluminum crucible (Al 40  $\mu$ L) closed with perforated lid (0.5 mm), in dynamic (50 ml/min) nitrogen atmosphere, in the temperature range from 0 to 300 °C at the heating rate  $\beta = 10$  °C/min.

**Chemical structure.** Fourier transform infrared spectroscopy (FTIR) was used to identify the chemical structure of the sodium alginate films with chestnut extract and various plasticizers and possible interactions between their components. The FTIR spectra were measured using a Spectrum Two spectrometer (Perkin Elmer). The spectra were averaged for 25 scans recorded at a resolution of 2  $\text{cm}^{-1}$  in the range from 4000 to 650  $\text{cm}^{-1}$ .

## Results and discussion

**Mechanical properties.** The effect of the bio-based plasticizers incorporated in the formulations of sodium alginate with chestnut extract on the tensile strength and elongation at break of the films was investigated. All films had a similar thickness of ca. 50  $\mu$ m. Typical stress-strain curves are shown in Fig. 2. It can be seen that the highest tensile strength values, 75–76 MPa, exhibited films containing MP1 mixture and commercially available glycerol, sample CP1. The values are about 70% higher than the values for films with the other plasticizers. The lowest tensile strength value, ca. 35 MPa, was noted for CP3 sample, wherein epoxidized palm oil was used as a plasticizer. Almost equally low value was observed for MP3 sample with the epoxidized mixture of synthesized plasticizers. The highest values of elongation at break were recorded for the synthesized plasticizer mixtures, i.e. MP1 and MP2 (about 4.5% and 5.5%, respectively). In this case, the values were about 50% higher than for other samples investigated. Such significantly better elongation at break is related to the increased flexibility of the polymer chains and compatibility between polymer matrix and plasticizer. It was confirmed by SEM images (Fig. 5), wherein the structures of MP1 and MP2 samples are much more homogeneous than that of the other samples. Zactiti and Kieckbusch<sup>62</sup> also studied sodium alginate-based films plasticized with glycerol and they obtained values of about 120 MPa and 4.5% for tensile strength and elongation at break, respectively. On the other hand, Paixão et al.<sup>29</sup> studied sodium alginate films plasticized with glycerol, tributyl citrate or tributyl citrate/glycerol mixture. They noted that sodium alginate plasticized with tributyl citrate showed the highest tensile strength (about 150 MPa), while for the material plasticized with glycerol it was only ca. 104 MPa. In contrast, the elongation at break value was the highest for films plasticized with glycerol and it was equal to ca. 6%. Aadil and Jha<sup>28</sup> proposed two plasticizers other than glycerol for sodium alginate, i.e. epichlorohydrin and polyethylene glycol. They found that the addition of the latter leads to an increase in the intermolecular space due to a decrease in the hydrogen bonds between lignin and sodium alginate, resulting in a decrease in glass transition temperature and melting point, which in turn improves the flexibility and processing properties of the film.

**Hydrophilic properties.** Moisture content and total soluble matter values of the obtained films with chestnut extract and various plasticizers are shown in Fig. 3A. The results show that the highest MC value, about 20%,

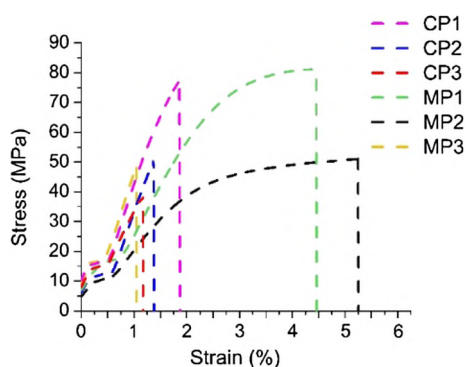


**Figure 2.** Effect of the bio-based plasticizers on tensile strength and elongation at break for sodium alginate films.



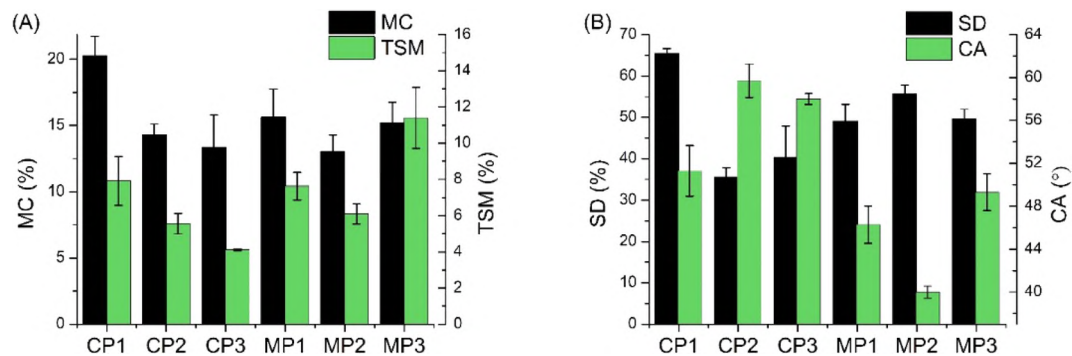


**Figure 3.** (A) Moisture content and total soluble matter; (B) swelling degree and water contact angle of the plasticized sodium alginate films.

was recorded for the sample plasticized with glycerol, i.e. CP1. MC for the other samples was comparable, at around 15%. Analyzing the TSM values, the highest value for MP3, about 11%, and the lowest for CP3, about 3%, can be observed. Among the synthesized plasticizer mixtures, the lowest TSM value was recorded for MP2, at around 6%. In contrast, SD results, Fig. 3B, showed that CP1 has the highest swelling properties, about 65%, and the lowest was recorded for CP2 and CP3, about 40%. The results are similar to those obtained in others studies on sodium alginate films<sup>63,64</sup>. In contrast, Eltabakh et al.<sup>65</sup> proposed sodium alginate maltodextrins-based films with phenolic extract of *Azolla pinnata* fern leaves for which slightly lower hydrophilicity results were obtained. In this case, a noteworthy effect was decrease in MC, SD and TSM values which was associated with the use of the phenolic extract. On the other hand, Abdin et al.<sup>66</sup> proposed sodium alginate arabic gum based films with *Syzygium cumini* seeds extract. Also in this case, a decrease in the hydrophilic properties of the obtained films with the addition of the extract was noted. However, in both cases, the values were slightly lower for the control samples (without the extract) than the results obtained for the films investigated in our studies. This suggests that the lower hydrophilic character of the films was influenced primarily by the addition of maltodextrins and arabic gum. Contact angle studies confirmed that all of the obtained sodium alginate-based films are hydrophilic (contact angle  $< 90^\circ$ ). Nevertheless, significant differences were noted for samples containing different plasticizers. The most hydrophilic character was observed for MP2 (CA about  $40^\circ$ ). It is worth noting that the epoxidation of the plasticizer caused a decrease in the hydrophilic character of the film, as its CA increased from  $40^\circ$  (MP2) to about  $50^\circ$  (MP3). Lu et al.<sup>67</sup> prepared similar films based on sodium alginate crosslinked with  $\text{CaCl}_2$  and plasticized with glycerol but their recipes were enriched with nano-silica and oregano essential oil. The CA value of the resulting films was about  $30^\circ$ , which also indicates the hydrophilic nature of these films. A similar finding was observed by Hou et al.<sup>68</sup>, who used films prepared with sodium alginate and agar and modified with nano  $\text{SiO}_2$ —the resulting CA value was about  $60^\circ$ . This suggests that neither  $\text{CaCl}_2$  crosslinking or presence of the forementioned plasticizers or nano additive change the nature of the films to hydrophobic.

**Barrier properties.** The effect of different plasticizers on the barrier properties of the sodium alginate films with chestnut extract is shown in Figure 4. Many factors can affect the gas permeability of a film, such as its thickness, water sensitivity and crystallinity<sup>69</sup>. According to Jouki et al.<sup>69</sup>, polymers with high crystallinity, due to their ordered structure, show significantly lower gas permeability than polymers with low crystallinity. This is primarily because the amorphous phase of the polymer is mainly responsible for the mass transfer of gases. The oxygen permeability (OP) of food packaging materials is essential for food preservation<sup>70,71</sup>. As shown in Fig. 4A, the oxygen permeability values were relatively low for all samples (about  $6 \times 10^{-11} \text{ cm}^3/\text{m}^2$ ) compared

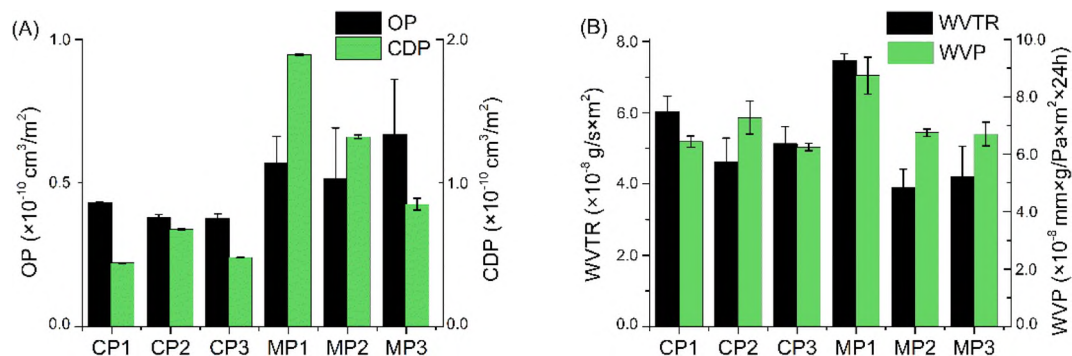


**Figure 4.** (A) Permeability of oxygen (OP) and carbon dioxide (CDP); (B) water vapor transmission rate (WVTR) and water vapor permeability (WVP) of the plasticized sodium alginate films.

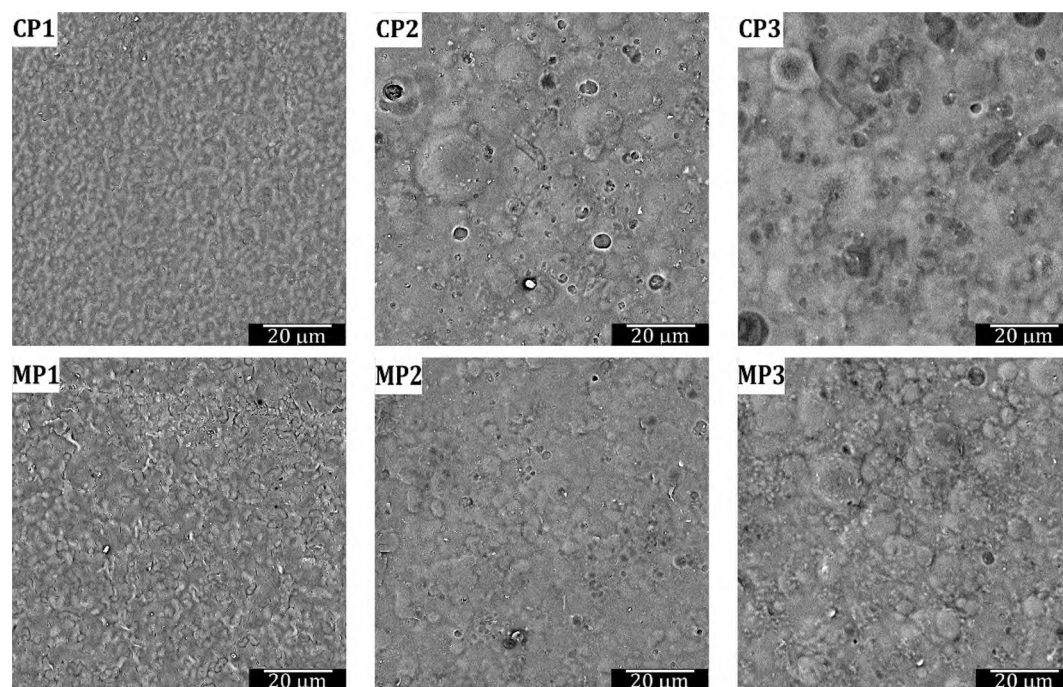


**Figure 5.** SEM images of sodium alginate film surfaces prepared with different plasticizers.

to commercially available polylactide film<sup>41</sup>. Carbon dioxide barrier properties for films used for packaging are as important as OP because they affect respiration or oxidation reactions in food and also affect the shelf life of products<sup>72</sup>. In our case, CO<sub>2</sub> permeability was also relatively low for all samples—about  $5 \times 10^{-11}$  cm<sup>3</sup>/m<sup>2</sup>. However, it is worth noting that epoxidation of the plasticizer led to a decrease in CDP. Despite the slightly higher OP and CDP for the films with the plasticizers synthesized in our study, their values were still lower or nearly equal than for the commercially available polylactide film, for which the values are on the order of  $10^{-9}$  and  $10^{-10}$ , respectively<sup>41</sup>. Water vapor permeability (WVP) is another parameter that determines the water sensitivity of films. It plays an important role in the broad applications of biodegradable films<sup>73</sup>. In the present study, Fig. 4B, the overall WVP and WVTR increased slightly only for MP1, and for the other samples it was without significant changes compared to CP1.

**Surface morphology.** To evaluate the homogeneity and structure of the sodium alginate film surfaces, their SEM images and interferometric optical profiles are shown in Figs. 5, 6, respectively. It can be noted that all films are quite uniform in roughness, with the average  $S_a$  of 50 nm (Table 2). It can be noted that the films with glycerol (CP1) and with the two synthesized plasticizers (MP1 and MP2) presented a more homogeneous and uniform surface structure (as evidenced in their SEM images) than the films prepared with the other plasticizers

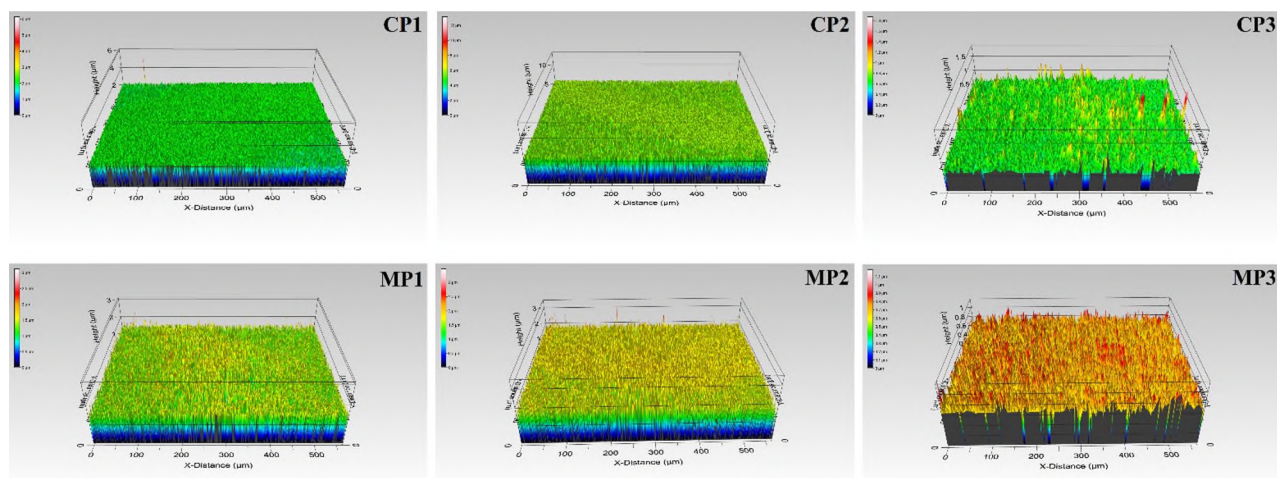


**Figure 6.** Optical profiles of sodium alginate film surfaces prepared with different plasticizers.

Symbol	CP1	CP2	CP3	MP1	MP2	MP3
Roughness ( $S_a$ , nm)	51.8 ± 1.1	49.4 ± 0.7	55.3 ± 5.6	64.6 ± 4.5	56.5 ± 7.5	38.7 ± 2.2

**Table 2.** Surface roughness of sodium alginate film surfaces prepared with different plasticizers.

under investigation, even though the smoothest surface is represented by MP3 ( $S_a = 38.7 \pm 2.2$  nm). This homogeneous structure mainly influenced the mechanical properties of the obtained sodium alginate-based films. They exhibited better tensile strength and elongation at break values compared to samples with a heterogeneous structure. Such a non-uniform surface with aggregate structures was observed for films prepared with epoxidized plasticizers (CP2, CP3 and MP3), what can be attributed to the limited compatibility of the components with the polysaccharide matrix<sup>72,74</sup>. The observed difference in the morphology of the films was also in line with the gas barrier properties (the non-uniform surface and aggregates resulted in higher barrier properties).

**Antimicrobial activity.** The results of microbiological studies, Figs. 7A,C, demonstrate that all alginate-based films containing chestnut extract exhibited strong antibacterial activity against both gram-negative *E. coli* and gram-positive *S. epidermidis* with up to 7 to 8-fold reduction in the recovered CFU/ml, respectively. In the case of fungi *C. albicans*, only a two–three-fold inhibition relative to the control disc was observed, Fig. 7B. Interestingly, the highest antibacterial effects were shown by sodium alginate films containing chestnut extract and synthesized plasticizers, particularly MP2 and MP3, which were found to decrease the bacterial presence to single cells (Table S1, Supplementary). The results are in line with previous research<sup>75–77</sup> showing antimicrobial properties of fatty acid esters. In the case of alginate films containing both chestnut extract and fatty acid based plasticizers, a synergistic effects are observed in relation to their antimicrobial activity. Even though chestnut extract-containing sodium alginate films were not found to exhibit as strong antifungal properties as antibacterial ones, still, a significant decrease in the number of cells was observed on the surface of alginate films plasticized with CP2, MP2 and MP3. These observations can be also attributed to the presence of fatty acids in the plasticizers used for the fabrication of materials. Although chestnut extract does not exhibit strong antifungal properties, fatty acids and their esters are known to be efficient antifungal agents<sup>77</sup>. Since soybean oil contains higher content of linoleic acid (characterized by a low minimum inhibitory concentration<sup>78</sup> than palm oil, also CP2 is more active against *C. albicans* than CP3.

**Thermal analysis.** The effect of various plasticizers on the thermal properties of sodium alginate films with chestnut extract was evaluated by thermogravimetric analysis and differential scanning calorimetry. TG and DTG curves in nitrogen atmosphere are shown in Fig. 8A,B, respectively. It can be seen that for all samples the first peaks in the DTG curves, below 200 °C, correspond to the evaporation of physically absorbed water. For neat sodium alginate (Control), the second weight loss is around 230 °C ( $T_{onset}$  in TG curves), while the maximum of degradation occurred at 235 °C ( $T_{peak}$  in DTG curve), which corresponds to the decomposition of polysaccharides by the fracture of glycosidic bonds, decarboxylation, decarbonylation and loss of bonded water. The final degradation occurred at around 500 °C, which might be attributed to the degradation of the formed intermediate compounds in the second stage and char formation<sup>19,79</sup>. For the plasticized alginate films, the degradation process has slightly decreased. Initial decomposition temperature ( $T_{onset}$ ) has decreased, compared to pure sodium alginate. Moreover neat alginate degradation gave a sharp peak while for plasticized films degradation peak was broader and a shoulder appeared indicating that the crosslink structure is shifting the alginate degradation to relatively higher temperatures. As shown in Table S2 (Supplementary Data), a similar relationship was observed in air atmosphere. Hence, these findings indicate that the addition of plasticizers retarded the initial thermal degradation and prolongs the degradations process<sup>26</sup>. Furthermore, the CP1 and MP1 films showed the lowest  $T_{onset}$  values, respectively 207.4 °C and 208.9 °C. This suggests in CP1 and MP1 samples the plasticizers could easily locate into alginate network and disrupt the intermolecular interactions. These disorders

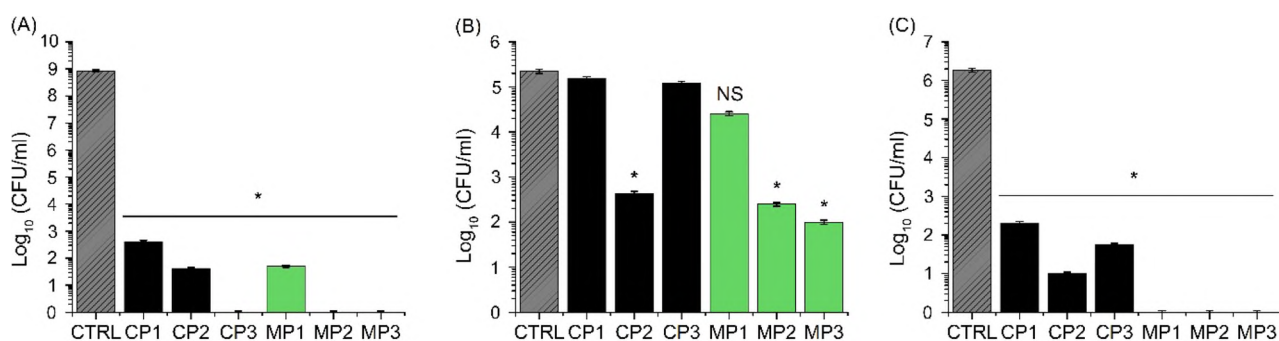


**Figure 7.** Antimicrobial activity of plasticized sodium alginate films against *E. coli* (A), *C. albicans* (B) and *S. epidermidis* (C). Asterisk represents statistically significant difference ( $p < 0.05$ ). NS = no significance difference relative to the control (CTRL-plasticized sodium alginate film without chestnut extract).



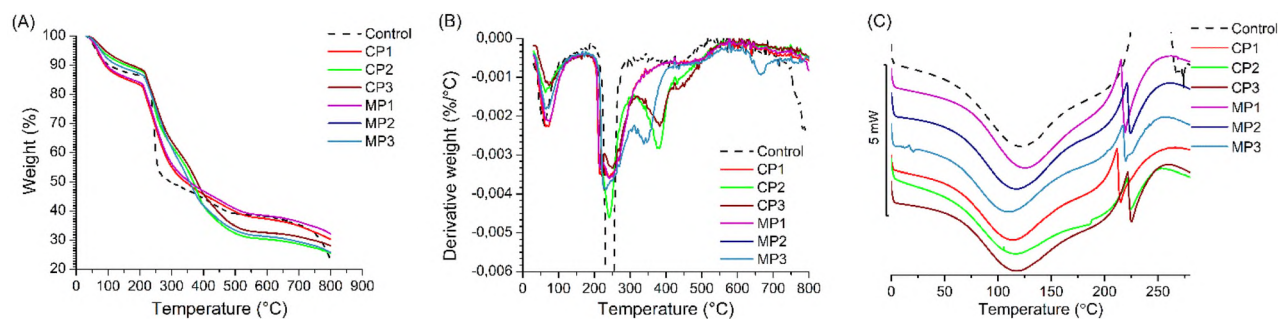


**Figure 8.** Thermal curves of neat sodium alginate and plasticized sodium alginate-based films: (A) TG in nitrogen; (B) DTG in nitrogen; (C) DSC, where Control- neat sodium alginate.

cause softening of the polymer structure, which results in increased chain mobility, making less packed chains more susceptible to degradation processes<sup>8,26</sup>.

Figure 8C shows DSC results. Thermograms for all samples showed a broad endothermic peak centered at 120 °C, confirming the evaporation of adsorbed water. The intensity of this DSC peak changes, what indicates a different amount of adsorbed water, but does not affect the hydrogen bonds between alginate molecules. The thermograms illustrate also the emergence of a sharp endothermic peak at 220 °C, probably corresponding to cleavage of calcium–carboxylate bonds within the complex. Such sharp endothermic peak indicates a highly ordered molecular arrangement forming the so-called “egg-box” structure within calcium alginate matrix<sup>80,81</sup>. Moreover, calcium crosslinking led to upward shift of the exothermic band from 240 to 281 °C indicative for increased alginate resistance to thermal oxidation<sup>20</sup>. However, no significant relationship between the type of plasticizer and the DSC curves shape was observed.

**Chemical structure.** The FT-IR spectra of unplasticized and plasticized sodium alginate films with chestnut extract are shown in Fig. 9. The characteristic peaks of neat sodium alginate (Control) were observed at 3606–3018  $\text{cm}^{-1}$  (broad, attributed to O–H stretching vibrations), 2975–2913  $\text{cm}^{-1}$  (–CH stretching vibrations), 1604  $\text{cm}^{-1}$  (asymmetric –COO– vibrations) and 1415  $\text{cm}^{-1}$  (symmetric –COO– vibrations) and 1090–1017  $\text{cm}^{-1}$  (C–O–C antisymmetric stretching vibrations)<sup>24,82</sup>. The absorbance bands at 1200–960  $\text{cm}^{-1}$  attributed to the skeletal vibrations of pyranose ring of alginate<sup>83</sup>. Plasticized alginate films showed the same FT-IR patterns as the unplasticized ones. For the plasticized alginate films, a characteristic broad band was observed between 3700 and 3000  $\text{cm}^{-1}$ , which was attributed to the O–H stretching vibration. The intensity of this band increased with the addition of a plasticizer; the highest intensities were observed for CP3 and MP2, while the lowest for CP1 and MP1, suggesting hydrogen bonding between the plasticizer and alginate matrix. The bands at ca. 1600  $\text{cm}^{-1}$  and 1405  $\text{cm}^{-1}$ , which were observed for each plasticized film, are characteristic for asymmetric and symmetric stretching vibrations of the COO– groups, respectively<sup>84</sup>. For CP2, CP3, MP2 and MP3, a band at 1748–1741  $\text{cm}^{-1}$  was observed which can be attributed to the double carbonyl bonds (C=O) formation; the most intense peak was observed for MP2. The least intensive bands at 1758–1754  $\text{cm}^{-1}$  were observed for CP1 and MP1, which also correspond to C=O stretching vibrations<sup>28</sup>. For CP1, C–H stretching vibration bands were observed at 2975  $\text{cm}^{-1}$ , while for the other samples at 2920  $\text{cm}^{-1}$  and 2850  $\text{cm}^{-1}$ . The most intensive bands were observed for CP3, MP2 and MP3, confirming the presence of hydrocarbon chains in the structure of the used plasticizers

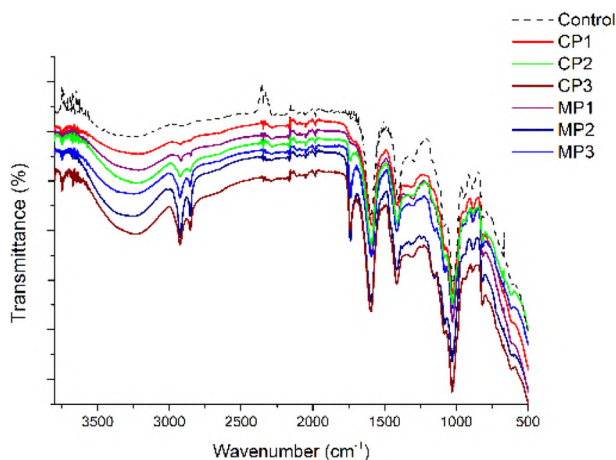


**Figure 9.** FT–IR spectra of sodium alginate films with different plasticizers, where Control- neat sodium alginate.

(they contain fatty acids)<sup>59</sup>. The bands at 1090 cm<sup>-1</sup> and 1020 cm<sup>-1</sup> were attributed to C–O–C antisymmetric stretching vibrations present in all plasticized alginate films.

## Conclusion

In order to develop new antibacterial and environmentally friendly sodium alginate-based films for food packaging, the selection of proper plasticizer is essential. The obtained results confirmed that each investigated plasticizer modifies the structure of the polymer but in a different way. Films CP1, MP1 and MP2 showed a more homogeneous structure, suggesting that the plasticizers are more compatible with sodium alginate than the epoxidized ones (CP2, CP3 or MP3). It was found that the film plasticized with mixed esters of propylene glycol and acetic acid of propylene glycol (MP1) and the film plasticized with glycerol (CP1), showed better mechanical properties (tensile strength and elongation at break) than the other films studied in this paper. It was due to a more homogeneous structure, that did not show morphological changes with the appearance of agglomerations, which promote increased film brittleness. All the films showed a hydrophilic character (contact angle < 90°) and high barrier properties to oxygen, carbon dioxide and water vapor compared to commercially used polylactide or polyethylene films. In addition, the presence of plasticizers, both commercially available or synthesized ones, was found to increase the antibacterial activity of sodium alginate films with chestnut extract for both gram-negative and gram-positive bacterial strains. The highest antibacterial activity showed sodium alginate films containing chestnut extract and the synthesized plasticizer mixtures, particularly MP2 and MP3, which was due to the synergistic effects between chestnut extract and fatty acid-derived plasticizers in relation to their antimicrobial activity. As the sodium alginate-based films plasticized with the synthesized MP1 and MP2 showed better elongation at break and significantly better antibacterial properties compared to glycerol, further work is planned with these plasticizers to improve the mechanical properties of the films even more. Expanded research is also planned in terms of their application in the food packaging sector, such as migration studies of the plasticizers and the active compound, among others. In addition, the obtained results suggest the need to look for other additives that could enhance low hydrophobicity of the sodium alginate-based films.

## Data availability

The datasets used and/or analysed during the current study available from the corresponding author on reasonable request.

Received: 26 April 2023; Accepted: 14 July 2023

Published online: 17 July 2023

## References

- Jafarzadeh, S. *et al.* Biodegradable green packaging with antimicrobial functions based on the bioactive compounds from tropical plants and their by-products. *Trends Food Sci. Technol.* **100**, 262–277 (2020).
- Rosenboom, J.-G., Langer, R. & Traverso, G. Bioplastics for a circular economy. *Nat. Rev. Mater.* **7**, 117–137 (2022).
- Li, Q., Wang, S., Jin, X., Huang, C. & Xiang, Z. The application of polysaccharides and their derivatives in pigment, barrier, and functional paper coatings. *Polymers* **12**, 1837 (2020).
- Mahcene, Z. *et al.* Development and characterization of sodium alginate based active edible films incorporated with essential oils of some medicinal plants. *Int. J. Biol. Macromol.* **145**, 124–132 (2020).
- Benavides, S., Villalobos-Carvajal, R. & Reyes, J. E. Physical, mechanical and antibacterial properties of alginate film: Effect of the crosslinking degree and oregano essential oil concentration. *J. Food Eng.* **110**, 232–239 (2012).
- Chen, J. *et al.* Characterization of sodium alginate-based films incorporated with thymol for fresh-cut apple packaging. *Food Control* **126**, 108063 (2021).
- Bt Ibrahim, S. F., Mohd Azam, N. A. N. & Mat Amin, K. A. Sodium alginate film: the effect of crosslinker on physical and mechanical properties, in *IOP Conference Series: Materials Science and Engineering*, Vol 509, 012063 (2019).
- Russo, R., Malinconico, M. & Santagata, G. Effect of cross-linking with calcium ions on the physical properties of alginate films. *Biomacromol* **8**, 3193–3197 (2007).
- Zhao, Y., Qiu, J., Xu, J., Gao, X. & Fu, X. Effects of crosslinking modes on the film forming properties of kelp mulching films. *Algal Res.* **26**, 74–83 (2017).
- Li, D., Wei, Z. & Xue, C. Alginate-based delivery systems for food bioactive ingredients: An overview of recent advances and future trends. *Compr. Rev. Food Sci. Food Saf.* **20**, 5345–5369 (2021).
- Girón-Hernández, J., Gentile, P. & Benlloch-Tinoco, M. Impact of heterogeneously crosslinked calcium alginate networks on the encapsulation of  $\beta$ -carotene-loaded beads. *Carbohydr. Polym.* **271**, 118429 (2021).
- Parreidt, T. S., Müller, K. & Schmid, M. Alginate-based edible films and coatings for food packaging applications. *Foods* **7**, 170 (2018).
- Di Donato, P. *et al.* Vegetable wastes derived polysaccharides as natural eco-friendly plasticizers of sodium alginate. *Carbohydr. Polym.* **229**, 115427 (2020).
- Gao, C., Pollet, E. & Avérous, L. Properties of glycerol-plasticized alginate films obtained by thermo-mechanical mixing. *Food Hydrocoll.* **63**, 414–420 (2017).
- Vieira, M. G. A., da Silva, M. A., dos Santos, L. O. & Beppu, M. M. Natural-based plasticizers and biopolymer films: A review. *Eur. Polymer J.* **47**, 254–263 (2011).
- Kadzińska, J., Bryś, J., Ostrowska-Ligeza, E., Estéve, M. & Janowicz, M. Influence of vegetable oils addition on the selected physical properties of apple–sodium alginate edible films. *Polym. Bull.* **77**, 883–900 (2020).
- Avella, M. *et al.* Addition of glycerol plasticizer to seaweeds derived alginates: Influence of microstructure on chemical–physical properties. *Carbohydr. Polym.* **69**, 503–511 (2007).
- López, O. V. *et al.* Thermoplastic starch plasticized with alginate–glycerol mixtures: Melt-processing evaluation and film properties. *Carbohydr. Polym.* **126**, 83–90 (2015).
- Giz, A. S. *et al.* A detailed investigation of the effect of calcium crosslinking and glycerol plasticizing on the physical properties of alginate films. *Int. J. Biol. Macromol.* **148**, 49–55 (2020).
- Castro-Yobal, M. A. *et al.* Evaluation of physicochemical properties of film-based alginate for food packing applications. *E-Polymers* **21**, 82–95 (2021).

21. Jost, V., Kobsik, K., Schmid, M. & Noller, K. Influence of plasticiser on the barrier, mechanical and grease resistance properties of alginate cast films. *Carbohydr. Polym.* **110**, 309–319 (2014).
22. Jost, V. & Stramm, C. Influence of plasticizers on the mechanical and barrier properties of cast biopolymer films. *J. Appl. Polym. Sci.* **133**, 42513 (2016).
23. Olivas, G. I. & Barbosa-Cánovas, G. V. Alginate–calcium films: Water vapor permeability and mechanical properties as affected by plasticizer and relative humidity. *LWT Food Sci. Technol.* **41**, 359–366 (2008).
24. Gao, C., Pollet, E. & Avérous, L. Innovative plasticized alginate obtained by thermo-mechanical mixing: Effect of different biobased polyols systems. *Carbohydr. Polym.* **157**, 669–676 (2017).
25. Can Karaca, A., Erdem, I. G. & Ak, M. M. Effects of polyols on gelation kinetics, gel hardness, and drying properties of alginates subjected to internal gelation. *LWT* **92**, 297–303 (2018).
26. El Miri, N. *et al.* Effect of plasticizers on physicochemical properties of cellulose nanocrystals filled alginate bionanocomposite films. *Adv. Polym. Technol.* **37**, 3171–3185 (2018).
27. Musa, M. T., Shaari, N. & Kamarudin, S. K. Characterization of sodium alginate membrane plasticized by polyols and polyamine for DMFC applications. *Key Eng. Mater.* **908**, 20–25 (2022).
28. Aadil, K. R. & Jha, H. Physico-chemical properties of lignin–alginate based films in the presence of different plasticizers. *Iran Polym J* **25**, 661–670 (2016).
29. Paixão, L. C., Lopes, I. A., Barros Filho, A. K. D. & Santana, A. A. Alginate biofilms plasticized with hydrophilic and hydrophobic plasticizers for application in food packaging. *J. Appl. Polym. Sci.* **136**, 48263 (2019).
30. Motelica, L. *et al.* Antibacterial biodegradable films based on alginate with silver nanoparticles and lemongrass essential oil-innovative packaging for cheese. *Nanomaterials (Basel)* **11**, 2377 (2021).
31. Łopusiewicz, Ł. *et al.* Alginate biofunctional films modified with melanin from watermelon seeds and zinc oxide/silver nanoparticles. *Materials* **15**, 2381 (2022).
32. Li, H., Liu, C., Sun, J. & Lv, S. Bioactive edible sodium alginate films incorporated with tannic acid as antimicrobial and antioxidative food packaging. *Foods* **11**, 3044 (2022).
33. Mallakpour, S. & Mohammadi, N. Development of sodium alginate-pectin/TiO<sub>2</sub> nanocomposites: Antibacterial and bioactivity investigations. *Carbohydr. Polym.* **285**, 119226 (2022).
34. Norajit, K. & Ryu, G. H. Preparation and properties of antibacterial alginate films incorporating extruded white ginseng extract. *J. Food Process. Preserv.* **35**, 387–393 (2011).
35. Wang, T. *et al.* Polyvinyl alcohol/sodium alginate hydrogels incorporated with silver nanoclusters via green tea extract for antibacterial applications. *Des. Monomers Polym.* **23**, 118–133 (2020).
36. Dai, Q., Huang, X., Jia, R., Fang, Y. & Qin, Z. Development of antibacterial film based on alginate fiber, and peanut red skin extract for food packaging. *J. Food Eng.* **330**, 111106 (2022).
37. Aydin, G. & Zorlu, E. B. Characterisation and antibacterial properties of novel biodegradable films based on alginate and roselle (*Hibiscus sabdariffa* L.) Extract. *Waste Biomass Valor.* **13**, 2991–3002 (2022).
38. Kowalonek, J., Stachowiak, N., Bolczak, K. & Richert, A. Physicochemical and antibacterial properties of alginate films containing tansy (*Tanacetum vulgare* L.) essential oil. *Polymers* **15**, 260 (2023).
39. Giyatmi, G., Irianto, H. E., Anggoro, B. & Fransiska, D. Use of basil leaf ethanol extract in alginate base edible film. *J. Phys. Conf. Ser.* **1933**, 012001 (2021).
40. da Costa, M. C. *et al.* Brown propolis bioactive compounds as a natural antimicrobial in alginate films applied to *Piper nigrum* L.. *Cienc. Rural* **53**, e20210805 (2023).
41. Janik, W. *et al.* Antibacterial and biodegradable polysaccharide-based films for food packaging applications: comparative study. *Materials* **15**, 3236 (2022).
42. Körge, K., Bajić, M., Likožar, B. & Novak, U. Active chitosan–chestnut extract films used for packaging and storage of fresh pasta. *Int. J. Food Sci. Technol.* **55**, 3043–3052 (2020).
43. Körge, K., Šeme, H., Bajić, M., Likožar, B. & Novak, U. Reduction in spoilage microbiota and cyclopiazonic acid mycotoxin with chestnut extract enriched chitosan packaging: Stability of inoculated gouda cheese. *Foods* **9**, 1645 (2020).
44. Song, B., Fan, X. & Gu, H. Chestnut-tannin-crosslinked, antibacterial, antifreezing, conductive organohydrogel as a strain sensor for motion monitoring, flexible keyboards, and velocity monitoring. *ACS Appl. Mater. Interfaces* **15**, 2147–2162 (2023).
45. Shao, K. *et al.* Green synthesis and antimicrobial study on functionalized chestnut-shell-extract Ag nanoparticles. *Antibiotics* **12**, 201 (2023).
46. Pinto, G. *et al.* Polyphenol profiling of chestnut pericarp, integument and curing water extracts to qualify these food by-products as a source of antioxidants. *Molecules* **26**, 2335 (2021).
47. Silva, V. *et al.* Evaluation of the phenolic profile of *Castanea sativa* Mill. By-products and their antioxidant and antimicrobial activity against multiresistant bacteria. *Antioxidants (Basel)* **9**, 87 (2020).
48. Aimone, C., Grillo, G., Boffa, L., Giovando, S. & Cravotto, G. Tannin extraction from chestnut wood waste: From lab scale to semi-industrial plant. *Appl. Sci.* **13**, 2494 (2023).
49. Cushnie, T. P. T. & Lamb, A. J. Recent advances in understanding the antibacterial properties of flavonoids. *Int. J. Antimicrob. Agents* **38**, 99–107 (2011).
50. das Neves, M. D. S. *et al.* antibacterial activity of biodegradable films incorporated with biologically-synthesized silver nanoparticles and the evaluation of their migration to chicken meat. *Antibiotics* **12**, 178 (2023).
51. Wrońska, N. *et al.* antimicrobial effect of chitosan films on food spoilage bacteria. *Int. J. Mol. Sci.* **22**, 5839 (2021).
52. McClements, D. J. & Xiao, H. Is nano safe in foods? Establishing the factors impacting the gastrointestinal fate and toxicity of organic and inorganic food-grade nanoparticles. *Npj Sci. Food* **1**, 6 (2017).
53. Suvarna, V., Nair, A., Mallya, R., Khan, T. & Omri, A. Antimicrobial nanomaterials for food packaging. *Antibiotics (Basel)* **11**, 729 (2022).
54. Anvar, A. A., Ahari, H. & Atae, M. Antimicrobial properties of food nanopackaging: A new focus on foodborne pathogens. *Front. Microbiol.* **12**, 690706 (2021).
55. He, X. & Hwang, H.-M. Nanotechnology in food science: Functionality, applicability, and safety assessment. *J. Food Drug Anal.* **24**, 671–681 (2016).
56. Onyeaka, H., Passaretti, P., Miri, T. & Al-Sharif, Z. T. The safety of nanomaterials in food production and packaging. *Curr. Res. Food Sci.* **5**, 763–774 (2022).
57. Liu, Y., Zhu, S., Gu, Z., Chen, C. & Zhao, Y. Toxicity of manufactured nanomaterials. *Particulology* **69**, 31–48 (2022).
58. Janik, W. *et al.* Chitosan-based films with alternative eco-friendly plasticizers: Preparation, physicochemical properties and stability. *Carbohydr. Polym.* <https://doi.org/10.1016/j.carbpol.2022.120277> (2022).
59. Ledniowska, K. *et al.* Effective, environmentally friendly PVC plasticizers based on succinic acid. *Polymers* **14**, 1295 (2022).
60. Aguirre-Loredo, R. Y., Rodríguez-Hernández, A. I., Morales-Sánchez, E., Gómez-Aldapa, C. A. & Velázquez, G. Effect of equilibrium moisture content on barrier, mechanical and thermal properties of chitosan films. *Food Chem.* **196**, 560–566 (2016).
61. Jiménez-Regalado, E. J., Caicedo, C., Fonseca-García, A., Rivera-Vallejo, C. C. & Aguirre-Loredo, R. Y. Preparation and physicochemical properties of modified corn starch-chitosan biodegradable films. *Polymers* **13**, 4431 (2021).
62. Zactiti, E. M. & Kieckbusch, T. G. Release of potassium sorbate from active films of sodium alginate crosslinked with calcium chloride. *Packag. Technol. Sci.* **22**, 349–358 (2009).



63. Bhatia, S. *et al.* Preparation and physiochemical characterization of bitter orange oil loaded sodium alginate and casein based edible films. *Polymers* **14**, 3855 (2022).
64. Al-Harrasi, A. *et al.* Effect of drying temperature on physical, chemical, and antioxidant properties of ginger oil loaded gelatin-sodium alginate edible films. *Membranes* **12**, 862 (2022).
65. Eltabakh, M., Kassab, H., Badawy, W., Abdin, M. & Abdelhady, S. Active bio-composite sodium alginate/maltodextrin packaging films for food containing azolla pinnata leaves extract as natural antioxidant. *J Polym Environ* **30**, 1355–1365 (2022).
66. Abdin, M., El-Beltagy, A. E., El-sayed, M. E. & Naeem, M. A. Production and characterization of sodium alginate/gum arabic based films enriched with syzygium cumini seeds extracts for food application. *J Polym Environ* **30**, 1615–1626 (2022).
67. Lu, W. *et al.* Development of antioxidant and antimicrobial bioactive films based on Oregano essential oil/mesoporous nano-silica/sodium alginate. *Food Packag. Shelf Life* **29**, 100691 (2021).
68. Hou, X. *et al.* Effect of SiO<sub>2</sub> nanoparticle on the physical and chemical properties of eco-friendly agar/sodium alginate nanocomposite film. *Int. J. Biol. Macromol.* **125**, 1289–1298 (2019).
69. Jouki, M., Yazdi, F. T., Mortazavi, S. A. & Koocheki, A. Physical, barrier and antioxidant properties of a novel plasticized edible film from quince seed mucilage. *Int. J. Biol. Macromol.* **62**, 500–507 (2013).
70. Cichello, S. A. Oxygen absorbers in food preservation: A review. *J. Food Sci. Technol.* **52**, 1889–1895 (2015).
71. Bourbon, A. I. *et al.* Physico-chemical characterization of chitosan-based edible films incorporating bioactive compounds of different molecular weight. *J. Food Eng.* **106**, 111–118 (2011).
72. Nallan, S. *et al.* Characterization of composite edible films based on pectin/alginate/whey protein concentrate. *Materials* **12**, 2454 (2019).
73. Wang, F. *et al.* Gelatin/Chitosan films incorporated with curcumin based on photodynamic inactivation technology for antibacterial food packaging. *Polymers* **14**, 1600 (2022).
74. Galus, S. & Lenart, A. Development and characterization of composite edible films based on sodium alginate and pectin. *J. Food Eng.* **115**, 459–465 (2013).
75. Huang, C. B., George, B. & Ebersole, J. L. Antimicrobial activity of n-6, n-7 and n-9 fatty acids and their esters for oral microorganisms. *Arch. Oral Biol.* **55**, 555–560 (2010).
76. McGaw, L. J., Jäger, A. K. & van Staden, J. Antibacterial effects of fatty acids and related compounds from plants. *S. Afr. J. Bot.* **68**, 417–423 (2002).
77. Chandrasekaran, M., Senthilkumar, A. & Venkatesalu, V. Antibacterial and antifungal efficacy of fatty acid methyl esters from the leaves of *Sesuvium portulacastrum* L.. *Eur. Rev. Med. Pharmacol. Sci.* **15**, 775–780 (2011).
78. Dilika, F., Bremner, P. D. & Meyer, J. J. M. Antibacterial activity of linoleic and oleic acids isolated from *Helichrysum pedunculatum*: A plant used during circumcision rites. *Fitoterapia* **71**, 450–452 (2000).
79. Marangoni Júnior, L. *et al.* Preparation and characterization of sodium alginate films with propolis extract and nano-SiO<sub>2</sub>. *Food Hydrocoll. Health* **2**, 100094 (2022).
80. Anbinder, P., Deladino, L., Navarro, A., Amaly, J. & Martino, M. Yerba mate extract encapsulation with alginate and chitosan systems: Interactions between active compound encapsulation polymers. *J. Encapsulation Adsorpt. Sci.* **1**, 80–87 (2011).
81. Abulatefeh, S. R. & Taha, M. O. Enhanced drug encapsulation and extended release profiles of calcium-alginate nanoparticles by using tannic acid as a bridging cross-linking agent. *J. Microencapsul.* **32**, 96–105 (2015).
82. Gao, C., Guo, J. & Xie, H. The effect of alginate on the mechanical, thermal, and rheological properties of nano calcium carbonate-filled polylactic acid composites. *Polym. Eng. Sci.* **59**, 1882–1888 (2019).
83. Xiao, Q., Gu, X. & Tan, S. Drying process of sodium alginate films studied by two-dimensional correlation ATR-FTIR spectroscopy. *Food Chem.* **164**, 179–184 (2014).
84. Çaykara, T., Demirci, S., Eroğlu, M. S. & Güven, O. Poly(ethylene oxide) and its blends with sodium alginate. *Polymer* **46**, 10750–10757 (2005).

## Acknowledgements

This research was co-financed by the Ministry of Education and Science of Poland under grant No DWD/4/21/2020.

## Author contributions

W.J, S.K. and G.D. conceived the idea of this work, designed the film preparation and characterization experiments, discussed the results and prepared the manuscript text and figures, W.J., M.N., K.L., D.Y.S., K.K., R.T., E.S. and S.F. conducted the experiments and contributed to the analysis of the results. All authors reviewed the manuscript.

## Competing interests

The authors declare no competing interests.

## Additional information

**Supplementary Information** The online version contains supplementary material available at <https://doi.org/10.1038/s41598-023-38794-3>.

**Correspondence** and requests for materials should be addressed to W.J.

**Reprints and permissions information** is available at [www.nature.com/reprints](http://www.nature.com/reprints).

**Publisher's note** Springer Nature remains neutral with regard to jurisdictional claims in published maps and institutional affiliations.



**Open Access** This article is licensed under a Creative Commons Attribution 4.0 International License, which permits use, sharing, adaptation, distribution and reproduction in any medium or format, as long as you give appropriate credit to the original author(s) and the source, provide a link to the Creative Commons licence, and indicate if changes were made. The images or other third party material in this article are included in the article's Creative Commons licence, unless indicated otherwise in a credit line to the material. If material is not included in the article's Creative Commons licence and your intended use is not permitted by statutory regulation or exceeds the permitted use, you will need to obtain permission directly from the copyright holder. To view a copy of this licence, visit <http://creativecommons.org/licenses/by/4.0/>.

© The Author(s) 2023

SUPPLEMENTARY DATA

# Modulation of Physicochemical Properties and Antimicrobial Activity of Sodium Alginate Films through the Use of Chestnut Extract and Plasticizers

Weronika Janik, Michał Nowotarski, Kerstin Ledniewska, Divine Yufetar Shyntum, Katarzyna Krukiewicz, Roman Turczyn, Ewa Sabura, Simona Furgol, Stanisław Kudła, and Gabriela Dudek

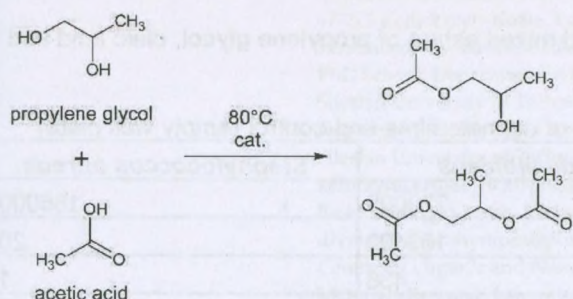


**Figure S1.** Schematic route of the synthesis of mixed esters of propylene glycol and acetic acid (sample MP1)

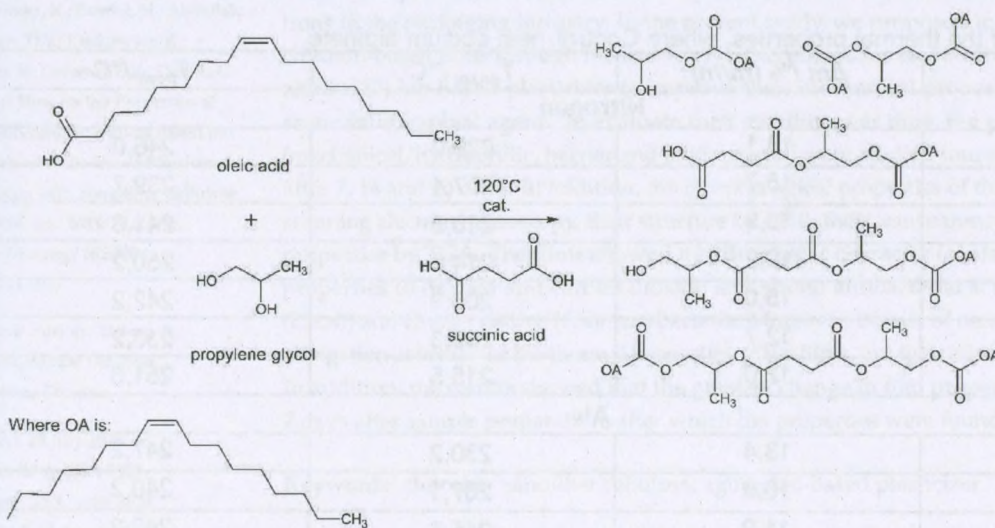
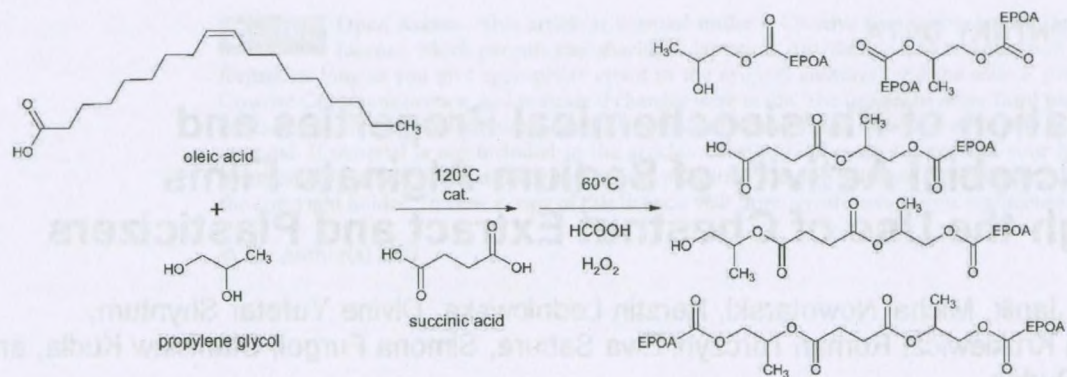


**Figure S2.** Schematic route of the synthesis of mixed esters of propylene glycol, oleic acid and succinic acid (sample MP2)





Where EPOA is:

**Figure S3.** Schematic route of the synthesis of epoxidized mixed esters of propylene glycol, oleic acid and succinic acid (sample MP3)

**Table S1.** Number of colony-forming units on the surface of alginate films and control (empty well plate)

	<i>Escherichia coli</i>	<i>Candida albicans</i>	<i>Staphylococcus aureus</i>
Control	850000000	222000	1850000
CP1	410	153400	200
CP2	42	436	10
CP3	1	122000	55
MP1	51	25644	1
MP2	1	249	1
MP3	1	100	1

**Table S2.** Results of the thermal properties, where Control=neat sodium alginate

	$\Delta m$ /% (m/m)	$T_{onset}$ /°C	$T_{peak}$ /°C
<b>Nitrogen</b>			
Control	13,1	229,0	246,0
CP1	15,7	207,4	239,7
CP2	10,9	218,3	241,3
CP3	10,2	214,3	250,2
MP1	15,0	208,9	242,2
MP2	12,7	215,3	233,2
MP3	12,0	215,5	251,5
<b>Air</b>			
Control	13,4	230,2	247,2
CP1	16,6	207,1	240,2
CP2	11,9	215,2	240,2
CP3	12,3	211,6	245,2
MP1	15,0	208,7	247,7
MP2	13,5	215,0	228,3
MP3	11,3	214,0	254,5



Article

# Effect of Time on the Properties of Bio-Nanocomposite Films Based on Chitosan with Bio-Based Plasticizer Reinforced with Nanofiber Cellulose

Weronika Janik <sup>1,2</sup> , Michał Nowotarski <sup>3</sup>, Kerstin Ledniowska <sup>1,2</sup> , Natalia Biernat <sup>1</sup>, Abdullah <sup>2,3</sup> , Divine Yufetar Shyntum <sup>4</sup> , Katarzyna Krukiewicz <sup>3,5</sup> , Roman Turczyn <sup>3,5</sup> , Klaudiusz Gołombek <sup>6</sup> and Gabriela Dudek <sup>3,\*</sup>

- <sup>1</sup> Lukaszewicz Research Network—Institute of Heavy Organic Synthesis “Blachownia”, 47-225 Kędzierzyn-Koźle, Poland; weronika.janik@icso.lukasiewicz.gov.pl (W.J.); kerstin.ledniowska@icso.lukasiewicz.gov.pl (K.L.); natalia.biernat@icso.lukasiewicz.gov.pl (N.B.)
- <sup>2</sup> PhD School, Department of Physical Chemistry and Technology of Polymers, Silesian University of Technology, 44-100 Gliwice, Poland; abdullah.abdullah@polsl.pl
- <sup>3</sup> Department of Physical Chemistry and Technology of Polymers, Faculty of Chemistry, Silesian University of Technology, 44-100 Gliwice, Poland; michnow566@student.polsl.pl (M.N.); katarzyna.krukiewicz@polsl.pl (K.K.); roman.turczyn@polsl.pl (R.T.)
- <sup>4</sup> Biotechnology Centre, Silesian University of Technology, 44-100 Gliwice, Poland; divine.yufetar.shyntum@polsl.pl
- <sup>5</sup> Centre for Organic and Nano hybrid Electronics, Silesian University of Technology, 44-100 Gliwice, Poland
- <sup>6</sup> Materials Research Laboratory, Faculty of Mechanical Engineering, Silesian University of Technology, 44-100 Gliwice, Poland; klaudiusz.golombek@polsl.pl
- \* Correspondence: gabriela.maria.dudek@polsl.pl; Tel.: +48-32-237-10-67



**Citation:** Janik, W.; Nowotarski, M.; Ledniowska, K.; Biernat, N.; Abdullah, Shyntum, D.Y.; Krukiewicz, K.; Turczyn, R.; Gołombek, K.; Dudek, G. Effect of Time on the Properties of Bio-Nanocomposite Films Based on Chitosan with Bio-Based Plasticizer Reinforced with Nanofiber Cellulose. *Int. J. Mol. Sci.* **2023**, *24*, 13205. <https://doi.org/10.3390/ijms241713205>

Academic Editors: Tatiana A. Akopova, Sankar Bhuniya and Tatiana Demina

Received: 28 July 2023

Revised: 22 August 2023

Accepted: 23 August 2023

Published: 25 August 2023



**Copyright:** © 2023 by the authors. Licensee MDPI, Basel, Switzerland. This article is an open access article distributed under the terms and conditions of the Creative Commons Attribution (CC BY) license (<https://creativecommons.org/licenses/by/4.0/>).

**Abstract:** The deterioration of the performance of polysaccharide-based films over time, particularly their hydrophilicity and mechanical properties, is one of the main problems limiting their applications in the packaging industry. In the present study, we proposed to improve the performance of chitosan-based films through the use of: (1) nanocellulose as an additive to reduce their hydrophilic nature; (2) bio-based plasticizer to improve their mechanical properties; and (3) chestnut extract as an antimicrobial agent. To evaluate their stability over time, the properties of as-formed films (mechanical, hydrophilic, barrier and antibacterial) were studied immediately after preparation and after 7, 14 and 30 days. In addition, the morphological properties of the films were characterized by scanning electron microscopy, their structure by FTIR, their transparency by UV-Vis and their thermal properties by TGA. The films showed a hydrophobic character (contact angle above 100°), barrier properties to oxygen and carbon dioxide and strong antibacterial activity against Gram-negative (*E. coli*) and Gram-positive (*S. aureus*) bacteria. Moreover, the use of nanofillers did not deteriorate the elongation at breaks or the thermal properties of the films, but their addition reduced the transparency. In addition, the results showed that the greatest change in film properties occurred within the first 7 days after sample preparation, after which the properties were found to stabilize.

**Keywords:** chitosan; nanofiber cellulose; aging; bio-based plasticizer

## 1. Introduction

The research interest in the development of innovative and environmentally friendly biocomposites based on biodegradable polymers and fillers to improve material strength properties has continued to grow rapidly over the last few decades. Among the various fillers for biopolymers, nanofillers are among the most popular, not only for their reinforcing properties but also for providing additional advantages, such as barrier properties or antibacterial activity [1]. Nanofillers play an important role in the design of biopolymer-based materials for various applications. Their main task is to improve the mechanical

properties of the material, which has already been confirmed in numerous studies [2–5]. The most commonly used biopolymer nanofillers for food packaging films are cellulose, starch, chitin and chitosan [6]. Some of the nanofillers, such as nanochitosan, improve not only the mechanical properties of the film but also its antimicrobial properties [7].

Among the previously mentioned nanofillers, nanocellulose (NC) is the most popular. It is a biodegradable and renewable nanofiller, obtained as a result of the decomposition of cellulose fibers [8]. The high interest in it is mainly due to its wide availability—cellulose is the main polysaccharide accumulating in plant biomass [2]. It is estimated that plants produce about 75 billion tons of cellulose per year, making it a highly available material [9]. Three types of nanocellulose are used in applications that improve material mechanical properties: cellulose nanofibers, cellulose nanocrystals and bacterial nanocellulose. The first two are isolated from plants and the last from bacteria [2]. Cellulose fibers, with or without chemical pretreatment, are mechanically fragmented in water into nanocellulose. The obtained products are distinguished depending on their morphology into nanofibrils and nanocrystals [8].

The use of NC is becoming also increasingly popular due to its properties, such as high strength, high extensibility, non-toxicity and biodegradability [10]. The incorporation of NC into the polymer matrix allows for the formation of a material with improved performance without compromising its biodegradability [11]. The effect of introducing NC into bio-based materials has been widely studied [4,7,12,13]. Attempts to obtain NC-reinforced chitosan nanocomposites suitable for use in the food industry, e.g., as active packaging films, have been described [2,11,14]. It has been observed that the addition of nanocellulose leads to the improvement of the mechanical properties, thermal stability, hydrophobicity and oxygen barrier of the film. Moreover, NC-loaded films showed bactericidal activity against Gram-positive and Gram-negative bacteria and fungicidal activity against *Candida albicans* [11]. In addition, chitosan films with NC reduce total volatile basic nitrogen (TVB-N), which is considered an indicator of food freshness under refrigeration conditions [11].

Despite ongoing research into combining chitosan with NC for use as bioactive packaging films, the impact of time on such systems remains unclear [11]. This information is crucial from the perspective of applying these materials for food packaging. The issue of the instability of chitosan–glycerol compositions has already been addressed by us in our previous study [15], in which we proved that replacing glycerol with esters of propylene glycol and acetic acid resulted in a more stable material over time. Therefore, in the present study, the esters of propylene glycol and acetic acid were also used for plasticization and were tested not only immediately after receiving them but also after 7, 14 and 30 days. The maximum time was determined based on our previous studies conducted on films based on chitosan and sodium alginate [15,16]. To obtain bioactive films, chestnut extract was used. To further improve the properties of chitosan, a biocomposite was obtained using NC as a filler. Mechanical properties, hydrophilic properties, oxygen, carbon dioxide and water vapor permeability and antibacterial activity were determined for the obtained sample immediately after receiving the samples and after 7, 14 and 30 days. To evaluate the morphology, structure, transparency and thermal properties of the obtained samples, scanning electron microscopy, Fourier transform infrared spectroscopy, ultraviolet-visible spectroscopy and thermal gravimetry were used, respectively.

## 2. Results and Discussion

### 2.1. Mechanical Properties

The mechanical performance of polymeric materials is one of the most important properties determining their applicability. Tensile strength (TS) and elongation at break (EB) for bio-nanocomposite films based on chitosan were measured immediately after the film preparation and after storage at room temperature for 7, 14 and 30 days to determine the effects of time on the mechanical properties. The characteristic stress–strain curves of the bio-nanocomposite films are illustrated in Figure 1. The strongest effect of time on mechanical performance can be observed within the first 7 days after sample preparation.



The TS value drops during this time from 7 MPa (NC/0) to 3.48 MPa (NC/7), and then for the subsequent days, the values are statistically equal. After 14 days of sample preparation, the TS value was 3.65 MPa (NC/14), and after 30 days, it increased slightly to 4.68 MPa (NC/30). The presented results show that the first 7 days have the greatest effect on the deterioration of TS. In contrast, the EB results show a slightly different relationship, as the elongation increased slightly over time. Indeed, newly prepared film showed an EB of 63% (NC/0), while after 7 days, this value increased to 75% (NC/7), and then for the subsequent days, the values were statistically equal. For NC/14, the EB was 74%, and for NC/30, it was 72%. This outcome is primarily related to the deteriorating properties of TS, which mostly cause the EB to increase [17,18]. Comparing the results of our previous studies [15] conducted without the use of NC, it can be seen that the presence of nanofibers significantly affects the increase in TS. Chitosan films prepared with the same plasticizer but without NC showed a TS of 6 MPa, while the use of nanofibers increased this value to 7 MPa (NC/0), and after 30 days, it dropped to 4.5 MPa (NC/30). In contrast, EB values remained at the same level, i.e., about 70%. The same relationship was observed by other researchers [3,5,7,11], who also reported a significant effect of nanofiller on TS and not on EB. For example, Costa et al. [11] added cellulose nanocrystals to a chitosan film and observed that, as the amount of NC increased, TS increased, while EB remained unchanged. Nevertheless, this relationship is not confirmed in every case, as in the study described by Jannatyh et al. [3], the addition of cellulose nanocrystals to the chitosan film resulted in an increase in TS and a simultaneous decrease in EB. This outcome may be related to poor dispersion of the nanofiller, incompatible structures or agglomeration of the nanoparticles [19]. Also worth mentioning is the effect of the chestnut extract itself used in the present samples. It has been shown that the addition of chestnut extract causes an increase in TS, but a decrease in EB [20,21]. This finding was confirmed, among others, by the study of K orge et al. [21], who observed a significant increase in TS and decrease in EB for chitosan-based films after the addition of chestnut extract.

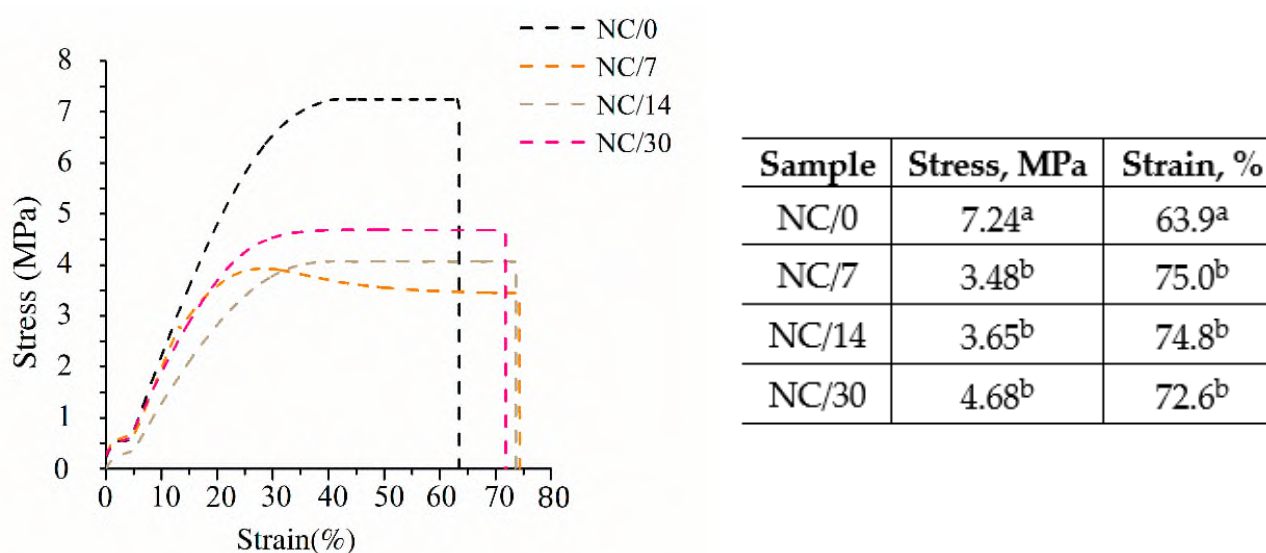


**Figure 1.** Stress vs. strain curves with exact values of bio-nanocomposite films based on chitosan; different lowercase letters indicate significantly different values at  $p < 0.05$  using Tukey's multiple range test.

## 2.2. Hydrophobic Properties

The hydrophobic properties of polymeric materials are as important as the mechanical properties for the determination of their applicability. Moisture content (MC, Figure 2A), total soluble matter (TSM, Figure 2A), swelling degree (SD, Figure 2A) and dynamic contact angle (CA, Figures 2B and 3) for chitosan-based bio-nanocomposite films were measured immediately after film preparation and after storing the films for 7, 14 and 30 days to

determine the effects of time on the hydrophobic properties. The results showed that all of these values decreased slightly over time. For MC, the initial value dropped from 15% (NC/0) to about 11% for the other samples (i.e., NC/7, NC/14 and NC/30). TSM values also dropped slightly, from about 18% for NC/0 to about 14% for NC/30. In the case of SD, the values increased after 7 days from 50% to 85% (for NC/0 and NC/7, respectively) and then dropped slightly to 81% and 78% (for NC/14 and NC/30, respectively). Most of these results also showed that the stabilization of the material occurred after 7 days, as the largest changes were recorded during this time, and the other values were statistically the same. A similar conclusion was observed in the mechanical properties discussed earlier, which decreased over 7 days related to the decrease in moisture content and thus to the formation of a less flexible structure through a reduction in plasticization of the amorphous areas of the polymer network [22,23].

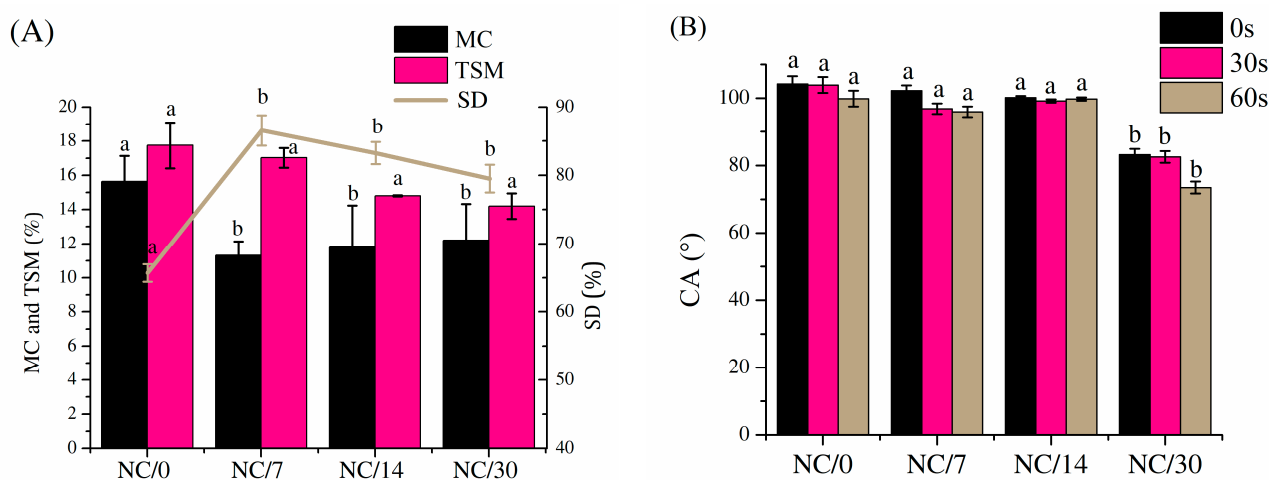


**Figure 2.** Moisture content (MC), total soluble matter (TSM) and swelling degree (SD) (A) and dynamic contact angle (CA) (B) for bio-nanocomposite films based on chitosan; different lowercase letters indicate significantly different values at  $p < 0.05$  using Tukey's multiple range test.

In contrast, the wetting angle results shown in Figures 2B and 3 indicate that the sample tested immediately after preparation showed a hydrophobic character ( $100^\circ$  at 0 s and about  $98^\circ$  at 30 s, NC/0) and this value, despite the decreasing MC value over time, remained unchanged until 14 days ( $100^\circ$ ; NC/14). However, tests performed on day 30 showed a decrease in the wetting angle value to about  $82^\circ$  (NC/30), demonstrating that the samples became hydrophilic over time. It is also worth mentioning the effects of NC and chestnut extract itself on these properties. Referring to the results obtained in previous studies [15], MC, TSM or SD for pure film without NC is practically the same as for film with nanofiller. In contrast, the CA results showed that the use of NC shifted the nature of the film decisively from hydrophilic to hydrophobic (from  $70^\circ$  to  $105^\circ$  for films without NC and with NC, respectively). The improvement of hydrophobic properties was also observed by Lavrič et al. [2], in which the addition of cellulose nanocrystals to the chitosan film led to an increase in the contact angle from  $75^\circ$  to  $108^\circ$ . This relationship was also confirmed by Mao et al. [4], who showed that, after adding cellulose nanocrystals to the chitosan film, CA increased. Moreover, the value continuously increased by increasing the NC content. On the other hand, in the case of the addition of chestnut extract, Bajić et al. [20] and Kõrge et al. [21] observed that, with an increase in its amount (0.5–1%), the hydrophilicity decreased. This outcome was attributed to the presence of a large number of hydrolysable tannins in the chestnut extract; this component has many interaction sites that crosslink the polymer chain, so they tend to saturate the hydrogen bonds in chitosan.

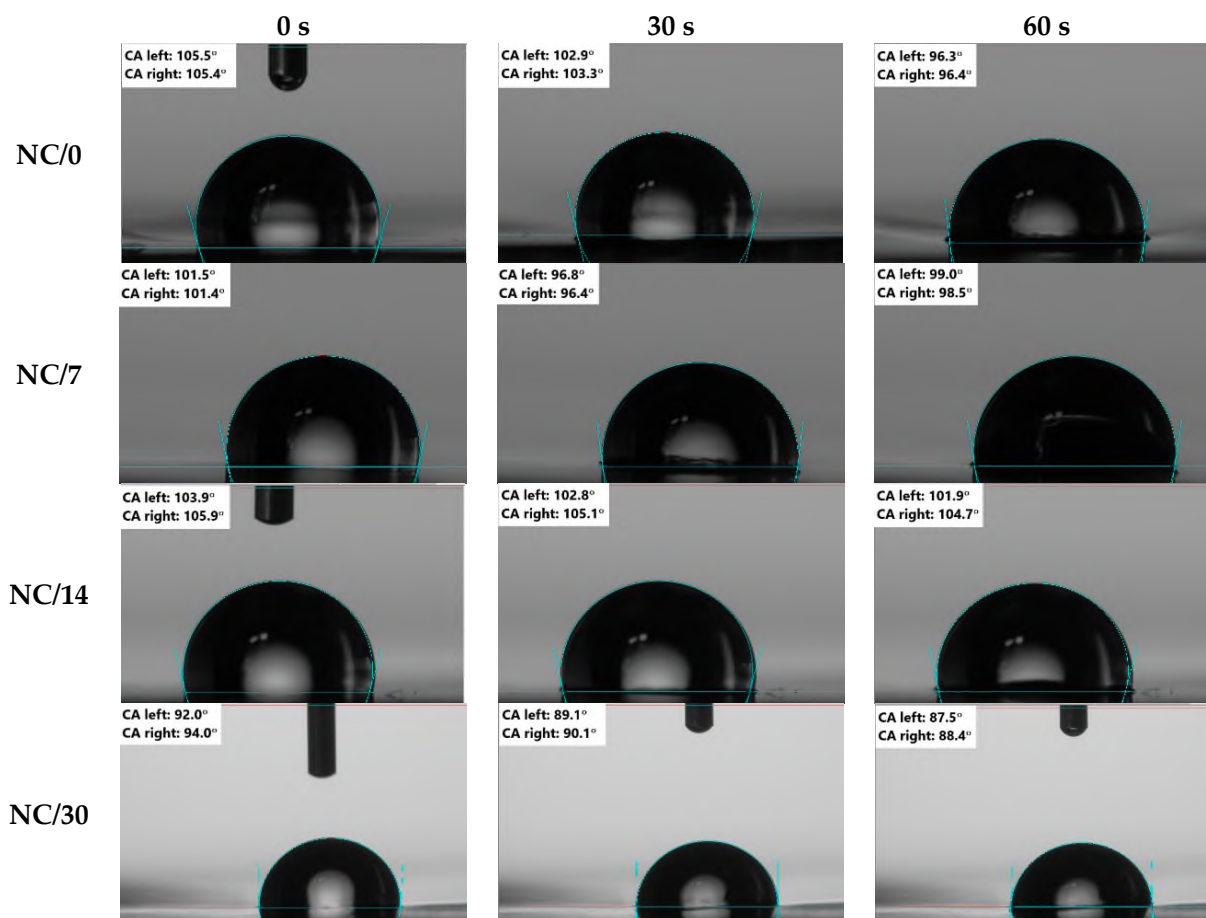


**Figure 3.** Dynamic contact angle images of bio-nanocomposite films based on chitosan.

### 2.3. Gas Permeability

The barrier properties of polymer films play an important role in the food packaging industry. The film is designed to delay the transfer of molecules between food and the environment to preserve food quality. Measuring properties, such as the permeability of oxygen, carbon dioxide or water vapor, makes it possible to estimate the shelf life of a product. The most commonly studied properties of biodegradable films are water vapor permeability and oxygen permeability because the proper amount of water keeps products fresh and crispy, while oxygen spoils food through oxidation reactions but is necessary for respiration of fresh vegetables and fruits [24].

Oxygen and carbon dioxide permeability (Figure 4A) and water vapor transmission rate and water vapor permeability (Figure 4B) for chitosan-based bio-nanocomposite films were measured immediately after film preparation and after storing the films for 7, 14 and 30 days to determine the effects of time on barrier properties. The obtained results of both OP and CDP for the tested films were relatively low (at a level of  $10^{-10}$   $\text{cm}^3/\text{m}^2$ ) compared to commercially available polylactide film or low-density polyethylene (PE-LD) [25] and slightly decreased over time. The OP for NC/0 was about  $2.5 \times 10^{-10}$   $\text{cm}^3/\text{m}^2$ , and after 30 days, this value decreased to about  $1.5 \times 10^{-10}$   $\text{cm}^3/\text{m}^2$  (NC/30). In contrast, the CDP for NC/0 was about  $3 \times 10^{-10}$   $\text{cm}^3/\text{m}^2$ , and after 30 days, the value dropped to about  $2 \times 10^{-10}$   $\text{cm}^3/\text{m}^2$  (NC/30). Despite the notable decline in values, none of these results were statistically different from each other. The OP of chitosan films is influenced by the concentration of plasticizer, as well as storage time. Leceta et al. [26] reported that OP values increased with increasing glycerol content. In addition, Butler et al. [27] reported that OP increased not only with the plasticizer concentration but also after film storage time. A similar decreasing relationship over time was noted for WVP and WVTR. The



obtained values were relatively low and close to each other, and after 30 days, they reached a value of about  $5 \times 10^{-8} \text{ mm} \times \text{g} / \text{Pa} \times \text{m}^2 \times 24 \text{ h}$  (NC/30). As in the previously described studies, i.e., mechanical and hydrophobic properties, the greatest changes for WVP and WVTR were observed after 7 days of storage, whereas for OP and CDP, a decrease in these values was observed after 14 days of storage. Nevertheless, also in this case, the results were not statistically different from each other. It is worth mentioning that slightly higher WVP values may be related to higher relative humidity in the environment [28–30] because chitosan has amino and hydroxyl groups that interact with water molecules through hydrogen bonds without modifying the chemical structure [22,31]. Adsorption of water molecules allows for a more flexible structure by plasticizing the amorphous regions of the polymer network and promoting internal rearrangement, consequently facilitating gas transport through the polymer matrix [22,23]. Moreover, WVP is closely related to the MC of the material: as WVP increases, MC also increases [18]. In our study, MC decreased over time, which was also observed for WVP, OP and CDP, due to the evaporation of water from the polymer matrix under the storage conditions. As the water content of the material decreases, its elasticity decreases, making the structure more compact and resistant to water and gas permeability [32].

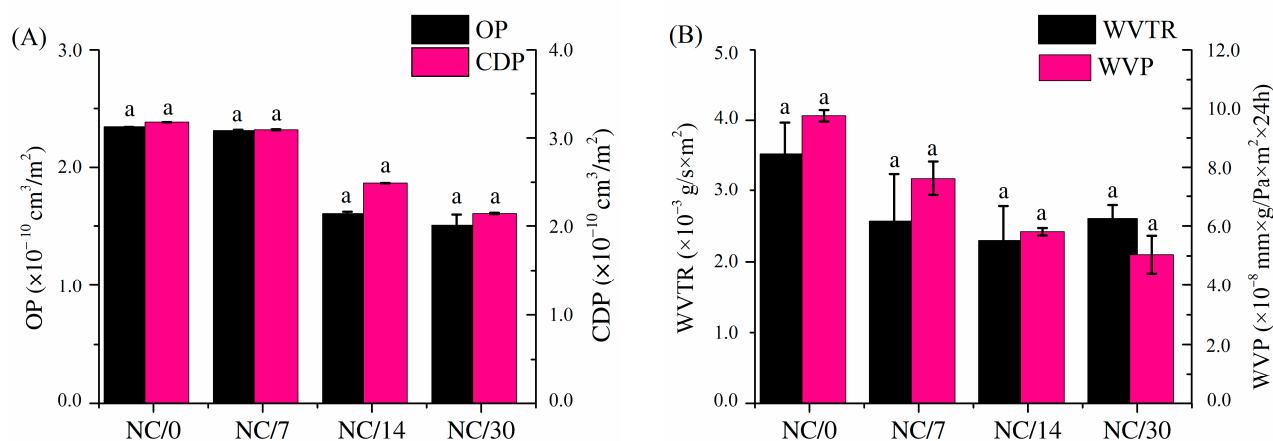


**Figure 4.** Oxygen (OP) and carbon dioxide permeability (CDP) (A) and water vapor transmission rate (WVTR) and water vapor permeability (WVP) (B) for bio-nanocomposite films based on chitosan; different lowercase letters indicate significantly different values at  $p < 0.05$  using Tukey's multiple range test.

Comparing the barrier properties (OP, CDP and WVP) obtained for plasticized chitosan film without nanofillers in our previous study [15] to the results obtained with the addition of NC, it can be seen that the addition of nanofiller slightly increased the values of OP, CDP and WVP, but these values were still relatively low values, and the obtained barrier results were satisfying because the barrier properties of the obtained bio-nanocomposite films based on chitosan films exceeded or were almost equal to the commercial food packaging films currently used, such as those based on PLA or PE-LD [25,26]. The introduction of NC deteriorated the barrier properties of the film because it facilitated the diffusion of the gas molecules through the film structure. NC in the form of fibers creates channels that facilitate the passage of oxygen, carbon dioxide or water vapor molecules through the film [33]. For pure chitosan film, Kerch et al. [34] reported that WVP increases at room temperature during storage (30 days). In contrast, Khan et al. [35] studied the effect of NC concentration on the WVP of chitosan films. They reported that WVP values decreased with increasing NC concentrations. In their case, crystalline NC was used and not the fiber form, which had a significant impact on the results.

#### 2.4. Morphology

To study the structure of the obtained bio-nanocomposite films based on chitosan, surface and cross-sectional images (Figure 5A,B, respectively) were taken to evaluate the homogeneity of the obtained materials. SEM microphotographs show the homogeneity of the NC-loaded film, as confirmed by both its surface and cross-sectional images. The surface of the chitosan films was found to be smooth, which indicated good film homogenization of chitosan and NC in aqueous medium. Considering the possibility of agglomeration of the used nanofiller in the film, no significant inhomogeneities that could indicate a large agglomeration of the filler were noted. The films showed a homogeneous and dense structure, indicating proper NC dispersion in the chitosan matrix.

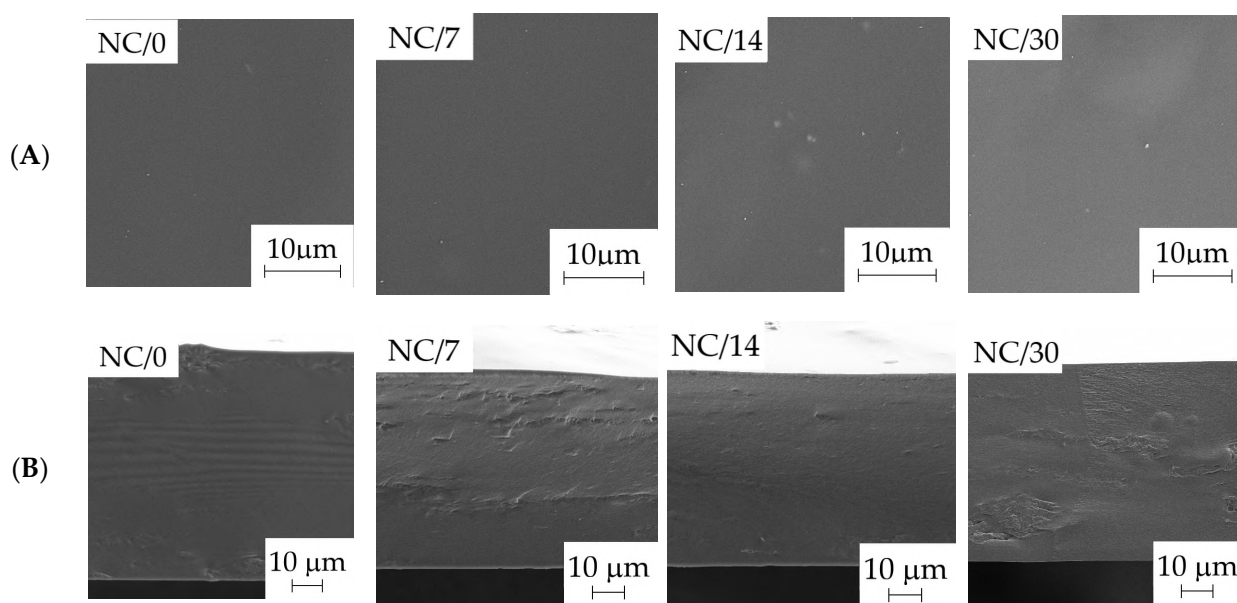
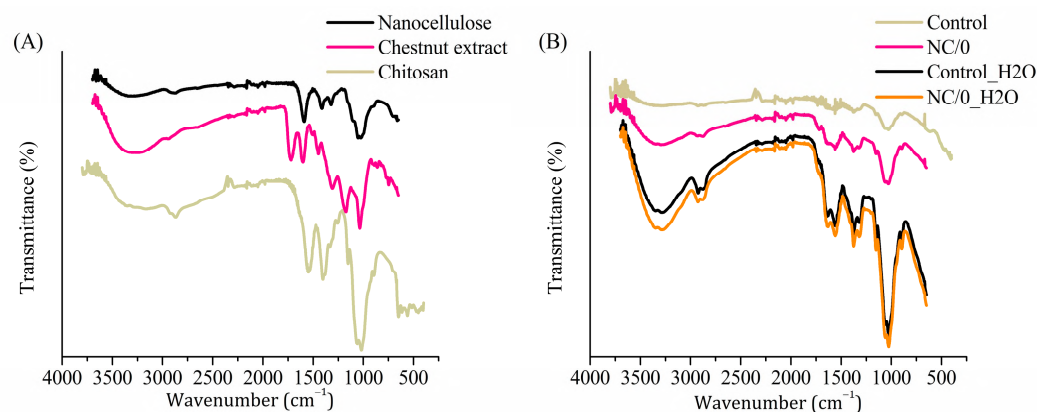


**Figure 5.** SEM images of the bio-nanocomposite films based on chitosan: surface (A) and cross-section (B).

#### 2.5. Fourier Transform Infrared Spectroscopy

FTIR analysis was carried out to evaluate the structural interactions among chitosan, NC and chestnut extract and the structural changes of the film after exposure to water for 24 h. Figure 6A shows the spectra of NC, chestnut extract and chitosan powders, and Figure 6B showed the plasticized chitosan film with chestnut extract (Control), with chestnut extract and nanocellulose (NC/0) and after their immersion in water for 24 h (Control\_H2O and NC/0\_H2O, respectively). The FTIR spectrum of NC powder (Figure 6A) showed several typical bands, namely the very broad bands located in the region of  $3200\text{--}3500\text{ cm}^{-1}$ , corresponding to stretching vibrations of the O–H groups of cellulose, a C–H stretch band at  $2900\text{ cm}^{-1}$  and absorption bands of  $\beta$ -glycoside bonds at  $1591$  and  $1057\text{ cm}^{-1}$  [11,36–38]. The powder spectrum of chestnut extract (Figure 6A) also showed its characteristic bands in the region of  $3100\text{--}3500\text{ cm}^{-1}$ , corresponding to the O–H stretching vibrations derived from different chemical environments, characteristic of polyphenolic extracts [39,40]. In the region of  $2800\text{--}2985\text{ cm}^{-1}$ , the C–H stretching vibrations, derived from carbohydrates and sugars, could be observed and, between  $1661$  and  $1769\text{ cm}^{-1}$ , the C=O stretching vibrations of esters of hydrolysable tannins. In the region of  $1422\text{--}1620\text{ cm}^{-1}$  the C=C-C aromatic bonds [39] and, in the region from  $1123$  to  $1380\text{ cm}^{-1}$  and from  $959$  to  $1082\text{ cm}^{-1}$ , the bands for C–O were observed, respectively [39,40]. Structural analysis of chitosan powder (Figure 6A) also showed characteristic bands, i.e., between  $3100$  and  $3500\text{ cm}^{-1}$ , the overlapping broad band from both O–H and N–H stretching vibrations and, at  $2920\text{--}2850\text{ cm}^{-1}$ , the symmetric and asymmetric modes of C–H stretching vibrations at methylene and methyl carbon [41,42]. Since the chitosan grade is 90% DD, the characteristic peaks representing the I amide band (C=O

stretching in nondeacetylated amide) were only weakly visible in the slope of the free amine N–H bending and C–N stretching located at  $1555\text{ cm}^{-1}$ . The weak resolved broad peak with a maximum at  $1400\text{ cm}^{-1}$  is attributed to the combined C–H bending in –CH and –CH<sub>2</sub>, as well as –CH<sub>3</sub> symmetrical deformations and –CH<sub>2</sub> wagging [26]. The absorption band at  $1038\text{ cm}^{-1}$  could be attributed to the C–O stretching and asymmetric stretching of the C–O–C bridge in the saccharides ring. The signal at  $893\text{ cm}^{-1}$  corresponds to the out of the plane C–H bending of the saccharides ring [26].



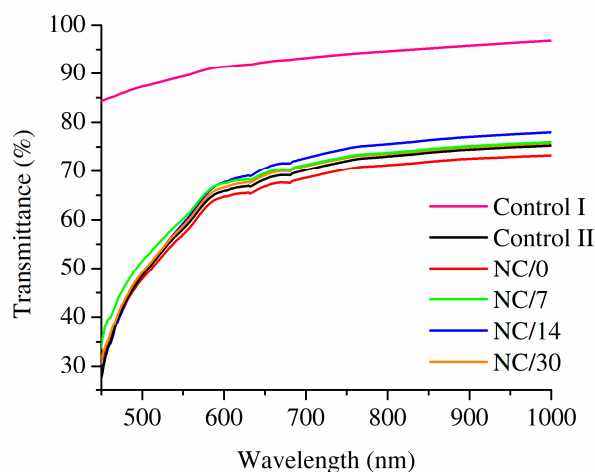
**Figure 6.** FTIR spectra of the NC, chestnut extract and chitosan powders (A), of the obtained films before and after immersion in water (B), where control indicates plasticized chitosan film with chestnut extract, and H<sub>2</sub>O indicates after immersion in water.

Figure 6B shows the plasticized chitosan film with chestnut extract (Control) and the film with chestnut extract and nanocellulose (NC/0), as well as after their immersion in water for 24 h (Control\_H<sub>2</sub>O and NC/0\_H<sub>2</sub>O, respectively). Comparing the spectra before and after soaking in water, a significant increase in band intensity was observed for both Control\_H<sub>2</sub>O and NC/0\_H<sub>2</sub>O. After soaking the spectra, all of the characteristic features of the bio-composite were retained. More intensive stretching vibrations of the O–H groups in the region of  $3100\text{--}3500\text{ cm}^{-1}$  were noted, which can be attributed to the absorbed residual water. The observed increase in the intensity and sharpness of the peaks characteristic for chitosan indicated that 24 h of soaking in water led to its swelling and backbone relaxation, and the residual water likely partially softened the composite, ensuring its better adherence to the UATR crystal surface. No evident release of bio-composite components, such as plasticizer or fillers, was observed.

## 2.6. Optical Properties

An important property of food packaging materials is their transparency since it allows consumers to evaluate food freshness and general appearance by visual inspection before purchasing [43]. Based on the UV-Vis spectra of the obtained bio-nanocomposite films based on chitosan, as well as chitosan films with and without a chestnut extract (Figure 7), it can be observed that the presence of chestnut extract decreased the transmittance of films, even without the presence of NC fibers. While the transmittance of a pristine chitosan film was noted between 84% (at 450 nm) and 97% (at 1000 nm), it dropped to 28–75% for chestnut extract-containing chitosan film. The presence of NC decreased transmittance further, but this feature was found to increase with time, as the process of aging occurred. The observed discoloration should be associated with the limited stability of chestnut extract and its partial degradation [44].





**Figure 7.** UV-Vis spectra of the obtained NC-loaded films based on chitosan, as well as chitosan films without (Control I) and with chestnut extract (Control II).

### 2.7. Antimicrobial Activity

Antimicrobial activity of NC-loaded films was assessed toward *Escherichia coli*, *Staphylococcus aureus* and *Candida albicans*, which represent model foodborne pathogens that are Gram-negative bacteria, Gram-positive bacteria and fungi, respectively [45–47]. Their morphology after 24 h of incubation on the surface of NC/0 is presented in Figure 8. Observed phenotypes indicated that the pathogens entered the multiplication stage of growth that occurred after their attachment to the surface. Therefore, 24 h was found to be an appropriate timepoint to investigate the effect of the material on the viability of pathogens, eliminating the risk of false-positive results based on the presence of pathogens entering the death phase [48].

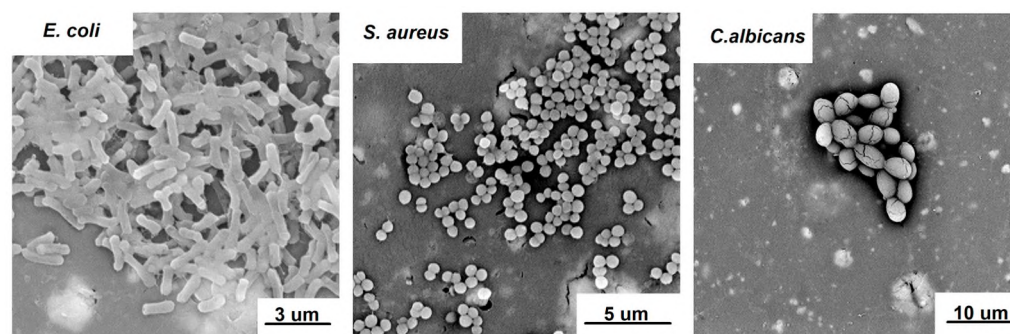


**Figure 8.** SEM images of *E. coli*, *S. aureus* and *C. albicans* inoculated overnight on the surface of NC/0 films.

The results of the antimicrobial tests (Figure 9) showed that the chitosan-based bio-nanocomposite films obtained in this study caused a strong reduction in the growth of both model Gram-negative (*E. coli*) and Gram-positive (*S. aureus*) bacteria and slight fungicidal activity against *C. albicans*. In particular, a 6–7 log reduction in the growth of *E. coli* and *S. aureus* was observed, while only a 1–2 log reduction was observed for *C. albicans*. In addition, the study showed that the chitosan-based bio-nanocomposite films were stable over time and retained their antibacterial activity against each pathogen. It is important to mention that the source of the antimicrobial activity of the studied films was the presence of both chestnut extract, which is a rich source of polyphenols, such as phenolic acids and tannins [49], and NC, which also exhibits antibacterial activity [50]. The antimicrobial activity of chestnut extract was proven in previous studies [21,25,51], in which its antimicrobial properties were demonstrated against model Gram-positive bacteria (*Staphylococcus epidermidis* ATCC12228), Gram-negative bacteria (*Escherichia coli* ATCC25922) and yeast

(*Candida albicans* ATCC18804). Körde et al. [51] also confirmed the antibacterial activity of chestnut extract against *Escherichia coli* K12 and *Bacillus subtilis* DSM 402. Dehnad et al. [14] prepared films of glycerol-plasticized chitosan and nanocellulose, studying their effects on inhibitory activity against both Gram-positive (*S. aureus*) and Gram-negative bacteria (*E. coli* and *S. enteritidis*). The results proved that, for all of the aforementioned bacteria, there was a decrease in their growth. In turn, Costa et al. [11] investigated the potential of chitosan/cellulose nanocrystal films for use as active pads in meat packaging to extend shelf life and preserve properties over time. Several concentrations of nanocellulose (5, 10, 25 and 50 wt.%) were used, and the films were produced by solvent casting. The study showed that the films obtained in this way exhibited antibacterial activity against Gram-positive and Gram-negative bacteria and slight fungicidal activity against *C. albicans*.

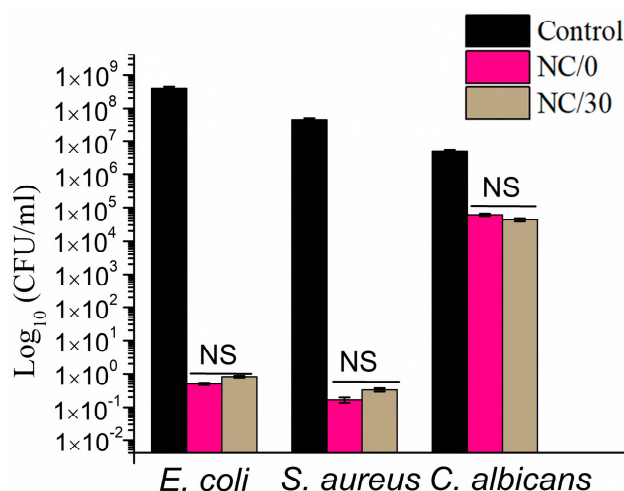


**Figure 9.** Antimicrobial activity of bio-nanocomposite films based on chitosan against *E. coli*, *S. aureus* and *C. albicans*, where Control—chitosan-based film without NC; NS = no significant difference relative to the controls. Comparisons among groups were performed by one-way ANOVA, followed by Bonferroni's multiple comparison post-hoc test. Statistical significance was considered at  $p < 0.05$ .

### 2.8. Thermal Analysis

Thermal degradation of the obtained bio-nanocomposite films based on chitosan (NC/0) was analyzed and compared to the film without NC (Control) and to the used neat chitosan, nanocellulose and chestnut extract (Figure 10). This analysis helped to determine the temperature at which the material is stable and the change in mass as a function of temperature change. Because of the law of NC content, the results indicated that the film with nanocellulose (NC/0) exhibited similar thermal degradation behavior to the film without nanocellulose (Control). They underwent an initial slight weight loss at around 100 °C, followed by a rapid weight loss between 250 and 400 °C. The first stage is associated with the evaporation of water and residual acetic acid present in the polymer matrix [52], while the second thermal event is attributed to the complex decomposition of chitosan [53]. Concerning chitosan, the main stage of thermal degradation begins at 300 °C, which is associated with the greatest weight loss ( $\approx 60\%$ ). This result can be attributed to degradation of the polysaccharide and deacetylation of chitosan [54]. In the case of nanocellulose, two steps were also noted, namely dehydration and degradation. The complete release of absorbed water took place at around 100 °C, followed by sharp decomposition noted at around 320–350 °C. In the case of the nanocellulose, the degradation occurred at ca. 50–70 °C lower than that typical for cellulose. The same relationship was also observed in previous work [55], indicating that nanocellulose should not be processed at temperatures higher than 200 °C. In the case of chestnut extract, initial weight loss was observed due to water evaporation, and the moisture was completely evaporated at about 150°, followed by the second phase, described as multistep complex thermal degradation (starting around 220 °C) [56].

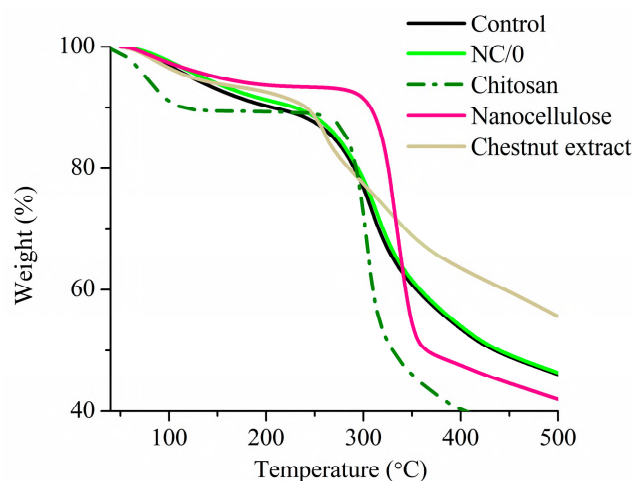


**Figure 10.** TG curves of the chitosan-based films, neat chitosan, nanocellulose and chestnut extract powder, where Control indicates plasticized chitosan film with chestnut extract.

### 3. Materials and Methods

#### 3.1. Materials

Chitosan 0.03–0.1 Pa  $\times$  s (MW = 250 kg/mol, DD  $\geq$  90%) was purchased from Sigma-Aldrich (Steinheim, Germany). Acetic acid was purchased from Avantor (Gliwice, Poland) (99.5–99.9%), and Farmatan chestnut extract ( $\geq$ 76% tannins) was provided by Tanin Sevnica (Sevnica, Slovenia). Propylene glycol, cyclohexene (pure p.a.) and sodium hydrogen carbonate (pure p.a.) were purchased from Chempur (Piekary Śląskie, Poland). Methanesulfonic acid (>99.0%) was provided by TCI (Zwijndrecht, Belgium). Nanofibrillated cellulose (10–20 nm wide, 2–3  $\mu$ m length) was purchased from Nanografi Nano Technology (Ankara, Türkiye).

#### 3.2. Preparation of the Bio-Based Plasticizer

Plasticizer mixtures were prepared as described in our previous study [15,57]. In short, propylene glycol was esterified with acetic acid for 24 h at 80  $^{\circ}$ C using methanesulfonic acid as a catalyst. Cyclohexane was used to remove water as a byproduct of the reaction. The esterification product was purified using a saturated solution of sodium hydrogen carbonate, distilled water and cyclohexane.

#### 3.3. Preparation of the Bio-Nanocomposite Films

Bio-nanocomposite films based on chitosan with a bio-based plasticizer reinforced with nanofiber cellulose were prepared by a casting method as described in our previous study [15]. Chitosan (2%, *w/v*) was dissolved in 1.0% (*v/v*) acetic acid aqueous solution with 30% (*w/w*) bio-based plasticizer based on the mass of chitosan by stirring with a magnetic stirrer at 800 rpm at room temperature for 24 h. Chestnut extract (0.75% (*w/v*)) was added, and the solution was homogenized for 5 min at 6000 rpm. Then, 0.5% (*w/v*) nanocellulose was added and homogenized for 1 min at 800 rpm. These solutions were left overnight to let the air bubbles disappear. Finally, bio-nanocomposite chitosan solutions were cast over Petri dishes (46 g per 12 cm  $\times$  12 cm dish) and dried at room temperature. In this way, bio-nanocomposite films with a thickness of about 94  $\mu$ m were obtained and tested directly (sample NC/0) and after 7, 14, and 30 days (sample NC/7, NC/14, and NC/30, respectively) of storage at 23  $^{\circ}$ C  $\pm$  2  $^{\circ}$ C and 50  $\pm$  5% relative humidity with access to light and air.

#### 3.4. Mechanical Properties

Tensile tests were performed at room temperature using an Instron 4466 testing machine. The specimens were cut in rectangular shapes 80 mm in length and 20 mm in width. The samples were conditioned before testing for 24 h at 23  $\pm$  2  $^{\circ}$ C and 50  $\pm$  2%



RH and were stretched at a crosshead speed of 5 mm/min. All tests were carried out on a minimum of five samples, and the final results were calculated as an average. The entire procedure was repeated for films stored for 7, 14 and 30 days.

### 3.5. Hydrophilic Properties

The hydrophilicity of the films was analyzed by moisture content—MC, swelling degree—SD, total soluble matter—TSM and water contact angle—CA. MC, SD and TSM were analyzed using a three-step gravimetric method; i.e., film samples with surface area of 1 cm<sup>2</sup> were weighed ( $M_1$ ), dried at 100 °C for 24 h and weighed again ( $M_2$ ).

$$MC(\%) = \frac{(M_1 - M_2)}{M_1} \times 100 \quad (1)$$

The samples were then placed in 30 mL of distilled water, left at room temperature for 24 h and weighed again ( $M_3$ ).

$$SD(\%) = \frac{(M_3 - M_2)}{M_2} \times 100 \quad (2)$$

In the final step, the samples were dried at 100 °C for 24 h and weighed ( $M_4$ ). Measurements were repeated five times, and the average value was calculated. TSM values were calculated using the following formula:

$$TSM(\%) = \frac{(M_2 - M_4)}{M_2} \times 100 \quad (3)$$

The dynamic water contact angle of the film surface was measured using a semi-automatic goniometer for dynamic contact angle and contour analysis systems (OCA15EC, DataPhysic, Filderstadt, Germany). A droplet of 5  $\mu$ L of deionized water was applied on the film surface according to the device's instructions. The measurement was taken immediately upon contact with the surface, after 30 s and after 60 s. The dynamic water contact angle was determined based on the average of the three measurements. The entire procedure was repeated for films stored for 7, 14 and 30 days.

### 3.6. Gas Permeability

Oxygen and carbon dioxide permeability through the bio-nanocomposite films were determined using an isobaric apparatus [15]. The samples for oxygen and carbon dioxide barrier testing, in the form of discs (60 mm<sup>2</sup>), were degassed for 24 h and conditioned with the appropriate gas in the apparatus prior to testing for 2 h. Then, the diffusion chamber was sealed, and compressed oxygen (class 5.0) or carbon dioxide (technical gas) was supplied at a controlled flow rate to keep the pressure constant. The permeation coefficient was determined as follows:

$$P = \frac{V \times l}{S \times \Delta p} \quad (4)$$

where  $V$  is the volumetric flow (mol·s<sup>-1</sup>),  $l$  is the sample thickness (m),  $S$  is the sample area (m<sup>2</sup>), and  $\Delta p$  is the pressure difference on both sides of the sample (Pa). The entire procedure was repeated for films stored for 7, 14 and 30 days.

Water vapor transmission rate (WVTR) and water vapor permeability (WVP) were determined according to the methodology proposed by Aguirre-Loredo et al. [32]. The samples in the form of discs (24.64 mm<sup>2</sup>), were mounted on a glass container with silica gel in its interior (~0% relative humidity, RH) and sealed with liquid paraffin. After the paraffin solidified, the cup was weighed to calculate the initial weight. The covered glass container was then placed in a desiccator containing a supersaturated saline solution of BaCl<sub>2</sub> (90% RH), generating a water-vapor differential pressure of 2854.23 Pa. The glass

container was weighed seven times at 60-min intervals. The determinations were made in triplicate. The entire procedure was repeated for films stored for 7, 14 and 30 days. The WVTR and WVP values were determined as follows:

$$\text{WVTR} = \frac{\Delta m}{\Delta t A} \quad (5)$$

$$\text{WVP} = \text{WVTR} \times L \Delta p \quad (6)$$

where  $\Delta m/\Delta t$  is the moisture weight gain in time (g/s),  $A$  is the exposed surface area of the film ( $\text{m}^2$ ),  $L$  is the thickness of the film (mm), and  $\Delta p$  is the difference in partial pressure (Pa).

### 3.7. Morphology

The morphology of the bio-nanocomposite films was examined by a scanning electron microscope (ZEISS Supra 35) at 10 kV of accelerating voltage, equipped with an energy dispersive X-ray detector (EDS) (Thermo Scientific™ EDX UltraDry).

### 3.8. Fourier Transform Infrared Spectroscopy

Fourier transform infrared (FTIR) spectra of the composite films were recorded in the range of  $3700\text{--}650\text{ cm}^{-1}$  with resolution of  $2\text{ cm}^{-1}$  using a Spectrum Two spectrometer equipped with a diamond UATR accessory (Perkin Elmer). For each spectrum, 16 scans were taken. These analyses were performed in duplicate at room temperature. In addition, the films were also tested after soaking for 24 h in water. For this purpose, the films were cut into small disks and stirred in water at room temperature for 24 h. The following films were dried at  $80^\circ\text{C}$ , and spectrum scans were performed according to the above procedure.

### 3.9. Transparency

The transparency of NC-loaded films was measured with the use of UV-Vis spectrophotometry (Hewlett Packard 8453 UV/Vis Diode Array Spectrophotometer) in the wavelength range from 450 nm to 1000 nm. UV-Vis spectra of NC-loaded chitosan films were compared with UV-Vis spectra of pristine chitosan films with and without chestnut extract.

### 3.10. Antimicrobial Activity

The antimicrobial activity of bio-nanocomposite films based on chitosan was determined against *Escherichia coli* ATCC25922, *Staphylococcus aureus* ATCC23235 and *Candida albicans* ATCC18804. They all represent foodborne pathogens [45–47], and numerous studies have used these pathogens to validate the antimicrobial activity of various materials, including food packaging materials [58,59]. Samples in the form of discs (10 mm in diameter) were placed in 12-well plates containing 500  $\mu\text{L}$  of M9 minimal medium supplemented with glucose as the sole carbon source. Thereafter, 20  $\mu\text{L}$  of the targeted bacterial culture, normalized to  $10^4$  CFU/mL, was inoculated into each well and incubated overnight at  $37^\circ\text{C}$  with shaking at 250 rpm. Overnight cultures were serially diluted in double-distilled autoclaved water and plated on LB agar to determine CFU/mL of recovered targeted bacteria. In control experiments, bacteria were inoculated in M9 media in the absence of NC. Surviving bacteria were quantified by serial dilution and plating on LB agar. All experiments were performed in triplicate and repeated three times.

To visualize and analyze the morphology of pathogens, a scanning electron microscope (Phenom ProX, Thermo Fisher Scientific, Waltham, MA, USA) at 15 kV of accelerating voltage was used. The materials were first fixed with 3% glutaraldehyde (Fisher BioReagents, Waltham, MA, USA) for 24 h and dehydrated by immersing the samples in solutions of ethanol (Acros Organics) with increasing concentrations (30%, 50%, 70%, 80%, 90%, 95%, 99.8%) and then dried for 24 h at  $50^\circ\text{C}$ . Subsequently, the samples were sputter-coated with a gold layer (20 min, 20 mA; Q150R Quorum Technologies, Lewes, UK).

### 3.11. Thermal Analysis

Thermogravimetric analysis (TGA) was carried out using a TGA 8000 thermogravimetric analyzer (PerkinElmer Inc., Waltham, MA, USA). The samples (ca. 10 mg) were heated in an open ceramic sample pan in the temperature range of 50–1000 °C, with the heating rate  $\beta = 20$  °C/min in a dynamic (20 mL/min) nitrogen atmosphere. The thermographs were collected and analyzed using Pyris<sup>TM</sup> 11 software (Waltham, MA, USA).

### 3.12. Statistical Analysis

Experimental data in Sections 3.1–3.3 were analyzed for statistical significance by analysis of variance (ANOVA) and Tukey's multiple range test with a  $p < 0.05$  significance level. Data were evaluated by OriginPro software, version 8.5.0 (OriginLab, Northampton, MA, USA), whereas for the experimental data in Section 3.6, the analysis was performed by one-way ANOVA, followed by Bonferroni's multiple comparison post-hoc test. Statistical significance was considered at  $p < 0.05$ .

## 4. Conclusions

Nanocomposite films have been made from chitosan, bio-based plasticizer and nanocellulose. The properties of these films were evaluated immediately after preparation and after 7, 14 and 30 days to determine changes over time. Interestingly, the greatest changes in film properties occurred within the first 7 days, after which the properties were found to stabilize. This outcome shows that significant changes occur in the first few days after sample preparation, such as a decrease in MC, which affects the other properties of the obtained films. Immediately after preparation, the tested films showed tensile stress at around 7 MPa, which dropped to 4.5 MPa after 7 days and oscillated around 4 MPa after 14 and 30 days. Elongation at break, on the other hand, increased slightly over time, rising from 60% for the initial sample to about 75% for the remaining ones. In this case, the greatest change also occurred within the first 7 days. The introduction of nanocellulose into the films mainly increased their hydrophobic character (the contact angle was about 105°). Based on the results, the use of nanocellulose to enhance the hydrophobic character of the films may be an interesting method to obtain films with better hydrophobic properties. Due to the presence of chestnut extract and NC, all films exhibited strong antibacterial activity against Gram-negative (*E. coli*) and Gram-positive (*S. aureus*) bacteria and slight fungicidal activity against *C. albicans*, which were maintained over time. The use of nanofillers did not affect the thermal properties of the film, but their addition reduced the transparency. In addition, the results show that testing bio-films not only immediately after testing but also over time can provide more meaningful results. The results presented in this article show not only the possibility of obtaining a more hydrophobic (due to the nanocellulose), more antibacterial (due to the synergistic effect of the chestnut extract, nanocellulose and bioplasticizer) and more durable (due to the bioplasticizer and nanocellulose) chitosan-based film than those without the above-mentioned components, but they also prove that, during the first 7 days, the film's properties can significantly deteriorate. In our case especially, a significant decrease in tensile strength was noted. Considering that the mechanical properties are among the most problematic properties of chitosan-based films, it is worth noting that films tested directly can provide misleading results. Nevertheless, properties such as antibacterial activity and barrier properties did not deteriorate over time, allowing us to conclude that the films obtained in the present study can successfully serve as active food packaging that extends the life of the product. However, to confirm their applicability to food, further research is needed, including mainly studies of migration performed in terms of the bioplasticizer, as well as the chestnut extract and nanocellulose.



**Author Contributions:** Conceptualization, W.J. and G.D.; methodology, W.J., G.D., K.K., A., D.Y.S., R.T., K.L. and K.G.; software, W.J., N.B., K.G. and M.N.; validation, W.J., G.D., M.N., K.L., N.B., A., R.T. and D.Y.S.; formal analysis, G.D.; investigation, W.J.; resources, W.J. and G.D.; data curation, M.N. and K.L.; writing—original draft preparation, W.J.; writing—review and editing, G.D. and K.K.; visualization, W.J.; supervision, G.D.; project administration, G.D.; funding acquisition, G.D. All authors have read and agreed to the published version of the manuscript.

**Funding:** This research was co-financed by the Ministry of Education and Science of Poland under grant no. DWD/4/21/2020. G.D. would like to thank the Ministry of Education and Science of Poland for funding under project no. SKN/SP/569054/2023 and the Silesian University of Technology for providing partial financial support under grant no. 31/010/SDU20/0006-10.

**Institutional Review Board Statement:** Not applicable.

**Informed Consent Statement:** Not applicable.

**Data Availability Statement:** Not applicable.

**Conflicts of Interest:** The authors declare no conflict of interest.

## References

- Jamróz, E.; Kulawik, P.; Kopel, P. The Effect of Nanofillers on the Functional Properties of Biopolymer-Based Films: A Review. *Polymers* **2019**, *11*, 675. [[CrossRef](#)] [[PubMed](#)]
- Lavrič, G.; Oberlintner, A.; Filipova, I.; Novak, U.; Likozar, B.; Vrabič-Brodnjak, U. Functional Nanocellulose, Alginate and Chitosan Nanocomposites Designed as Active Film Packaging Materials. *Polymers* **2021**, *13*, 2523. [[CrossRef](#)] [[PubMed](#)]
- Xu, Y.; Willis, S.; Jordan, K.; Sismour, E. Chitosan Nanocomposite Films Incorporating Cellulose Nanocrystals and Grape Pomace Extracts. *Packag. Technol. Sci.* **2018**, *31*, 631–638. [[CrossRef](#)]
- Mao, H.; Wei, C.; Gong, Y.; Wang, S.; Ding, W. Mechanical and Water-Resistant Properties of Eco-Friendly Chitosan Membrane Reinforced with Cellulose Nanocrystals. *Polymers* **2019**, *11*, 166. [[CrossRef](#)]
- Azeredo, H.M.C.; Mattoso, L.H.C.; Avena-Bustillos, R.J.; Filho, G.C.; Munford, M.L.; Wood, D.; McHugh, T.H. Nanocellulose Reinforced Chitosan Composite Films as Affected by Nanofiller Loading and Plasticizer Content. *J. Food Sci.* **2010**, *75*, N1–N7. [[CrossRef](#)]
- Priyadarshi, R.; Roy, S.; Ghosh, T.; Biswas, D.; Rhim, J.-W. Antimicrobial Nanofillers Reinforced Biopolymer Composite Films for Active Food Packaging Applications—A Review. *Sustain. Mater. Technol.* **2022**, *32*, e00353. [[CrossRef](#)]
- Jannatyha, N.; Shojaee-Aliabadi, S.; Moslehishad, M.; Moradi, E. Comparing Mechanical, Barrier and Antimicrobial Properties of Nanocellulose/CMC and Nanochitosan/CMC Composite Films. *Int. J. Biol. Macromol.* **2020**, *164*, 126187. [[CrossRef](#)]
- Isogai, A. Cellulose Nanofibers: Recent Progress and Future Prospects. *J. Fiber Sci. Technol.* **2020**, *76*, 310–326. [[CrossRef](#)]
- Ahankari, S.S.; Subhedar, A.R.; Bhadauria, S.S.; Dufresne, A. Nanocellulose in Food Packaging: A Review. *Carbohydr. Polym.* **2021**, *255*, 117479. [[CrossRef](#)]
- Trache, D.; Tarchoun, A.F.; Derradji, M.; Hamidon, T.S.; Masruchin, N.; Brosse, N.; Hussin, M.H. Nanocellulose: From Fundamentals to Advanced Applications. *Front. Chem.* **2020**, *8*, 392. [[CrossRef](#)]
- Costa, S.M.; Ferreira, D.P.; Teixeira, P.; Ballesteros, L.F.; Teixeira, J.A.; Figueiro, R. Active Natural-Based Films for Food Packaging Applications: The Combined Effect of Chitosan and Nanocellulose. *Int. J. Biol. Macromol.* **2021**, *177*, 241–251. [[CrossRef](#)] [[PubMed](#)]
- Mujtaba, M.; Salaberria, A.M.; Andres, M.A.; Kaya, M.; Gunyakti, A.; Labidi, J. Utilization of Flax (*Linum Usitatissimum*) Cellulose Nanocrystals as Reinforcing Material for Chitosan Films. *Int. J. Biol. Macromol.* **2017**, *104*, 944–952. [[CrossRef](#)]
- Fahma, F.; Febiyanti, I.; Lisdayana, N.; Arnata, I.; Sartika, D. Nanocellulose as a New Sustainable Material for Various Applications: A Review. *Arch. Mater. Sci. Eng.* **2021**, *2*, 49–64. [[CrossRef](#)]
- Dehnad, D.; Mirzaei, H.; Emam-Djomeh, Z.; Jafari, S.-M.; Dadashi, S. Thermal and Antimicrobial Properties of Chitosan–Nanocellulose Films for Extending Shelf Life of Ground Meat. *Carbohydr. Polym.* **2014**, *109*, 148–154. [[CrossRef](#)] [[PubMed](#)]
- Janik, W.; Ledniowska, K.; Nowotarski, M.; Kudła, S.; Knapczyk-Korczak, J.; Stachewicz, U.; Nowakowska-Bogdan, E.; Sabura, E.; Nosal-Kovalenko, H.; Turczyn, R.; et al. Chitosan-Based Films with Alternative Eco-Friendly Plasticizers: Preparation, Physicochemical Properties and Stability. *Carbohydr. Polym.* **2022**, *301*, 120277. [[CrossRef](#)]
- Janik, W.; Nowotarski, M.; Ledniowska, K.; Shyntum, D.Y.; Krukiewicz, K.; Turczyn, R.; Sabura, E.; Furgoł, S.; Kudła, S.; Dudek, G. Modulation of Physicochemical Properties and Antimicrobial Activity of Sodium Alginate Films through the Use of Chestnut Extract and Plasticizers. *Sci. Rep.* **2023**, *13*, 11530. [[CrossRef](#)]
- Zhang, X.; Ismail, B.B.; Cheng, H.; Jin, T.Z.; Qian, M.; Arabi, S.A.; Liu, D.; Guo, M. Emerging Chitosan–Essential Oil Films and Coatings for Food Preservation—A Review of Advances and Applications. *Carbohydr. Polym.* **2021**, *273*, 118616. [[CrossRef](#)]
- Hosseinzadeh, S.; Partovi, R.; Talebi, F.; Babaei, A. Chitosan/TiO<sub>2</sub> Nanoparticle/Cymbopogon Citratus Essential Oil Film as Food Packaging Material: Physico-Mechanical Properties and Its Effects on Microbial, Chemical, and Organoleptic Quality of Minced Meat during Refrigeration. *J. Food Process. Preserv.* **2020**, *44*, e14536. [[CrossRef](#)]

19. Šupová, M.; Simha Martynková, G.; Cech Barabaszova, K. Effect of Nanofillers Dispersion in Polymer Matrices: A Review. *Sci. Adv. Mater.* **2010**, *3*, 1–25. [[CrossRef](#)]
20. Bajić, M.; Oberlintner, A.; Körge, K.; Likozar, B.; Novak, U. Formulation of Active Food Packaging by Design: Linking Composition of the Film-Forming Solution to Properties of the Chitosan-Based Film by Response Surface Methodology (RSM) Modelling. *Int. J. Biol. Macromol.* **2020**, *160*, 971–978. [[CrossRef](#)]
21. Körge, K.; Šeme, H.; Bajić, M.; Likozar, B.; Novak, U. Reduction in Spoilage Microbiota and Cyclopiazonic Acid Mycotoxin with Chestnut Extract Enriched Chitosan Packaging: Stability of Inoculated Gouda Cheese. *Foods* **2020**, *9*, 1645. [[CrossRef](#)]
22. Bourtoom, T.; Chinnan, M.S. Preparation and Properties of Rice Starch–Chitosan Blend Biodegradable Film. *LWT—Food Sci. Technol.* **2008**, *41*, 1633–1641. [[CrossRef](#)]
23. Pereda, M.; Aranguren, M.I.; Marcovich, N.E. Water Vapor Absorption and Permeability of Films Based on Chitosan and Sodium Caseinate. *J. Appl. Polym. Sci.* **2009**, *111*, 2777–2784. [[CrossRef](#)]
24. Cazón, P.; Vázquez, M. Mechanical and Barrier Properties of Chitosan Combined with Other Components as Food Packaging Film. *Environ. Chem. Lett.* **2020**, *18*, 257–267. [[CrossRef](#)]
25. Janik, W.; Nowotarski, M.; Shyntum, D.Y.; Banaś, A.; Krukiewicz, K.; Kudła, S.; Dudek, G. Antibacterial and Biodegradable Polysaccharide-Based Films for Food Packaging Applications: Comparative Study. *Materials* **2022**, *15*, 3236. [[CrossRef](#)] [[PubMed](#)]
26. Leceta, I.; Guerrero, P.; De La Caba, K. Functional Properties of Chitosan-Based Films. *Carbohydr. Polym.* **2013**, *93*, 339–346. [[CrossRef](#)] [[PubMed](#)]
27. Butler, B.L.; Vergano, P.J.; Testin, R.F.; Bunn, J.M.; Wiles, J.L. Mechanical and Barrier Properties of Edible Chitosan Films as Affected by Composition and Storage. *J. Food Sci.* **1996**, *61*, 953–956. [[CrossRef](#)]
28. Kurek, M.; Guinault, A.; Voilley, A.; Galić, K.; Debeaufort, F. Effect of Relative Humidity on Carvacrol Release and Permeation Properties of Chitosan Based Films and Coatings. *Food Chem.* **2014**, *144*, 9–17. [[CrossRef](#)]
29. Masclaux, C.; Gouanvé, F.; Espuche, E. Experimental and Modelling Studies of Transport in Starch Nanocomposite Films as Affected by Relative Humidity. *J. Membr. Sci.* **2010**, *363*, 221–231. [[CrossRef](#)]
30. Stading, M.; Rindlav-Westling, Å.; Gatenholm, P. Humidity-Induced Structural Transitions in Amylose and Amylopectin Films. *Carbohydr. Polym.* **2001**, *45*, 209–217. [[CrossRef](#)]
31. Srinivasa, P.C.; Ramesh, M.N.; Tharanathan, R.N. Effect of Plasticizers and Fatty Acids on Mechanical and Permeability Characteristics of Chitosan Films. *Food Hydrocoll.* **2007**, *21*, 1113–1122. [[CrossRef](#)]
32. Aguirre-Loredo, R.Y.; Rodríguez-Hernández, A.I.; Morales-Sánchez, E.; Gómez-Aldapa, C.A.; Velazquez, G. Effect of Equilibrium Moisture Content on Barrier, Mechanical and Thermal Properties of Chitosan Films. *Food Chem.* **2016**, *196*, 560–566. [[CrossRef](#)] [[PubMed](#)]
33. Borys, P.; Pawelek, K.; Grzywna, Z.J. On the Magnetic Channels in Polymer Membranes. *Phys. Chem. Chem. Phys.* **2011**, *13*, 17122–17129. [[CrossRef](#)] [[PubMed](#)]
34. Kerch, G.; Korkhov, V. Effect of Storage Time and Temperature on Structure, Mechanical and Barrier Properties of Chitosan-Based Films. *Eur. Food Res. Technol.* **2011**, *232*, 17–22. [[CrossRef](#)]
35. Khan, A.; Khan, R.A.; Salmieri, S.; Le Tien, C.; Riedl, B.; Bouchard, J.; Chauve, G.; Tan, V.; Kamal, M.R.; Lacroix, M. Mechanical and Barrier Properties of Nanocrystalline Cellulose Reinforced Chitosan Based Nanocomposite Films. *Carbohydr. Polym.* **2012**, *90*, 1601–1608. [[CrossRef](#)]
36. Helmiyati, H.; Budiman, Y.; Abbas, G.H.; Dini, F.; Khalil, M. Highly Efficient Synthesis of Biodiesel Catalyzed by a Cellulose@hematite-Zirconia Nanocomposite. *Heliyon* **2021**, *7*, e06622. [[CrossRef](#)]
37. Li, M.; He, B.; Chen, Y.; Zhao, L. Physicochemical Properties of Nanocellulose Isolated from Cotton Stalk Waste. *ACS Omega* **2021**, *6*, 25162–25169. [[CrossRef](#)]
38. Wulandari, W.; Rochliadi, A.; Arcana, I.M. Nanocellulose Prepared by Acid Hydrolysis of Isolated Cellulose from Sugarcane Bagasse. *IOP Conf. Ser. Mater. Sci. Eng.* **2016**, *107*, 012045. [[CrossRef](#)]
39. dos Santos Grasel, F.; Ferrão, M.F.; Wolf, C.R. Development of Methodology for Identification the Nature of the Polyphenolic Extracts by FTIR Associated with Multivariate Analysis. *Spectrochim. Acta A Mol. Biomol. Spectrosc.* **2016**, *153*, 94–101. [[CrossRef](#)]
40. Fernández, K.; Agosin, E. Quantitative Analysis of Red Wine Tannins Using Fourier-Transform Mid-Infrared Spectrometry. *J. Agric. Food Chem.* **2007**, *55*, 7294–7300. [[CrossRef](#)]
41. Indrani, D.J.; Lukitowati, F.; Yulizar, Y. Preparation of Chitosan/Collagen Blend Membranes for Wound Dressing: A Study on FTIR Spectroscopy and Mechanical Properties. *IOP Conf. Ser. Mater. Sci. Eng.* **2017**, *202*, 012020. [[CrossRef](#)]
42. Varma, R.; Vasudevan, S. Extraction, Characterization, and Antimicrobial Activity of Chitosan from Horse Mussel *Modiolus Modiolus*. *ACS Omega* **2020**, *5*, 20224–20230. [[CrossRef](#)] [[PubMed](#)]
43. Guzman-Puyol, S.; Benítez, J.J.; Heredia-Guerrero, J.A. Transparency of Polymeric Food Packaging Materials. *Food Res. Int.* **2022**, *161*, 111792. [[CrossRef](#)] [[PubMed](#)]
44. Cortés-Rojas, D.F.; Souza, C.R.F.; Oliveira, W.P. Assessment of Stability of a Spray Dried Extract from the Medicinal Plant *Bidens pilosa* L. *J. King Saud Univ. Eng. Sci.* **2016**, *28*, 141–146. [[CrossRef](#)]
45. Fetsch, A.; Jöhler, S. *Staphylococcus Aureus* as a Foodborne Pathogen. *Curr. Clin. Microbiol. Rep.* **2018**, *5*, 88–96. [[CrossRef](#)]
46. Ma, Y.; Ding, S.; Fei, Y.; Liu, G.; Jang, H.; Fang, J. Antimicrobial Activity of Anthocyanins and Catechins against Foodborne Pathogens *Escherichia Coli* and *Salmonella*. *Food Control* **2019**, *106*, 106712. [[CrossRef](#)]

47. Krishnamoorthy, R.; Gassem, M.A.; Athinarayanan, J.; Periyasamy, V.S.; Prasad, S.; Alshatwi, A.A. Antifungal Activity of Nanoemulsion from Cleome Viscosa Essential Oil against Food-Borne Pathogenic Candida Albicans. *Saudi J. Biol. Sci.* **2021**, *28*, 286–293. [[CrossRef](#)]
48. Czerwińska-Główka, D.; Przysaś, W.; Zabłocka-Godlewska, E.; Student, S.; Cwalina, B.; Łapkowski, M.; Krukiewicz, K. Bacterial Surface Colonization of Sputter-Coated Platinum Films. *Materials* **2020**, *13*, 2674. [[CrossRef](#)]
49. Aimone, C.; Grillo, G.; Boffa, L.; Giovando, S.; Cravotto, G. Tannin Extraction from Chestnut Wood Waste: From Lab Scale to Semi-Industrial Plant. *Appl. Sci.* **2023**, *13*, 2494. [[CrossRef](#)]
50. Li, J.; Cha, R.; Mou, K.; Zhao, X.; Long, K.; Luo, H.; Zhou, F.; Jiang, X. Nanocellulose-Based Antibacterial Materials. *Adv. Healthc. Mater.* **2018**, *7*, 1800334. [[CrossRef](#)]
51. Kõrge, K.; Bajić, M.; Likožar, B.; Novak, U. Active Chitosan–Chestnut Extract Films Used for Packaging and Storage of Fresh Pasta. *Int. J. Food Sci. Technol.* **2020**, *55*, 3043–3052. [[CrossRef](#)]
52. Souza, V.G.L.; Pires, J.R.A.; Rodrigues, C.; Rodrigues, P.F.; Lopes, A.; Silva, R.J.; Caldeira, J.; Duarte, M.P.; Fernandes, F.B.; Coelho, I.M.; et al. Physical and Morphological Characterization of Chitosan/Montmorillonite Films Incorporated with Ginger Essential Oil. *Coatings* **2019**, *9*, 700. [[CrossRef](#)]
53. Szymańska, E.; Winnicka, K. Stability of Chitosan—A Challenge for Pharmaceutical and Biomedical Applications. *Mar. Drugs* **2015**, *13*, 1819–1846. [[CrossRef](#)] [[PubMed](#)]
54. Corazzari, I.; Nisticò, R.; Turci, F.; Faga, M.G.; Franzoso, F.; Tabasso, S.; Magnacca, G. Advanced Physico-Chemical Characterization of Chitosan by Means of TGA Coupled on-Line with FTIR and GCMS: Thermal Degradation and Water Adsorption Capacity. *Polym. Degrad. Stab.* **2015**, *112*, 1–9. [[CrossRef](#)]
55. Gan, P.G.; Sam, S.T.; Abdullah, M.F.b.; Omar, M.F. Thermal Properties of Nanocellulose-Reinforced Composites: A Review. *J. Appl. Polym. Sci.* **2020**, *137*, 48544. [[CrossRef](#)]
56. Çiçek Özkan, B.; Güner, M. Isolation, Characterization, and Comparison of Nanocrystalline Cellulose from Solid Wastes of Horse Chestnut and Chestnut Seed Shell. *Cellulose* **2022**, *29*, 6629–6644. [[CrossRef](#)]
57. Ledniowska, K.; Nosal-Kovalenko, H.; Janik, W.; Krasuska, A.; Stańczyk, D.; Sabura, E.; Bartoszewicz, M.; Rybak, A. Effective, Environmentally Friendly PVC Plasticizers Based on Succinic Acid. *Polymers* **2022**, *14*, 1295. [[CrossRef](#)] [[PubMed](#)]
58. Zulfa, Z.; Chia, C.T.; Rukayadi, Y. In Vitro Antimicrobial Activity of Cymbopogon Citratus (Lemongrass) Extracts against Selected Foodborne Pathogens. *Int. Food Res. J.* **2016**, *23*, 1262–1267.
59. Becerril, R.; Gómez-Lus, R.; Goñi, P.; López, P.; Nerín, C. Combination of Analytical and Microbiological Techniques to Study the Antimicrobial Activity of a New Active Food Packaging Containing Cinnamon or Oregano against *E. Coli* and *S. Aureus*. *Anal. Bioanal. Chem.* **2007**, *388*, 1003–1011. [[CrossRef](#)]

**Disclaimer/Publisher’s Note:** The statements, opinions and data contained in all publications are solely those of the individual author(s) and contributor(s) and not of MDPI and/or the editor(s). MDPI and/or the editor(s) disclaim responsibility for any injury to people or property resulting from any ideas, methods, instructions or products referred to in the content.



Gliwice, 30.08.2023 r.

mgr inż. Weronika Janik

Sieć Badawcza Łukasiewicz –  
Instytut Ciężkiej Syntezy Organicznej "Blachownia"  
Energetyków 9, 47-225 Kędzierzyn-Koźle

Katedra Fizykochemii i Technologii Polimerów  
Szkoła Doktorów  
Politechnika Śląska  
Akademicka 2a, 44-100 Gliwice  
[weronika.janik@icso.lukasiewicz.gov.pl](mailto:weronika.janik@icso.lukasiewicz.gov.pl)

### OŚWIADCZENIE O WSPÓLAUTORSTWIE

Niniejszym oświadczam, że w pracy:

Janik, W., Wojtala, A., Pietruszka, A., Dudek, G., & Sabura, E. (2021). Environmentally Friendly Melt-Processed Chitosan/Starch Composites Modified with PVA and Lignin. *Polymers*, 13, 2685, <https://doi.org/10.3390/polym13162685> mój udział polegał na współtworzeniu wspólnej koncepcji, wykonaniu badań laboratoryjnych, współtworzeniu metod badawczych, współudziale w analizie i interpretacji wyników, współtworzeniu oryginalnego manuskryptu, korekcie tekstu po recenzjach, przygotowaniu odpowiedzi do recenzentów, pełnieniu roli autora korespondencyjnego. Mój udział szacuję na 60%.

Janik, W., Nowotarski, M., Shyntum, D. Y., Banaś, A., Krukiewicz, K., Kudła, S., & Dudek, G. (2022). Antibacterial and Biodegradable Polysaccharide-Based Films for Food Packaging Applications: Comparative Study. *Materials*, 15(9). <https://doi.org/10.3390/ma15093236> mój udział polegał na współtworzeniu wspólnej koncepcji, współtworzeniu metod badawczych, współudziale w analizie i interpretacji wyników, modyfikacji polimerów, współtworzeniu oryginalnego manuskryptu, korekcie tekstu po recenzjach, przygotowaniu odpowiedzi do recenzentów, pełnieniu roli autora korespondencyjnego. Mój udział szacuję na 50%.

Janik, W., Ledniowska, K., Nowotarski, M., Kudła, S., Knapczyk-Korczak, J., Stachewicz, U., Nowakowska-Bogdan, E., Sabura, E., Nosal-Kovalenko, H., Turczyn, R., & Dudek, G. (2022). Chitosan-based films with alternative eco-friendly plasticizers: Preparation, physicochemical properties and stability. *Carbohydrate Polymers*, 120277. <https://doi.org/10.1016/j.carbpol.2022.120277> mój udział polegał na współtworzeniu wspólnej koncepcji, udziale w wykonaniu badań laboratoryjnych, współtworzeniu metod badawczych, współudziale w analizie i interpretacji wyników, współtworzeniu oryginalnego manuskryptu,



korekcie tekstu po recenzjach, przygotowaniu odpowiedzi do recenzentów, pełnieniu roli autora korespondencyjnego. Mój udział szacuję na 40%.

Janik, W., Nowotarski, M., Ledniowska, K., Shyntum, D. Y., Krukiewicz, K., Turczyn, R., Sabura, E., Furgoń, S., Kudła, S., & Dudek, G. (2023). Modulation of physicochemical properties and antimicrobial activity of sodium alginate films through the use of chestnut extract and plasticizers. *Scientific Reports*, 13(1), <https://doi.org/10.1038/s41598-023-38794-3> mój udział polegał na współtworzeniu wspólnej koncepcji, udziale w wykonaniu badań laboratoryjnych, współtworzeniu metod badawczych, współudziale w analizie i interpretacji wyników, współtworzeniu oryginalnego manuskryptu, korekcie tekstu po recenzjach, przygotowaniu odpowiedzi do recenzentów, pełnieniu roli autora korespondencyjnego. Mój udział szacuję na 40%.

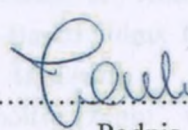
Janik, W., Nowotarski, M., Ledniowska, K., Biernat N., Abdullah, Shyntum, D. Y., Krukiewicz, K., Turczyn R., Gołombek, K. & Dudek, G. (2023). Effect of Time on the Properties of Bio-Nanocomposite Films Based on Chitosan with Bio-Based Plasticizer Reinforced with Nanofiber Cellulose. *International Journal of Molecular Sciences* 24(17), <https://doi.org/10.3390/ijms241713205> udział polegał na współtworzeniu wspólnej koncepcji, udziale w wykonaniu badań laboratoryjnych, współtworzeniu metod badawczych, współudziale w analizie i interpretacji wyników, współtworzeniu oryginalnego manuskryptu, korekcie tekstu po recenzjach oraz przygotowaniu odpowiedzi do recenzentów. Mój udział szacuję na 40%.

Janik, W., Nowotarski, M., Ledniowska, K., Biernat N., Abdullah, Shyntum, D. Y., Krukiewicz, K., Turczyn R., Gołombek, K. & Dudek, G. (2023). Effect of Time on the Properties of Bio-Nanocomposite Films Based on Chitosan with Bio-Based Plasticizer Reinforced with Nanofiber Cellulose. *International Journal of Molecular Sciences* 24(17), <https://doi.org/10.3390/ijms241713205> udział polegał na współtworzeniu wspólnej koncepcji, udziale w wykonaniu badań laboratoryjnych, współtworzeniu metod badawczych, współudziale w analizie i interpretacji wyników, współtworzeniu oryginalnego manuskryptu oraz korekcie tekstu po recenzjach. Mój udział szacuję na 40%.

Janik, W., Nowotarski, M., Shyntum, D. Y., Nowak, A., Krukiewicz, K., Kudła, S., & Dudek, G. (2022). Antimicrobial and Biodegradable Polymeric Films for Food Packaging Applications. *Composites* 2022, <https://doi.org/10.3390/com2216131216> mój udział polegał na współtworzeniu wspólnej koncepcji, współtworzeniu metod badawczych, współudziale w analizie i interpretacji wyników, współtworzeniu oryginalnego manuskryptu oraz korekcie tekstu po recenzjach. Mój udział szacuję na 40%.

Janik, W., Ledniowska, K., Nowotarski, M., Kudła, S., Knapczyk-Kozłak, J., Szańbiewska, T., Nowakowska, Eugenia, E., Sabura, E., Nowak-Kondratyć, U., Turczyn, R., & Dudek, G. (2022). Chitosan-based films with alginate-chitosan-bio-based plasticizer: Preparation, physicochemical properties and stability. *Carbohydrate Polymers*, 220277, <https://doi.org/10.1016/j.carpol.2022.112817> mój udział polegał na współtworzeniu wspólnej koncepcji, współtworzeniu metod badawczych, współudziale w analizie i interpretacji wyników, współtworzeniu oryginalnego manuskryptu oraz korekcie tekstu po recenzjach. Mój udział szacuję na 40%.

Janik, W., Nowotarski, M., Ledniowska, K., Shyntum, D. Y., Krukiewicz, K., Turczyn, R., Sabura, E., Furgoń, S., Kudła, S., & Dudek, G. (2023). Modulation of physicochemical properties and antimicrobial activity of sodium alginate films through the use of chestnut extract and plasticizers. *Scientific Reports*, 13(1), <https://doi.org/10.1038/s41598-023-38794-3> mój

  
.....  
Podpis



Gliwice, 29.08.2023 r.

dr hab. inż. Gabriela Dudek, profesor PŚ

Katedra Fizykochemii i Technologii Polimerów

Wydział Chemiczny

Politechnika Śląska

Ks. M. Strzody 9, 44-100 Gliwice

[gmdudek@polsl.pl](mailto:gmdudek@polsl.pl)

### OŚWIADCZENIE O WSPÓLAUTORSTWIE

Niniejszym oświadczam, że w pracy:

Janik, W., Wojtala, A., Pietruszka, A., Dudek, G., & Sabura, E. (2021). Environmentally Friendly Melt-Processed Chitosan/Starch Composites Modified with PVA and Lignin. *Polymers*, 13, 2685, <https://doi.org/10.3390/polym13162685> mój udział polegał na współtworzeniu wspólnej koncepcji, współtworzeniu metod badawczych, współudziale w analizie i interpretacji wyników, współtworzeniu oryginalnego manuskryptu oraz korekcie tekstu po recenzjach. Mój udział szacuję na 15%.

Janik, W., Nowotarski, M., Shyntum, D. Y., Banaś, A., Krukiewicz, K., Kudła, S., & Dudek, G. (2022). Antibacterial and Biodegradable Polysaccharide-Based Films for Food Packaging Applications: Comparative Study. *Materials*, 15(9). <https://doi.org/10.3390/ma15093236> mój udział polegał na współtworzeniu wspólnej koncepcji, współtworzeniu metod badawczych, współudziale w analizie i interpretacji wyników, współtworzeniu oryginalnego manuskryptu oraz korekcie tekstu po recenzjach. Mój udział szacuję na 15%.

Janik, W., Ledniowska, K., Nowotarski, M., Kudła, S., Knapczyk-Korczak, J., Stachewicz, U., Nowakowska-Bogdan, E., Sabura, E., Nosal-Kovalenko, H., Turczyn, R., & Dudek, G. (2022). Chitosan-based films with alternative eco-friendly plasticizers: Preparation, physicochemical properties and stability. *Carbohydrate Polymers*, 120277. <https://doi.org/10.1016/j.carbpol.2022.120277> mój udział polegał na współtworzeniu wspólnej koncepcji, współtworzeniu metod badawczych, współudziale w analizie i interpretacji wyników, współtworzeniu oryginalnego manuskryptu oraz korekcie tekstu po recenzjach. Mój udział szacuję na 10%.

Janik, W., Nowotarski, M., Ledniowska, K., Shyntum, D. Y., Krukiewicz, K., Turczyn, R., Sabura, E., Furgoń, S., Kudła, S., & Dudek, G. (2023). Modulation of physicochemical properties and antimicrobial activity of sodium alginate films through the use of chestnut extract and plasticizers. *Scientific Reports*, 13(1), <https://doi.org/10.1038/s41598-023-38794-3> mój



udział polegał na współtworzeniu wspólnej koncepcji, współtworzeniu metod badawczych, współudziale w analizie i interpretacji wyników, współtworzeniu oryginalnego manuskryptu oraz korekcie tekstu po recenzjach. Mój udział szacuję na 15%.

Janik, W., Nowotarski, M., Ledniowska, K., Biernat N., Abdullah, Shyntum, D. Y., Krukiewicz, K., Turczyn R., Gołombek, K. & Dudek, G. (2023). Effect of Time on the Properties of Bio-Nanocomposite Films Based on Chitosan with Bio-Based Plasticizer Reinforced with Nanofiber Cellulose. *International Journal of Molecular Sciences* 24(17), <https://doi.org/10.3390/ijms241713205> mój udział polegał na współtworzeniu wspólnej koncepcji, współtworzeniu metod badawczych, współudziale w analizie i interpretacji wyników, współtworzeniu oryginalnego manuskryptu oraz korekcie tekstu po recenzjach. Mój udział szacuję na 10%.



Signed by /  
Podpisano przez:

Gabriela Maria  
Dudek  
Politechnika Śląska

Date / Data:  
2023-08-29 11:06

Podpis



Gliwice, 28.08.2023 r.

dr hab. Stanisław Kudła

Sieć Badawcza Łukasiewicz –  
Instytut Ciężkiej Syntezy Organicznej "Błachownia"  
Energetyków 9, 47-225 Kędzierzyn-Koźle  
[stanislaw.kudla@icso.lukasiewicz.gov.pl](mailto:stanislaw.kudla@icso.lukasiewicz.gov.pl)

## OŚWIADCZENIE O WSPÓLAUTORSTWIE

Niniejszym oświadczam, że w pracy:

Janik, W., Nowotarski, M., Shyntum, D. Y., Banaś, A., Krukiewicz, K., Kudła, S., & Dudek, G. (2022). Antibacterial and Biodegradable Polysaccharide-Based Films for Food Packaging Applications: Comparative Study. *Materials*, 15(9). <https://doi.org/10.3390/ma15093236> mój udział polegał współudziale w analizie i interpretacji wyników, wsparciu merytorycznym podczas opracowywaniu wyników badań oraz korekcie tekstu. Mój udział szacuję na 5%.

Janik, W., Ledniowska, K., Nowotarski, M., Kudła, S., Knapczyk-Korczak, J., Stachewicz, U., Nowakowska-Bogdan, E., Sabura, E., Nosal-Kovalenko, H., Turczyn, R., & Dudek, G. (2022). Chitosan-based films with alternative eco-friendly plasticizers: Preparation, physicochemical properties and stability. *Carbohydrate Polymers*, 120277. <https://doi.org/10.1016/j.carbpol.2022.120277> mój udział polegał współudziale w analizie i interpretacji wyników, wsparciu merytorycznym podczas opracowywaniu wyników badań oraz korekcie tekstu. Mój udział szacuję na 5%.

Janik, W., Nowotarski, M., Ledniowska, K., Shyntum, D. Y., Krukiewicz, K., Turczyn, R., Sabura, E., Furgol, S., Kudła, S., & Dudek, G. (2023). Modulation of physicochemical properties and antimicrobial activity of sodium alginate films through the use of chestnut extract and plasticizers. *Scientific Reports*, 13(1), <https://doi.org/10.1038/s41598-023-38794-3> mój udział polegał współudziale w analizie i interpretacji wyników, wsparciu merytorycznym podczas opracowywaniu wyników badań oraz korekcie tekstu. Mój udział szacuję na 5%.



.....  
Podpis



Gliwice, 25.08.2023 r.

mgr inż. Michał Nowotarski  
Katedra Fizykochemii i Technologii Polimerów  
Wydział Chemiczny  
Politechnika Śląska  
Ks. M. Strzody 9, 44-100 Gliwice  
[michnow566@student.polsl.pl](mailto:michnow566@student.polsl.pl)

## OŚWIADCZENIE O WSPÓLAUTORSTWIE

Niniejszym oświadczam, że w pracy:

Janik, W., Nowotarski, M., Shyntum, D. Y., Banaś, A., Krukiewicz, K., Kudła, S., & Dudek, G. (2022). Antibacterial and Biodegradable Polysaccharide-Based Films for Food Packaging Applications: Comparative Study. *Materials*, 15(9). <https://doi.org/10.3390/ma15093236> mój udział polegał na przeprowadzaniu badań właściwości hydrofilowych i barierowych, obróbce danych. Mój udział szacuję na 10%.

Janik, W., Ledniowska, K., Nowotarski, M., Kudła, S., Knapczyk-Korczak, J., Stachewicz, U., Nowakowska-Bogdan, E., Sabura, E., Nosal-Kovalenko, H., Turczyn, R., & Dudek, G. (2022). Chitosan-based films with alternative eco-friendly plasticizers: Preparation, physicochemical properties and stability. *Carbohydrate Polymers*, 120277. <https://doi.org/10.1016/j.carbpol.2022.120277> mój udział polegał na przeprowadzaniu badań właściwości hydrofilowych i barierowych, obróbce danych. Mój udział szacuję na 5%.

Janik, W., Nowotarski, M., Ledniowska, K., Shyntum, D. Y., Krukiewicz, K., Turczyn, R., Sabura, E., Furgoń, S., Kudła, S., & Dudek, G. (2023). Modulation of physicochemical properties and antimicrobial activity of sodium alginate films through the use of chestnut extract and plasticizers. *Scientific Reports*, 13(1), <https://doi.org/10.1038/s41598-023-38794-3> mój udział polegał na przeprowadzaniu badań właściwości hydrofilowych i barierowych, obróbce danych. Mój udział szacuję na 10%.

Janik, W., Nowotarski, M., Ledniowska, K., Biernat N., Abdullah, Shyntum, D. Y., Krukiewicz, K., Turczyn R., Gołombek, K. & Dudek, G. (2023). Effect of Time on the Properties of Bio-Nanocomposite Films Based on Chitosan with Bio-Based Plasticizer Reinforced with Nanofiber Cellulose. *International Journal of Molecular Sciences* 24(17), <https://doi.org/10.3390/ijms241713205> mój udział polegał na przeprowadzaniu badań właściwości hydrofilowych i barierowych i obróbce danych eksperymentalnych. Mój udział szacuję na 5%.

*Michał Nowotarski*

Podpis



Kędzierzyn-Koźle, 25.08.2023 r.

mgr inż. Kerstin Ledniowska

Sieć Badawcza Łukasiewicz –  
Instytut Ciężkiej Syntezy Organicznej "Blachownia"  
Energetyków 9, 47-225 Kędzierzyn-Koźle

Katedra Fizykochemii i Technologii Polimerów  
Szkoła Doktorów  
Politechnika Śląska  
Akademicka 2a, 44-100 Gliwice  
[kerstin.ledniowska@icso.lukasiewicz.gov.pl](mailto:kerstin.ledniowska@icso.lukasiewicz.gov.pl)

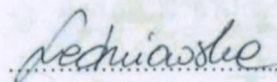
### OŚWIADCZENIE O WSPÓLAUTORSTWIE

Niniejszym oświadczam, że w pracy:

Janik, W., Ledniowska, K., Nowotarski, M., Kudła, S., Knapczyk-Korczak, J., Stachewicz, U., Nowakowska-Bogdan, E., Sabura, E., Nosal-Kovalenko, H., Turczyn, R., & Dudek, G. (2022). Chitosan-based films with alternative eco-friendly plasticizers: Preparation, physicochemical properties and stability. *Carbohydrate Polymers*, 120277. <https://doi.org/10.1016/j.carbpol.2022.120277> mój udział polegał na przygotowaniu metodologii i syntezie bioplastyfikatorów, obróbce i analizie danych, redagowaniu pracy, omówieniu wyników. Mój udział szacuję na 10%.

Janik, W., Nowotarski, M., Ledniowska, K., Shyntum, D. Y., Krukiewicz, K., Turczyn, R., Sabura, E., Furgoń, S., Kudła, S., & Dudek, G. (2023). Modulation of physicochemical properties and antimicrobial activity of sodium alginate films through the use of chestnut extract and plasticizers. *Scientific Reports*, 13(1), <https://doi.org/10.1038/s41598-023-38794-3> mój udział polegał na przygotowaniu metodologii i syntezie bioplastyfikatorów oraz na analizie wyników. Mój udział szacuję na 5%.

Janik, W., Nowotarski, M., Ledniowska, K., Biernat N., Abdullah, Shyntum, D. Y., Krukiewicz, K., Turczyn R., Golombek, K. & Dudek, G. (2023). Effect of Time on the Properties of Bio-Nanocomposite Films Based on Chitosan with Bio-Based Plasticizer Reinforced with Nanofiber Cellulose. *International Journal of Molecular Sciences* 24(17), <https://doi.org/10.3390/ijms241713205> mój udział polegał na przygotowaniu metodologii i syntezie bioplastyfikatorów oraz na analizie wyników. Mój udział szacuję na 5%.



Podpis



Kędzierzyn-Koźle, 4.08.2023 r.

dr Ewa Sabura

Sieć Badawcza Łukasiewicz –  
Instytut Ciężkiej Syntezy Organicznej "Blachownia"  
Energetyków 9, 47-225 Kędzierzyn-Koźle  
[ewa.sabura@icso.lukasiewicz.gov.pl](mailto:ewa.sabura@icso.lukasiewicz.gov.pl)

## OŚWIADCZENIE O WSPÓLAUTORSTWIE

Niniejszym oświadczam, że w pracy:

Janik, W., Wojtala, A., Pietruszka, A., Dudek, G., & Sabura, E. (2021). Environmentally Friendly Melt-Processed Chitosan/Starch Composites Modified with PVA and Lignin. *Polymers*, 13, 2685, <https://doi.org/10.3390/polym13162685> mój udział polegał na współtworzeniu metod badawczych (analiza termiczna) oraz udziale w analizie wyników. Mój udział szacuję na 5%.

Janik, W., Ledniowska, K., Nowotarski, M., Kudła, S., Knapczyk-Korczak, J., Stachewicz, U., Nowakowska-Bogdan, E., Sabura, E., Nosal-Kovalenko, H., Turczyn, R., & Dudek, G. (2022). Chitosan-based films with alternative eco-friendly plasticizers: Preparation, physicochemical properties and stability. *Carbohydrate Polymers*, 120277. <https://doi.org/10.1016/j.carbpol.2022.120277> mój udział polegał na współtworzeniu metodologii, analizie danych i omówieniu wyników z zakresu analizy termicznej. Mój udział szacuję na 5%.

Janik, W., Nowotarski, M., Ledniowska, K., Shyntum, D. Y., Krukiewicz, K., Turczyn, R., Sabura, E., Furgoń, S., Kudła, S., & Dudek, G. (2023). Modulation of physicochemical properties and antimicrobial activity of sodium alginate films through the use of chestnut extract and plasticizers. *Scientific Reports*, 13(1), <https://doi.org/10.1038/s41598-023-38794-3> mój udział polegał na przygotowaniu metodologii i na analizie wyników z zakresu analizy termicznej. Mój udział szacuję na 5%.

Sabura

Podpis



Gliwice, 30.08.2023 r.

dr inż. Roman Turczyn  
Katedra Fizykochemii i Technologii Polimerów  
Wydział Chemiczny  
Politechnika Śląska  
Ks. M. Strzody 9, 44-100 Gliwice  
roman.turczyn@polsl.pl

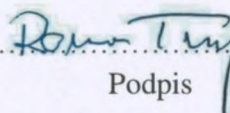
## OŚWIADCZENIE O WSPÓLAUTORSTWIE

Niniejszym oświadczam, że w pracy:

Janik, W., Ledniowska, K., Nowotarski, M., Kudła, S., Knapczyk-Korczak, J., Stachewicz, U., Nowakowska-Bogdan, E., Sabura, E., Nosal-Kovalenko, H., Turczyn, R., & Dudek, G. (2022). Chitosan-based films with alternative eco-friendly plasticizers: Preparation, physicochemical properties and stability. *Carbohydrate Polymers*, 120277. <https://doi.org/10.1016/j.carbpol.2022.120277> mój udział polegał na współtworzeniu metod badawczych, współudziale w analizie i interpretacji wyników oraz korekcie tekstu po recenzjach. Mój udział szacuję na 5%.

Janik, W., Nowotarski, M., Ledniowska, K., Shyntum, D. Y., Krukiewicz, K., Turczyn, R., Sabura, E., Furgoń, S., Kudła, S., & Dudek, G. (2023). Modulation of physicochemical properties and antimicrobial activity of sodium alginate films through the use of chestnut extract and plasticizers. *Scientific Reports*, 13(1), <https://doi.org/10.1038/s41598-023-38794-3> mój udział polegał na współtworzeniu metod badawczych, współudziale w analizie i interpretacji wyników oraz korekcie tekstu po recenzjach. Mój udział szacuję na 5%.

Janik, W., Nowotarski, M., Ledniowska, K., Biernat N., Abdullah, Shyntum, D. Y., Krukiewicz, K., Turczyn R., Gołombek, K. & Dudek, G. (2023). Effect of Time on the Properties of Bio-Nanocomposite Films Based on Chitosan with Bio-Based Plasticizer Reinforced with Nanofiber Cellulose. *International Journal of Molecular Sciences* 24(17), <https://doi.org/10.3390/ijms241713205> mój udział polegał na współtworzeniu metod badawczych, współudziale w analizie i interpretacji wyników oraz korekcie tekstu po recenzjach. Mój udział szacuję na 10%.

  
.....  
Podpis



Gliwice, 25.08.2023 r.

dr hab. inż. Katarzyna Krukiewicz, profesor PŚ  
Katedra Fizykochemii i Technologii Polimerów  
Wydział Chemiczny  
Politechnika Śląska  
Ks. M. Strzody 9, 44-100 Gliwice  
[katarzyna.krukiewicz@polsl.pl](mailto:katarzyna.krukiewicz@polsl.pl)

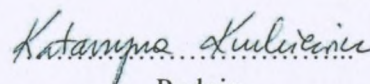
## OŚWIADCZENIE O WSPÓLAUTORSTWIE

Niniejszym oświadczam, że w pracy:

Janik, W., Nowotarski, M., Shyntum, D. Y., Banaś, A., Krukiewicz, K., Kudła, S., & Dudek, G. (2022). Antibacterial and Biodegradable Polysaccharide-Based Films for Food Packaging Applications: Comparative Study. *Materials*, 15(9). <https://doi.org/10.3390/ma15093236> mój udział polegał na współtworzeniu metod badawczych, współudziale w analizie i interpretacji wyników z zakresu właściwości antybakteryjnych, współtworzeniu oryginalnego manuskryptu oraz korekcie tekstu po recenzjach. Mój udział szacuję na 10%.

Janik, W., Nowotarski, M., Ledniowska, K., Shyntum, D. Y., Krukiewicz, K., Turczyn, R., Sabura, E., Furgoł, S., Kudła, S., & Dudek, G. (2023). Modulation of physicochemical properties and antimicrobial activity of sodium alginate films through the use of chestnut extract and plasticizers. *Scientific Reports*, 13(1), <https://doi.org/10.1038/s41598-023-38794-3> mój udział polegał na współtworzeniu metod badawczych, współudziale w analizie i interpretacji wyników z zakresu właściwości antybakteryjnych, współtworzeniu oryginalnego manuskryptu oraz korekcie tekstu po recenzjach. Mój udział szacuję na 5%.

Janik, W., Nowotarski, M., Ledniowska, K., Biernat N., Abdullah, Shyntum, D. Y., Krukiewicz, K., Turczyn R., Gołombek, K. & Dudek, G. (2023). Effect of Time on the Properties of Bio-Nanocomposite Films Based on Chitosan with Bio-Based Plasticizer Reinforced with Nanofiber Cellulose. *International Journal of Molecular Sciences* 24(17), <https://doi.org/10.3390/ijms241713205> mój udział polegał na współtworzeniu metod badawczych, współudziale w analizie i interpretacji wyników z zakresu właściwości antybakteryjnych, współtworzeniu oryginalnego manuskryptu oraz korekcie tekstu po recenzjach. Mój udział szacuję na 10%.



Podpis

Kędzierzyn-Koźle, 28.07.2023 r.

dr Anna Pietruszka

Sieć Badawcza Łukasiewicz – Instytut  
Ciężkiej Syntezy Organicznej "Błachownia"  
Energetyków 9, 47-225 Kędzierzyn-Koźle  
[anna.pietruszka@icso.lukasiewicz.gov.pl](mailto:anna.pietruszka@icso.lukasiewicz.gov.pl)

### OŚWIADCZENIE O WSPÓLAUTORSTWIE

Niniejszym oświadczam, że w pracy:

Janik, W., Wojtala, A., Pietruszka, A., Dudek, G., & Sabura, E. (2021). Environmentally Friendly Melt-Processed Chitosan/Starch Composites Modified with PVA and Lignin. *Polymers*, 13, 2685, <https://doi.org/10.3390/polym13162685> mój udział polegał na współtworzeniu manuskryptu oraz udziale w analizie wyników. Mój udział szacuję na 10%.



Podpis



Kędzierzyn-Koźle, 31.07.2023 r.

dr Anna Wojtala

Sieć Badawcza Łukasiewicz – Instytut  
Ciężkiej Syntezy Organicznej "Blachownia"  
Energetyków 9, 47-225 Kędzierzyn-Koźle  
[anna.wojtala@icso.lukasiewicz.gov.pl](mailto:anna.wojtala@icso.lukasiewicz.gov.pl)

### OŚWIADCZENIE O WSPÓLAUTORSTWIE

Niniejszym oświadczam, że w pracy:

Janik, W., Wojtala, A., Pietruszka, A., Dudek, G., & Sabura, E. (2021). Environmentally Friendly Melt-Processed Chitosan/Starch Composites Modified with PVA and Lignin. *Polymers*, 13, 2685, <https://doi.org/10.3390/polym13162685> mój udział polegał na współtworzeniu metod badawczych oraz udziale w analizie wyników. Mój udział szacuję na 10%.

Anna Wojtala  
.....  
Podpis



Kędzierzyn-Koźle, 28.07.2023 r.

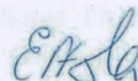
dr Ewa Nowakowska-Bogdan

Sieć Badawcza Łukasiewicz – Instytut  
Ciężkiej Syntezy Organicznej "Blachownia"  
Energetyków 9, 47-225 Kędzierzyn-Koźle  
[ewa.nowakowska@icso.lukasiewicz.gov.pl](mailto:ewa.nowakowska@icso.lukasiewicz.gov.pl)

### OŚWIADCZENIE O WSPÓLAUTORSTWIE

Niniejszym oświadczam, że w pracy:

Janik, W., Ledniowska, K., Nowotarski, M., Kudła, S., Knapczyk-Korczak, J., Stachewicz, U., Nowakowska-Bogdan, E., Sabura, E., Nosal-Kovalenko, H., Turczyn, R., & Dudek, G. (2022). Chitosan-based films with alternative eco-friendly plasticizers: Preparation, physicochemical properties and stability. *Carbohydrate Polymers*, 120277. <https://doi.org/10.1016/j.carbpol.2022.120277> mój udział polegał na współtworzeniu metod badawczych plastyfikatorów (GC-MS), na ich analizie oraz na wsparciu merytorycznym. Mój udział szacuję na 5%.



.....  
Podpis

Gliwice, 25.08.2023 r.

dr Divine Yufetar Shyntum

Centrum Biotechnologii

Politechnika Śląska

Bolesława Krzywoustego 8, 44-100 Gliwice

[divine.yufetar.shyntum@polsl.pl](mailto:divine.yufetar.shyntum@polsl.pl)

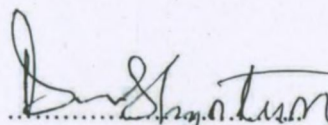
## OŚWIADCZENIE O WSPÓLAUTORSTWIE

Niniejszym oświadczam, że w pracy:

Janik, W., Nowotarski, M., Shyntum, D. Y., Banaś, A., Krukiewicz, K., Kudła, S., & Dudek, G. (2022). Antibacterial and Biodegradable Polysaccharide-Based Films for Food Packaging Applications: Comparative Study. *Materials*, 15(9). <https://doi.org/10.3390/ma15093236> mój udział polegał na współtworzeniu metod badawczych, wykonaniu badań właściwości antybakteryjnych oraz współudziale w ich analizie i interpretacji. Mój udział szacuję na 5%.

Janik, W., Nowotarski, M., Ledniowska, K., Shyntum, D. Y., Krukiewicz, K., Turczyn, R., Sabura, E., Furgoń, S., Kudła, S., & Dudek, G. (2023). Modulation of physicochemical properties and antimicrobial activity of sodium alginate films through the use of chestnut extract and plasticizers. *Scientific Reports*, 13(1), <https://doi.org/10.1038/s41598-023-38794-> mój udział polegał na współtworzeniu metod badawczych, wykonaniu badań właściwości antybakteryjnych oraz współudziale w ich analizie i interpretacji. Mój udział szacuję na 5%.

Janik, W., Nowotarski, M., Ledniowska, K., Biernat N., Abdullah, Shyntum, D. Y., Krukiewicz, K., Turczyn R., Gołombek, K. & Dudek, G. (2023). Effect of Time on the Properties of Bio-Nanocomposite Films Based on Chitosan with Bio-Based Plasticizer Reinforced with Nanofiber Cellulose. *International Journal of Molecular Sciences* 24(17), <https://doi.org/10.3390/ijms241713205> mój udział polegał na współtworzeniu metod badawczych, wykonaniu badań właściwości antybakteryjnych oraz współudziale w ich analizie i interpretacji. Mój udział szacuję na 5%.



Podpis



Kraków, 8.08.2023 r.

dr inż. Joanna Knapczyk-Korczak

Akademia Górniczo-Hutnicza im. Stanisława Staszica w Krakowie

al. Adama Mickiewicza 30

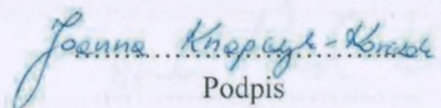
30-059 Kraków

[jknapczyk@agh.edu.pl](mailto:jknapczyk@agh.edu.pl)

## OŚWIADCZENIE O WSPÓLAUTORSTWIE

Niniejszym oświadczam, że w pracy:

Janik, W., Ledniowska, K., Nowotarski, M., Kudła, S., Knapczyk-Korczak, J., Stachewicz, U., Nowakowska-Bogdan, E., Sabura, E., Nosal-Kovalenko, H., Turczyn, R., & Dudek, G. (2022). Chitosan-based films with alternative eco-friendly plasticizers: Preparation, physicochemical properties and stability. *Carbohydrate Polymers*, 120277. <https://doi.org/10.1016/j.carbpol.2022.120277> mój udział polegał na analizie ładunku powierzchniowego folii za pomocą potencjału zeta oraz na wsparciu merytorycznym. Mój udział szacuję na 5%.

  
Podpis



Kędzierzyn-Koźle, 28.07.2023 r.

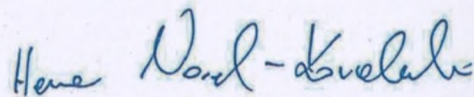
dr Hanna Nosal-Kovalenko

Sieć Badawcza Łukasiewicz – Instytut  
Ciężkiej Syntezy Organicznej "Blachownia"  
Energetyków 9, 47-225 Kędzierzyn-Koźle  
[hanna.nosal@icso.lukasiewicz.gov.pl](mailto:hanna.nosal@icso.lukasiewicz.gov.pl)

### OŚWIADCZENIE O WSPÓLAUTORSTWIE

Niniejszym oświadczam, że w pracy:

Janik, W., Ledniowska, K., Nowotarski, M., Kudła, S., Knapczyk-Korczak, J., Stachewicz, U., Nowakowska-Bogdan, E., Sabura, E., Nosal-Kovalenko, H., Turczyn, R., & Dudek, G. (2022). Chitosan-based films with alternative eco-friendly plasticizers: Preparation, physicochemical properties and stability. *Carbohydrate Polymers*, 120277. <https://doi.org/10.1016/j.carbpol.2022.120277> mój udział polegał na współtworzeniu metod badawczych plastyfikatorów oraz na wsparciu merytorycznym. Mój udział szacuję na 5%.



.....  
Podpis

Kędzierzyn-Koźle, 25.08.2023 r.

mgr inż. Natalia Biernat

Sieć Badawcza Łukasiewicz –

Instytut Ciężkiej Syntezy Organicznej "Błachownia"

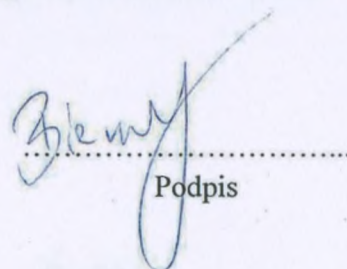
Energetyków 9, 47-225 Kędzierzyn-Koźle

[natalia.biernat@icso.lukasiewicz.gov.pl](mailto:natalia.biernat@icso.lukasiewicz.gov.pl)

## OŚWIADCZENIE O WSPÓŁAUTORSTWIE

Niniejszym oświadczam, że w pracy:

Janik, W., Nowotarski, M., Ledniowska, K., Biernat N., Abdullah, Shyntum, D. Y., Krukiewicz, K., Turczyn R., Gołombek, K. & Dudek, G. (2023). Effect of Time on the Properties of Bio-Nanocomposite Films Based on Chitosan with Bio-Based Plasticizer Reinforced with Nanofiber Cellulose. *International Journal of Molecular Sciences* 24(17), <https://doi.org/10.3390/ijms241713205> mój udział polegał na obróbce danych eksperymentalnych i analizie wyników. Mój udział szacuję na 5%.

  
.....  
Podpis



Gliwice, 8.08.2023 r.

Angelika Banaś

Wydział Chemiczny

Politechnika Śląska

Ks. M. Strzody 9, 44-100 Gliwice

[angeb429@student.polsl.pl](mailto:angeb429@student.polsl.pl)

## OŚWIADCZENIE O WSPÓLAUTORSTWIE

Niniejszym oświadczam, że w pracy:

Janik, W., Nowotarski, M., Shyntum, D. Y., Banaś, A., Krukiewicz, K., Kudła, S., & Dudek, G. (2022). Antibacterial and Biodegradable Polysaccharide-Based Films for Food Packaging Applications: Comparative Study. *Materials*, 15(9). <https://doi.org/10.3390/ma15093236> mój udział polegał na przeprowadzaniu badań antybakteryjnych i obróbce danych. Mój udział szacuję na 5%.

.....  
Banaś.....  
Podpis

Gliwice, 25.08.2023 r.

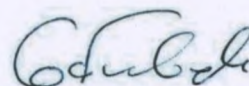
dr hab. inż. Klaudiusz Gołombek, profesor PŚ

Laboratorium Badania Materiałów  
Wydział Mechaniczny Technologiczny  
Politechnika Śląska  
ul. Konarskiego 18a, 44-100 Gliwice  
[kladiusz.golombek@polsl.pl](mailto:kladiusz.golombek@polsl.pl)

### OŚWIADCZENIE O WSPÓLAUTORSTWIE

Niniejszym oświadczam, że w pracy:

Janik, W., Nowotarski, M., Ledniowska, K., Biernat N., Abdullah, Shyntum, D. Y., Krukiewicz, K., Turczyn R., Gołombek, K. & Dudek, G. (2023). Effect of Time on the Properties of Bio-Nanocomposite Films Based on Chitosan with Bio-Based Plasticizer Reinforced with Nanofiber Cellulose. *International Journal of Molecular Sciences* 24(17), <https://doi.org/10.3390/ijms241713205> mój udział polegał na współtworzeniu metod badawczych z zakresu badania morfologii otrzymanych materiałów, wykonaniu zdjęć SEM oraz ich analizie. Mój udział szacuję na 5%.



.....  
Podpis



Gliwice, 25.08.2023 r.

Abdullah

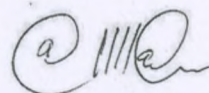
Katedra Fizykochemii i Technologii Polimerów  
Wydział Chemiczny  
Politechnika Śląska  
Ks. M. Strzody 9, 44-100 Gliwice

Szkoła Doktorów  
Politechnika Śląska  
Akademicka 2a, 44-100 Gliwice  
[abdullah.abdullah@polsl.pl](mailto:abdullah.abdullah@polsl.pl)

### OŚWIADCZENIE O WSPÓLAUTORSTWIE

Niniejszym oświadczam, że w pracy:

Janik, W., Nowotarski, M., Ledniowska, K., Biernat N., Abdullah, Shyntum, D. Y., Krukiewicz, K., Turczyn R., Gołombek, K. & Dudek, G. (2023). Effect of Time on the Properties of Bio-Nanocomposite Films Based on Chitosan with Bio-Based Plasticizer Reinforced with Nanofiber Cellulose. *International Journal of Molecular Sciences* 24(17), <https://doi.org/10.3390/ijms241713205> mój udział polegał na współtworzeniu metod badawczych z zakresu badania właściwości antybakteryjnych oraz wykonaniu zdjęć SEM bakterii. Mój udział szacuję na 5%.



.....  
Podpis

Kędzierzyn-Koźle, 1.08.2023 r.

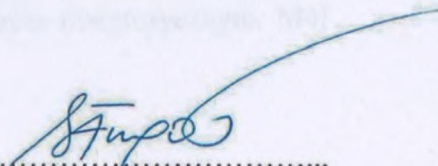
mgr inż. Simona Furgoł

Sieć Badawcza Łukasiewicz –  
Instytut Ciężkiej Syntezy Organicznej "Blachownia"  
Energetyków 9, 47-225 Kędzierzyn-Koźle  
[simona.furgol@icso.lukasiewicz.gov.pl](mailto:simona.furgol@icso.lukasiewicz.gov.pl)

## OŚWIADCZENIE O WSPÓLAUTORSTWIE

Niniejszym oświadczam, że w pracy:

Janik, W., Nowotarski, M., Ledniowska, K., Shyntum, D. Y., Krukiewicz, K., Turczyn, R., Sabura, E., Furgoł, S., Kudła, S., & Dudek, G. (2023). Modulation of physicochemical properties and antimicrobial activity of sodium alginate films through the use of chestnut extract and plasticizers. *Scientific Reports*, 13(1), <https://doi.org/10.1038/s41598-023-38794-3> mój udział polegał na analizie danych eksperymentalnych z analizy termicznej wraz z ich obróbką i opisem. Mój udział szacuję na 5%.



.....  
Podpis



Kraków, 21.08.2023 r.

Prof. dr hab. inż. Urszula Stachewicz

Akademia Górniczo-Hutnicza im. Stanisława Staszica w Krakowie

al. Adama Mickiewicza 30


30-059 Kraków

[ustachew@agh.edu.pl](mailto:ustachew@agh.edu.pl)

## OŚWIADCZENIE O WSPÓLAUTORSTWIE

Niniejszym oświadczam, że w pracy:

Janik, W., Ledniowska, K., Nowotarski, M., Kudła, S., Knapczyk-Korczak, J., Stachewicz, U., Nowakowska-Bogdan, E., Sabura, E., Nosal-Kovalenko, H., Turczyn, R., & Dudek, G. (2022). Chitosan-based films with alternative eco-friendly plasticizers: Preparation, physicochemical properties and stability. *Carbohydrate Polymers*, 120277. <https://doi.org/10.1016/j.carbpol.2022.120277> mój udział polegał na analizie ładunku powierzchniowego folii za pomocą potencjału zeta oraz na wsparciu merytorycznym. Mój udział szacuję na 5%.

  
.....  
Podpis

